science › environment › community

October 26, 2020

FINAL REPORT

Santa Susana Field Laboratory

Evaluation of Off-site Impacts from the Woolsey Fire Burning on Portions of the Santa Susana Field Laboratory Site

Submitted to Gibson, Dunn & Crutcher LLP

RAC Report No. 01-SSFL-2020-FINAL

RAC
RISK ASSESSMENT
CORPORATION

October 26, 2020

FINAL REPORT

Santa Susana Field Laboratory

Evaluation of Off-site Impacts from the Woolsey Fire Burning on Portions of the Santa Susana Field Laboratory Site

Authors
Arthur S. Rood, M.S., K-Spar, Inc.
H. Justin Mohler, M.S., Bridger Scientific, Inc.
Helen A. Grogan, Ph.D., Cascade Scientific, Inc.
Emily A. Caffrey, Ph.D., Radian Scientific, LLC
Colby Mangini, Ph.D., CHP, Paragon Scientific, LLC

Principal Investigator
John E. Till, Ph.D., Risk Assessment Corporation

RAC Report No. 01-SSFL-2020-FINAL

Executive Summary

The purpose of this study was to determine if any radioactive material from the SSFL was released to the atmosphere during the Woolsey Fire and transported downwind by the smoke plume to the surrounding communities. Addressing this question involved computer modeling, soil sampling and environmental data analysis.

Modeling was performed to understand the progression of the fire on the SSFL, where the plume of smoke likely travelled during this time interval and the potential deposition of particulate matter associated with it. A timeline of fire progression on the SSFL was constructed using meteorological data in combination with video footage taken during the fire at air sampling stations operated by Boeing and NASA along with supporting information. Air monitoring data from the Department of Energy (DOE) was also utilized. The fire was segregated into 10 regions covering the time from when the fire began to when it ceased active burning on the SSFL. The Fire Emission Production Simulator model was used to calculate emissions of particulate matter from each segment, and output from this model was coupled with the CALPUFF Version 7 model to calculate transport and deposition of particulate matter. Any radionuclides on vegetation and in surface soil released by the fire were assumed to follow the particulate matter release and deposition. The predicted particulate matter deposition plume trended southwest from the SSFL and formed the basis for identifying soil sampling locations. Highest PM_{10} deposition offsite (See Section 3.4) was determined to be northeast of the Oak Park community which is located about 6 km southwest of SSFL. Any impacts farther west from Oak Park would be lower because of dilution and dispersion.

Based on the modeling described above, 16 soil sampling locations were identified that included locations across the plume and several background locations that were not impacted by the Woolsey Fire while it burned on the SSFL. Sampling focused on the region of highest predicted off-site particulate deposition. Depth-profile sampling was used to evaluate whether radionuclides of SSFL origin were potentially emitted and deposited during the Woolsey fire. Samples were taken in 0–3 cm, 3–6 cm, and 6–12 cm layers. If radionuclides had been deposited from the Woolsey Fire, then they would be detected in the surface (0–3 cm) layer (See Section 5.3) and would be expected to be higher within the plume footprint than outside it.

Soil sampling was carried out August 5–8, 2019 at the 16 locations and 3 depth intervals for a total of 48 soil samples. Each sample was analyzed for 61 radionuclides by GEL Laboratories, LLC. Twenty-eight radionuclides were detected in at least one soil sample. Radionuclides detected were determined to be background, either naturally occurring or of global weapons testing fallout origin, and not from the SSFL. Weighted average concentrations were compared to background concentrations determined by the U.S. Environmental Protection Agency for SSFL (HydroGeologic Inc. 2011). Radionuclides were considered of natural origin if the concentrations were generally uniform with depth. Occurrences of natural occurring radionuclides at concentrations above the established background for the SSFL were attributed to natural variability in geologic formations and not the SSFL because the concentration depth profiles were generally uniform. No anthropogenic radionuclides were measured at levels above those expected from global weapons testing fallout.

Based on the soil sampling, we found no evidence of SSFL impact in off-site soils as a result of the Woolsey fire. Moreover, we found no radionuclide impact on the off-site soils we sampled from past operations of the SSFL.

Contents

Figures

Tables

Acronyms and Abbreviations

AFB	Air Force Base
ASER	Annual Site Environmental Report
BTV	background threshold value
CALMET	a diagnostic three-dimensional meteorological model
CALPOST	a post-processing package for the CALPUFF output
CALPUFF	an air quality dispersion model
DCS	Derived Concentration Standard
DOE	U.S. Department of Energy
DTSC	Department of Toxic Substance Control
EPA	U.S. Environmental Protection Agency
ETEC	Energy Technology Engineering Center
FEPS	Fire Emissions Production Simulator
FRMAC	Federal Radiological Monitoring and Assessment Center
GPS	Global Positioning System
ICRP	International Commission on Radiation Protection
MDA	minimum detectable activity
MDC	minimum detectable concentration
NASA	National Aeronautics and Space Administration
NCRP	National Council on Radiation Protection and Measurements
PM	particulate matter: the term for a mixture of solid particles and liquid droplets found in the air
$PM_{2.5}$	fine inhalable particles, with diameters that are generally 2.5 micrometers (µm) and smaller
PM_{10}	inhalable particles, with diameters that are generally less than 10 micrometers (µm)
PST	pacific standard time
RMHF	Radioactive Material Handling Facility
RRC	radionuclide reference concentration
SSFL	Santa Susana Field Laboratory
UTM	Universal Transverse Mercator

Unit Conversion Table

Imperial unit		SI unit
Radiation activities		
1 Ci	=	3.7×10^{10} Bq
~27 pCi L^{-1}	=	1 Bq L^{-1}
~27 pCi m^{-3}	=	1 Bq m^{-3}
~27 pCi kg^{-1}	=	1 Bq kg^{-1}
Radiation dose quantities		
100 rad	=	1 Gy
100 mrem	=	1 mSv
100 µrem hr^{-1}	=	1 µSv hr^{-1}
Radiation exposure		
3.9×10^3 Roentgen	=	1 C kg^{-1}

Scientific Notation (E-format)

Some of the numbers in this report are presented in scientific notation. Scientific notation is useful for presenting very large or very small numbers, or numbers that are different by many orders of magnitude. In scientific notation, numbers are expressed as the product of two terms; a digit term and an exponential term. For example, the number 723 expressed in scientific notation would be 7.23×10^2 where 7.23 is the digit term and 10^2 (10 raised to the power of 2 or 100) is the exponential term. The power is the number of places to shift the decimal point to present the number in long format. If the power is positive, then shift the decimal point to the right. If the power is negative, then shift the decimal point to the left. Here are some examples.

4,231 $= 4.231\times10^3$
1,230,000 $= 1.23\times10^6$
0.0361 $= 3.61\times10^{-2}$

Computers print scientific notation slightly different where the exponential term is reported as "E" followed by the power term. Thus, in the preceding example, 723 in computer scientific notation is 7.23E+02. Both forms of scientific notation are used in this report. Finally, for numbers between 1 and 10, the power term is zero because any number raised to the zero power is 1. Thus 7.23 expressed in scientific notation is 7.23×10^0 or 7.23E+00 in computer scientific notation.

Common Unit Prefixes

p	pico	10^{-12}	k	kilo	10^3
µ	micro	10^{-6}	M	mega	10^6
m	milli	10^{-3}			

1. Introduction

The Woolsey Fire was reported to have ignited at 14:24 Pacific Standard Time (PST) on November 8, 2018, in the vicinity of the northern boundary of the Santa Susana Field Laboratory (SSFL) site (Citygate 2019) and burned quickly due to powerful Santa Ana winds. The Woolsey Fire was declared 100% contained on November 21, 2018 (CAL FIRE 2019). The objective of this work was to determine if any radioactive material from the SSFL was released to the atmosphere during the Woolsey Fire and transported downwind by the smoke plume to the surrounding communities. The progression of the Woolsey Fire on the SSFL was modeled to aid in the design of a soil-sampling plan that was subsequently carried out. Sampling locations were based on the modeled smoke plume and the areas that were predicted to be impacted by deposition of particulate matter if materials were released while the Woolsey Fire burned on the SSFL. These locations included downwind areas where atmospheric deposition of particulates was anticipated to be largest, as well as locations that were outside the deposition plume of the fire and remained unimpacted. The analysis draws upon environmental monitoring data taken before, during, and after the Woolsey Fire. These data were obtained from the Department of Energy (DOE), the National Aeronautics and Space Administration (NASA) and Boeing.

1.1. Brief Summary of SSFL History and Site Operations

The following summary was adapted from Sapere Consulting and Boeing (2005) and HydroGeologic (2011) and Boeing[1]. The SSFL began operations in 1947 on land acquired by North American Aviation in the Simi Hills between Simi Valley and San Fernando Valley. The facility is located in southeastern Ventura County and borders Los Angeles County on its eastern boundary. The facility's mission initially was rocket engine testing. In 1955, part of Area IV, located in the northwestern corner of the site, was set aside for nuclear research and testing by Atomics International (Figure 1-1[2]). In 1984, Atomics International merged with Rocketdyne, which was purchased in 1996 by The Boeing Company. The remainder of the site was used by NASA and the Department of Defense for rocket and laser testing. Boeing owns Area IV, a portion of which was leased to the DOE and its predecessor agencies in the past for nuclear research activities.

[1] https://www.boeing.com/principles/environment/santa-susana/extraordinary-past.page

[2] Geographical information system data (GIS) and resources are documented in Appendix C.

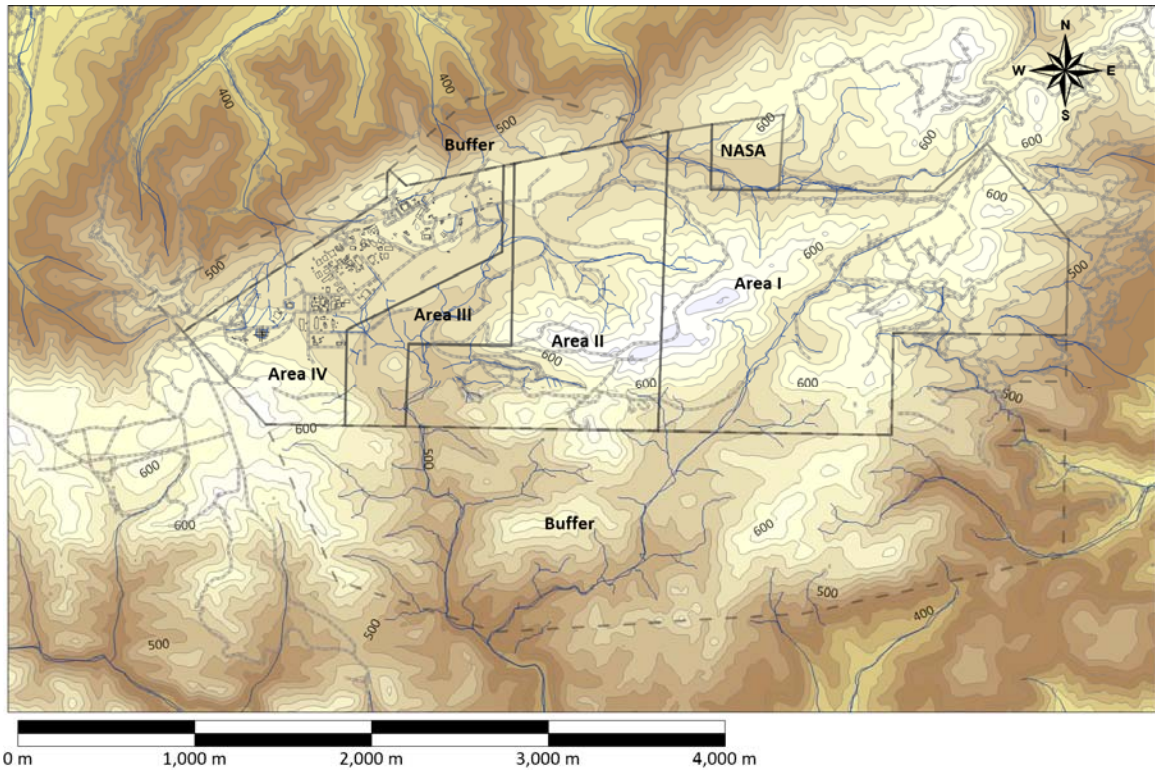

Figure 1-1. Santa Susana Field Laboratory (SSFL) showing administrative areas and buffer zone. DOE operations were confined to Area IV.

The DOE and its predecessors operated the Energy Technology Engineering Center (ETEC) located in Area IV, which represented a group of facilities used for nuclear research and other experimental activities involving radioactive materials. From the mid-1950s until the mid-1980s, nuclear operations included the construction and operation of nuclear research reactors; the fabrication, disassembly, and examination of nuclear reactor fuel; and other radioactive materials research were sponsored by DOE and its predecessor agencies. Nuclear operations at ETEC included 10 nuclear research reactors and seven critical facilities. These facilities included the Hot Laboratory, the Nuclear Materials Development Facility, the Radioactive Materials Handling Facility, and various radioactive material storage areas.

Nuclear research in the ETEC facility of Area IV ended in 1988. Activities conducted by the ETEC have resulted in soil contamination in Area IV. The DOE is responsible for remediation of Area IV soils. As of 2020, some of the contaminated soils have been excavated and removed, and the majority of buildings have been decommissioned and removed[3].

2. Progression and Modeling of the Woolsey Fire on the SSFL

The Woolsey Fire was reported to have begun on November 8, 2018, at 14:24 PST near a Southern California Edison substation located near the northern boundary of the SSFL (Figure 2-1) (Citygate 2019). A second suspected ignition point ~500 m (~550 yds) west of the first ignition

[3] On May 19, 2020, DOE and DTSC entered into a Consent Order regarding the demolition and offsite disposal of ten (10) additional DOE buildings from this area of the SSFL.

point was also identified by CAL FIRE (2019). The fire quickly spread to the southwest pushed by strong Santa Ana winds reaching speeds of about 21 m s^{-1} (47 mph), as measured at the SSFL. The fire spread off-site during the late afternoon/evening and was reported to be burning near the community of Oak Park at 9:00 PM the evening of November 8th (Citygate 2019). The fire jumped U.S. Route 101 between Liberty Canyon Road and Palo Comado Canyon Road overpass at 5:13 AM on the morning of November 9th (Citygate 2019). During the day of November 9, the fire spread rapidly westward (Citygate 2019). The fire also spread to portions of Thousand Oaks, Bell Canyon, West Lake Village, and West Hills during the day (Wildfire Today 2019). The total burned area of the SSFL was 2,268 acres, which encompassed most of the site excluding an east-west strip of land along the northern boundary. The Woolsey Fire was declared 100% contained on November 21 at 18:11 PST (CAL FIRE 2019). The suspected ignition points were provided in the CAL FIRE incident management report (CAL FIRE 2019) and were visually inspected by RAC during a visit to the area on June 4, 2019.

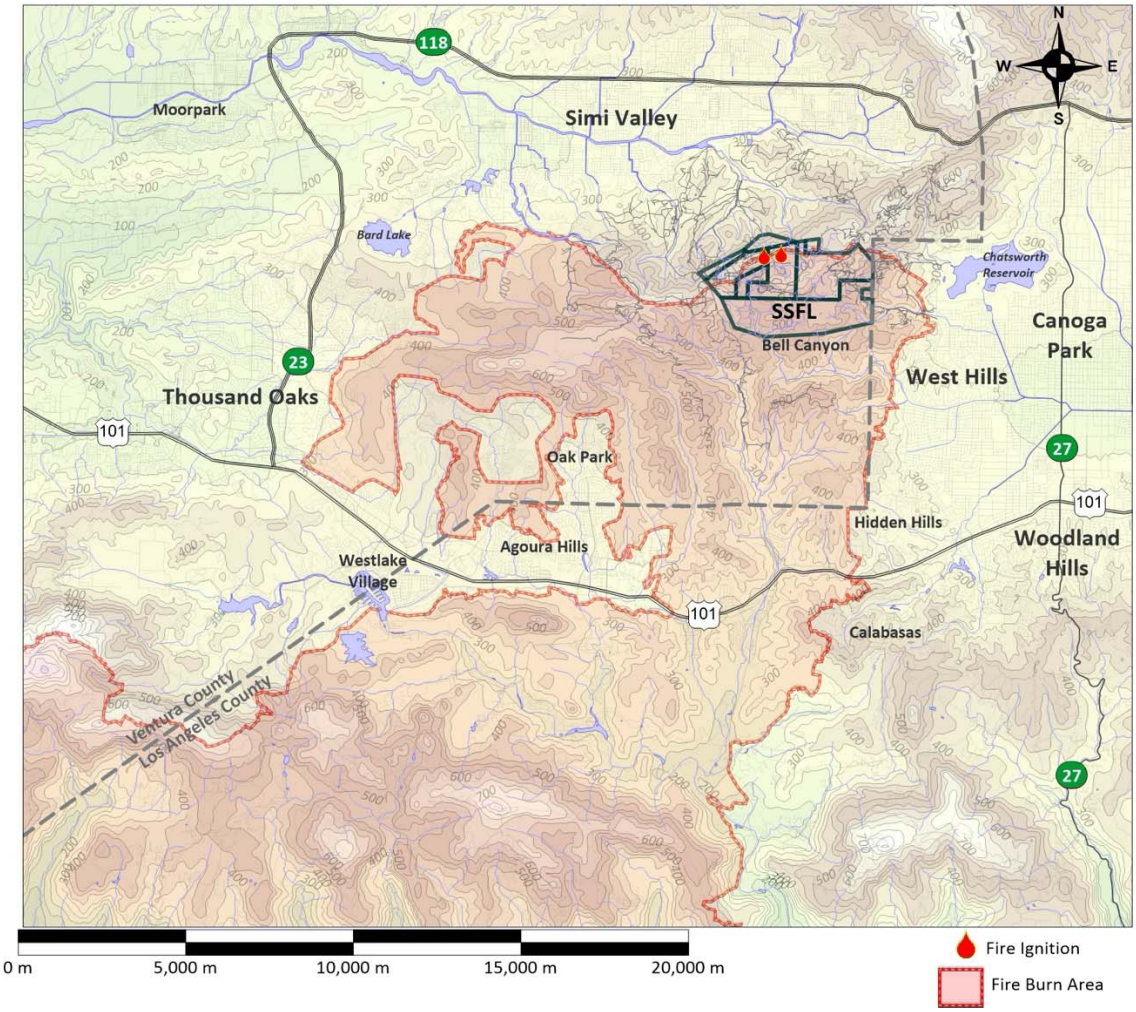

Figure 2-1. Region around the SSFL where the Woolsey Fire burned. Suspected ignition points identified by CAL FIRE are depicted by fire symbol. Fire outline was obtained from LA County (2019).

A timeline of the Woolsey Fire on the SSFL was constructed using different sources of information including meteorological data, video from webcams located at Boeing air monitoring stations and details regarding the fire progression (Figure 2-2 and Table 2.1). Ten regions were identified by date and time of burning. Initially, the fire burned toward the southwest from its ignition point and crossed the western boundary of the SSFL during the late afternoon/evening of November 8. During the late evening of November 8 to the early morning of November 9, a portion of the Woolsey Fire burned through Bell Canyon, which borders the southern boundary of SSFL (Citygate 2019). Around 22:00 PST on November 9, a portion of the fire then burned toward the north, and then back toward the west in the early morning of November 10. Areas of burning at the SSFL continued during November 10 and active burning ceased by the morning of November 11.

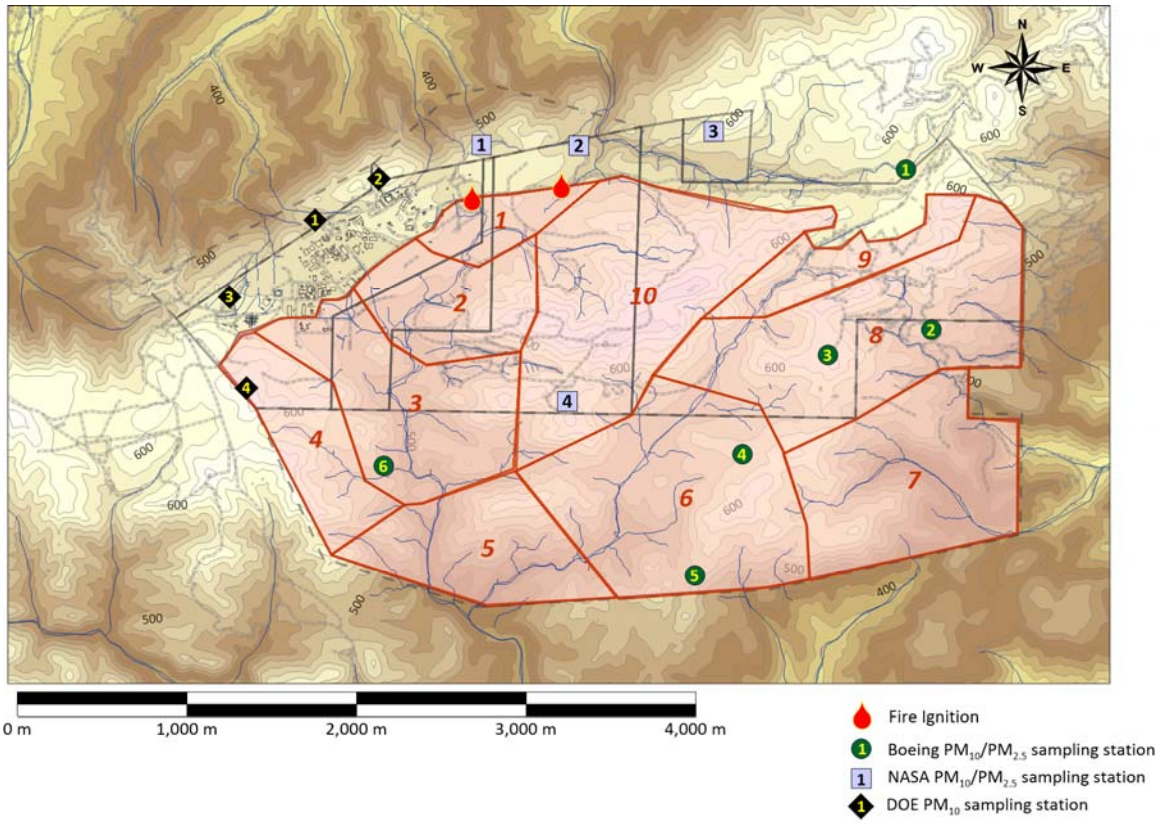

Figure 2-2. Map developed by RAC to show progression of fire on the SSFL. The fire was segregated into 10 regions numbered sequentially from starting region (1) on November 8 at 14:30 (rounded to the nearest half-hour) to ending region (10). Active fire burning on SSFL ceased on the early morning of November 11, but all regions smoldered for some time after active burning.

Table 2.1. Fire Regions on the SSFL, Area Burned, and Date and Time

Region ID	Area (m^2)	Area (acres)	Consumption rate (acres hr^{-1})	Date and time (PST)
1	206502.7	51.0	34.0	11/08/2018, 1430–1600
2	576969.7	142.6	35.6	11/08/2018, 1600–2000
3	988611.0	244.3	244.3	11/08/2018, 2000–2100
4	549912.6	135.9	135.9	11/08/2018, 2100–2200
5	730145.4	180.4	180.4	11/08/2018 2200–2300
6	1509361.7	373.0	124.3	11/09/2018 0000–0300
7	1144709.9	282.9	40.4	11/09/2018 0300–1000
8	1477440.3	365.1	73.0	11/09/2018 1000–1500
9	373000.4	92.2	11.5	11/09/2018 1500–2300
10	1620482.3	400.4	14.3	11/10/2018, 0000 to 11/11 0400

2.1. Model Simulation of Fire

Each region of the Woolsey Fire on SSFL was modeled using the Fire Emission Production Simulator (FEPS) Version 1.1.0 (Anderson et al. 2004) computer program. This model takes as input the beginning and ending time of the fire, the area burned, fuel loading, relative humidity, wind speed, temperature, and atmospheric stability. Fuel loading is defined from the National Fire Danger Rating System 1978 Fuel Model Definitions (Deeming et al. 1977). Fuel model B was selected for the model because it represents California's mixed chaparral ecosystem that covers the SSFL. Dominant plant species in a mixed chaparral ecosystem include scrub oak, chaparral oak, and several species of ceanothus and manzanita (Ornduff 1974). The default fuel loads for this material are 11.5 tons per acre of shrub, 4.5 tons per acre of woody material, and 3.5 tons per acre of litter (Deeming et al. 1977).

The fuel condition was assumed to be very dry based on the meteorological conditions recorded at the Boeing and NASA meteorological tower. The FEPS default moisture percentages for very dry fuels are 4%, 6%, 8%, and 8% for the 1-hr, 10-hr, 100-hr, and 1,000-hr times, respectively. The FEPS default live material moisture percentage was 60%, and litter was 25%. Wind speed, relative humidity, and temperature obtained from the Boeing meteorological tower located in the northeast corner of the SSFL are presented in Figure 2-3, Figure 2-4, and Figure 2-5. Temperatures were relatively mild for Santa Ana conditions with a maximum of about 22º C (~72 º F) recorded on November 10. Atmospheric stability was estimated for each hour based on Pasquill-Gifford classification using Turner's method (Turner 1964). High wind speeds and clear skies resulted in neutral stability conditions for most of the time during the fire.

The total area of each fire region on the SSFL was divided by the number of hours the region actively burned to provide the consumption rate that was entered into FEPS (i.e., acres per hour or tons of fuel per hour). Thus, Region 3, which burned during the highest recorded wind speeds, had the highest burn rate (see Table 2-1). Lower burn rates corresponded to periods of relatively light wind speeds, which were recorded on the evening of the November 9 and on the morning of November 10. This facilitates separate modeling of each region of the Woolsey Fire on the SSFL

and assumes linear growth of the Woolsey Fire across each region. The estimated emission rate for particulate matter with diameters less than 2.5 microns ($PM_{2.5}$) from all sources as a function of time (Figure 2-6) shows that the highest emission rates occurred in the late afternoon and evening of November 8 and the early morning of November 9 during the period of highest wind speeds.

The FEPS model produces emission estimates as a function of time for carbon monoxide, methane and $PM_{2.5}$. For this application, only the $PM_{2.5}$ was included in the atmospheric dispersion model because (1) measurements at the Boeing air samplers included $PM_{2.5}$ and PM_{10} (particulate matter with diameters less than 10 µm) and (2) radionuclides potentially present in vegetation and surface soil would be released with the burning of vegetation and the suspension of soil in a similar manner that particulate matter is released from a fire (Grogan et al. 2007). Historical vegetation measurements are discussed Section 4.1.1. Emissions and mass of vegetation burned for each region are summarized in Table 2-2.

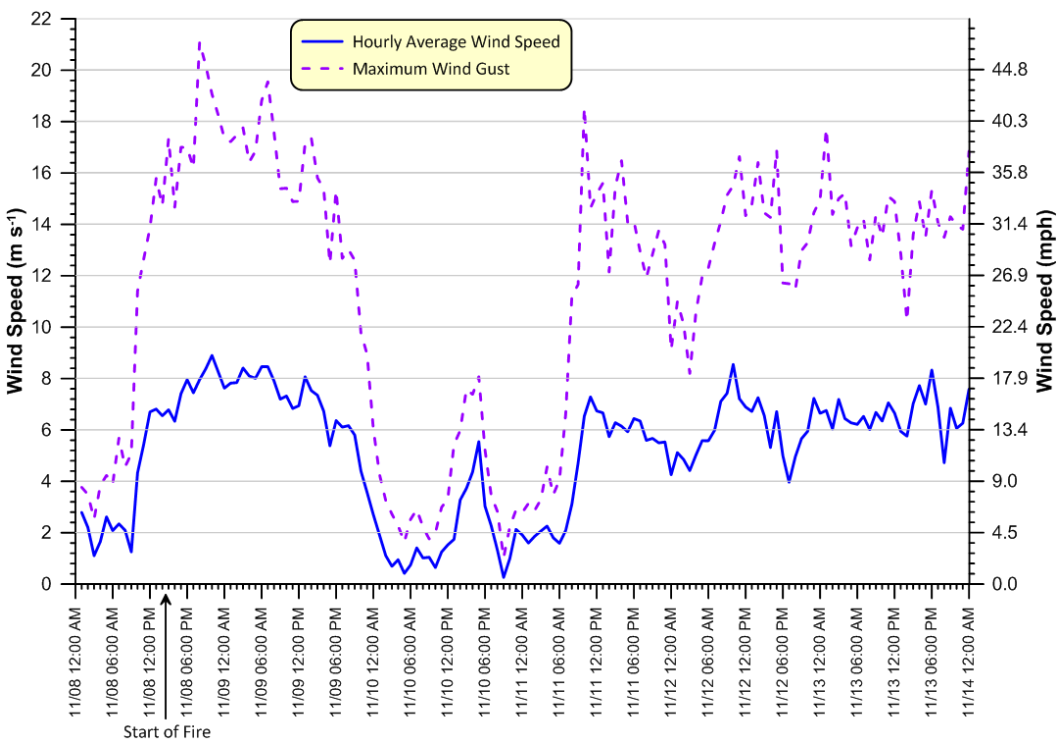

Figure 2-3. Wind speed as a function of time measured at Boeing meteorological tower during Woolsey Fire.

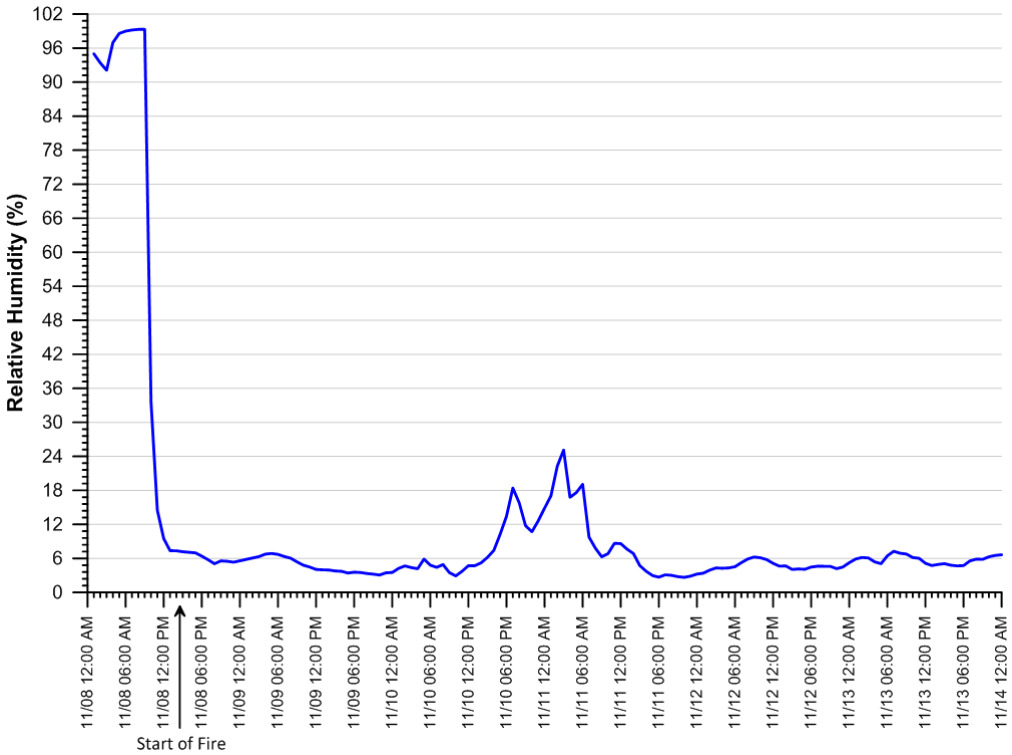

Figure 2-4. Relative humidity as a function of time measured at Boeing meteorological tower during Woolsey Fire.

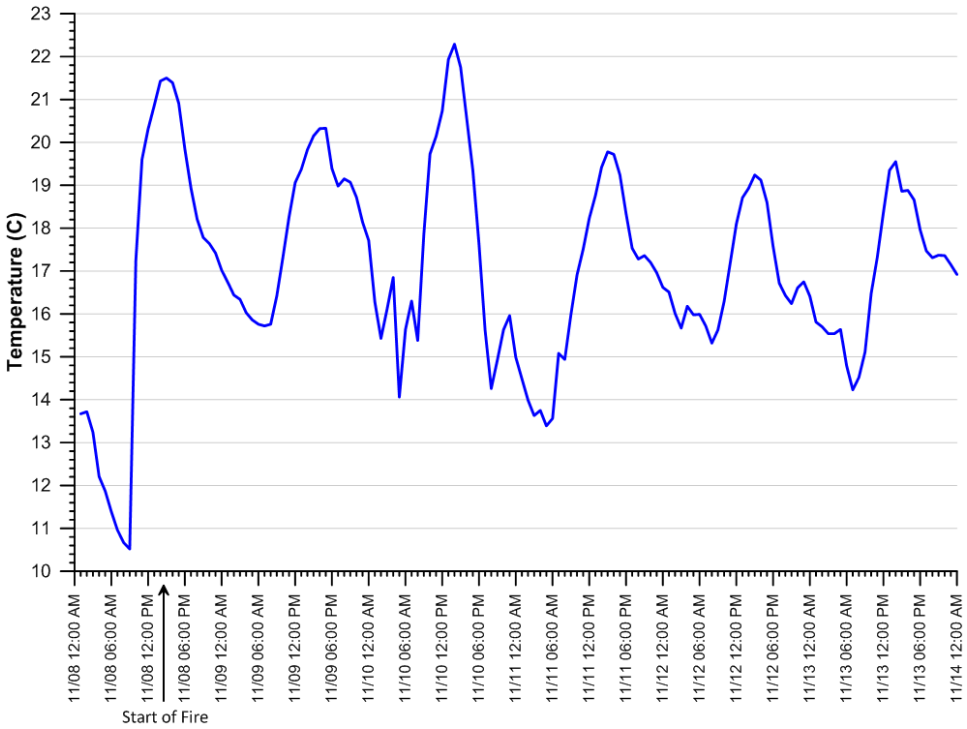

Figure 2-5. Temperature as a function of time measured at Boeing meteorological tower during Woolsey Fire.

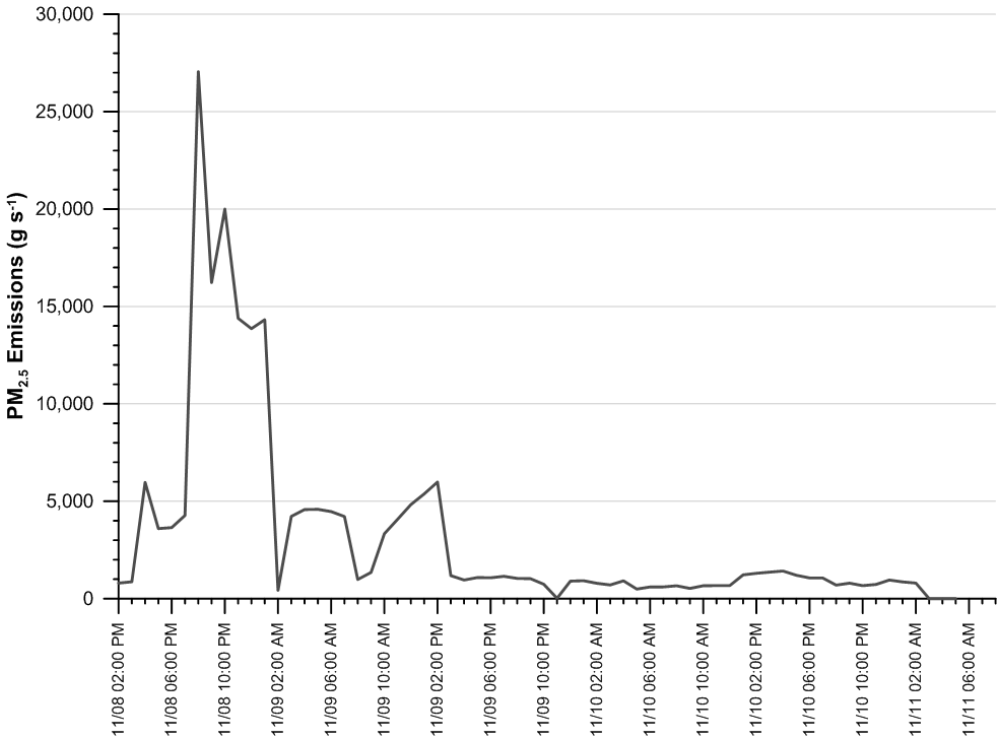

Figure 2-6. FEPS-predicted release rate of $PM_{2.5}$ as a function of time from Woolsey Fire burning on the SSFL.

Table 2.2. FEPS-Predicted $PM_{2.5}$ Emissions and Biomass Consumed during Woolsey Fire

Region	Total $PM_{2.5}$ emissions (g)	Area (m^2)	Area (acres)	$PM_{2.5}$ emissions per unit area ($g\ m^{-2}$)	Total biomass consumption (kg)
1	1.644E+07	206,503	51.03	7.962E+01	1.16E+06
2	5.298E+07	576,970	142.57	9.182E+01	3.67E+06
3	9.992E+07	988,611	244.29	1.011E+02	6.83E+06
4	5.722E+07	549,913	135.88	1.041E+02	3.90E+06
5	7.240E+07	730,145	180.42	9.915E+01	4.96E+06
6	1.526E+08	1,509,362	372.96	1.011E+02	1.04E+07
7	8.790E+07	1,144,710	282.86	7.679E+01	6.23E+06
8	8.550E+07	1,477,440	365.08	5.787E+01	6.37E+06
9	2.913E+07	373,000	92.17	7.810E+01	2.06E+06
10	8.895E+07	1,620,482	400.42	5.489E+01	6.70E+06
Total	7.431E+08	9,177,136	2268	N/A	3.794E+09

3. Model Simulation of Atmospheric Transport of Particulate Matter Emitted from the Woolsey Fire on the SSFL

As noted in previous sections, if radionuclides were present and released in burning vegetation and suspended from the surface soil, the release, transport and deposition would be similar to particulate matter from the fire (Grogan et al. 2007). A fraction of the particulate matter that is released to the atmosphere will deposit from the plume on the soil as it is transported downwind. Likewise, radionuclides entrained in the plume will also deposit on the soil as they are transported downwind. Therefore, the purpose of the modeling was to estimate the deposition pattern of particulate matter from the Woolsey Fire while it burned on the SSFL.

The plume was modeled using the CALPUFF (Scire et al. 2000) modeling system Version 7. CALPUFF is an advanced non-steady-state meteorological and air quality modeling system used to compute particulate and gaseous concentrations of material emitted to the atmosphere. The model has been listed by the U.S. Environmental Protection Agency (EPA) as an approved model for assessing long range transport of pollutants and their impacts on Federal Class I areas[4] and for certain near-field applications involving complex meteorological conditions. Version 7 is the EPA-approved version (Version 5.8) but includes additional enhancements. Enhancements in Version 7 include an interface between FEPS and CALPUFF so that the output from FEPS can be processed and used directly in a CALPUFF simulation. The CALPUFF modeling system consists of three primary codes: A meteorological model (CALMET), a complex terrain Lagrangian puff dispersion model (CALPUFF), and a post-processing program (CALPOST). There are also numerous preprocessors for developing input data that include surface and upper air meteorological data, terrain and land-use data, and the source-term data provided by FEPS.

3.1. Model Domain and Computational Grid

The total region that is modeled is referred to as the model domain and is illustrated in Figure 2-1. The model domain measures 33.1 km east-west by 27.5 km north-south covering an area of 910.25 km^2 (224,928 acres). Terrain in the SSLF region is characterized as complex and rugged. Elevations above mean sea level within the model domain ranged from 55 m (180 ft) to 917 m (3,008 ft), with a median elevation of 331 m (1,086 ft). The rugged terrain required a refined horizontal grid spacing of 100 m resulting in 332 east-west nodes and 276 north-south nodes for a total of 91,632 nodes. The 100-m grid spacing allowed spatial resolution of the steep terrain in the vicinity of the SSFL.

The vertical discretization of the atmosphere was segregated into 10 layers having upper bounds of 20 m, 40 m, 80 m, 160 m, 320 m, 640 m,1,200 m, 2,000 m, 3,000 m, and 4,000 m above ground surface.

3.2. Meteorological Data

Meteorological towers on the SSFL are illustrated in Figure 3-1. The tower operated by Boeing is located in the northeastern corner of the facility. NASA operates the tower near the center of the

[4] Federal Class I areas include areas such as national parks and national wilderness areas. These areas are granted special air quality protections under Section 162(a) of the federal Clean Air Act.

facility and DOE operates a tower in the northwest portion of the facility. The DOE tower was inoperable during the fire and thus provided no data in the model simulation. The Boeing and NASA towers remained operational during the fire and these data were the primary source of on-site meteorological data. Wind speed and direction were measured at 10 m or 15 m, which is optimal for surface measurements and generally recommended by EPA.

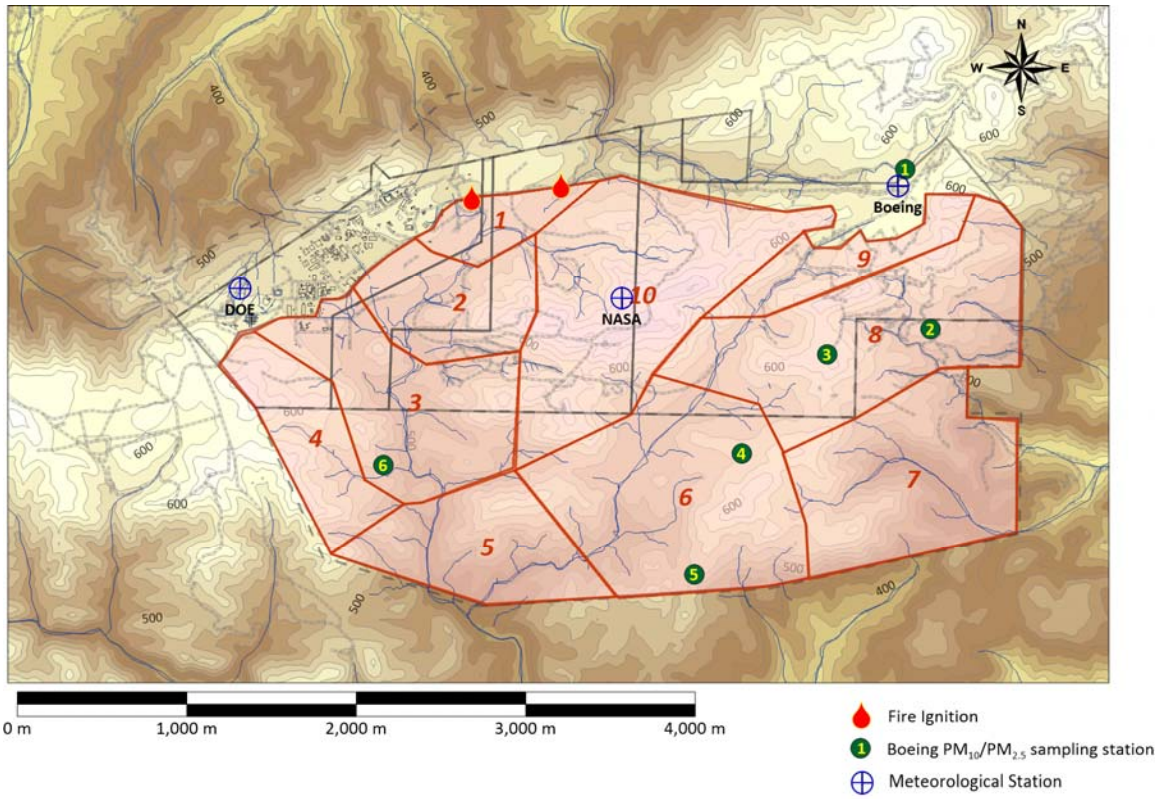

Figure 3-1. Location of the three meteorological towers at SSFL. Meteorological data were also collected at Boeing PM_{10} sampling stations at the 2-m level.

Boeing also measures windspeed and direction at six particulate air monitoring stations that are illustrated in Figure 3-1 and labeled 1 through 6. These data are measured at the 2-m level, and supplemented data from the towers. Tower data was preferable because at the 2-m level, ground obstructions can influence the measurements.

Meteorological data from the Burbank and Van Nuys airports were also obtained and used in the simulation. Although these stations were outside the model domain, they provided required data on cloud cover and barometric pressure. Cloud cover and barometric pressure were not likely to differ from conditions at the SSFL.

CALMET also requires upper air sounding from the nearest upper air station. The nearest upper air station was at Vandenberg AFB and the twice daily sounding during the fire were obtained and used in the simulation.

Wind roses during the most active burning period of the fire at the two operational towers and the six Boeing air monitoring locations (Figure 3-2 and Figure 3-3) show winds predominantly out of the north-northeast to northeast direction; however, the Boeing main tower had winds predominately out of the east-northeast and Boeing station 4 had winds predominantly out of the

north. It is likely that terrain channeling influenced the wind direction at Boeing station 4. Wind speeds were highest at the NASA tower, which is at the highest elevation of all the stations. Wind speeds for the Boeing air monitoring stations (2-m measurement height) generally exhibited lower windspeeds than the meteorological towers. The Boeing main tower and Boeing monitoring station 1 are relatively close to each another but exhibited different predominant wind directions. This observation is likely due to different measurement heights and the chaotic nature of the winds during the fire.

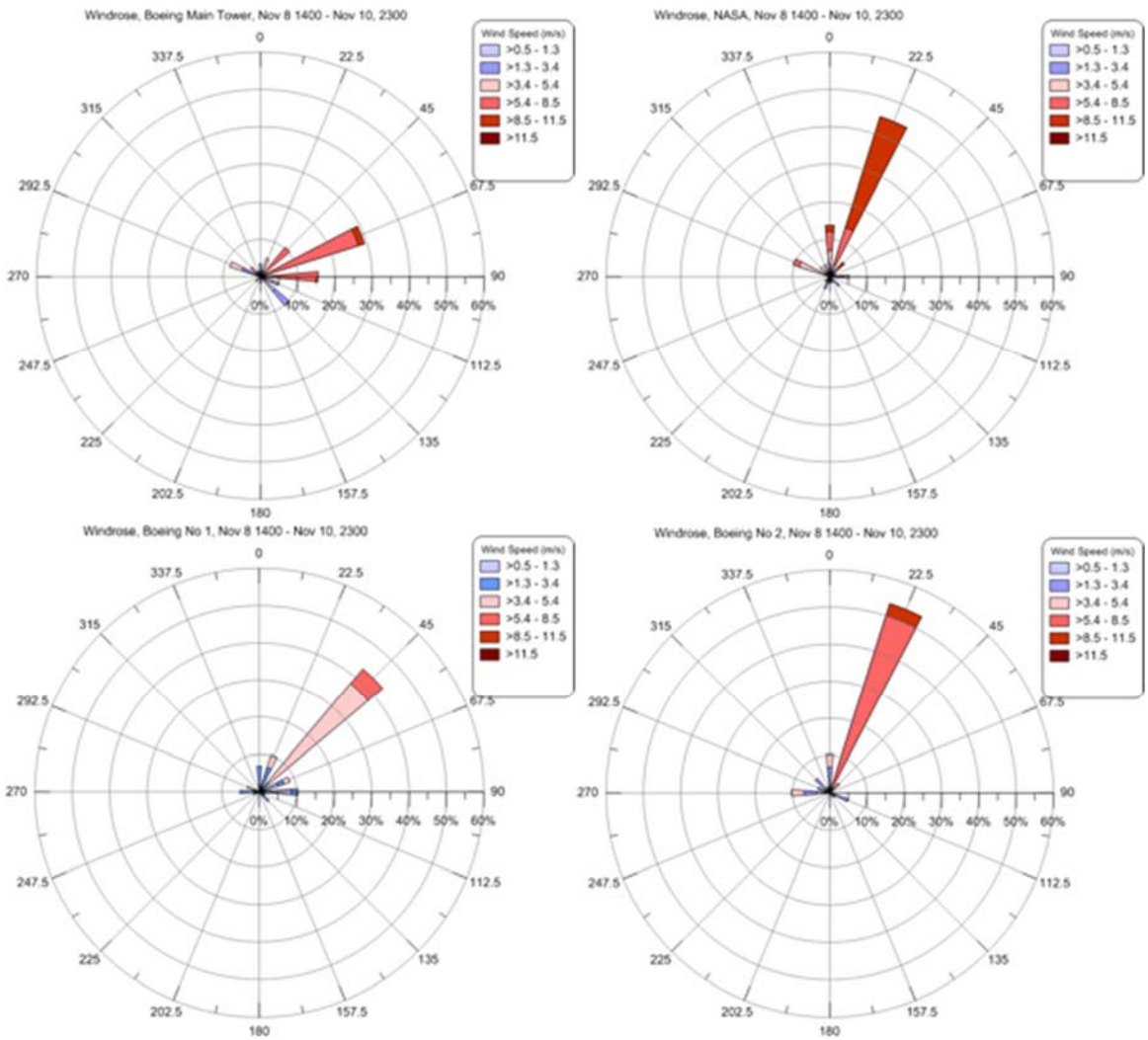

Figure 3-2. Wind roses during the fire for Boeing and NASA towers and particulate monitors 1 and 2. Instruments on the towers were at 10 to 15-m height and meteorological instruments at the particulate monitors were at 2-m height.

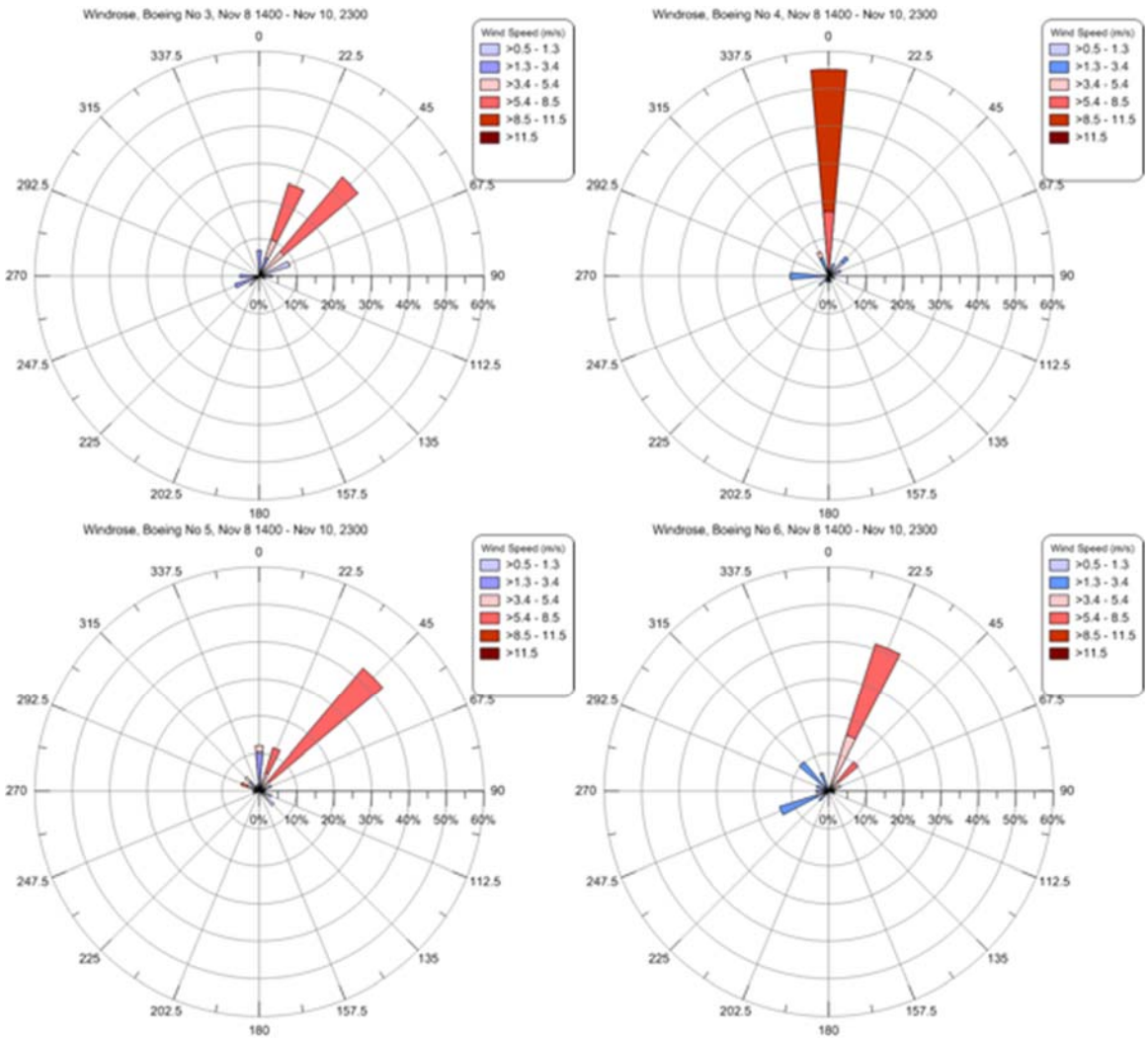

Figure 3-3. Wind roses during the fire for particulate monitors 3, 4, 5, and 6. Meteorological instruments at the particulate monitors were at 2-m height.

3.3. CALMET and CALPUFF Technical Options

In general, default technical options and parameters were used in the CALMET and CALPUFF simulations. Model parameters and options with no default value or where the default was not selected are discussed below.

3.3.1. CALMET Bias Variable

The bias variable weights the surface and upper air readings in the wind field interpolation scheme. A bias value of –1 reduces the weight of the upper air stations by 100%, and a bias value of 1 reduces the weight of a surface station by 100%. Integer bias values range between –1 and 1 (i.e., a bias value of –0.3 weights the upper air observations by 30% and applies a weight of 70% to the surface stations). In this application a gradational approach was used (as recommended in CALPUFF) so that at the surface layer, the surface stations are weighted by 100%; in the uppermost

layer, the upper air station is weighted by 100%. Bias values for each layer from the surface to the highest layer were –1, –0.9, –0.8, –0.7, –0.4, 0.0, 0.7, 1.0, 1.0, 1.0.

3.3.2. CALMET Radius of Influence and Kinematic Effects

The CALMET default is to use all stations weighted by the distance squared. Because conditions can vary significantly across the SSFL, the varying radius of influence option was used in the simulation. For surface stations, all stations within 2 km of the grid point were used in the wind field interpolation. If no stations were found within 2 km, then the nearest station was used. For upper air stations, this value was 100 km because only one station was used. Radius of influence for terrain features was 0.5 km. That is, terrain features within 0.5 km of a grid point were included in the simulation. Observations within 0.5 km of a grid point were given equal weighting between the observation and the first-guess wind field as prescribed in CALMET.

Kinematic effects (the change in air properties due to the advection of air parcels) by default are not included in CALMET but were included in this simulation because of the strong and chaotic nature of Santa Ana winds that drove the fire. A sensitivity case was also run using only the CALMET defaults, which do not include kinematic effects or varying radius of influence. The difference between the simulations were minimal.

3.3.3. CALPUFF Dispersion Coefficient Option

The dispersion coefficients used in this CALPUFF simulation are determined from internally calculated micrometeorological variables that account for the physical and dynamic occurrences within a shallow stratum of air adjacent to the ground and provide a non-biased estimate of air concentrations. This represents the current state-of-the art in atmospheric dispersion modeling.

3.4. Predicted and Observed $PM_{2.5}$ Concentrations

Boeing, NASA, and DOE operate a total of 14 PM_{10} monitors on the SSFL, and at three monitoring stations (Boeing stations 1 and 4, NASA station 2) there is also a $PM_{2.5}$ monitor (Figure 2-2, Table 3-1, Table 3-2, Table 3-3). These monitoring stations are discussed in Section 4. Particulate matter emission is one of the natural consequences of wildfires and the measurements show a clear increase in particulate matter emissions during the Woolsey Fire.

The CALPUFF simulation calculates the 24-hour average $PM_{2.5}$ concentration at each of the monitoring stations from $PM_{2.5}$ emitted while the Woolsey Fire burned in the different areas of the SSFL. Because the CALPUFF predicted concentration represents a net value that does not include the contribution from background, the average background $PM_{2.5}$ concentration (11.7 $\mu g\ m^{-3}$) was added to the predicted concentration at each location for comparison to the measured concentration. This background $PM_{2.5}$ concentration was calculated from pre-fire data measured at Boeing stations 1 and 4 and NASA station 2 (see Table 4-1). The pre-fire Boeing data spanned from April 15, 2018 to the start of the Woolsey Fire and the pre-fire NASA data spanned from November 1, 2018 to the start of the Woolsey Fire. For stations that only measured PM_{10}, the $PM_{2.5}$ concentration was estimated using Equation 3-1 by dividing the PM_{10} concentration by the average PM_{10} to $PM_{2.5}$ ratio measured during the fire (2.05).

$$PM_{2.5} = \frac{PM_{10}}{2.05}, \text{ for samplers with only } PM_{10} \text{ measurements} \quad (3\text{-}1)$$

Table 3.1. Measured 24-hr Average PM_{10} and $PM_{2.5}$ Concentrations at Boeing Samplers

	Boeing 1		Boeing 2	Boeing 3	Boeing 4		Boeing 5	Boeing 6
Date	PM_{10} (µg m^{-3})	$PM_{2.5}$ (µg m^{-3})	PM_{10} (µg m^{-3})	PM_{10} (µg m^{-3})	PM_{10} (µg m^{-3})	$PM_{2.5}$ (µg m^{-3})	PM_{10} (µg m^{-3})	PM_{10} (µg m^{-3})
11/8/2018	46.1	7.9	76.2	46.0	52.8	19.5	48.8	614.9
11/9/2018	23.0	4.0	716.1	640.5	825.4	436.1	923.2	163.8
11/10/2018	54.0	43.7	71.1	63.0	57.4	48.8	71.4	42.5
11/11/2018	26.8	15.2	106.7	107.0	79.6	22.5	67.8	64.7

Table 3.2. Measured 24-hr Average PM_{10} and $PM_{2.5}$ Concentrations at NASA Samplers

	NASA 1	NASA 2		NASA 3	NASA 4
Date	PM_{10} (µg m^{-3})	PM_{10} (µg m^{-3})	$PM_{2.5}$ (µg m^{-3})	PM_{10} (µg m^{-3})	PM_{10} (µg m^{-3})
11/8/2018	57.2	52.2	16.4	53.2	56.6
11/9/2018	22.8	19.5	5.0	16.5	744.1
11/10/2018	32.4	87.3	75.6	59.0	52.6
11/11/2018	36.2	28.8	19.0	26.5	63.5

Table 3.3. Measured 24-hr Average PM_{10} Concentrations at DOE Samplers

	DOE 1	DOE 2	DOE 3	DOE 4
Date	PM_{10} (µg m^{-3})	PM_{10} (µg m^{-3})	PM_{10} (µg m^{-3})	PM_{10} (µg m^{-3})
11/8/2018	55.1	66.1	51.3	a
11/9/2018	23.5	30.4	30.4	a
11/10/2018	21.9	21.5	25.2	a
11/11/2018	30.3	28.8	30.4	a

a. DOE Sampler 4 ceased operation on November 8 and was repaired on December 19, 2018

Predicted and measured $PM_{2.5}$ concentrations (Table 3-4, Table 3-5, Table 3-6) show that predicted concentrations are approximately within a factor of 2 of the observations (i.e. overpredict or underpredict the measured concentration by a factor of 2). Model predictions within a factor of 2 of the observations are generally considered acceptable model performance (Chang and Hanna 2004). Previous modeling studies of wildfires show that PM_{10} was predicted generally within a factor of 2 of the observations (Grogan et al. 2007). The average observed value across all samplers was 63.8 µg m^{-3}, the average predicted value was 37.1 µg m^{-3}, and the P/O ratio of the averages was 0.58. However, the measured data may include not only $PM_{2.5}$ generated by the Woolsey Fire burning on the SSFL, but also $PM_{2.5}$ generated by the Woolsey Fire burning on land outside the SSFL boundary, whereas the modeled

concentrations only include $PM_{2.5}$ generated by the Woolsey Fire burning on SSFL land. Consequently, some model underprediction would be expected.

Table 3.4. Measured and Predicted Net 24-hr Average $PM_{2.5}$ Concentrations at the Boeing Samplers (µg m^{-3})

Date	Measured Boeing 1	Measured[b] Boeing 2	Measured[b] Boeing 3	Measured Boeing 4	Measured[b] Boeing 5	Measured[b] Boeing 6
11/8/2018	7.9	37.2	22.4	19.5	23.8	299.9
11/9/2018	4.0	338.6	301.8	436.1	450.3	79.9
11/10/2018	43.7	24.1	20.1	48.8	34.8	20.7
11/11/2018	15.2	41.4	41.6	22.5	33.1	31.6
Average	17.7	110.3	96.5	131.7	135.5	108.0
Average measured over all samplers: 100 µg m^{-3}.						
Date	Predicted Boeing 1	Predicted Boeing 2	Predicted Boeing 3	Predicted Boeing 4	Predicted Boeing 5	Predicted Boeing 6
11/8/2018	11.7	11.7	11.7	11.7	12.2	259.2
11/9/2018	38.6	150.4	52.1	102.1	61.2	26.1
11/10/2018	17.5	23.3	33.6	241.3	37.3	74.0
11/11/2018	11.7	11.7	11.9	14.6	15.0	12.4
Average	19.8	49.3	27.3	92.4	31.4	92.9
Average predicted over all samplers: 52.2 µg m^{-3}.						
P/O[a]	1.1	0.45	0.28	0.70	0.23	0.86
P/O of sampler average: 0.52						

[a.] Predicted-to-observed (measured) ratio of sampler time average.
[b.] Calculated from PM_{10} measurement based on Equation 3-1.

Table 3.5. Measured and Predicted Net 24-hr Average $PM_{2.5}$ Concentrations at the NASA Samplers (µg m^{-3})

Date	Measured [b] NASA 1	Measured NASA 2	Measured [b] NASA 3	Measured [b] NASA 4
11/8/18	28.0	16.4	26.0	27.7
11/9/18	11.1	5.0	8.1	363.8
11/10/18	15.8	75.6	28.8	25.7
11/11/18	17.7	19.0	13.0	31.0
Average	18.2	29.0	19.0	112.1
Average measured over all samplers: 44.5 µg m^{-3}.				
Date	**Predicted NASA 1**	**Predicted NASA 2**	**Predicted NASA 3**	**Predicted NASA 4**
11/8/18	11.7	11.7	11.7	12.0
11/9/18	16.6	16.4	17.4	39.7
11/10/18	25.4	18.4	17.4	110.9
11/11/18	11.8	11.8	11.8	24.0
Average	16.4	14.6	14.6	46.7
Average predicted over all samplers: 23 µg m^{-3}.				
P/O[a]	0.90	0.50	0.77	0.42
P/O of sampler average: 0.52				

[a.] Predicted-to-observed (measured) ratio of sampler time average.
[b.] Calculated from PM_{10} measurement based on Equation 3-1.

Table 3.6. Measured and Predicted Net 24-hr Average $PM_{2.5}$ Concentrations at the DOE Samplers (µg m^{-3})

Date	Measured [c] DOE 1	Measured [c] DOE 2	Measured [c] DOE 3	Measured [c] DOE 4
11/8/18	27.0	32.3	25.1	b
11/9/18	11.5	14.9	14.9	b
11/10/18	10.7	10.5	12.3	b
11/11/18	14.8	14.1	14.9	b
Average	16.0	18.0	16.8	---
Average measured over all samplers: 16.9 µg m^{-3}.				
Date	**Predicted DOE 1**	**Predicted DOE 2**	**Predicted DOE 3**	**Predicted DOE 4**
11/8/18	11.7	11.7	11.8	b
11/9/18	17.3	16.8	18.2	b
11/10/18	73.7	40.9	71.9	b
11/11/18	11.7	11.7	11.7	b
Average	28.6	20.3	28.4	---
Average predicted over all samplers: 25.7 µg m^{-3}.				
P/O[a]	1.8	1.1	1.7	---
P/O of sampler average: 1.5				

[a.] Predicted-to-observed (measured) ratio of sampler time average.
[b.] DOE Sample 4 ceased operation on November 8 and was repaired on December 19, 2018. Because no corresponding measurements existed during the fire, no model predictions were made for DOE-4
[c.] Calculated from PM_{10} measurement based on Equation 3-1.

The distribution of individual P/O ratios had an average value of 1.4 (standard deviation 1.90) and a median value of 0.69 indicating the distribution is closer to a lognormal distribution. The geometric mean P/O ratio was 0.80 and geometric standard deviation was 2.75.

Predicted ambient air concentrations of $PM_{2.5}$ above background are illustrated in Figure 3-4. The contours represent the average $PM_{2.5}$ concentration from November 8, 1400 to November 10, 2200 (57 hours). $PM_{2.5}$ plumes from areas burned on November 8 traveled southwest of SSFL, and then funneled down a north-south drainage skirting the community of Oak Park. Average concentrations were typically 60 to 90 µg m^{-3} in this uninhabited region but were lower in the residential areas (20 to 50 µg m^{-3}) of Oak Park and Agoura Hills. A second $PM_{2.5}$ plume from SSFL that burned on November 9 and 10 traveled almost directly south down Bell Canyon, but at concentrations less than those at Oak Park and Agoura Hills. Concentrations of the SSFL derived $PM_{2.5}$ southwest of the model domain and in the community of Malibu would have been considerably lower due to atmospheric dispersion and dilution than depicted in Figure 3-4.

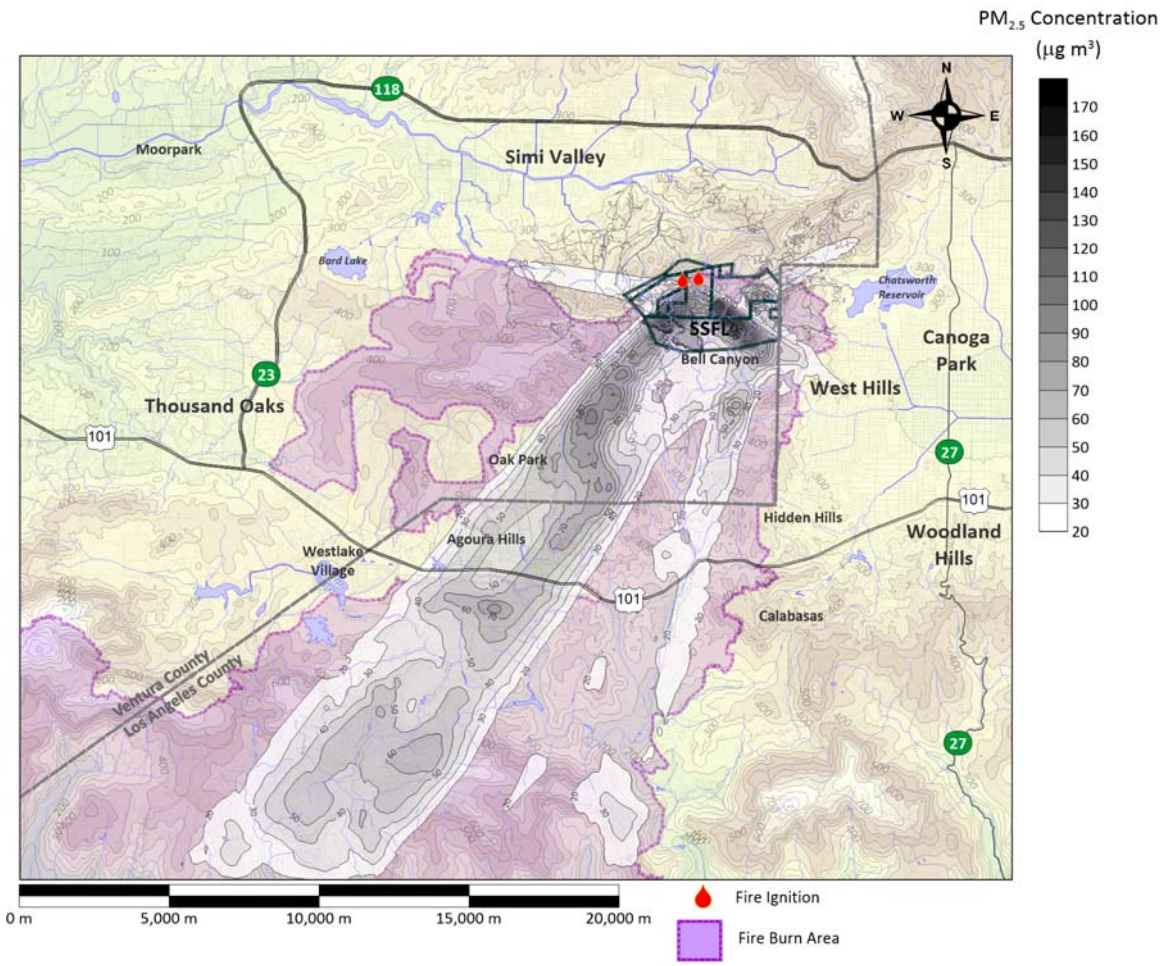

Figure 3-4. Average $PM_{2.5}$ ambient air concentration from the fire burning across the SSFL from November 8, 1400 to November 10, 2200.

3.5. Deposition Pattern of Particulate Matter

Airborne particulate matter from the burning of vegetation and suspended from soil during the fire will eventually deposit on the land surface according to the dry deposition velocity. For this evaluation, the $PM_{2.5}$ deposition across the model domain was scaled to PM_{10} (using the previously discussed $PM_{10}/PM_{2.5}$ ratio in Section 3.4) and plotted in the form of an isopleth map (Figure 3-5). This deposition pattern is from PM_{10} generated only while the Woolsey Fire burned on the SSFL and does not include deposition from burned areas outside the SSFL boundaries. The deposition pattern generally follows the regional northeast winds at the time of the fire. Any particulate radionuclides on vegetation or in the surface soil that was potentially suspended during the fire would have followed a similar deposition pattern. Highest deposition of particulate matter from the fire outside the SSFL boundary was east of the community of Oak Park in a region of hilly uninhabited terrain. Other areas of enhanced deposition correspond to elevated terrain where the lofted plume intersected the ground surface. Deposition of SSFL derived PM_{10} southwest of the model domain and in the community of Malibu (~23 km SSW of the SSFL) would have been considerably lower than depicted in Figure 3-5. For example, PM_{10} deposition decreased from

~1.25 g m^2 at Oak Park to ~0.45 g m^2 at the southern edge of the model domain (~ 10 km distance and reduction factor of 2.8). Malibu is about 10 km south of southern boundary of the model domain so we could expect a similar reduction in deposition resulting from further atmospheric dispersion and dilution. Thus, deposition in Malibu would be about a factor of 5 less than the deposition at Oak Park.

During the first day of the Woolsey Fire (November 8), particulate emissions and fire consumption rates on the SSFL were the greatest. A plot of the PM_{10} deposition from PM_{10} emissions on November 8 (Figure 3-6) shows a similar pattern and magnitude to Figure 3-5 and indicates that most of the total PM_{10} deposited was generated when the Woolsey Fire burned on the SSFL on November 8.

These isopleth maps served as a guide for defining a soil sampling program to determine if radionuclides located on the SSFL property were released when the Woolsey Fire burned on the site. If radionuclides located on the SSFL property were released during the Woolsey Fire, then their presence would be detected in surface soil within the deposition plume.

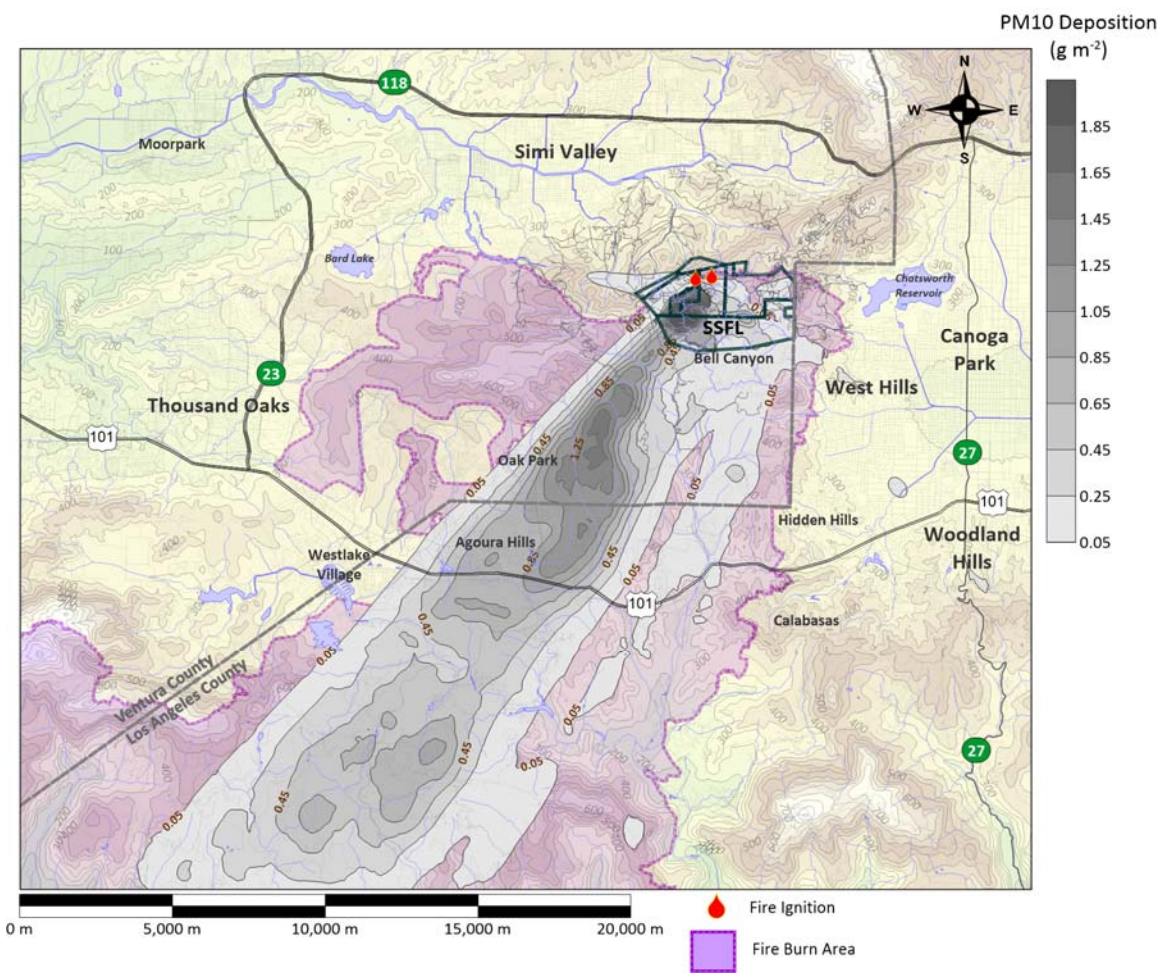

Figure 3-5. Isopleth map showing predicted total deposition of PM_{10} from Woolsey Fire burning on the SSFL from November 8 to November 11, 2018. Woolsey Fire outline is also shown.

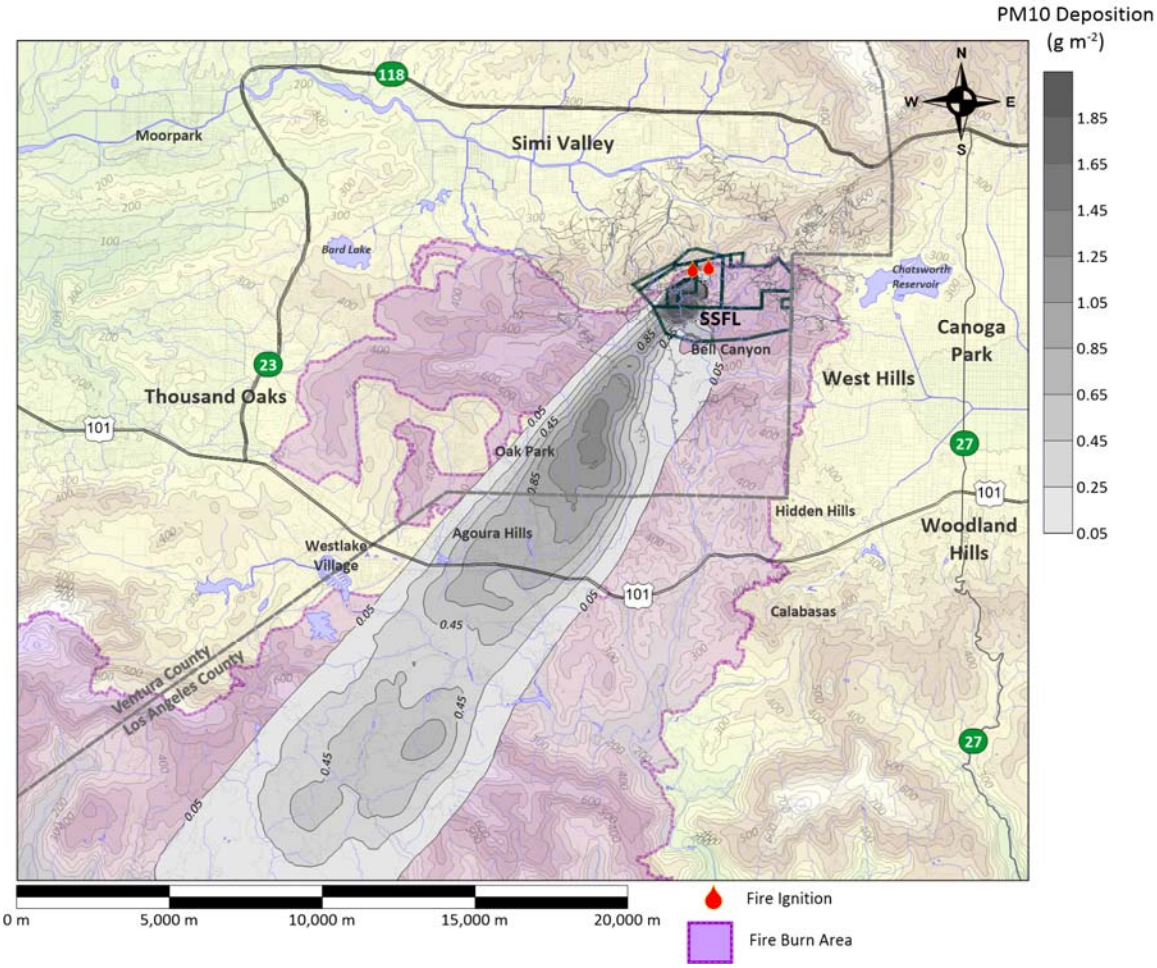

Figure 3-6. Isopleth map showing predicted total deposition of PM_{10} from Woolsey Fire burning on the SSFL on November 8. Woolsey Fire outline is also shown.

3.5.1. Potential Dose that Soil Sampling is Capable of Detecting

Calculations were performed to determine the dose an individual would receive if radionuclides of SSFL origin were detected above background concentrations in surface soil. These calculations are important because they demonstrate the sensitivity in terms of individual dose that the soil sampling program is capable of detecting. This was done by first calculating the amount of radionuclide deposition that would be required to give a particular annual effective dose to an individual residing in the community of Oak Park. Three annual effective doses were evaluated: 0.01 mrem, 0.1 mrem, and 1.0 mrem. The annual effective dose limit above background from human sources recommended by the International Commission on Radiological Protection (ICRP), National Council on Radiation Protection and Measurements (NCRP) and implemented in DOE-Order 458.1 (DOE 2011b) is 100 mrem. The annual effective dose of 0.01 mrem, 0.1 mrem, and 1.0 mrem are a factor of 10,000, 1,000, and 100 times lower than the dose limit, respectively, and much lower than the annual effective dose, on average, to persons in the U.S. from natural background which is about 310 mrem (NCRP 2009). Relevant exposure pathways that were considered for the period included inhalation of radionuclides in the smoke plume and external exposure from radionuclides deposited on soil. The deposition amounts corresponding to the annual

effective dose were then converted to a soil concentration in the surface layer and compared to radionuclide-specific background levels and minimum detectable concentrations (*MDC*) in soil. Details of the calculation are presented in Appendix E. The results showed that soil sampling would be sensitive enough to detect deposition of radionuclides above background for ^{137}Cs, ^{90}Sr, and ^{239}Pu equivalent to an annual effective dose of 0.1 mrem.

3.5.2. Comparison to DTSC Report

Shortly after the Woolsey Fire, the California Environmental Protection Agency (CalEPA) and Department of Toxic Substances Control (DTSC) produced an interim summary report evaluating impacts of the Woolsey Fire on surrounding communities (DTSC 2018). The report summarized sampling work done between November 8 and 30, 2018, to address community concerns about the possibility that the Woolsey Fire caused radionuclides and hazardous materials on-site to migrate into surrounding communities.

The report presented available soil/ash and air sampling data, mostly for hazardous materials, but also some radionuclide measurements and exposure rates. Appendix C of the report contained plots provided as part of the U.S. DOE Radiological Assistance Program and approved by the DOE Federal Radiological Monitoring and Assessment Center (FRMAC).

Based on different lines of evidence including modeling and measurements, the DTSC concluded that no radiation or hazardous materials from the SSFL were detected in communities following the Woolsey Fire.

3.5.3. Summary of Findings Based on Atmospheric Release and Transport Modeling

This section presented a model simulation of particulate matter ($PM_{2.5}$ and PM_{10}) generated from the Woolsey Fire burning on the SSFL and extended that simulation for radionuclides that might have been present on vegetation and in the soil. Predicted air concentrations of particulate matter were compared to measurements, and the average concentrations predicted during the fire were less than a factor of 1.7 different than the corresponding measured values. This is good agreement for such modeling. Scoping calculations were used to assess the likelihood of detecting releases from the SSFL in the soil. Based on the dispersion and deposition factors calculated for the Oak Park community located about 6 km southwest of SSFL, soil sampling data quality objectives would be sufficient to detect radionuclides released from the fire that would have resulted in a dose to a person living in the area of 0.1 mrem (one-thousand times less than the annual dose limit to the public).

4. Environmental Monitoring Data

Measurements of radionuclides in the environment before, during, and following the fire are an important aspect of understanding and quantifying potential impacts from the Woolsey Fire. It is well understood that all wildfires, even in the absence of anthropogenic contamination, release and mobilize radionuclides and other chemicals to the environment (Nance et al. 1993; Lambert et al. 1991; and Le Cloarec et al. 1995). The available air and soil data related to samples collected in the vicinity of the SSFL are described and evaluated in the following sections to investigate the potential for significant impacts at off-site locations.

4.1. SSFL Environmental Monitoring Program and Available Data

Routine environmental monitoring has been carried out at the SSFL since 1956 and has included analysis of air, vegetation, soil, surface water, and groundwater samples (AI 1960). Results of the environmental monitoring program have been reported in the annual site environmental reports (ASERs)[5] (e.g., Boeing [2001]). Both Rocketdyne (SSFL 1996) and the EPA (HydroGeologic 2011) have collected samples and conducted analyses as part of site area and background level characterizations.

In April 2018, a baseline air monitoring program was developed at the SSFL to evaluate baseline conditions and provide a basis for evaluating any impacts from on-site remediation activities at the SSFL (NASA/Boeing/DOE 2017). Included in the program was monitoring for particulate matter, volatile organic compounds, and radionuclides. Data resulting from the baseline air monitoring program for samples collected before, during, and after the fire were obtained from DOE (North Wind 2019a, 2019b), NASA (2019), and Boeing (Rutherford 2019; Boeing 2018).

Figure 4-1 shows the locations of the Boeing, DOE, and NASA air samplers at SSFL along with the approximate area impacted by the Woolsey Fire. To characterize background concentrations of natural and anthropogenic radionuclides in soil from geological formations that underlie the SSFL, the EPA used the Bridal Peak, Lang Ranch, and Rocky Peak locations shown in Figure 4-1 (HydroGeologic 2011).

[5] https://www.etec.energy.gov/Environmental_and_Health/ASER.php.

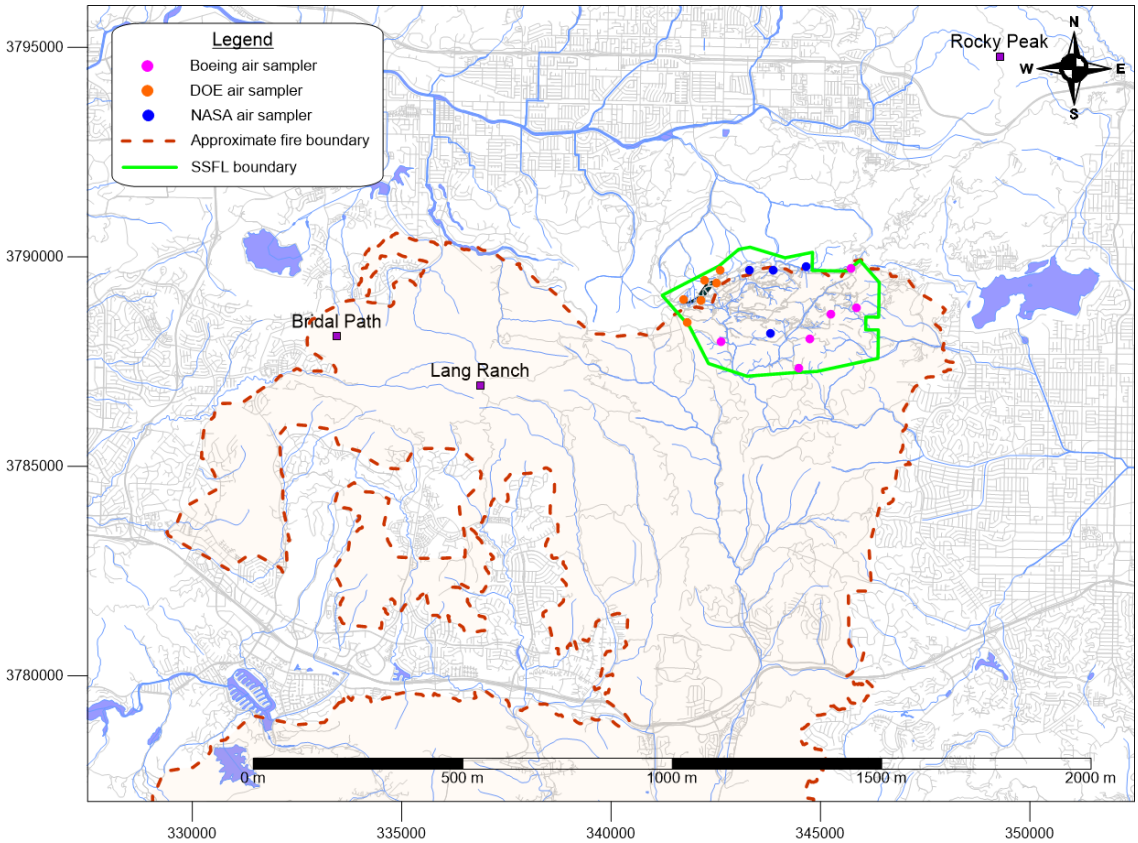

Figure 4-1. Map showing locations of baseline air samplers at the SSFL along with the area burned by the fire.

Radionuclide monitoring was established for a subset of the samplers, including the DOE samplers in Area IV and two Boeing samplers near the Area I Burn Pit that was used to burn materials no longer needed in the operations (samplers 4 and 5). Samples are analyzed according to the procedures described by NASA/Boeing/DOE (2017). After a minimum 120-hour holding time to allow the decay of short-lived radon and thoron daughters, the samples are simultaneously counted for gross alpha and beta activity with a low-background, thin-window, gas-flow proportional-counting system continually purged with P-10 argon/methane counting gas over a preset time interval. Individual filters are typically composited for quarterly isotopic analysis, and specific radionuclides are measured by gamma spectroscopy (^{7}Be, ^{40}K, ^{54}Mn, ^{60}Co, ^{137}Cs), gas flow proportional counting (^{90}Sr, ^{228}Ra), alpha spectroscopy (^{210}Po, ^{228}Th, ^{230}Th, ^{232}Th, ^{234}U, ^{235}U, ^{238}U, ^{238}Pu, $^{239/240}$Pu, ^{241}Am), and liquid scintillation techniques (^{241}Pu, ^{226}Ra) (NASA/Boeing/DOE 2017).

Figure 4-2 shows the locations of each of the air samplers, with the DOE samplers positioned within Area IV in the northwest of the SSFL site, the Boeing samplers positioned along the east and south of the site, and the NASA samplers along the north of the site with an additional NASA sampler near the Area I Burn Pit.

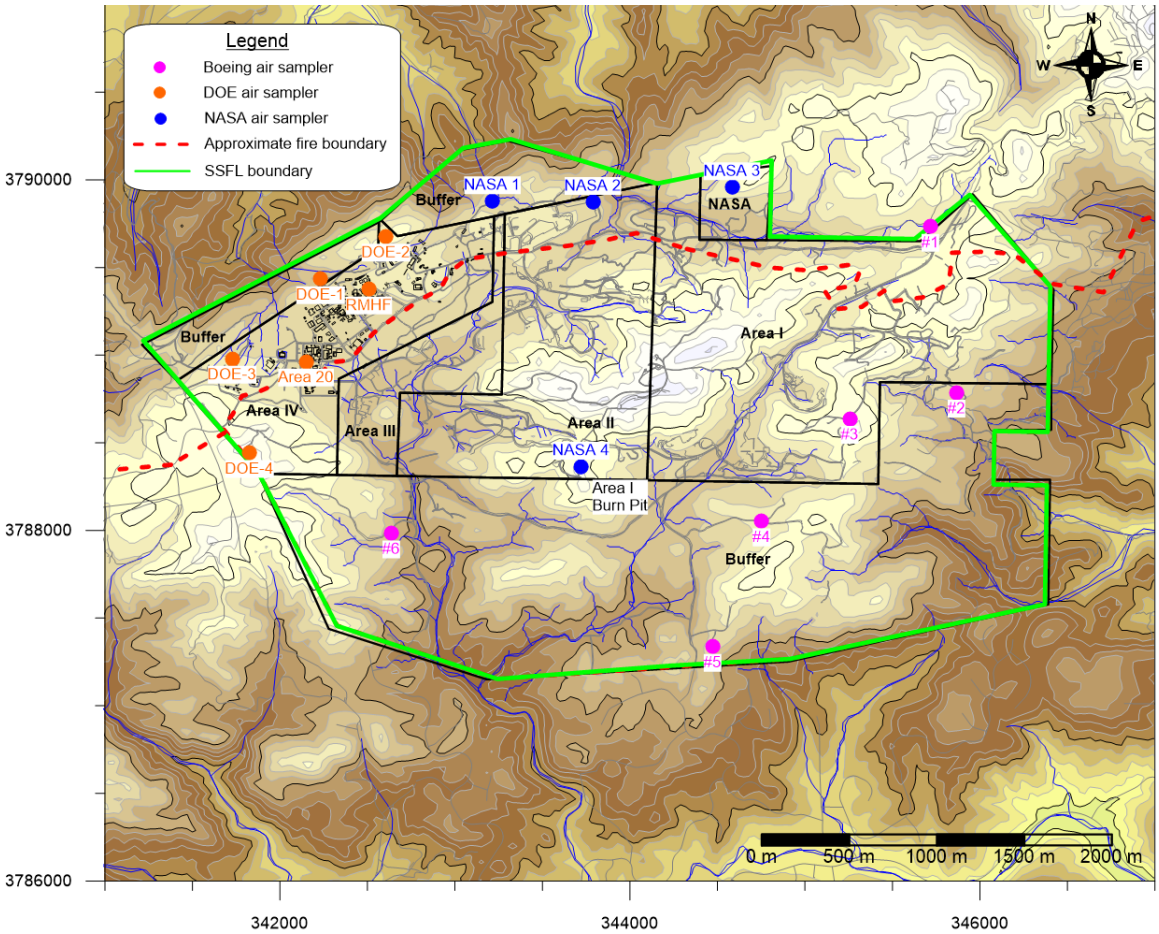

Figure 4-2. Detailed map showing locations of Boeing, DOE, and NASA air samplers at SSFL.

The Boeing samplers 4 and 5 collect airborne particles on glass fiber (Type A/E) filters that are changed approximately twice a week and counted for gross alpha and beta activity. Both air monitors were operational during the Woolsey Fire. All six Boeing samplers measured PM_{10}, and measurements for $PM_{2.5}$ were made at samplers 1 and 4.

The DOE samplers 1 through 4 employed the same sampling and measurement protocol as described for the Boeing samplers. North Wind, Inc., operates the samplers for DOE. All four DOE samplers were operational during the Woolsey Fire. Damage to the electrical connections at sampler 4 caused it to be turned off on November 12 at 10:31 am (North Wind 2019a). The blower on sampler 1 failed due to heavy rain on December 17, and the sampler at station 4 was moved to station 1 on that same day. Samplers 1 through 3 were generally operational through the end of the year, but samplers 1 and 2 were shut off multiple times for a few hours because of heavy rain (North Wind 2019a).

Samples are also collected at two additional DOE samplers within the ETEC site, which encompasses most of the DOE facilities within Area IV. These two samplers (Area 20 and RMHF) are operated continuously with samples collected weekly on glass fiber filters. Both samplers were operational during the fire but did not operate after the fire because electric line power was lost. These two samplers operated sporadically through the end of 2018 using battery and generator power (North Wind 2019a).

The individual samples collected at the two Boeing stations and the six DOE stations during the fire were sent for isotopic analysis in addition to the routine gross alpha and gross beta analyses that were done.

4.2. Background Concentrations

An integral part of any thorough environmental data evaluation is understanding and quantifying radionuclide concentrations that would be present if the site or facility did not exist. This is referred to as background and is associated with naturally occurring decay chains, long-lived materials in the earth's crust, cosmogenic materials (e.g., uranium and thorium decay chain nuclides, ^{7}Be, ^{40}K and other singly occurring radionuclides whose half-lives are long relative to the age of the earth) and anthropogenic radionuclides deposited world-wide as part of atmospheric weapons tests. Background concentrations vary spatially. The geology of an area affects the levels of many naturally occurring radionuclides. Concentrations that are significantly greater than background may indicate contributions from sources other than naturally occurring materials or atmospheric weapons testing fallout.

Background levels are typically established by measuring concentrations in environmental samples collected from locations that would not be affected by site operations (e.g., at sufficient distances and/or in upwind directions) and that are representative (i.e., same geologic materials since different rock types may exhibit different background levels) of the site environment, or in samples collected prior to the start of site operations. Background levels can then be compared to measurements at various locations around a facility to identify instances where measurements exhibit impact from the facility. A general description of background radionuclides found in soils is discussed first followed by background radionuclide concentrations in air and soil in the vicinity of SSFL.

4.2.1. Radionuclides Found in the Environment from Natural and Anthropogenic Sources

All soils contain naturally occurring radionuclides of primordial and cosmogenic origin. Primordial radionuclides originated during formation of the solar system four billion years ago. These radionuclides are long-lived and include the ^{238}U (Figure 4-3), ^{232}Th (Figure 4-4), and ^{235}U (Figure 4-5) decay chains in addition to ^{40}K and other singly occurring radionuclides whose half-lives are long relative to the age of the earth. Plutonium-239 (which decays to ^{235}U) and ^{237}Np (Figure 4-6) were also formed during the solar system's formation, but their half-lives are relatively short compared to the age of the earth so they have decayed. Natural occurrence of ^{239}Pu and ^{237}Np has been observed in regions of high uranium concentrations and in natural nuclear reactors such as at Oklo in the central African state of Gabon (Choppin and Rydberg 1983) but these occurrences are not ubiquitous.

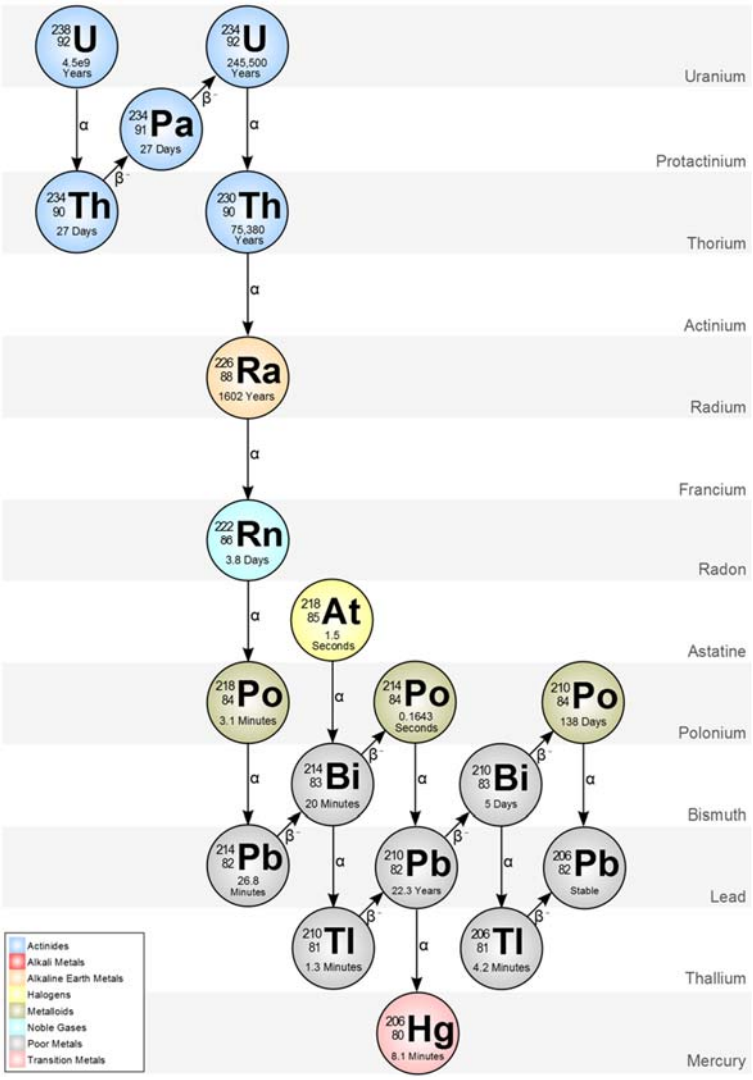

Figure 4-3. Uranium-238 decay scheme showing short-lived progeny that will be present alongside the parent. Uranium-238 and its progeny are naturally occurring radionuclides and present in most soils and rocks (from http://metadata.berkeley.edu/nuclear-forensics/Decay%20Chains.html).

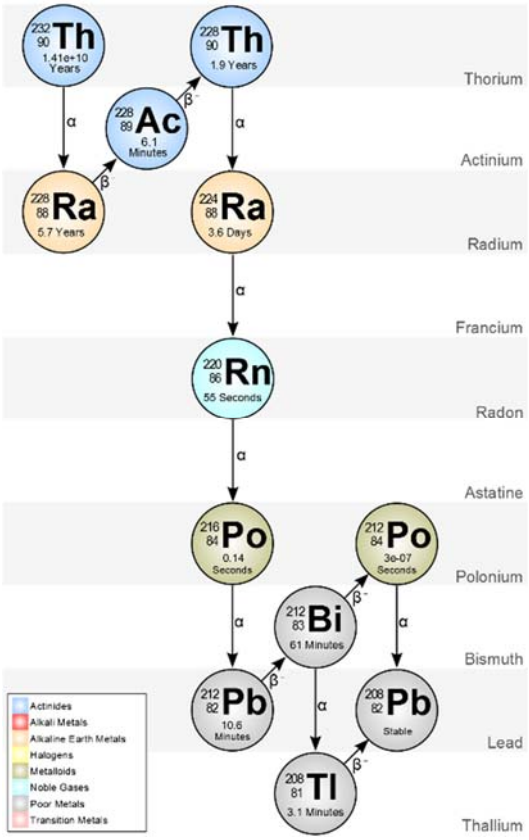

Figure 4-4. Thorium-232 decay series showing short-lived progeny that will be present alongside the parent. Thorium-232 and its progeny are naturally occurring radionuclides and present in most soils and rocks (from http://metadata.berkeley.edu/nuclear-forensics/Decay%20Chains.html).

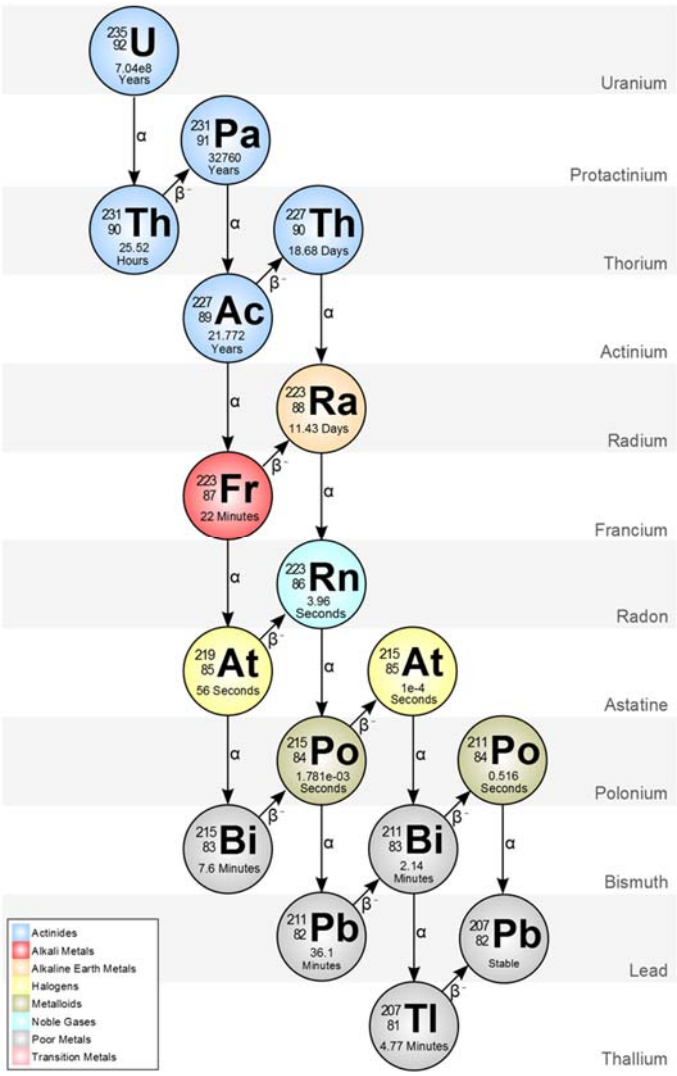

Figure 4-5. Uranium-235 decay series showing short-lived progeny that will be present alongside the parent. Uranium-235 and its progeny are naturally occurring radionuclides and present in most soils and rocks (from http://metadata.berkeley.edu/nuclear-forensics/Decay%20Chains.html).

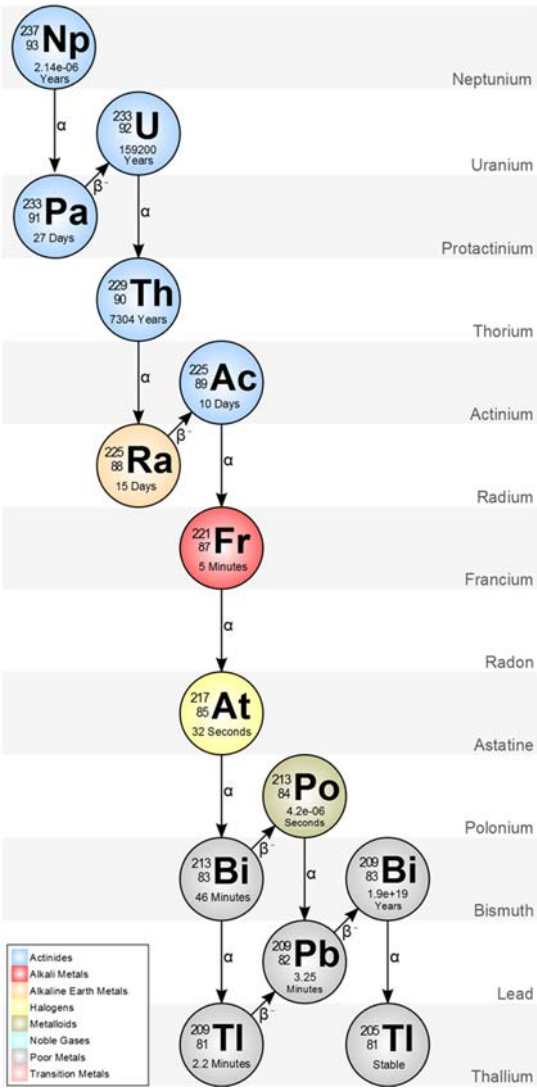

Figure 4-6. Neptunium-237 decay series showing short-lived progeny that will be present alongside the parent. Neptunium-237 and its progeny are radionuclides primarily derived from nuclear weapons fallout (from http://metadata.berkeley.edu/nuclear-forensics/Decay%20Chains.html).

Cosmogenic radionuclides are derived from reactions of cosmic radiation interacting with atoms in the atmosphere. Cosmogenic radionuclides include ^{14}C, ^{3}H, ^{7}Be, ^{10}Be, ^{22}Na, ^{26}Al, ^{35}S, ^{36}Cl, and ^{39}Cl (Choppin and Rydberg 1983) and many of these, such as ^{14}C, are found in equilibrium in the biosphere in more or less constant concentrations.

Global fallout from above-ground nuclear weapons testing resulted in deposition on surface soil of actinides including ^{237}Np, ^{238}Pu, $^{239/240}Pu$, ^{241}Pu, and ^{241}Am, and fission and activation products including ^{55}Fe, ^{90}Sr and ^{137}Cs (Efurd et al. 1982). Concentrations of fallout radionuclides are spatially variable and depend on the location latitude and altitude, proximity of aboveground tests, prevailing winds, precipitation patterns when these materials were airborne, soil chemistry, and erosion and other physical processes. Peak fallout from weapons testing occurred at latitudes between 40 and 50 degrees in both hemispheres and was greater in the northern hemisphere

(Whicker and Shultz 1982). Production of ^{90}Sr, ^{137}Cs, and ^{55}Fe per megaton of fission is approximately 0.1, 0.16, and 1.7×10^{7} MCi (Whicker and Shultz 1982). Iron-55 has a much shorter half-life (2.9 years) and thus most of it would have decayed, whereas ^{90}Sr and ^{137}Cs have longer half-lives (28.8 and 30.17 years, respectively) and are still observed in detectable quantities in present-day soil. Cesium has a high soil-water partition coefficient and consequently is relatively immobile in soil, whereas ^{90}Sr is much more mobile and tends to leach from surface soils over the ~55 years that have elapsed since global atmospheric weapons testing fallout. Because of its relative immobility in soil and its large global fallout inventory, ^{137}Cs can readily be detected in surface soil today. In soil undisturbed since weapons testing fallout, ^{137}Cs concentrations are highest in the surface layer and decrease with depth. Thus, a ^{137}Cs depth profile where the highest concentrations are not near the surface would indicate the soil has been disturbed since weapons fallout.

Plutonium isotopes from nuclear weapons testing fallout and nuclear accidents can also be detected in soils. During 1992 – 1994, Ibrahim et al. (1997) measured $^{239/240}Pu$ in soil near the Rocky Flats Plant in Colorado, northwest of Denver. Plutonium that was attributed to global fallout (i.e., not of Rocky Flats origin) was determined from isotopic ratios of $^{239}Pu/^{240}Pu$. In the 0–3 cm undisturbed surface soil layer, the $^{239/240}Pu$ concentration from global fallout was 0.054 pCi g^{-1} and 50% of the total $^{239/240}Pu$ soil inventory resided in the surface (0–3 cm) layer. Piekarz and Komosa (2014) reported ratios of $^{241}Pu/^{239}Pu$ in 0–5 cm soil from weapons testing was 4.6 in 1986. Accounting for decay of ^{241}Pu (14.35-year half-life) to the present results in a current ratio of about 0.93.

The April 1986 Chernobyl accident and the partial meltdown of the Fukushima-Daichi nuclear reactors and spent fuel in March 2011 emitted actinides and fission and activation products to the air that were later deposited onto surface soil. Immediately after the 1986 Chernobyl accident in Ukraine, the $^{241}Pu/^{239}Pu$ ratio was as high as 94.8 in the 0–5 cm layer but varied widely (Piekarz and Komosa 2014). In deeper layers, the ratio was much smaller, indicating the deeper layers reflect fallout from weapons testing while the surface layer reflects recent deposits. Ratios of $^{238}Pu/^{239}Pu$ after the Chernobyl accident were 0.42 and 0.13 in the 0–5 cm and 5–10 cm layers, respectively. Fallout from Chernobyl was limited mainly to eastern and northern Europe. Small amounts of ^{131}I and ^{137}Cs (<1% of weapons fallout) were detected in New York City (Feely et al. 1988) indicating appreciable quantities were not likely to have reached the western United States.

Following the Fukushima accident, the maximum estimated ^{241}Pu soil concentration in the 0–5 cm layer in Japan was 0.11 pCi g^{-1} (Yang et al. 2015)[6]. Concentrations measured by Zheng et al. (2012) in Japan after the Fukushima accident for ^{241}Pu and ^{239}Pu were 0.94 pCi g^{-1} and 0.0089 pCi g^{-1}, respectively in surface litter. In the 0–2 cm surface soil Zheng et al. (2012) measured 0.12 pCi g^{-1} and 0.0016 pCi g^{-1} for ^{241}Pu and ^{239}Pu, respectively. Cesium-137 activity in the same samples was 38,270 pCi g^{-1} in the surface litter and 310 pCi g^{-1} in the surface soil. Iodine-131 and ^{137}Cs were detected in wet deposition in the western United States following the Fukushima accident (Wetherbee et al. 2012). At a location ~85 km east of SSFL in the San Gabriel Mountains ^{134}Cs and ^{137}Cs wet deposition amounts were 1,270 pCi m^{-2} and 6,486 pCi m^{-2}, respectively (Wetherbee et al. 2011, 2012)[7]. It is therefore unlikely that the Fukushima accident contributed significantly to the

[6] Calculated from 240 Bq m^{-2} and assuming a bulk density in the 0–5 cm layer of 1.2 g cm^{-3}.

[7] These deposition amounts would equate to 0.035 pCi/g for ^{134}Cs and 0.18 pCi/g for ^{137}Cs assuming a 3 cm surface soil layer and a bulk density of 1.2 g cm^{-3}.

plutonium activity present in the surface soils in Southern California, but possibly had some minor contribution to the ^{134}Cs and ^{137}Cs surface soil inventory.

4.2.2. Measured Background Radionuclides in Air on the SSFL

Background concentrations of radionuclides and particulates in air were estimated using available data for samples collected before the Woolsey Fire. The pre-fire data obtained from DOE (North Wind 2019a, 2019b), NASA (2019), and Boeing (Rutherford 2019; Boeing 2018) included gross alpha, gross beta, and PM_{10} measurements (Table 4-1). Because of the relatively low environmental concentrations that were measured and the natural fluctuation in the instrument background, some concentrations are reported as negative. To avoid confusion and misleading values and because observations of negative concentrations in the environment are not feasible, the statistics shown in Table 4-1 are computed after substituting a value of 0 for all negative results (NRC 2010). The 5th and 95th percentile values are assumed to represent the range of background concentrations that could be expected. Additional data related to air samples collected and analyzed before the fire would be required to estimate isotope-specific background concentrations in air.

Table 4.1. Background Concentrations in Air Based on Pre-Fire Data from Boeing, DOE, and NASA

Statistic[a]	Gross alpha (µCi mL^{-1})		Gross beta (µCi mL^{-1})		PM_{10} (µg m^{-3})		
	Boeing	DOE	Boeing	DOE	Boeing	NASA	DOE
Mean	1.3E-15	6.5E-15	3.6E-14	8.5E-14	21.7	17.8	18.1
Median	6.2E-16	6.0E-15	3.7E-14	5.7E-14	20.1	11.7	17.4
Min	0	0	0	0	3.3	2.3	3.9
Max	8.0E-15	2.1E-14	9.4E-14	3.3E-12	150.5	46.0	40.5
5th	0	0	6.1E-15	0	8.5	3.9	6.9
95th	4.2E-15	1.5E-14	6.4E-14	1.9E-13	38.8	39.8	32.8
n	121	252	121	252	1218	28	116

[a.] Statistics computed after substituting a value of 0 for all negative results.

Because elevated radionuclide concentrations in soil primarily exist in Area IV (see Section 4.3.3), the DOE samplers in that area are less suitable for establishing background levels than are the Boeing samplers, which are more than a mile southeast of Area IV and less likely to be impacted by any elevated concentrations that might exist on-site. Differences between background concentrations in the different areas (i.e., Area IV and the area around Boeing 4 and 5 stations) may also be attributed to geologic variations in baseline soil concentrations in each geologic area. For example, the Santa Susana formation appears to have generally higher soil concentrations for most of the naturally occurring radionuclides, including isotopes of radium, uranium, and thorium (HydroGeologic 2011). This in turn could lead to higher gross alpha concentrations in suspended soil collected by the air samplers in Area IV. Greater levels of mechanical disturbances that result in the suspension of dust (such as vehicle traffic) could also result in higher air concentrations. The presence of impact related to past SSFL operations in Area IV soil also may contribute to localized higher gross alpha concentrations in air, although detectable impact appears to be sporadic and confined to isolated time periods based on recent data reported in the site's Annual Site Environmental Reports (ASERs) (e.g., Boeing 2005, 2006, 2008; North Wind 2015, 2018).

The range (i.e., 5th and 95th percentile values) of PM_{10} background concentrations estimated using the Boeing data is similar to the range estimated using the NASA data as shown in Table 4-1.

4.2.3. Background Radionuclides in Soil on the SSFL

The EPA conducted a study to estimate the background concentrations of radionuclides on the SSFL (HydroGeologic 2011). Background included naturally occurring radionuclides and fallout radionuclides from weapons testing. The EPA developed background threshold values (BTVs) for the SSFL region based on samples collected in August, September, and November of 2009 and analyzed by Pace Analytical Services, Inc[8]. The maximum non-detect value was assumed as the BTV for radionuclides with fewer than five detections, and the 95% upper simultaneous limit (USL95) was used for the remaining radionuclides. The USL95 statistic represents the value such that all observations, not some proportion or percentile, from the established background data set will be less than or equal to USL95 with a confidence coefficient (CC) of 95% (HydroGeologic 2011).

Samples were collected from unimpacted radiological background reference areas (RBRAs) approximately 3 to 6 miles outside the SSFL property boundaries (see Figure 4-1). In addition, sampling at distance test locations (DTLs) was done, which confirmed that surface soils at the RBRAs had not been impacted by historical releases from SSFL. The RBRA sample locations were selected to represent the surface and subsurface soils overlying the two geologic formations present at the SSFL: the Chatsworth and Santa Susana formations. A single BTV was estimated for each radionuclide based on a combination of all the data from the different soil horizons and geologic formations that were sampled (Table 4.2). The soil horizon from 0 to 6 inches was used to characterize the surface soil background concentrations (HydroGeologic 2011). These background values were used to determine if there is evidence of impact on surface soil samples collected and analyzed as part of this work.

Soil sampling at Area IV identified radionuclides detected above the radionuclide reference concentration (RRC) as priority-1 radionuclides for cleanup activities (HydroGeologic 2012). The RRC is the maximum of either the BTV or the laboratory MDC plus 1.645 (e.g., 1-sigma) times the laboratory method uncertainty. These radionuclides are identified in Table 4.2. Radionuclides that were not identified as priority 1 had measured concentrations that were not significantly above background.

[8] Pace Analytical Services, Inc, 1800 Elm Street SE, Minneapolis, MN 55414.

Table 4.2. Radionuclide Background Threshold Values (BTV) and Radionuclides Identified as Priority-1 Radionuclides

Radionuclide	BTV (pCi g^{-1})	Radionuclide	BTV (pCi g^{-1})
Actinium-227	0.127	Plutonium-238	0.00425
Actinium-228[b]	2.3	Plutonium-239/240[b]	0.0142
Americium-241	0.0162	Plutonium-241	0.349
Americium-243	0.0134	Plutonium-242[a]	0.00246
Antimony-125	0.321	Plutonium-244	0.00156
Barium-137m[a]	0.183	Polonium-210[a]	2.09
Bismuth-212[b]	2.04	Potassium-40	30.5
Bismuth-214[b]	1.57	Promethium-147	4.96
Cadmium-113m[d]	2950	Protactinium-231	0.791
Carbon-14	2.54	Radium-226[c]	1.88
Cesium-134	0.03	Radium-228[a,c]	2.3
Cesium-137[b]	0.193	Radon-220[a]	2.27
Cobalt-60[b]	0.00556	Radon-222[a]	1.61
Curium-243/244	0.0147	Sodium-22	0.00787
Curium-245/246	0.0162	Strontium-90[b]	0.075
Curium-248	0.0234	Technetium-99	0.368
Europium-152[b]	0.0169	Tellurium-125m[a]	0.0761
Europium-154	0.0251	Thallium-208[b]	0.923
Europium-155	0.198	Thorium-228	3.67
Holmium-166m	0.0365	Thorium-229	0.0462
Iodine-129	2.08	Thorium-230[b]	2.04
Iron-55[a]	5.08	Thorium-231[a]	0.13
Lead-210[a]	2.07	Thorium-232[c]	2.95
Lead-212[b]	2.67	Thorium-234[b]	3.04
Lead-214[b]	1.68	Thulium-171	65.9
Neptunium-236	0.0314	Tin-126	0.0049
Neptunium-237	0.0109	Tritium (H-3) organic	7.38
Neptunium-239	0.0427	Uranium-232[a]	0.0565
Nickel-59[b]	0.344	Uranium-233/234[b]	1.87
Nickel-63	0.452	Uranium-235/236[b]	0.13
Niobium-94	0.0165	Uranium-238[b]	1.68
Plutonium-236	0.0184	Uranium-240[a]	0.00156

[a.] BTV taken from HydroGeologic (2011). All other BTVs taken from HydroGeologic (2012).
[b.] Priority-1 radionuclides as defined in HydroGeologic (2012).
[c.] Progeny of these parent radionuclides were defined as priority-1 radionuclides. The progeny does not exist in the environment without presence of the parent. Therefore, the parents were also defined as priority-1 radionuclides.
[d.] The BTV for Cd-113m is extremely high because this radionuclide emits a very low energy beta and very few gammas making it difficult to detect.

4.3. Data Analysis

The following sections discuss air concentration measurements of particulate matter and radionuclides and how they were used to help quantify and better understand the impacts of the fire, along with limitations associated with the data. The particulate matter measurements made during the fire were used to identify which stations were impacted by the fire to the greatest extent and when those impacts were highest. The gross alpha and beta measurements were used to evaluate the relative impact of the fire on radioactivity levels in the air by making comparisons to measurements before and after the fire. The isotope-specific measurements were used to determine whether radionuclides that could be attributed to SSFL site operations were present in the smoke and particulate matter created and suspended during the fire.

4.3.1. Particulate Matter in Air

Particulate matter samples were collected at the Boeing, NASA, and DOE stations. Figure 4-7 shows daily average PM_{10} concentrations measured at the six Boeing stations, along with the 5th and 95th percentile background values estimated using the pre-fire measurement data (Table 4-1). The data are consistent with our understanding of the fire progression, with Boeing station 6 being impacted first on November 8 and Boeing stations 2 through 5 being impacted on November 9. Much lower PM_{10} concentrations, but still somewhat above pre-fire levels, are seen through the duration of the Woolsey Fire on November 13. Boeing station 1, at the north end of the site, shows little, if any, impact from the Woolsey Fire.

Figure 4-8 shows daily average PM_{10} concentrations measured at the four NASA stations, along with the 5th and 95th percentile background values estimated using the pre-fire measurement data (Table 4-1). These data are consistent with the fire progression and with the Boeing PM_{10} data. The three NASA stations at the north edge of the site show minimal impact from the fire and station 4 to the south shows impact on November 9.

The $PM_{2.5}$ concentrations measured at the Boeing 1 and 4 stations and the NASA 2 station are consistent with the PM_{10} data. The greatest impact to $PM_{2.5}$ levels is at the Boeing 4 station on November 9, with a slight impact at the Boeing 1 and NASA 2 stations on November 10.

Figure 4-9 shows daily average PM_{10} concentrations measured at the four DOE stations, along with the 5th and 95th percentile background values estimated using the pre-fire measurement data (Table 4-1). As noted previously, the DOE-4 station went offline shortly after the fire started because of damage to the electrical connection (North Wind 2019a). There was significantly less impact to the PM_{10} concentrations at the three DOE operating samplers than to the most impacted Boeing and NASA samplers. This is not unexpected based on the location of the samplers relative to the Woolsey Fire boundary (Figure 4-2). The impact that is seen occurs on the first day of the Woolsey Fire (November 8) with little impact outside the range of expected background concentrations after that, which is consistent with our knowledge of the Woolsey Fire progression.

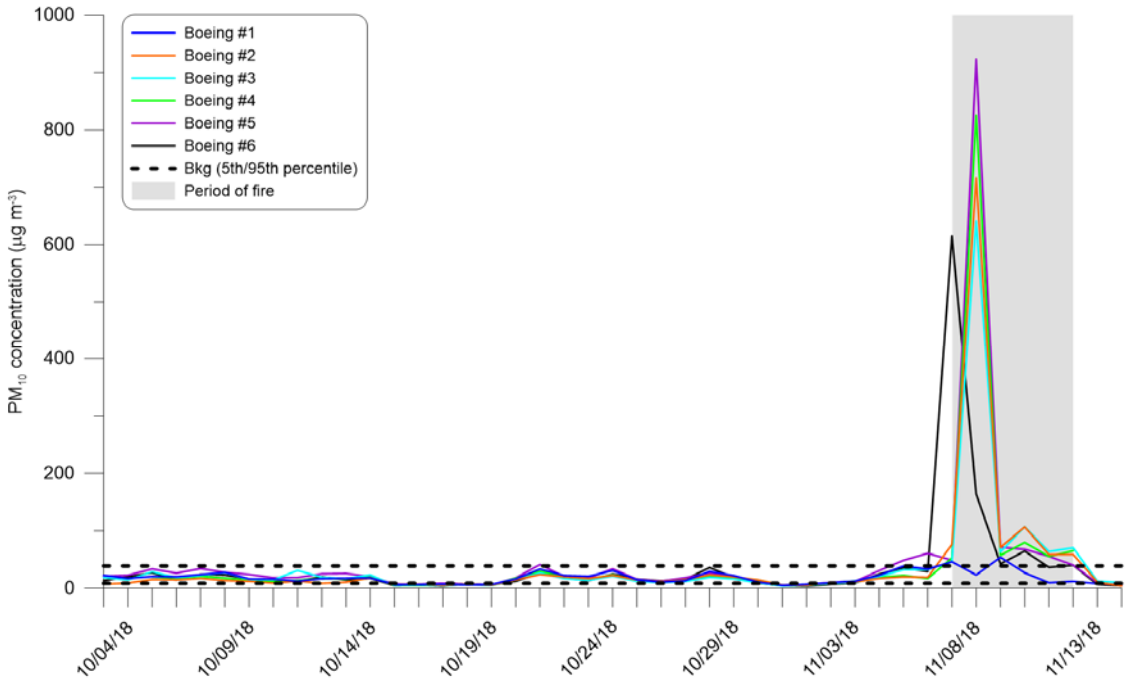

Figure 4-7. Time history of the daily average PM_{10} concentration measured at Boeing air sampling stations.

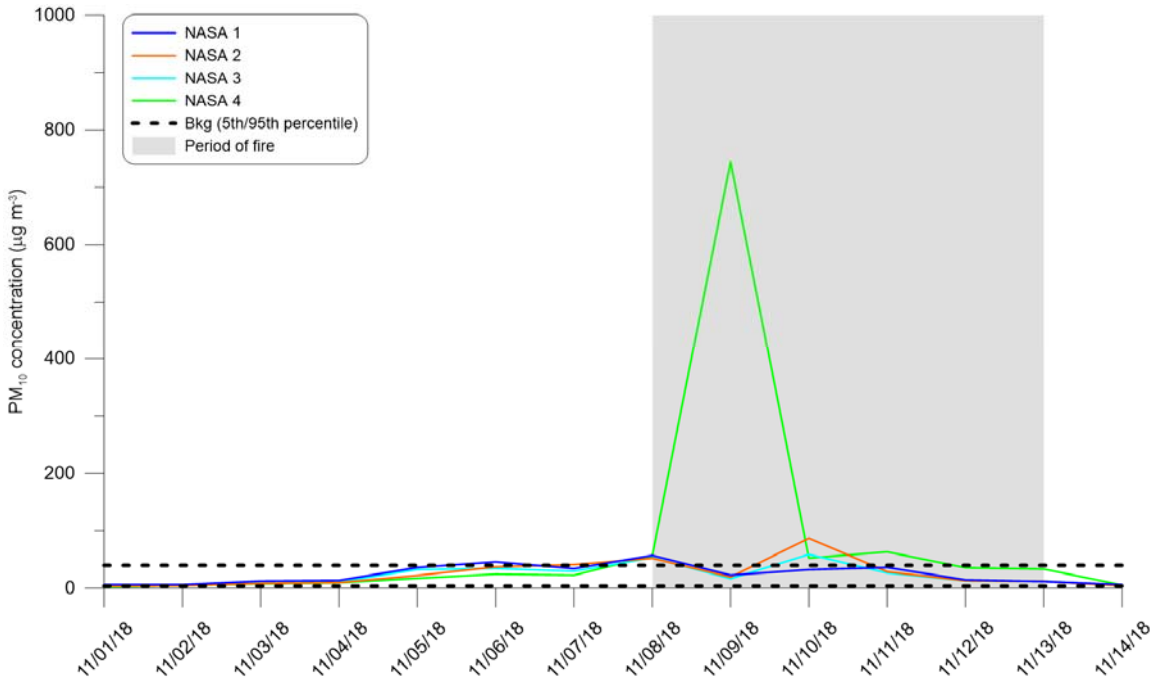

Figure 4-8. Time history of the daily average PM_{10} concentration measured at NASA air sampling stations.

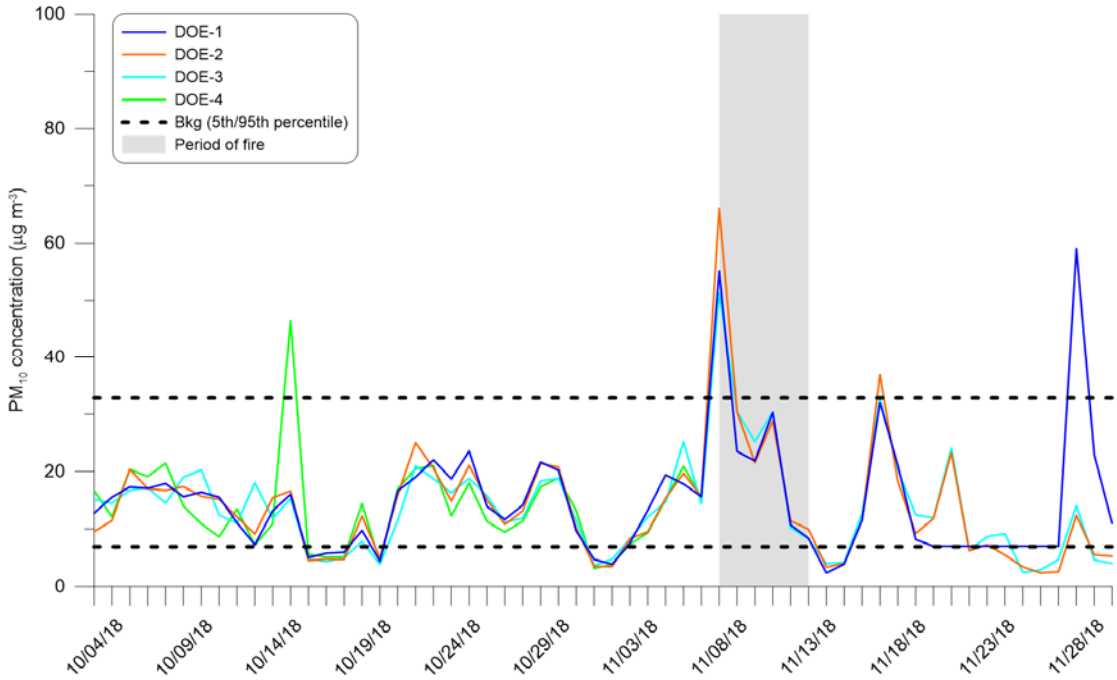

Figure 4-9. Time history of the daily average PM_{10} concentration measured at DOE air sampling stations.

4.3.2. Radionuclides in Air

Measurements of radionuclide concentrations in air before, during, and after the fire are used to determine whether there is evidence of any impact from the fire. These measurements also help to identify the potential source of any elevated concentrations, which would be expected to occur during any fire as a result of emission of naturally occurring radionuclides on vegetation and in the soil.

4.3.2.1. Gross Alpha and Gross Beta Measurements

Concentrations of gross alpha and gross beta in air were measured before, during, and after the Woolsey Fire by both Boeing and DOE. Figure 4-10 and Figure 4-11 show gross alpha concentrations in air measured by Boeing at stations 4 and 5, respectively, along with the 5th and 95th percentile background values estimated using the pre-fire measurement data (Table 4-1). Positive detections are identified as results greater than the detection limit and greater than the 2-sigma counting error for the Boeing data, and greater than the detection limit for DOE data since counter error information was unavailable. Positive detections occurred at both stations for the samples collected during the fire, as well as one additional sampling period in June 2018 at station 4. The concentration measured during the fire at station 4 is similar to that measured in June 2018 and to levels measured by DOE at the samplers in Area IV (North Wind 2015, 2018), indicating that the levels measured at station 4 during the fire were not significantly elevated above levels measured before the fire.

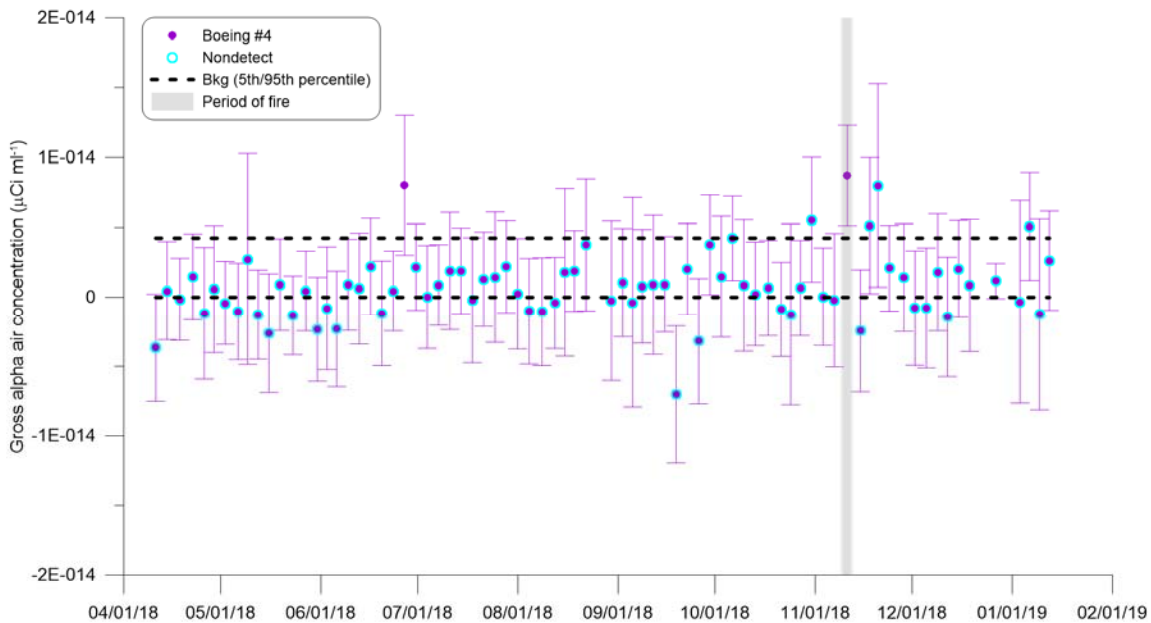

Figure 4-10. Gross alpha concentrations in air measured by Boeing at monitoring station 4. Error bars represent the 2-sigma analytical uncertainty for the measured concentration.

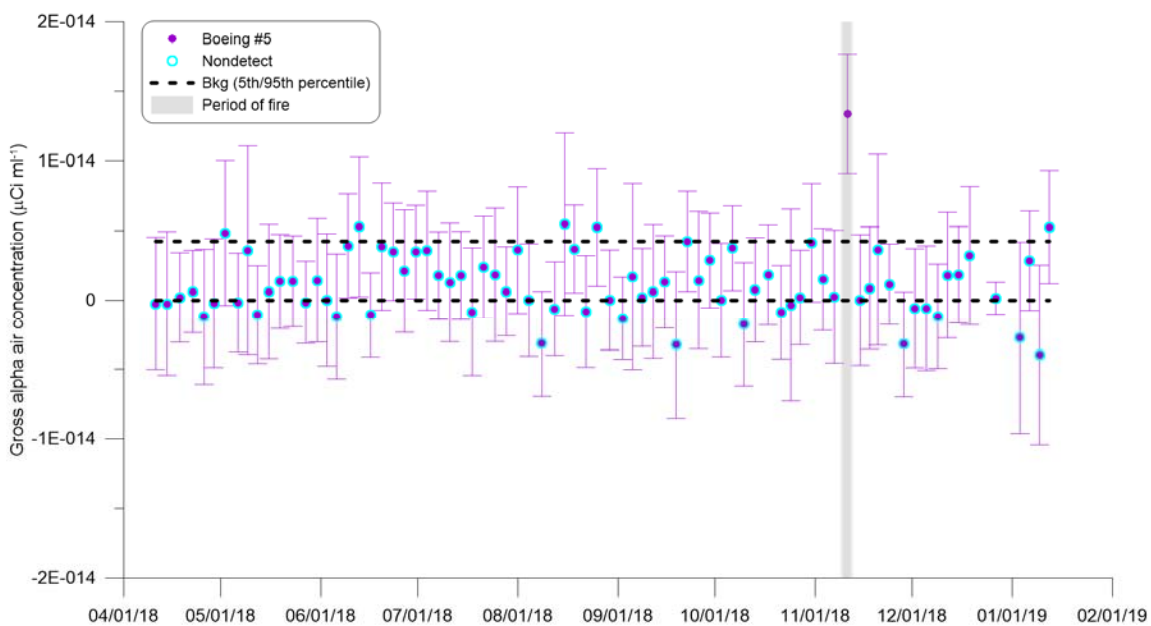

Figure 4-11. Gross alpha concentrations in air measured by Boeing at monitoring station 5. Error bars represent the 2-sigma analytical uncertainty for the measured concentration.

Figure 4-12 and Figure 4-13 show gross beta concentrations in air measured by Boeing at stations 4 and 5. Positive detections occurred at both stations during the fire, although higher concentrations were measured both before and following the fire, indicating little if any impact by the fire on gross beta concentrations.

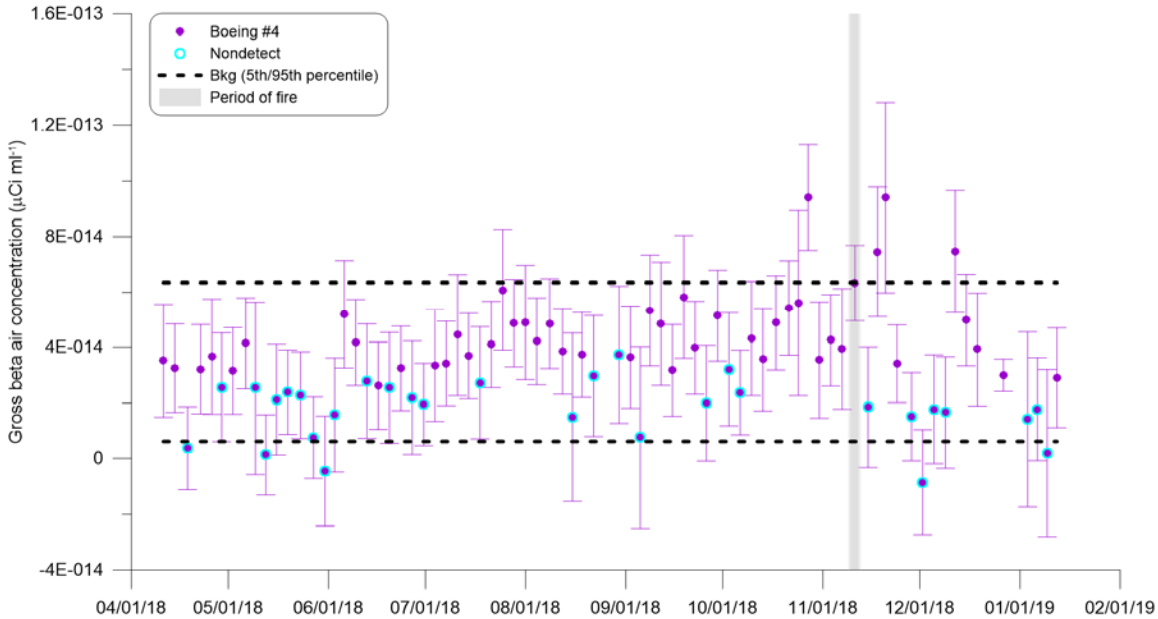

Figure 4-12. Gross beta concentrations in air measured by Boeing at monitoring station 4. Error bars represent the 2-sigma analytical uncertainty for the measured concentration.

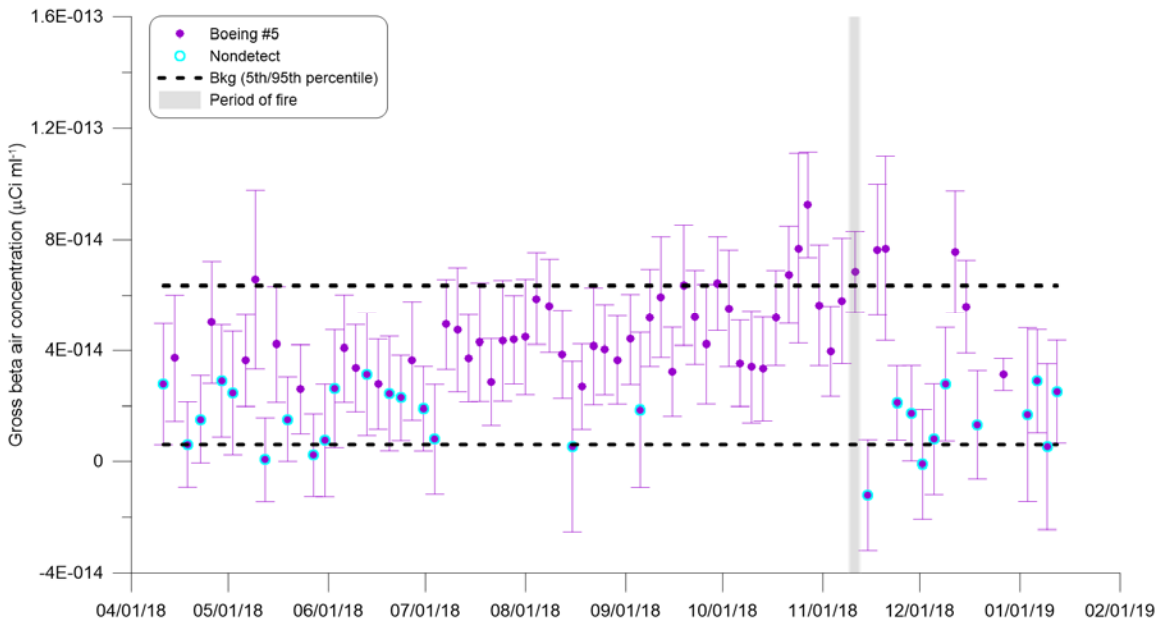

Figure 4-13. Gross beta concentrations in air measured by Boeing at monitoring station 5. Error bars represent the 2-sigma analytical uncertainty for the measured concentration.

Figure 4-14 shows gross alpha concentrations in air measured by DOE at the samplers maintained in Area IV. The samples collected during the fire all had concentrations less than the detection limit, although concentrations similar to those detected by Boeing at stations 4 and 5 had been detected at the DOE stations prior to the time of the fire.

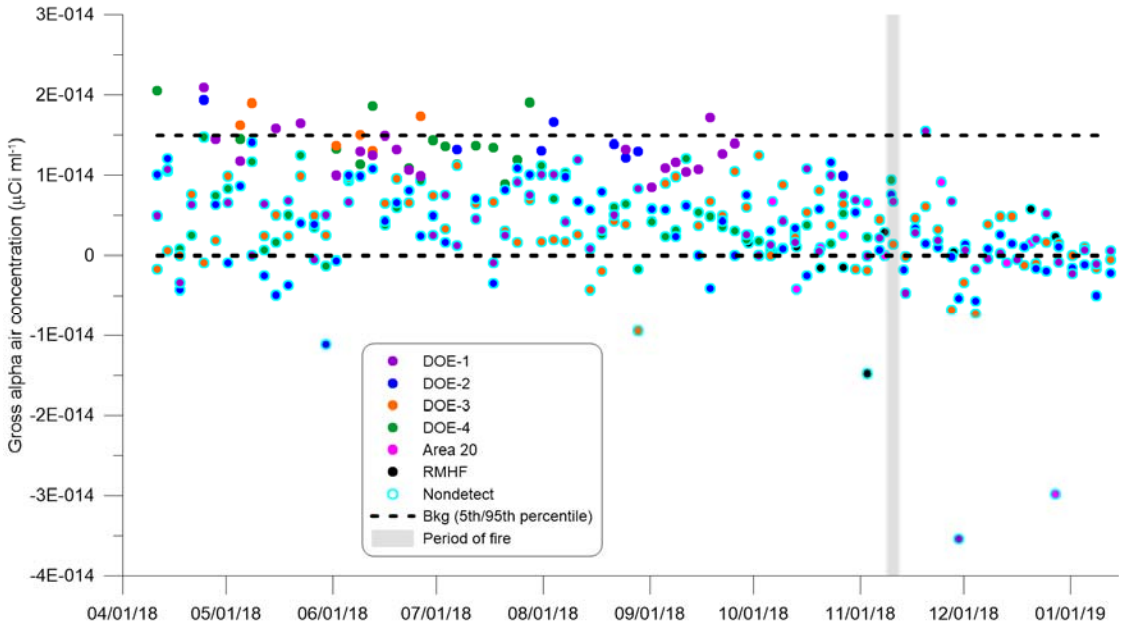

Figure 4-14. Gross alpha concentrations in air measured by DOE in Area IV. Analytical uncertainty was not provided with DOE sample results.

Figure 4-15 shows gross beta concentrations in air measured by DOE at the samplers maintained in Area IV. The sample collected during the fire at DOE-2 had a concentration greater than the detection limit, while the other samplers had concentrations less than the detection limit. Significantly greater gross beta concentrations were measured before the fire at the Area 20 and RMHF stations during the October 30 to November 7 sampling period and after the fire at the DOE-1 and DOE-2 stations during the November 19 to 21 sampling period.

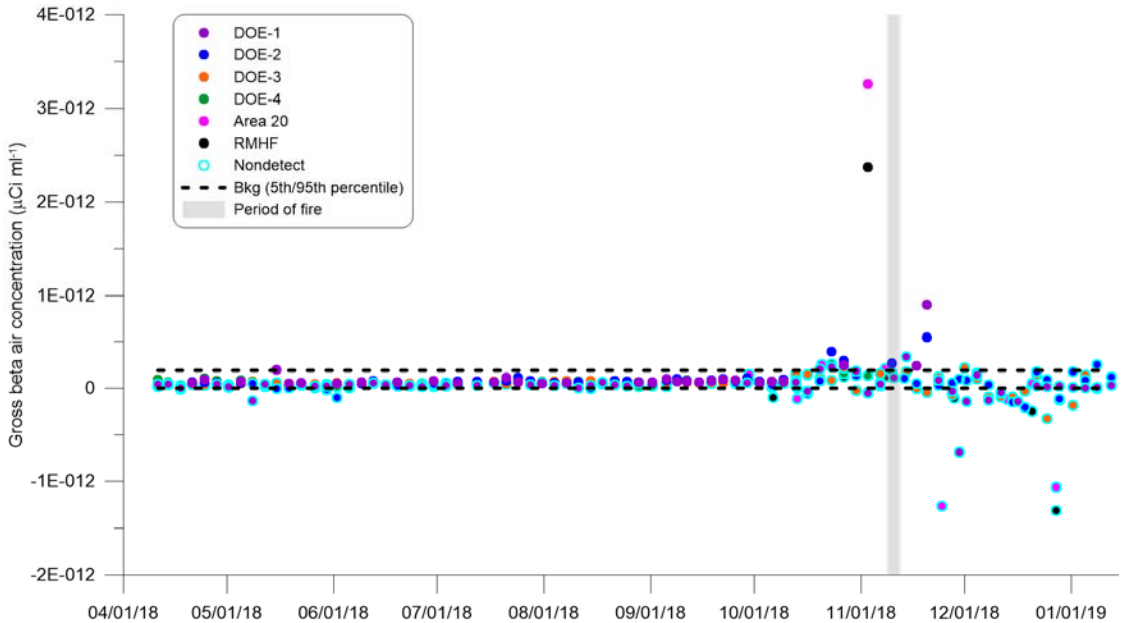

Figure 4-15. Gross beta concentrations in air measured by DOE in Area IV. Analytical uncertainty was not provided with DOE sample results.

The detected and slightly elevated gross alpha concentrations for some of the samples collected by Boeing during the fire are consistent with increases that would be expected during any wildfire (Nance et al. 1993; Lambert et al. 1991; and Le Cloarec et al. 1995). Gross alpha was not detected by the DOE samplers. The fire did not have a measurable impact on gross beta concentrations at any of the stations.

While it is not clear why higher gross beta concentrations were measured at some of the DOE stations before and following the fire, the concentrations are all less than 2 times the reported detection limit, which suggests less overall precision in the measurements in general. The analytical uncertainty was not provided with the DOE sample results, so it is not possible to analyze these elevated measurements in any more detail or investigate why gross alpha was not detected by the DOE samplers. Shorter than normal sample collection time and/or analytical count time could both lead to increased uncertainty associated with the measurements and impact the ability to detect the generally low concentrations that were present.

4.3.2.2. Radioisotopic Measurements

The samples collected by Boeing and DOE during the fire were submitted for isotopic analysis in addition to the gross alpha and beta measurements discussed above. Positive detections were seen for naturally occurring radionuclides ^{210}Po, ^{230}Th, and ^{232}Th at Boeing stations 4 and 5, which would be expected to be seen for air samples collected during any fire. No anthropogenic radionuclides attributable to SSFL site operations were detected at either station.

The samples from the DOE stations had positive detections for naturally occurring radionuclides ^{228}Ac, ^{228}Ra, ^{226}Ra, ^{230}Th, ^{234}U, ^{238}U, and ^{210}Po, which again would be expected to be detected in samples collected during a fire. There were also detections of ^{239}Pu and ^{90}Sr at the DOE-3 station and of ^{239}Pu at the Area 20 station, based on the analytical laboratory analysis report. Because ^{239}Pu and ^{90}Sr exist in Area IV soils, it is not surprising that concentrations of these nuclides would be detected in the air due to localized resuspension of soil from conditions and activities associated with the fire. Detections of both ^{239}Pu and ^{90}Sr have occurred in the past at Area IV samplers (e.g., Boeing 2005, 2006, 2008; North Wind 2015, 2018), which again is not unexpected due to the proximity of the samplers to soil with elevated concentrations and potential suspension of dust during high wind events.

Plutonium-239 and ^{90}Sr were both detected at Area IV samplers during the fire at concentrations equal to or less than a factor of 2 greater than the detection limit. The concentrations were also approximately an order of magnitude or more below the Derived Concentration Standard (DCS) (DOE 2011a) for both radionuclides (Table 4-3). The DCS is based on a 100 mrem dose and assumes continuous exposure for one year, so the dose from breathing air with these concentrations during the period of the fire would be significantly less than 1 mrem at that location on the SSFL based on the concentrations measured during the fire and the maximum possible exposure duration that could have occurred.

Table 4.3. Concentrations (µCi mL^{-1}) of ^{239}Pu and ^{90}Sr Measured in Air by DOE Samplers in Area IV

Station	Nuclide	Air concentration	Detection limit	Solubility class	DCS[a]	% of DCS
DOE-3	^{239}Pu	2.89E-15	2.43E-15	M	8.10E-14	3.6%
	^{90}Sr	3.43E-14	2.29E-14	M	1.00E-10	0.03%
Area 20	^{239}Pu	8.73E-15	8.73E-15	M	8.10E-14	10.8%

a. Source: DOE (2011a).

4.3.3. Radionuclides in Soil

Extensive soil sampling for radionuclides has been performed in areas of the SSFL with known contamination in soil. A summary of the historical soil sampling based on data from SSFL is in Table 4-4.

Table 4.4. Summary of Historical Detected Radionuclide Soil Concentrations Measured at the SSFL. Concentrations Include Natural Background and Weapons Fallout[a]

Radionuclide	Minimum (pCi g^{-1})	Maximum (pCi g^{-1})	Average (pCi g^{-1})	*n*
^{60}Co	0.0001	2.6	0.0268	253
^{137}Cs	0.0001	196	0.460	4142
^{152}Eu	0.0002	25.7	0.165	289
$^{239/240}$Pu	0.0002	2.1	0.0122	1299
^{226}Ra	0.19	18.8	1.27	701
^{228}Ra	0.54	2.87	1.24	218
^{90}Sr	0.008	28.1	0.425	1109
^{230}Th	0.07	6.4	0.918	3848
^{232}Th	0.063	3.7	1.17	4787
^{234}U	0.22	9.6	0.888	688
^{235}U	0.004	0.73	0.0618	811
^{238}U	0.09	8.6	0.869	5019

a. See Table 4-2 for the background concentrations estimated by EPA.

The soil data at SSFL were compared to the EPA BTVs for ^{239}Pu (Figure 4-16), ^{90}Sr (Figure 4-17) and ^{137}Cs (Figure 4-18) to examine the potential for impacts to off-site locations. Plutonium-239, ^{90}Sr, and ^{137}Cs were selected because of their occurrence at isolated locations in Area IV and because of the positive detections of ^{239}Pu and ^{90}Sr by Area IV air monitors during the Woolsey Fire. There is a limited area within Area IV where concentrations of ^{239}Pu, ^{90}Sr, and ^{137}Cs are above background.

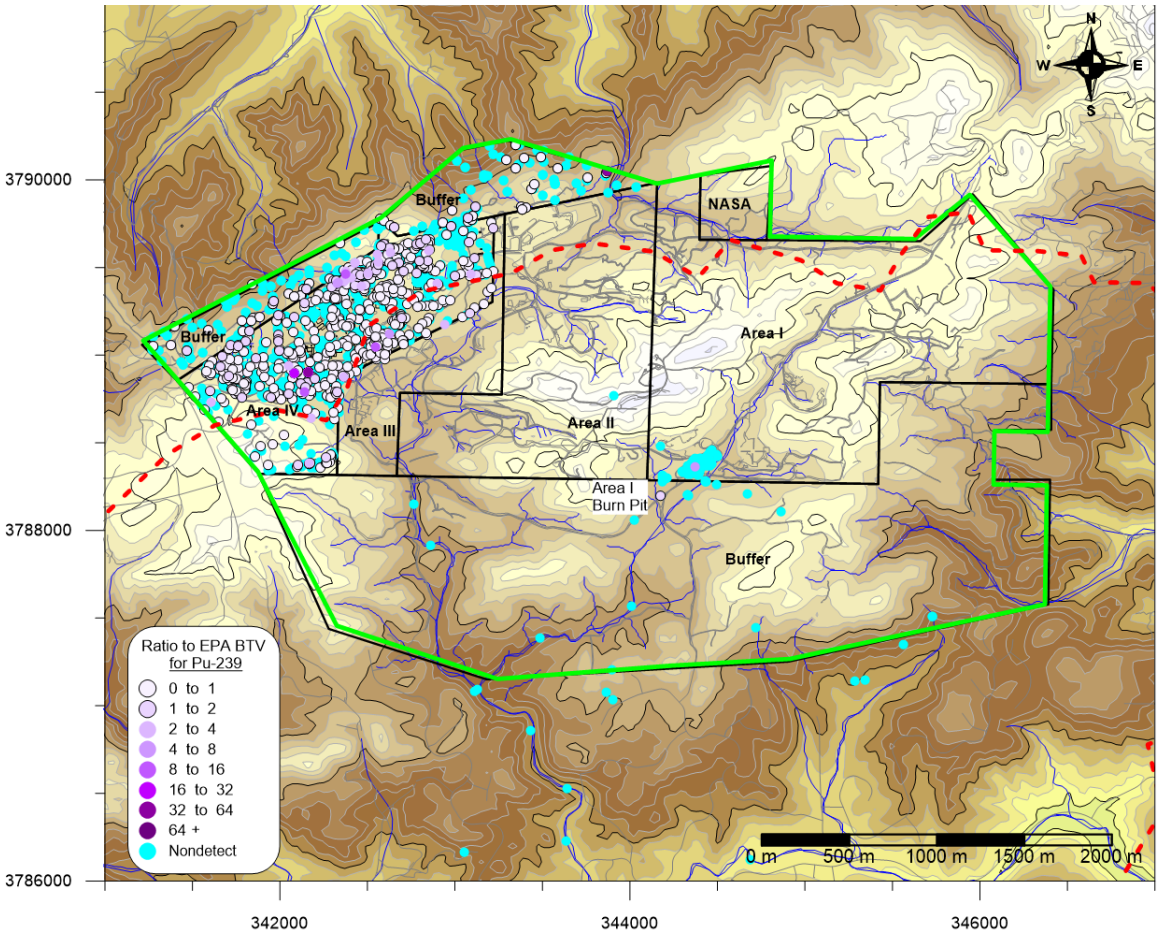

Figure 4-16. Plutonium-239 concentrations in soil compared to the EPA Background Threshold Value (BTV) (HydroGeologic 2011) of 0.0134 pCi g^{-1}. Red dotted line represents fire boundary.

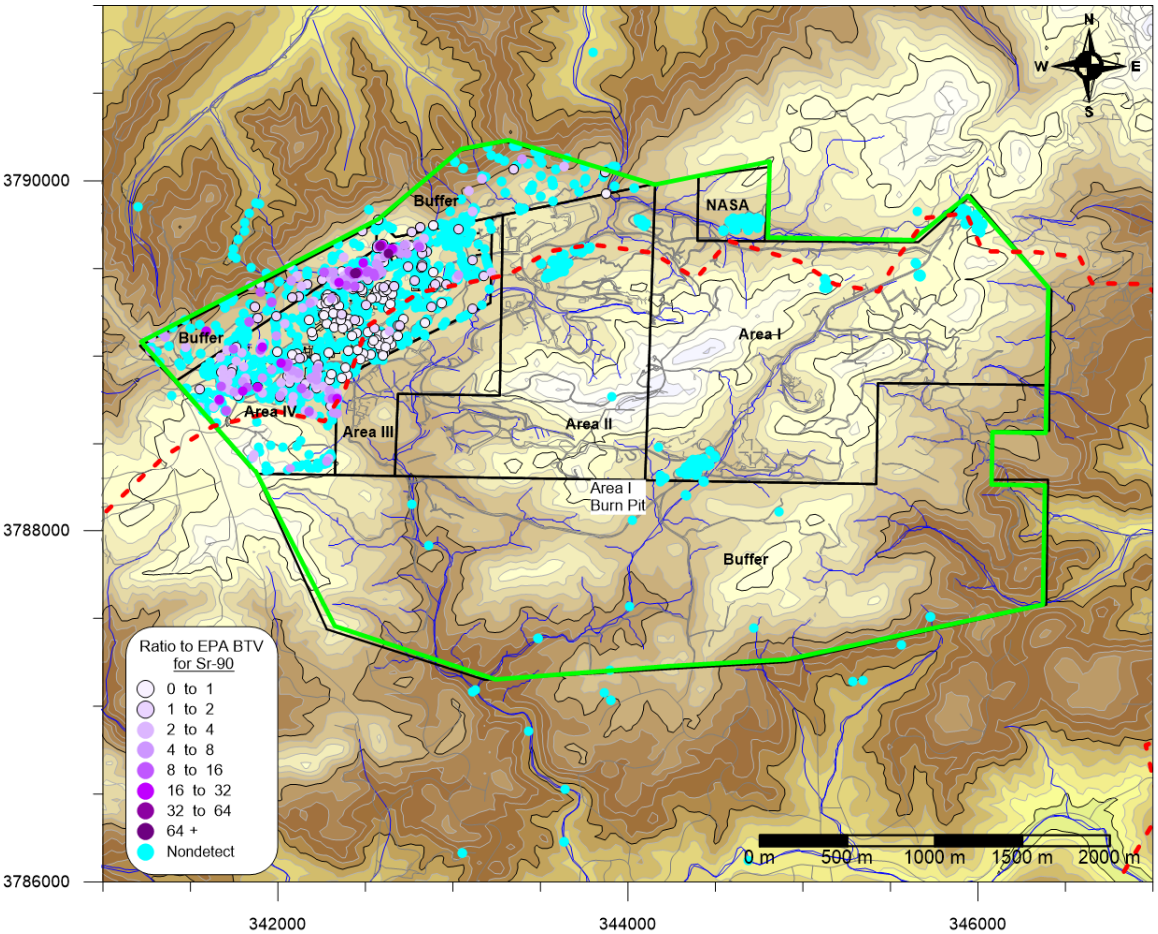

Figure 4-17. Strontium-90 concentrations in soil compared to the EPA Background Threshold Value (BTV) (HydroGeologic 2011) of 0.0735 pCi g^{-1}. Red dotted line represents fire boundary.

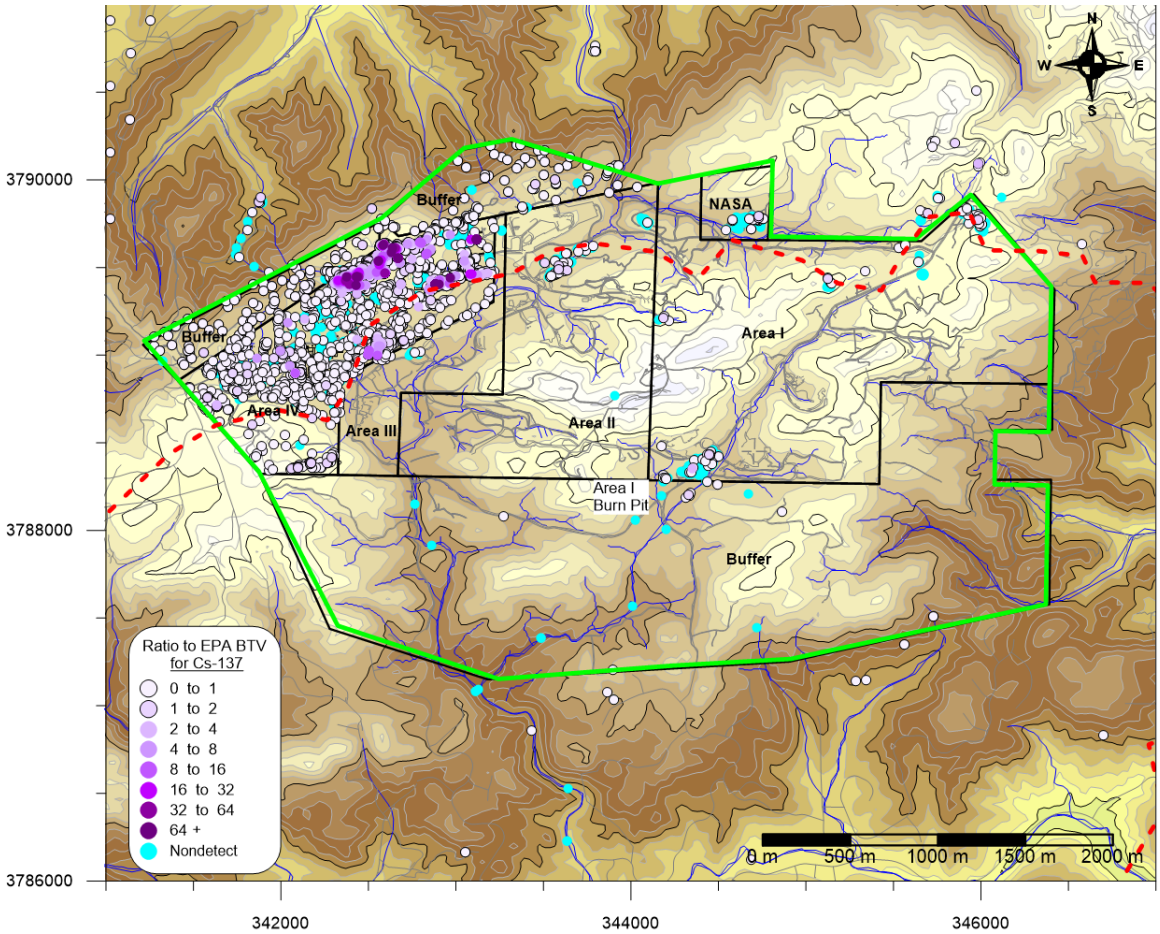

Figure 4-18. Cesium-137 concentrations in soil compared to the EPA Background Threshold Value (BTV) (HydroGeologic 2011) of 0.229 pCi g^{-1}. Red dotted line represents fire boundary.

A bounding estimate of the maximum potential radionuclide releases from the Woolsey Fire burning on the SSFL is to assume the entire radionuclide inventory in the surface soil, including background, was all released as particulates. The predicted hypothetical radionuclide concentration in 0–3 cm depth soil (C) from deposition in the Oak Park community (the region of highest off-site particulate matter deposition located about 6 km southwest of SSFL) is given by:

$$C = \frac{\left(C_{soil} \times \rho \times T \times A\right) \times \frac{\psi}{Q}}{\rho \times T} = C_{soil} A \times \frac{\psi}{Q} \tag{4-1}$$

where

C_{soil}	=	average soil concentration in Area IV of SSFL (pCi g^{-1})
ρ	=	bulk density (1.0×10^{-6} g m^{-3})
T	=	surface layer thickness (m)
ψ/Q	=	deposition factor (1.07×10^{-9} m^{-2}, see Appendix E, Equation E-1)
A	=	area of fire regions 1–5 (30,521,141 m^2).

The hypothetical concentration of ^{137}Cs, ^{90}Sr, ^{239}Pu, and ^{226}Ra in the 0–3 cm soil layer in the Oak Park community calculated using Equation 4-1 is either below the detection limit or is indistinguishable from background (Table 4-5). Equation 4-1 does not correct for background, and thus overestimates the actual SSFL-derived radionuclide inventory in soil. The results from applying Equation 4-1 demonstrate that the radionuclide inventory present on the SSFL is insufficient to produce a measurable impact in off-site soils.

A similar calculation can be made assuming the ^{137}Cs concentration in vegetation is at the MDC value of 0.046 pCi g^{-1} wet weight (see Section 4.3.4) with a total wet weight biomass of 19.5 tons per acre (4.26 kg m^{-2}) calculated from the fuel loads (see Section 2.1). The hypothetical inventory of ^{137}Cs that would be released assuming a concentration of 0.046 pCi g^{-1} wet weight in vegetation is 6.11×10^8 pCi, which is a factor of 345 less than the release inventory given in Table 4-5. The hypothetical deposition amounts based on vegetation sampling would also be a factor of 345 less than the values in Table 4-5. When it is assumed that the entire radionuclide inventory in soil at the SSFL (including both background and anthropogenic radionuclides), was released to the atmosphere during the Woolsey Fire, the maximum dose to an individual at Oak Park would be much less than 0.01 mrem (Appendix E presents calculation details). The annual dose limit for members of the public (DOE 2011b) is 10,000 times higher than a dose of 0.01 mrem. The soil sampling program described in Section 5 supports the conclusion that radiological impacts (doses) related to the Woolsey Fire burning on the SSFL are indistinguishable from background.

Table 4.5. Bounding Estimate of the Radionuclide Inventory in the 0–3 cm Layer on the SSFL, Predicted Deposition and Soil Concentration at Oak Park, and Comparison to Background BTV

Radio-nuclide	Average SSFL soil concentration (pCi g^{-1})	Average SSFL soil concentration (pCi m^{-2})	Inventory assumed released from SSFL (pCi)	Predicted deposition at Oak Park (pCi m^{-2})	0–3 cm concentration at Oak Park (pCi g^{-1})	Background BTV (pCi g^{-1})
^{137}Cs	4.6E-01	6.90E+04	2.11E+11	2.26E+02	7.52E-03	2.29E-01
^{239}Pu	1.22E-2	1.83E+03	5.59E+09	5.99E+00	2.00E-04	1.34E-02
^{90}Sr	4.25E-01	6.38E+04	1.95E+11	2.09E+02	6.95E-03	7.35E-02
^{226}Ra	1.24E+00	1.86E+05	5.68E+11	6.08E+02	2.03E-02	1.88E+00

4.3.4. Vegetation Monitoring

Vegetation was sampled from both on-site and off-site locations during the operational period from 1956 to 1989. Additional vegetation sampling occurred after 1989 during building demolition and site cleanup. Gross alpha and gross beta measurements were reported through 1985 (Moore 1986) and results for specific radionuclides were first reported in 1989 (Moore 1990). Most detected concentrations were for naturally occurring radionuclides (e.g., Rockwell International 1994, Table 5-16). Detections of anthropogenic radionuclides were limited to a measurement of 0.4 pCi g^{-1} of ^{60}Co in 1990 (Rockwell International 1991), two detections each of ^{60}Co (maximum = 0.02 pCi g^{-1}) and ^{137}Cs (maximum = 0.10 pCi g^{-1}) in 1991 (Rockwell International 1992), a maximum detection of 0.021 pCi g^{-1} of ^{137}Cs in 1993 (Rockwell International 1994), and a detection of 0.096 pCi g^{-1} of ^{137}Cs in 1997 (Robinson 1998). The 1989 data are reported on a dry weight basis, and the 2000 results are given on a wet weight basis. Dry or wet weight is not denoted for

the detected concentrations in the 1990s. For a given sample, concentrations reported on a dry weight basis will be greater than those reported on a wet weight basis. The ^{137}Cs detected is assumed to originate from global fallout (see Section 4.2.1).

A comprehensive vegetation sampling program was conducted in Area IV at the SSFL in 2000 in response to wildfires that had burned on a number of DOE facilities including Los Alamos National Laboratory, Hanford Nuclear Facility, and Idaho National Laboratory (Boeing 2001). The sampling was conducted in response to concerns that radionuclides would be emitted to the air from burning vegetation in contaminated areas. A composite vegetation sample was taken at each of the 28 legacy radiological facilities in Area IV and two off-site locations. The only radionuclide detected in measurable quantities was naturally occurring ^{40}K with concentrations ranging from the minimum detectable concentration (0.52 pCi g^{-1}) to 3.50 pCi g^{-1}. No anthropogenic radionuclides were detected in either on-site or off-site vegetation. The average MDC for the anthropogenic radionuclides ^{60}Co, ^{137}Cs, and ^{155}Eu were 0.054 pCi g^{-1}, 0.046 pCi g^{-1}, and 0.069 pCi g^{-1}, respectively.

4.3.5. Summary of Findings from Environmental Data Collected before and during the Fire

Several important conclusions can be drawn based on the measurement data:

- Air samplers equipped to measure radionuclide concentrations were positioned at various onsite locations in the direction the plume traveled and in areas with soil concentrations above background by samplers operated by both Boeing and DOE
- The response of the PM_{10} samplers is consistent with the fire progression. The unusually high mass loading corresponds to times at which smoke and suspended materials were known to be present, so it is clear that the samplers captured the impacts of the fire
- The fire had limited impact on gross alpha and beta concentrations measured in air. Some small increases in concentration were seen at the Boeing samplers with similar concentrations measured at different times before the fire.
- There was no impact of the fire observed at DOE samplers (i.e., concentrations measured before the fire are similar to or greater than concentrations measured during the fire)
- Detection of specific isotopes in air by DOE samplers in Area IV is likely due to their proximity to soil with concentrations above background in parts of Area IV within the defined fire boundary. Plutonium-239 and ^{90}Sr were the only anthropogenic nuclides detected in Area IV. All other detections in Area IV were for naturally occurring radionuclides.
- The concentrations of ^{239}Pu and ^{90}Sr detected in air in Area IV were well below concentration standards defined for human health protection assuming continuous exposure over a long period of time. Any exposures associated with the Woolsey Fire would be of short duration occurring only during the fire.
- The Boeing stations did not detect SSFL-related nuclides, nor did the other four DOE Area IV samplers, indicating that the slightly elevated air concentrations were limited to the immediate vicinity around areas of Area IV with soil concentrations above background
- Historical monitoring of vegetation resulted in a few sporadic detections of ^{137}Cs and ^{60}Co, and a comprehensive vegetation survey in 2000 did not detect any anthropogenic radionuclides in either onsite or offsite vegetation.

A soil sampling plan was designed to further investigate whether radionuclides of potential SSFL-origin were measured in areas impacted by deposition of particulates and associated radionuclides that might have been suspended during the fire. The concentrations in these post-fire soil samples were compared to the background soil concentrations discussed in this section to determine if there was any evidence of concentrations greater than background in areas downwind from the fire where materials suspended from SSFL might have been deposited. Details related to the soil sampling plan are discussed in Section 5.

5. Soil Sampling

The purpose of off-site soil sampling was to determine whether radionuclides from the SSFL were carried off site during the Woolsey Fire and deposited in the surrounding communities. The scoping calculations presented in Section 4.3.3, confirmed that soil sample analyses would detect ^{137}Cs and ^{239}Pu concentrations that could result in an effective dose of 0.1 mrem in Oak Park.

The approach used to identify the study sampling locations is described in Section 5.1. Quality assurance for the soil sampling and analysis program was implemented through the following elements:

- Establish written protocol for taking samples (Section 5.2)
- Establish chain-of-custody from sample collection to accredited analytical laboratory (Section 5.2.2)
- Sample duplicates (Section 5.2.1)
- Establish data quality objectives (Section 5.3.2)
- Data validation (Section 5.3).

5.1. Identifying Sampling Locations

Sampling locations were selected to include three distinct areas:

- Areas where potential deposition of any radionuclides from the Woolsey Fire burning on the SSFL would have been most likely to occur
- Areas on either side of the particulate deposition plume
- Areas upwind during the fire that would be unaffected. These samples were obtained to understand background concentrations of radionuclides.

A reconnaissance trip taken June 4 and 5, 2019, identified potential sampling locations based on their proximity to the particulate deposition plume and accessibility. Further reconnaissance was performed using Google Earth and Gaia GPS software to aid in identifying trail heads and access roads. Gaia GPS software typically has an accuracy ranging from ±5 m to ±10 m. This accuracy was more than adequate to identify sampling location coordinates. Land ownership for each potential sampling site was identified and written permissions were obtained to perform soil sampling.

Permissions were obtained for 16 sample locations, and these locations were sampled in August 2019. Figure 5-1 illustrates the location of each of the sampled sites with the modeled particulate deposition plume overlain. Sample location coordinates, ownership entity, and geologic formation are summarized in Table 5-1, and sampling location details are provided in Appendix A. Sampling was concentrated in the region of highest estimated particulate deposition (locations 13,

14, 15, 16, and 18) off the SSFL property. None of the locations have surface water that drains from SSFL.

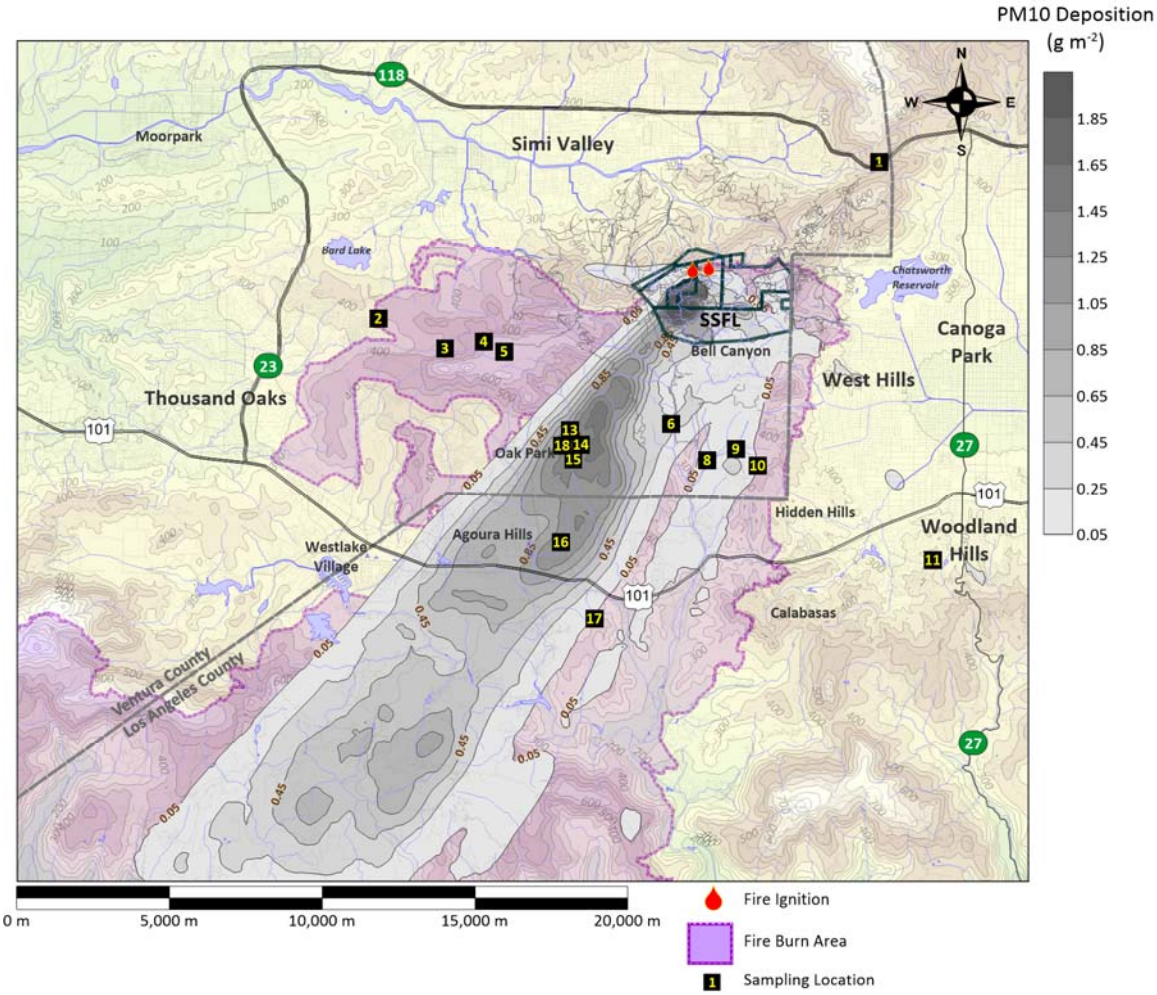

Figure 5-1. Sampling locations overlaying model predicted PM_{10} deposition plume and the Woolsey Fire burn extent. Samples 1, 2, and 5 were at or near EPA background locations that were sampled in 2011 (HydroGeologic 2011).

Table 5.1 Sample Location Coordinates, Geologic Formation, and Ownership Entity

Location number [a]	Latitude (dd)[b]	Longitude (dd)[b]	UTM E (m)[c]	UTM N (m)[d]	Geologic formation	Ownership entity[e]
1	34.2681	118.6373	349268	3793094	Chatsworth formation	MRCA
2	34.2193	118.8143	332872	3787960	Santa Susana formation	City of Thousand Oaks
3	34.2109	118.7904	335057	3786985	Chatsworth formation	Conejo Open Space
4	34.2131	118.7767	336326	3787207	Chatsworth formation	RSRPD
5	34.2102	118.7694	336992	3786880	Chatsworth formation	MRCA
6	34.1898	118.7097	342461	3784525	Alluvium	MRCA
8	34.1793	118.6967	343640	3783338	Modelo formation	MRCA
9	34.1827	118.6565	344579	3783702	Modelo formation	MRCA
10	34.1779	118.6788	345286	3783159	Towsley formation	MRCA
11	34.1508	118.6160	351021	3780058	Modelo formation	MRCA
13	34.1875	118.7456	339145	3784317	Calabasas formation	NPS
14	34.1832	118.7416	339504	3783843	Modelo formation	NPS
15	34.1789	118.7442	339252	3783363	Modelo formation	NPS
16	34.1543	118.7482	338842	3780645	Modelo formation	MRCA
17	34.1319	118.7358	339945	3778145	Calabasas formation	MRCA
18	34.1829	118.7483	338888	3783814	Modelo formation	NPS

a. Location 7 was deleted because of its proximity to location 6. Location 12 was deleted because we did not receive permission from the property owner to take a sample.
b. Decimal degrees.
c. Universal Transverse Mercator East.
d. Universal Transverse Mercator North.
e. MRCA: Mountain Recreation and Conservation Agency; RSRPD: Rancho Simi Recreation and Parks District; NPS: National Park Service.

5.1.1. Sample Location Geology

The local geology is important because naturally occurring radionuclides vary in abundance depending on the source rock. Naturally occurring radionuclides include the uranium and thorium series, and potassium-40. The EPA background study (HydroGeologic 2011) focused on samples taken from the same geologic formations exposed on the SSFL because they reflect the same natural abundance of naturally occurring radionuclides. EPA background samples at Lang Ranch and Rocky Peak were taken from the Chatsworth formation. Background samples identified as Bridal Path were taken in the Santa Susana formation. For some radionuclides, notably ^{232}Th, EPA noted higher concentrations in the Santa Susana formation compared to the Chatsworth formation. According to the EPA background study, about 80% of Area IV is underlain by the Chatsworth formation and the remainder is underlain by the Santa Susana formation. Most of the entire SSFL site, including the buffer areas, is underlain by the Chatsworth formation.

The oldest formation in the study area was the Cretaceous-age Chatsworth formation, which is composed of massive, thick-bedded medium to coarse-grained turbidite sandstone and well cemented conglomerate (Yerks and Campbell 2005). The conglomerate contains rounded clasts of porphyry and granitic rocks. The overlying early Eocene to late Paleocene-age Santa Susana formation consists of clay, shale, and fractured mud stone interbedded with fine- to medium-grained sandstone and pebble conglomerate. There are also lenses of gray limestone concretions

that are common in shale. Sample location 2 was located in the Santa Susana formation and samples 1, 3, 4, and 5 were located in the Chatsworth formation. Based on a U.S. Geologic Survey map of the region (Yerks and Campbell 2005), the Miocene-age Calabasas formation underlays sample locations 13 and 17, and the late Miocene age Modelo formation underlays samples 8, 9, 11, 14, 15, 16, 18. Sample location 13 may have been taken in a thin layer of Quaternary alluvium overlying the Calabasas formation based on the ^{137}Cs depth profile and its location in a canyon bottom. Sample location 10 is underlain by the early Pliocene/late Miocene age Towsley formation, which overlies and interfingers with the Modelo formation in the Santa Susana Mountains. Sample 6 was taken in Quaternary alluvium that overlies the Calabasas and Modelo formation. The Calabasas formation consists of interbedded clayey to silty sandstone and silty shale with local beds of sedimentary breccia. The Modelo formation lies unconformable above the Calabasas formation and consists of gray to brown, thin-bedded mudstone shale or siltstone with interbeds of very fine- to coarse-grained sandstone. Samples 8 and 9 lie within a subdivision of the Modelo consisting primarily of sandstone, and sample 11 is in a subdivision of the Modelo formation consisting of diatomaceous shale. The Towsley formation is the youngest formation and consists of interbedded sandstone, mudstone, and conglomerate.

5.2. Sample Protocol

The sampling protocol was adapted from the protocol used by Webb (1996) and Rood et al. (2008) to detect plutonium and uranium deposition from atmospheric plumes. The protocol uses depth profiles to determine activity levels in layers starting from the surface and extending to depth. Webb (1996) and Rood et al. (2008) demonstrated that most of the radionuclide deposition (>80%) that occurred 30 to 60 years ago remains in the top 6 cm of soil. Less than a year elapsed between potential deposition and the sampling in the case of the Woolsey Fire. Therefore, the activity contained within each layer provides evidence of the source because if activity were deposited from the atmosphere recently, most of the activity will reside in the first layer. This sampling strategy assumes that the soil has remained undisturbed from the time of deposition and this was verified during sampling.

Samples were taken at locations undisturbed since the fire with no obvious evidence of surface runoff, erosion, or soil accumulation. Cesium-137 is often used to determine soil disturbance because above-ground nuclear weapons testing resulted in worldwide deposition of ^{137}Cs in measurable quantities on soils. Most of the cesium remains in the surface layer because it is relatively immobile due to its relatively high soil-water partitioning coefficient. Thus, a depth profile that shows most of the ^{137}Cs activity in the surface layer would indicate the soil has been undisturbed since weapons fallout. In this case, soil would only have to be undisturbed since the Woolsey Fire. Cesium-137 is also a radionuclide detected in SSFL soils and thus may have potentially been emitted during the fire. If ^{137}Cs were emitted from the SSFL during the Woolsey Fire, then the surface soil concentration would be statistically greater than that associated with weapons testing fallout, the concentration of ^{137}Cs in the surface soil would have to be higher than in the subsurface layers, *and* the sample would have to have been taken within the Woolsey Fire deposition plume (see Figure 3-5).

5.2.1. Sampling Procedure

Before field sampling commenced, chain of custody, sampling forms, and sampling labels were printed; a 25 cm × 25 cm sampling frame was constructed; and a sample naming convention was established. Sample locations were numbered from 1 to 18 (with locations 7 and 12 subsequently omitted as discussed above). The sample ID was the sample location number followed by a depth designation letter (A=0–3 cm, B=3–6 cm, C=6–12 cm). Duplicate samples had "-D" after the depth designation letter. Sample split (sent to a different laboratory) was designated by "-S" following the depth designation letter. Sampling tools obtained included a steel scraper, hammer, chisel, trowel, small shovel, and funnel. Samples were placed in 2-liter sample bottles in the field, and the sample bottle was placed in a secondary plastic bag before shipment to the laboratory. A scintillometer was used to characterize the overall gamma exposure rate at each sampling site.

The excavation pit dimensions with the different layers are illustrated in Figure 5-2, and photos from sampling site 15 depicting the completed excavation pit is shown in Figure 5-3. The sampling procedure is outlined below:

1. At the sampling location, select an area that has no visible signs of disturbance from human or natural processes (i.e, water, burrowing animals).
2. Record the location of the sampling site using a GPS unit. The Gaia GPS iPhone application was used (www.gaiagps.com) for this task.
3. Carefully remove surface vegetation from the 25 cm × 25 cm sampling area.
4. Take a gamma exposure reading using a scintillometer with a detachable probe several inches above the sampling surface. A measurement is taken for each layer sampled.
5. Excavate soil from the 25 cm × 25 cm area using hand tools by soil layer. The target depth layers are 0–3 cm, 3–6 cm, and 6–12 cm. For depth layers greater than 6 cm, halve the area so the volume of the sample is the same as the higher layers (1.875 L). The actual depths and number of layers may vary from these standard values depending on the nature of the sampling site. Careful excavation is required around features such as large rocks or roots.
6. Place sample on disposable plastic sheet. When excavation is complete, transfer sample from plastic sheet to 2 L, wide-mouth sample bottle (one per sample). Discard disposable plastic sheet in trash bag.
7. Label each sample with sample label affixed with clear tape to the bottle. The sample label has the sample ID followed by a letter to designate depth layers: A=0–3 cm, B=3–6 cm, and C=6–12 cm. A "-D" designation following the sample ID indicates a sampling duplicate. A "-S" designation following the sample ID indicates a sampling split.
8. To avoid mixing of soil between layers, wash sampling tools between samples using a water spray bottle and wipe with clean paper towels.
9. Photograph excavation pit from several angles to illustrate the appearance of the soil profile and the local setting.
10. Record the following information to document the process:
    a. Date and time of sampling
    b. General description of location
    c. Length and width of each excavation layer
    d. Scintillometer reading (counts per minute)

e. Layer depth
f. Coordinates of sampling site (decimal degrees latitude and longitude)
g. Any other pertinent information.

11. Thoroughly clean sampling tools between sample sites using the spray bottle and paper towels.

The sample label and completed sample collection forms are presented in Appendix A. The scintillometer was a Ludlum model 3 (SN# 103609) rate meter with a detached 2.5 in × 2.5 in NaI(Tl) probe. The meter was calibrated on January 30, 2019, and it was checked with a source of known activity included with the meter every morning before sampling commenced.

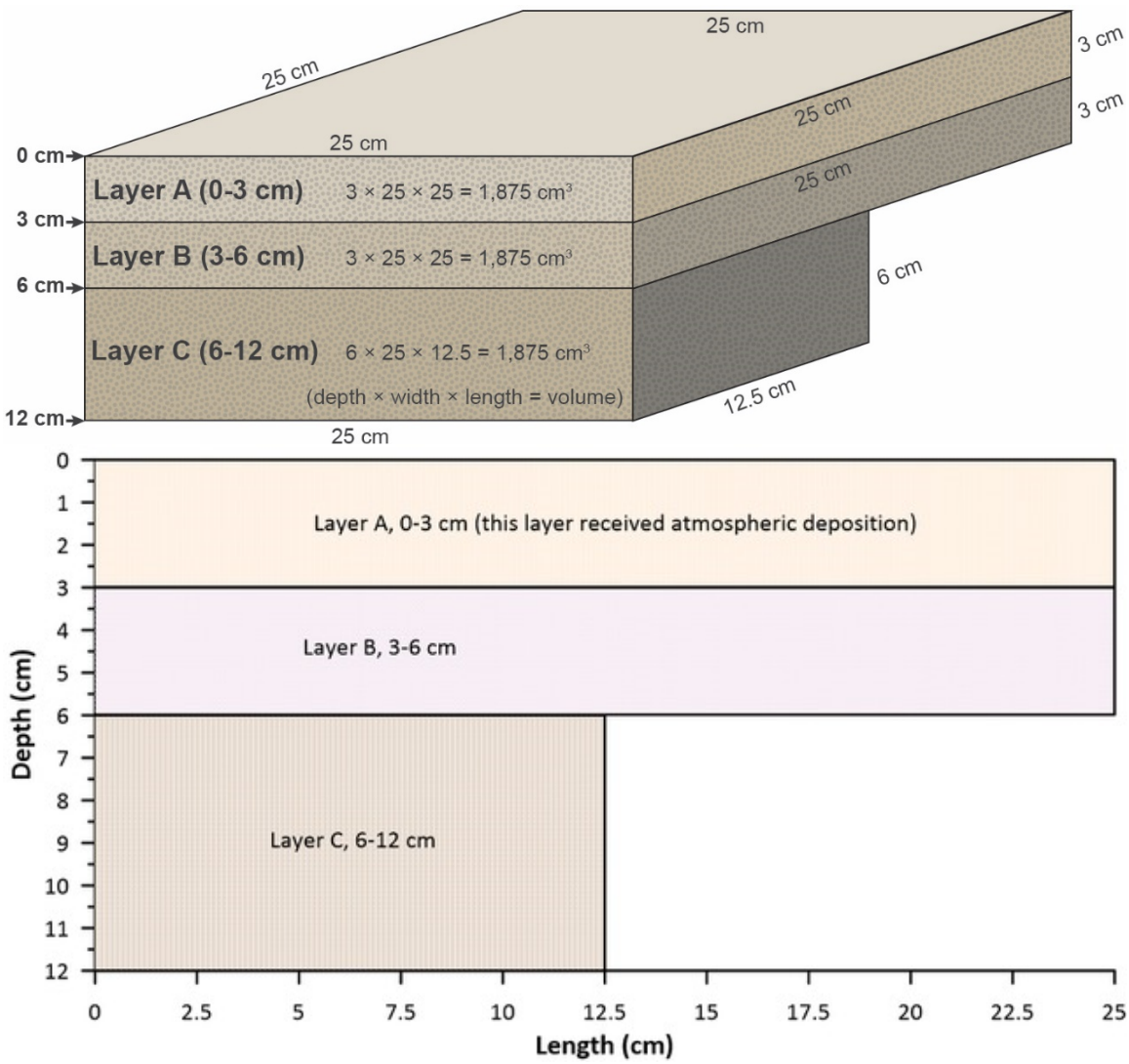

Figure 5-2. Depth profile sampling layers. Each layer contained 1,875 cm^3 of soil. The area of the lowest sampled layer (6–12 cm) was halved to 25 cm × 12.5 cm. The 0–3-cm top layer would contain atmospheric deposition from Woolsey Fire and ^{137}Cs from weapons fallout.

1 2 3

Figure 5-3. Field sampling procedure. (1) The 25 cm × 25 cm frame placed over soil surface before excavation and scintillometer reading made. (2) Surface layer (0–3 cm) excavation complete and sample bottled in 2 L container. (3) Excavation pit after all three layers were excavated.

5.2.2. Analytes and Laboratory Analysis

Samples were sent to GEL Laboratories, LLC., and one sample split was sent to TestAmerica, Inc. Chain-of-custody forms accompanied each shipment of samples. GEL Laboratories and TestAmerica have environmental accreditation in the State of California. Accreditation is used to verify that laboratories have an appropriate quality management system and can properly perform certain test methods (e.g., ANSI, ASTM, and ISO test methods) and calibration parameters according to their scopes of accreditation. GEL Laboratories and TestAmerica are participants in the DOE Mixed Analyte Performance Evaluation Program (MAPEP). The MAPEP provides quality assurance oversight for environmental analytical services by performing semiannual proficiency testing and evaluation of laboratories managed by the DOE, the U.S. Department of Defense, and other federal agencies; commercial analytical laboratories; and international analytical laboratories.

Radionuclides for which analysis was requested included all the radionuclides reported in the EPA background study (HydroGeologic 2011), with the exception of ^{113m}Cd, ^{222}Rn, and ^{220}Rn (Table 5-2). The GEL laboratory does not analyze for ^{113m}Cd because the analytical methods are incapable of detecting this radionuclide at concentrations that could conceivably be in soil. The ^{113m}Cd MDC in the EPA background study was 2,000 pCi g^{-1}. The radon isotopes were short half-life noble gases that are the progeny of ^{224}Ra and ^{226}Ra, respectively, and would not be present without the presence of their parent. Soil concentrations of radon isotopes in the environment depend on many factors because they readily diffuse in the gas phase. There were also a few radionuclides (^{225}Ac, ^{213}Bi, ^{90}Y) that were included in the GEL results but were not included in the EPA background suite. Results were provided for 61 radionuclides. Radionuclides identified as

priority-1 radionuclides were those that were detected above background by EPA in Area IV (HydroGeologic 2012) and above the radionuclide reference concentration (RRC).

There are several omissions from priority-1 radionuclides defined in HydroGeologic (2012). Namely, they identified ^{214}Bi, ^{214}Pb, ^{228}Ac, ^{212}Bi, ^{212}Pb, and ^{208}Tl as priority-1 radionuclides, but these radionuclides have short half-lives (less than 12 hours) and do not exist in the environment without the presence of their parent. Bisimuth-214 and ^{214}Pb are progeny of ^{226}Ra (^{238}U decay chain), and ^{228}Ac, ^{212}Bi, ^{212}Pb, and ^{208}Tl are progeny of ^{228}Ra (^{232}Th decay chain). Thus, for completeness ^{226}Ra, ^{228}Ra, and ^{232}Th were added to the priority-1 radionuclide list in this report.

5.2.3. Critical Levels and Minimum Detectable Concentrations

Two important quantities are necessary to evaluate analytical results, especially when concentrations are near background values. The first quantity is the *MDC*, which is derived from the minimum detectable activity (*MDA*). The *MDA* is defined as (Knoll 2010):

$$MDA = 4.653\sigma_{NB} + 2.706 \tag{5-1}$$

where

σ_{NB} = the 1-sigma (standard deviation) uncertainty in the background counts.

The *MDC* is calculated by factoring in percent recovery, detector efficiency, radiation yield per disintegration, and other factors specific to the analytical technique. The *MDA* is calculated such that there is less than a 5% probability that the activity detected in the sample is not actually present (i.e., false negative). The second quantity is the critical level (L_c), which is defined as (Knoll 2010):

$$L_c = 2.326\sigma_{NB} \tag{5-2}$$

The critical level (L_c) is the minimum activity in a sample such that the probability of a false positive (i.e., activity above background that is not actually present) will be no larger than 5%. The critical level can be converted to activity concentration in the same fashion as the *MDA*. Samples analyzed by the GEL laboratory were flagged as non-detect if the result was less than the *MDC*. Samples analyzed by TestAmerica laboratories were flagged as non-detect if the result was less than the L_c. A sample result greater than the *MDC* does not assure the activity present is from the radionuclide. Thus, samples were considered valid if they were (1) not flagged as non-detect, (2) the sample result exceeded the *MDC*, and (3) the sample result was greater than the 2-sigma uncertainty.

The *MDC* achieved by GEL varied between samples, but the requested *MDC* generally fell within the range of actual *MDCs* achieved. The *MDC* for samples analyzed by TestAmerica were lower for some radionuclides than those analyzed by GEL.

Table 5.2. Radionuclide List and Actual and Requested Minimum Detectable Concentrations

Radionuclide	Average reported MDC (pCi g^{-1})	Lowest reported MDC (pCi g^{-1})	Highest reported MDC (pCi g^{-1})	Requested MDC (pCi g^{-1})	Comments
Actinium-225	1.93	0.0102	4.58	N/A	
Actinium-227	0.08	0.0111	0.154	0.1	
Actinium-228	0.04	0.0074	0.074	0.05	Priority-1 radionuclide
Americium-241	0.02	0.00599	0.0538	0.015	
Americium-243	0.03	0.0139	0.0699	0.02	
Antimony-125	0.03	0.00369	0.0557	0.03	
Barium-137m	0.01	0.00152	0.0213	0.007	
Bismuth-212	0.14	0.0206	0.283	0.08	Priority-1 radionuclide
Bismuth-213	0.03	0.00438	0.0611	N/A	
Bismuth-214	0.02	0.00318	0.0388	0.02	Priority-1 radionuclide
Cadmium-113m				2000	Not analyzed
Carbon-14	2.63	2.28	3.03	3.5	
Cesium-134	0.02	0.00161	0.0367	0.04	
Cesium-137	0.01	0.00161	0.0225	0.007	Priority-1 radionuclide
Cobalt-60	0.01	0.00157	0.023	0.007	Priority-1 radionuclide
Curium-243/244	0.02	0.00516	0.0593	0.03	
Curium-245/246	0.01	0.00547	0.0329	0.03	
Curium-248	0.024	0.00424	0.0597	0.03	
Europium-152	0.03	0.0044	0.0576	0.03	Priority-1 radionuclide
Europium-154	0.04	0.00449	0.0788	0.04	
Europium-155	0.04	0.00485	0.0743	0.05	
Holmium-166m	0.02	0.00243	0.0362	0.015	
Iodine-129	0.73	0.193	1.34	1.7	
Iron-55	3.69	2.14	4.99	5	
Lead-210	2.44	0.13	5.95	0.2	
Lead-212	0.02	0.00291	0.0348	0.03	Priority-1 radionuclide
Lead-214	0.05	0.00375	0.135	0.02	Priority-1 radionuclide
Neptunium-236	0.02	0.00279	0.0343	0.04	
Neptunium-237	0.02	0.00981	0.034	0.008	
Neptunium-239	0.1	0.0121	0.17	0.07	
Nickel-59	1.43	0.194	2.4	0.5	Priority-1 radionuclide

Table 5.2. Radionuclide List and Actual and Requested Minimum Detectable Concentrations

Radionuclide	Average reported MDC (pCi g^{-1})	Lowest reported MDC (pCi g^{-1})	Highest reported MDC (pCi g^{-1})	Requested MDC (pCi g^{-1})	Comments
Nickel-63	0.65	0.402	0.821	0.7	
Niobium-94	0.01	0.0014	0.0214	0.06	
Plutonium-236	0.02	0.00279	0.0343	0.03	
Plutonium-238	0.019	0.00468	0.0465	0.004	
Plutonium-239/240	0.02	0.0109	0.0343	0.005	Priority-1 radionuclide
Plutonium-241	3.4	2.4	6.32	0.6	
Plutonium-242	0.02	0.0103	0.0341	0.005	
Plutonium-244	0.01	0.00558	0.0273	0.005	
Polonium-210	0.15	0.0415	0.397	0.2	
Potassium-40	0.09	0.0221	0.184	0.07	
Promethium-147	291.94	33.3	494	5	
Protactinium-231	0.14	0.0201	0.285	0.4	
Radium-226	0.02	0.00318	0.0388	0.07	Priority-1 radionuclide[a]
Radium-228	0.04	0.0074	0.074	0.04	Priority-1 radionuclide[a]
Sodium-22	0.01	0.00161	0.0284	0.01	
Strontium-90	0.01	0.00742	0.015	0.015	Priority-1 radionuclide
Technetium-99	0.62	0.409	0.802	0.3	
Tellurium-125m	5.53	0.376	9.89	0.006	
Thallium-208	0.01	0.00142	0.0209	0.01	Priority-1 radionuclide
Thorium-228	0.15	0.0846	0.55	0.03	Priority-1 radionuclide[a]
Thorium-229	0.12	0.0683	0.31	0.05	
Thorium-230	0.11	0.0471	0.355	0.03	Priority-1 radionuclide
Thorium-231	0.2	0.0271	0.401	0.03	
Thorium-232	0.08	0.0183	0.239	0.01	Priority-1 radionuclide[a]
Thorium-234	0.63	0.0685	1.35	0.2	Priority-1 radionuclide
Thulium-171	11.19	1.14	24.5	10	
Tin-126	0.03	0.00352	0.0531	0.008	
Tritium	3.95	3.5	4.6	5	
Uranium-232	0.09	0.0476	0.249	0.15	
Uranium-233/234	0.05	0.0298	0.12	0.05	Priority-1 radionuclide

Table 5.2. Radionuclide List and Actual and Requested Minimum Detectable Concentrations

Radionuclide	Average reported MDC (pCi g^{-1})	Lowest reported MDC (pCi g^{-1})	Highest reported MDC (pCi g^{-1})	Requested MDC (pCi g^{-1})	Comments
Uranium-235/236	0.04	0.0086	0.0813	0.05	Priority-1 radionuclide
Uranium-238	0.05	0.00933	0.117	0.03	Priority-1 radionuclide
Yttrium-90	0.01	0.00742	0.015	N/A	

[a.] See discussion in Section 5.3.2.

5.3. Evaluation of Sampling Results

Sample mass received by the GEL laboratory and the estimated bulk density are presented in Table 5-3. The bulk density was estimated by assuming every sample contained 1.875 L of soil. While every effort was made to collect 1.875 L in each sample, in practice, the sample volume varied among samples because of variable soil conditions. Radionuclide inventories can be calculated in each layer by multiplying the activity concentration (in pCi g^{-1}) by sample mass (g).

Table 5.3. Sample Depths, Mass, and Estimated Bulk Density

Sample number	Location	Top depth (cm)	Bottom depth (cm)	Mass (g)	Bulk density (g cm^{-3})
1 A	1	0	3	2520.9	1.34
1 A–D	1	0	3	2275.9	1.21
1 B	1	3	6	2542.1	1.36
1 B–D	1	3	6	2599.9	1.39
1 C	1	6	12	2386.1	1.27
1 C–D	1	6	12	2761.8	1.47
2 A	2	0	3	2004.2	1.07
2 B	2	3	6	1961.3	1.05
2 C	2	6	12	2158.6	1.15
3 A	3	0	3	2593.9	1.38
3 B	3	3	6	2585.6	1.38
3 C	3	6	12	1883.9	1.00
4 A	4	0	3	2241.1	1.20
4 B	4	3	6	2197.8	1.17
4 C	4	6	12	2009.7	1.07
5 A	5	0	3	2784.5	1.49
5 B	5	3	6	2136.2	1.14
5 C	5	6	12	2136.9	1.14
6 A	6	0	3	1786.8	0.95
6 B	6	3	6	1897.7	1.01

Table 5.3. Sample Depths, Mass, and Estimated Bulk Density

Sample number	Location	Top depth (cm)	Bottom depth (cm)	Mass (g)	Bulk density (g cm^{-3})
6 C	6	6	12	2047.1	1.09
8 A	8	0	3	2372.3	1.27
8 B	8	3	6	2393.1	1.28
8 C	8	6	12	2202.5	1.17
9 A	9	0	3	2174.9	1.16
9 B	9	3	6	2298.4	1.23
9 C	9	6	12	2140.6	1.14
10 A	10	0	3	1426.8	0.76
10 B	10	3	6	1379.4	0.74
10 C	10	6	12	1537.8	0.82
11 A	11	0	3	1615.8	0.86
11 B	11	3	6	1625.8	0.87
11 C	11	6	12	1883.9	1.00
13 A	13	0	3	1670.3	0.89
13 B	13	3	6	1624.5	0.87
13 C	13	6	12	1805.9	0.96
14 A	14	0	3	2106.1	1.12
14 B	14	3	6	2091.2	1.12
14 C	14	6	12	2274.6	1.21
15 A	15	0	3	1927.4	1.03
15 B	15	3	6	2010.4	1.07
15 C	15	6	12	2058.7	1.10
16 A	16	0	3	2795.3	1.49
16 B	16	3	6	2726.8	1.45
16 C	16	6	12	2760.9	1.47
17 A	17	0	3	1651.2	0.88
17 B	17	3	6	1714.0	0.91
17 C	17	6	12	1687.6	0.90
18 A	18	0	3	1651.2	0.88
18 B	18	3	6	1714.0	0.91
18 C	18	6	12	1687.6	0.90

A complete tabulation of results is presented in Appendix B. There were 28 radionuclides that were positively detected (above the *MDC* and above the 2-sigma uncertainty) by the GEL laboratory in at least one soil sample. Radionuclides detected were naturally occurring or of weapons fallout origin. Detected radionuclides in the 16 locations plus the sample duplicate taken at sample location 1 are listed in Table 5.4. For comparison, the 12-cm weighted average concentration was computed and compared to the BTV value. The BTV value was based on a soil

sampling depth of 6 inches (15 cm). Therefore, it was inappropriate to compare the soil concentration from individual layers (0–3, 3–6, and 6–12 cm) with the BTV; instead, the weighted average concentration (C_{wt}) was compared. The weighted average concentration was calculated using Equation 5-3:

$$C_{wt} = \frac{C_3 \times 3\text{ cm} + C_6 \times 3\text{ cm} + C_{12} \times 6\text{ cm}}{12\text{ cm}} \tag{5-3}$$

where

C_3 = radionuclide soil concentration in 0–3 cm layer (pCi g^{-1})
C_6 = radionuclide soil concentration in 3–6 cm layer (pCi g^{-1})
C_{12} = radionuclide soil concentration in 6–12 cm layer (pCi g^{-1}).

For radionuclides that had a non-detect result in one or two layers at a given location, the reported value was used in the weighted average concentration and the concentration was bolded and in decimal format in Table 5.4. Concentrations less than zero were reported as zero. Ten radionuclides had weighted average concentrations that exceeded the BTV value as indicated by a ratio value greater than 1.0 in the last column of Table 5.4. Of these 10 radionuclides, only five (^{230}Th, ^{234}Th, ^{234}U, ^{235}U, and ^{238}U) were identified as priority-1 radionuclides, and all were naturally occurring.

Table 5.4. Sample Results with Positive Detections, the Weighted Average Concentration, and Comparison of the Weighted Average Concentration with the BTV[a, b]

Radionuclide	Location[c]	0–3 cm (pCi g^{-1})	3–6 cm (pCi g^{-1})	6–12 cm (pCi g^{-1})	12-cm weighted average concentration (pCi g^{-1})	BTV (pCi g^{-1})	Ratio to BTV
Ac-228	1	1.60E+00	1.66E+00	1.72E+00	1.67E+00	2.30E+00	0.73
Ac-228	10	3.92E-01	4.26E-01	4.95E-01	4.52E-01	2.30E+00	0.20
Ac-228	11	1.37E+00	1.51E+00	1.50E+00	1.47E+00	2.30E+00	0.64
Ac-228	13	1.25E+00	1.18E+00	1.15E+00	1.18E+00	2.30E+00	0.51
Ac-228	14	1.05E+00	9.94E-01	1.06E+00	1.04E+00	2.30E+00	0.45
Ac-228	15	1.02E+00	1.01E+00	1.08E+00	1.05E+00	2.30E+00	0.46
Ac-228	16	1.03E+00	9.22E-01	9.61E-01	9.69E-01	2.30E+00	0.42
Ac-228	17	3.89E-01	3.72E-01	4.07E-01	3.94E-01	2.30E+00	0.17
Ac-228	18	1.22E+00	1.24E+00	1.26E+00	1.25E+00	2.30E+00	0.54
Ac-228	2	1.71E+00	1.72E+00	1.76E+00	1.74E+00	2.30E+00	0.76
Ac-228	3	1.71E+00	1.86E+00	1.91E+00	1.85E+00	2.30E+00	0.80
Ac-228	4	1.42E+00	1.50E+00	1.60E+00	1.53E+00	2.30E+00	0.67
Ac-228	5	1.73E+00	1.99E+00	1.55E+00	1.71E+00	2.30E+00	0.74
Ac-228	6	6.31E-01	8.96E-01	1.19E+00	9.77E-01	2.30E+00	0.42
Ac-228	8	9.21E-01	9.61E-01	1.07E+00	1.01E+00	2.30E+00	0.44
Ac-228	9	8.66E-01	9.55E-01	9.38E-01	9.24E-01	2.30E+00	0.40
Am-241	2	**0.0131**	1.49E-02	**0.00726**	1.06E-02	1.62E-02	0.66
Ba-137m	1	8.07E-02	3.68E-02	2.54E-02	4.21E-02	1.83E-01	0.23
Ba-137m	10	1.24E-01	1.15E-01	1.00E-01	1.10E-01	1.83E-01	0.60
Ba-137m	11	3.44E-02	1.63E-02	1.80E-02	2.17E-02	1.83E-01	0.12
Ba-137m	13	7.66E-02	7.82E-02	6.67E-02	7.21E-02	1.83E-01	0.39
Ba-137m	14	9.01E-02	6.68E-02	4.90E-02	6.37E-02	1.83E-01	0.35
Ba-137m	15	8.06E-02	7.93E-02	6.52E-02	7.26E-02	1.83E-01	0.40
Ba-137m	16	7.07E-02	5.54E-02	3.92E-02	5.11E-02	1.83E-01	0.28
Ba-137m	17	5.07E-02	2.88E-02	2.36E-02	3.17E-02	1.83E-01	0.17
Ba-137m	18	7.94E-02	8.28E-02	7.86E-02	7.99E-02	1.83E-01	0.44

Table 5.4. Sample Results with Positive Detections, the Weighted Average Concentration, and Comparison of the Weighted Average Concentration with the BTV[a, b]

Radionuclide	Location[c]	0–3 cm (pCi g^{-1})	3–6 cm (pCi g^{-1})	6–12 cm (pCi g^{-1})	12-cm weighted average concentration (pCi g^{-1})	BTV (pCi g^{-1})	Ratio to BTV
Ba-137m	2	5.75E-02	6.80E-02	4.44E-02	5.36E-02	1.83E-01	0.29
Ba-137m	3	1.00E-01	4.79E-02	**0.0113**	4.26E-02	1.83E-01	0.23
Ba-137m	4	5.66E-02	2.63E-02	1.18E-02	2.66E-02	1.83E-01	0.15
Ba-137m	5	2.90E-01	1.04E-01	3.36E-02	1.15E-01	1.83E-01	0.63
Ba-137m	6	2.99E-02	6.18E-02	8.30E-02	6.44E-02	1.83E-01	0.35
Ba-137m	8	6.24E-02	4.36E-02	3.08E-02	4.19E-02	1.83E-01	0.23
Ba-137m	9	1.38E-01	8.10E-02	5.65E-02	8.30E-02	1.83E-01	0.45
Bi-212	1	1.84E+00	1.74E+00	1.78E+00	1.78E+00	2.04E+00	0.87
Bi-212	10	3.75E-01	4.76E-01	4.86E-01	4.56E-01	2.04E+00	0.22
Bi-212	11	1.31E+00	1.49E+00	1.52E+00	1.46E+00	2.04E+00	0.72
Bi-212	13	1.34E+00	1.37E+00	1.30E+00	1.33E+00	2.04E+00	0.65
Bi-212	14	1.11E+00	9.84E-01	1.14E+00	1.09E+00	2.04E+00	0.54
Bi-212	15	1.23E+00	1.14E+00	1.13E+00	1.16E+00	2.04E+00	0.57
Bi-212	16	1.02E+00	1.06E+00	8.89E-01	9.65E-01	2.04E+00	0.47
Bi-212	17	4.06E-01	3.85E-01	3.43E-01	3.69E-01	2.04E+00	0.18
Bi-212	18	1.34E+00	1.24E+00	1.46E+00	1.38E+00	2.04E+00	0.67
Bi-212	2	1.83E+00	2.06E+00	1.67E+00	1.81E+00	2.04E+00	0.89
Bi-212	3	1.80E+00	1.86E+00	1.81E+00	1.82E+00	2.04E+00	0.89
Bi-212	4	1.50E+00	1.53E+00	1.59E+00	1.55E+00	2.04E+00	0.76
Bi-212	5	1.86E+00	1.93E+00	1.97E+00	1.93E+00	2.04E+00	0.95
Bi-212	6	5.68E-01	8.97E-01	1.36E+00	1.05E+00	2.04E+00	0.51
Bi-212	8	9.95E-01	1.08E+00	1.05E+00	1.04E+00	2.04E+00	0.51
Bi-212	9	9.42E-01	1.18E+00	8.90E-01	9.76E-01	2.04E+00	0.48
Cs-137	1	8.51E-02	3.89E-02	2.68E-02	4.44E-02	1.93E-01	0.23
Cs-137	10	1.31E-01	1.22E-01	1.06E-01	1.16E-01	1.93E-01	0.60
Cs-137	11	3.63E-02	1.72E-02	1.90E-02	2.29E-02	1.93E-01	0.12
Cs-137	13	8.09E-02	8.26E-02	7.05E-02	7.61E-02	1.93E-01	0.39
Cs-137	14	9.52E-02	7.06E-02	5.18E-02	6.74E-02	1.93E-01	0.35
Cs-137	15	8.52E-02	8.38E-02	6.89E-02	7.67E-02	1.93E-01	0.40
Cs-137	16	7.47E-02	5.86E-02	4.14E-02	5.40E-02	1.93E-01	0.28
Cs-137	17	5.35E-02	3.05E-02	2.50E-02	3.35E-02	1.93E-01	0.17
Cs-137	18	8.39E-02	8.75E-02	8.30E-02	8.44E-02	1.93E-01	0.44
Cs-137	2	6.08E-02	7.18E-02	4.69E-02	5.66E-02	1.93E-01	0.29
Cs-137	3	1.06E-01	5.06E-02	**0.012**	4.52E-02	1.93E-01	0.23
Cs-137	4	5.98E-02	2.78E-02	1.25E-02	2.82E-02	1.93E-01	0.15
Cs-137	5	3.06E-01	1.09E-01	3.55E-02	1.22E-01	1.93E-01	0.63
Cs-137	6	3.16E-02	6.53E-02	8.77E-02	6.81E-02	1.93E-01	0.35
Cs-137	8	6.60E-02	4.61E-02	3.25E-02	4.43E-02	1.93E-01	0.23
Cs-137	9	1.45E-01	8.55E-02	5.97E-02	8.75E-02	1.93E-01	0.45
Fe-55	10	**0.761**	3.35E+00	4.17E+00	3.11E+00	5.08E+00	0.61
Fe-55	6	**1.23**	**2.34**	6.63E+00	4.21E+00	5.08E+00	0.83
Fe-55	8	**1.61**	5.64E+00	3.35E+00	3.49E+00	5.08E+00	0.69
K-40	1	2.28E+01	2.35E+01	2.26E+01	2.29E+01	3.05E+01	0.75
K-40	10	1.25E+01	1.35E+01	1.32E+01	1.31E+01	3.05E+01	0.43
K-40	11	2.26E+01	2.36E+01	2.33E+01	2.32E+01	3.05E+01	0.76
K-40	13	2.34E+01	2.23E+01	2.01E+01	2.15E+01	3.05E+01	0.70
K-40	14	1.48E+01	1.55E+01	1.59E+01	1.55E+01	3.05E+01	0.51
K-40	15	2.55E+01	2.32E+01	2.48E+01	2.46E+01	3.05E+01	0.81
K-40	16	1.84E+01	1.81E+01	1.81E+01	1.82E+01	3.05E+01	0.60
K-40	17	2.39E+01	2.44E+01	2.70E+01	2.56E+01	3.05E+01	0.84
K-40	18	1.53E+01	1.53E+01	1.42E+01	1.48E+01	3.05E+01	0.48
K-40	2	2.24E+01	2.06E+01	2.25E+01	2.20E+01	3.05E+01	0.72
K-40	3	2.63E+01	2.64E+01	2.81E+01	2.72E+01	3.05E+01	0.89
K-40	4	2.20E+01	2.46E+01	2.45E+01	2.39E+01	3.05E+01	0.78

Table 5.4. Sample Results with Positive Detections, the Weighted Average Concentration, and Comparison of the Weighted Average Concentration with the BTV[a, b]

Radionuclide	Location[c]	0–3 cm (pCi g^{-1})	3–6 cm (pCi g^{-1})	6–12 cm (pCi g^{-1})	12-cm weighted average concentration (pCi g^{-1})	BTV (pCi g^{-1})	Ratio to BTV
K-40	5	2.56E+01	2.78E+01	2.00E+01	2.34E+01	3.05E+01	0.77
K-40	6	3.20E+01	3.23E+01	2.98E+01	3.10E+01	3.05E+01	1.02
K-40	8	1.64E+01	1.63E+01	1.69E+01	1.66E+01	3.05E+01	0.55
K-40	9	1.36E+01	1.39E+01	1.35E+01	1.36E+01	3.05E+01	0.45
Pb-210	1	**1.013**	**1.085**	***0.658***	8.54E-01	2.07E+00	0.41
Pb-210	10	2.23E+00	**0.554**	1.25E+00	1.32E+00	2.07E+00	0.64
Pb-210	13	**2.55**	1.93E+00	1.63E+00	1.94E+00	2.07E+00	0.93
Pb-210	14	1.48E+00	**0.777**	**1.52**	1.32E+00	2.07E+00	0.64
Pb-210	2	**1.02**	1.24E+00	**2.43**	1.78E+00	2.07E+00	0.86
Pb-210	3	**2.32**	1.62E+00	**2.14**	2.06E+00	2.07E+00	0.99
Pb-210	5	**4.22**	**2.41**	1.01E+00	2.16E+00	2.07E+00	1.04
Pb-210	6	**0.839**	**2.17**	1.26E+00	1.38E+00	2.07E+00	0.67
Pb-212	1	1.53E+00	1.64E+00	1.69E+00	1.63E+00	2.67E+00	0.61
Pb-212	10	3.73E-01	4.23E-01	4.65E-01	4.32E-01	2.67E+00	0.16
Pb-212	11	1.38E+00	1.49E+00	1.54E+00	1.49E+00	2.67E+00	0.56
Pb-212	13	1.29E+00	1.28E+00	1.06E+00	1.17E+00	2.67E+00	0.44
Pb-212	14	9.12E-01	9.76E-01	1.04E+00	9.92E-01	2.67E+00	0.37
Pb-212	15	1.07E+00	9.36E-01	1.06E+00	1.03E+00	2.67E+00	0.39
Pb-212	16	9.77E-01	9.56E-01	9.89E-01	9.78E-01	2.67E+00	0.37
Pb-212	17	3.87E-01	3.69E-01	3.97E-01	3.88E-01	2.67E+00	0.15
Pb-212	18	1.23E+00	1.24E+00	1.16E+00	1.20E+00	2.67E+00	0.45
Pb-212	2	1.69E+00	1.67E+00	1.73E+00	1.71E+00	2.67E+00	0.64
Pb-212	3	1.67E+00	1.73E+00	1.91E+00	1.81E+00	2.67E+00	0.68
Pb-212	4	1.30E+00	1.48E+00	1.61E+00	1.50E+00	2.67E+00	0.56
Pb-212	5	1.75E+00	2.02E+00	1.46E+00	1.67E+00	2.67E+00	0.63
Pb-212	6	6.03E-01	8.86E-01	1.16E+00	9.52E-01	2.67E+00	0.36
Pb-212	8	1.00E+00	9.42E-01	1.04E+00	1.01E+00	2.67E+00	0.38
Pb-212	9	8.29E-01	9.32E-01	9.24E-01	9.02E-01	2.67E+00	0.34
Po-210	1	1.20E+00	5.79E-01	6.54E-01	7.72E-01	2.09E+00	0.37
Po-210	10	1.38E+00	1.09E+00	1.50E+00	1.37E+00	2.09E+00	0.65
Po-210	11	2.85E+00	2.55E+00	1.87E+00	2.29E+00	2.09E+00	1.09
Po-210	13	1.48E+00	1.35E+00	1.66E+00	1.54E+00	2.09E+00	0.74
Po-210	14	1.26E+00	1.04E+00	9.55E-01	1.05E+00	2.09E+00	0.50
Po-210	15	1.20E+00	1.02E+00	6.42E-01	8.76E-01	2.09E+00	0.42
Po-210	16	9.60E-01	9.77E-01	9.88E-01	9.78E-01	2.09E+00	0.47
Po-210	17	4.17E-01	3.78E-01	2.03E-01	3.00E-01	2.09E+00	0.14
Po-210	18	1.25E+00	9.29E-01	9.92E-01	1.04E+00	2.09E+00	0.50
Po-210	2	8.91E-01	7.75E-01	7.63E-01	7.98E-01	2.09E+00	0.38
Po-210	3	1.75E+00	1.74E+00	1.30E+00	1.52E+00	2.09E+00	0.73
Po-210	4	1.32E+00	9.34E-01	8.48E-01	9.88E-01	2.09E+00	0.47
Po-210	5	1.58E+00	6.92E-01	7.97E-01	9.67E-01	2.09E+00	0.46
Po-210	6	1.85E+00	1.24E+00	1.49E+00	1.52E+00	2.09E+00	0.73
Po-210	8	2.54E+00	2.33E+00	5.45E-01	1.49E+00	2.09E+00	0.71
Po-210	9	1.44E+00	7.36E-01	8.85E-01	9.87E-01	2.09E+00	0.47
Ra-226	1	1.15E+00	1.11E+00	1.16E+00	1.14E+00	1.88E+00	0.61
Ra-226	10	1.06E+00	1.13E+00	1.25E+00	1.17E+00	1.88E+00	0.62
Ra-226	11	2.76E+00	3.16E+00	2.71E+00	2.84E+00	1.88E+00	1.51
Ra-226	13	2.35E+00	2.26E+00	2.00E+00	2.15E+00	1.88E+00	1.14
Ra-226	14	1.55E+00	1.47E+00	1.54E+00	1.53E+00	1.88E+00	0.81
Ra-226	15	1.27E+00	1.23E+00	1.33E+00	1.29E+00	1.88E+00	0.69
Ra-226	16	1.68E+00	1.53E+00	1.52E+00	1.56E+00	1.88E+00	0.83
Ra-226	17	3.62E-01	3.48E-01	3.41E-01	3.48E-01	1.88E+00	0.19
Ra-226	18	1.79E+00	1.76E+00	1.88E+00	1.83E+00	1.88E+00	0.97
Ra-226	2	1.29E+00	1.36E+00	1.43E+00	1.38E+00	1.88E+00	0.73

Table 5.4. Sample Results with Positive Detections, the Weighted Average Concentration, and Comparison of the Weighted Average Concentration with the BTV[a, b]

Radionuclide	Location[c]	0–3 cm (pCi g^{-1})	3–6 cm (pCi g^{-1})	6–12 cm (pCi g^{-1})	12-cm weighted average concentration (pCi g^{-1})	BTV (pCi g^{-1})	Ratio to BTV
Ra-226	3	1.45E+00	1.39E+00	1.50E+00	1.46E+00	1.88E+00	0.78
Ra-226	4	1.03E+00	1.10E+00	1.12E+00	1.09E+00	1.88E+00	0.58
Ra-226	5	1.31E+00	1.33E+00	1.17E+00	1.25E+00	1.88E+00	0.66
Ra-226	6	6.17E-01	9.42E-01	1.05E+00	9.15E-01	1.88E+00	0.49
Ra-226	8	2.16E+00	2.02E+00	2.05E+00	2.07E+00	1.88E+00	1.10
Ra-226	9	1.15E+00	1.29E+00	1.34E+00	1.28E+00	1.88E+00	0.68
Ra-228	1	1.60E+00	1.66E+00	1.72E+00	1.67E+00	2.30E+00	0.73
Ra-228	10	3.92E-01	4.26E-01	4.95E-01	4.52E-01	2.30E+00	0.20
Ra-228	11	1.37E+00	1.51E+00	1.50E+00	1.47E+00	2.30E+00	0.64
Ra-228	13	1.25E+00	1.18E+00	1.15E+00	1.18E+00	2.30E+00	0.51
Ra-228	14	1.05E+00	9.94E-01	1.06E+00	1.04E+00	2.30E+00	0.45
Ra-228	15	1.02E+00	1.01E+00	1.08E+00	1.05E+00	2.30E+00	0.46
Ra-228	16	1.03E+00	9.22E-01	9.61E-01	9.69E-01	2.30E+00	0.42
Ra-228	17	3.89E-01	3.72E-01	4.07E-01	3.94E-01	2.30E+00	0.17
Ra-228	18	1.22E+00	1.24E+00	1.26E+00	1.25E+00	2.30E+00	0.54
Ra-228	2	1.71E+00	1.72E+00	1.76E+00	1.74E+00	2.30E+00	0.76
Ra-228	3	1.71E+00	1.86E+00	1.91E+00	1.85E+00	2.30E+00	0.80
Ra-228	4	1.42E+00	1.50E+00	1.60E+00	1.53E+00	2.30E+00	0.67
Ra-228	5	1.73E+00	1.99E+00	1.55E+00	1.71E+00	2.30E+00	0.74
Ra-228	6	6.31E-01	8.96E-01	1.19E+00	9.77E-01	2.30E+00	0.42
Ra-228	8	9.21E-01	9.61E-01	1.07E+00	1.01E+00	2.30E+00	0.44
Ra-228	9	8.66E-01	9.55E-01	9.38E-01	9.24E-01	2.30E+00	0.40
Sr-90	5	2.48E-02	**0.0122**	1.67E-02	1.76E-02	7.50E-02	0.23
Th-228	1	1.36E+00	1.56E+00	1.39E+00	1.42E+00	3.67E+00	0.39
Th-228	10	4.16E-01	5.19E-01	3.77E-01	4.22E-01	3.67E+00	0.12
Th-228	11	9.79E-01	7.49E-01	1.14E+00	1.00E+00	3.67E+00	0.27
Th-228	13	9.87E-01	8.85E-01	8.95E-01	9.16E-01	3.67E+00	0.25
Th-228	14	8.32E-01	8.54E-01	8.75E-01	8.59E-01	3.67E+00	0.23
Th-228	15	7.47E-01	9.34E-01	7.15E-01	7.78E-01	3.67E+00	0.21
Th-228	16	9.36E-01	8.96E-01	8.91E-01	9.04E-01	3.67E+00	0.25
Th-228	17	2.26E-01	4.01E-01	3.11E-01	3.12E-01	3.67E+00	0.09
Th-228	18	8.83E-01	8.20E-01	7.86E-01	8.19E-01	3.67E+00	0.22
Th-228	2	1.18E+00	1.28E+00	1.30E+00	1.27E+00	3.67E+00	0.34
Th-228	3	1.53E+00	1.47E+00	1.43E+00	1.47E+00	3.67E+00	0.40
Th-228	4	1.27E+00	1.31E+00	1.31E+00	1.30E+00	3.67E+00	0.35
Th-228	5	1.54E+00	1.90E+00	1.55E+00	1.64E+00	3.67E+00	0.45
Th-228	6	6.40E-01	1.05E+00	7.83E-01	8.14E-01	3.67E+00	0.22
Th-228	8	8.32E-01	7.92E-01	***0.7115***	7.62E-01	3.67E+00	0.21
Th-228	9	7.35E-01	6.18E-01	6.71E-01	6.74E-01	3.67E+00	0.18
Th-229	1	**0.038**	**-0.0037**	1.59E-01	8.82E-02	4.62E-02	1.91
Th-229	4	**0.011**	1.28E-01	**0.0697**	6.95E-02	4.62E-02	1.50
Th-229	5	**2.68E-08**	1.29E-01	**0.0316**	4.81E-02	4.62E-02	1.04
Th-230	1	1.10E+00	1.31E+00	1.11E+00	1.16E+00	2.04E+00	0.57
Th-230	10	1.64E+00	1.82E+00	1.42E+00	1.58E+00	2.04E+00	0.77
Th-230	11	2.40E+00	2.67E+00	3.17E+00	2.85E+00	2.04E+00	1.40
Th-230	13	2.30E+00	2.37E+00	2.15E+00	2.24E+00	2.04E+00	1.10
Th-230	14	1.52E+00	1.33E+00	1.23E+00	1.33E+00	2.04E+00	0.65
Th-230	15	9.11E-01	1.12E+00	1.10E+00	1.06E+00	2.04E+00	0.52
Th-230	16	1.71E+00	1.63E+00	1.57E+00	1.62E+00	2.04E+00	0.79
Th-230	17	5.06E-01	3.53E-01	4.00E-01	4.15E-01	2.04E+00	0.20
Th-230	18	1.86E+00	1.82E+00	2.12E+00	1.98E+00	2.04E+00	0.97
Th-230	2	1.14E+00	8.20E-01	9.25E-01	9.53E-01	2.04E+00	0.47
Th-230	3	1.24E+00	1.30E+00	1.44E+00	1.36E+00	2.04E+00	0.66
Th-230	4	8.49E-01	1.01E+00	1.06E+00	9.95E-01	2.04E+00	0.49

Table 5.4. Sample Results with Positive Detections, the Weighted Average Concentration, and Comparison of the Weighted Average Concentration with the BTV[a, b]

Radionuclide	Location[c]	0–3 cm (pCi g^{-1})	3–6 cm (pCi g^{-1})	6–12 cm (pCi g^{-1})	12-cm weighted average concentration (pCi g^{-1})	BTV (pCi g^{-1})	Ratio to BTV
Th-230	5	1.09E+00	1.08E+00	1.26E+00	1.17E+00	2.04E+00	0.57
Th-230	6	8.02E-01	1.25E+00	1.07E+00	1.05E+00	2.04E+00	0.51
Th-230	8	2.52E+00	2.63E+00	2.65E+00	2.61E+00	2.04E+00	1.28
Th-230	9	2.08E+00	2.05E+00	2.05E+00	2.06E+00	2.04E+00	1.01
Th-232	1	1.21E+00	1.57E+00	1.14E+00	1.26E+00	2.95E+00	0.43
Th-232	10	3.78E-01	4.44E-01	3.55E-01	3.83E-01	2.95E+00	0.13
Th-232	11	7.09E-01	7.44E-01	7.94E-01	7.60E-01	2.95E+00	0.26
Th-232	13	8.83E-01	8.32E-01	8.48E-01	8.53E-01	2.95E+00	0.29
Th-232	14	8.29E-01	7.30E-01	6.15E-01	6.97E-01	2.95E+00	0.24
Th-232	15	6.99E-01	7.64E-01	7.26E-01	7.29E-01	2.95E+00	0.25
Th-232	16	8.61E-01	7.22E-01	7.67E-01	7.79E-01	2.95E+00	0.26
Th-232	17	3.66E-01	3.93E-01	3.28E-01	3.54E-01	2.95E+00	0.12
Th-232	18	9.14E-01	7.72E-01	8.64E-01	8.54E-01	2.95E+00	0.29
Th-232	2	1.59E+00	1.17E+00	1.28E+00	1.33E+00	2.95E+00	0.45
Th-232	3	1.32E+00	1.25E+00	1.25E+00	1.27E+00	2.95E+00	0.43
Th-232	4	1.12E+00	1.25E+00	1.18E+00	1.18E+00	2.95E+00	0.40
Th-232	5	1.30E+00	1.33E+00	1.33E+00	1.32E+00	2.95E+00	0.45
Th-232	6	4.92E-01	9.06E-01	6.00E-01	6.50E-01	2.95E+00	0.22
Th-232	8	7.71E-01	6.87E-01	8.34E-01	7.82E-01	2.95E+00	0.26
Th-232	9	7.82E-01	6.41E-01	6.07E-01	6.59E-01	2.95E+00	0.22
Th-234	1	1.29E+00	1.16E+00	1.11E+00	1.17E+00	3.04E+00	0.38
Th-234	10	1.68E+00	1.70E+00	1.76E+00	1.73E+00	3.04E+00	0.57
Th-234	11	3.99E+00	4.43E+00	3.67E+00	3.94E+00	3.04E+00	1.30
Th-234	13	1.47E+00	1.24E+00	1.04E+00	1.20E+00	3.04E+00	0.39
Th-234	14	1.27E+00	**0.656**	1.10E+00	1.03E+00	3.04E+00	0.34
Th-234	15	**0.65**	1.91E+00	**0.558**	9.19E-01	3.04E+00	0.30
Th-234	16	1.20E+00	1.03E+00	1.63E+00	1.37E+00	3.04E+00	0.45
Th-234	17	4.17E-01	**0.182**	**0.00**	1.50E-01	3.04E+00	0.05
Th-234	18	1.19E+00	1.65E+00	1.63E+00	1.53E+00	3.04E+00	0.50
Th-234	2	1.51E+00	1.42E+00	2.36E+00	1.91E+00	3.04E+00	0.63
Th-234	3	2.07E+00	1.55E+00	2.09E+00	1.95E+00	3.04E+00	0.64
Th-234	4	1.29E+00	9.03E-01	1.05E+00	1.07E+00	3.04E+00	0.35
Th-234	5	2.11E+00	1.27E+00	1.20E+00	1.45E+00	3.04E+00	0.48
Th-234	6	**0.00**	9.79E-01	1.12E+00	8.05E-01	3.04E+00	0.26
Th-234	8	2.43E+00	2.25E+00	2.89E+00	2.62E+00	3.04E+00	0.86
Th-234	9	**0.00**	1.04E+00	1.29E+00	9.05E-01	3.04E+00	0.30
Tl-208	1	4.94E-01	4.74E-01	5.39E-01	5.12E-01	9.23E-01	0.55
Tl-208	10	1.17E-01	1.21E-01	1.51E-01	1.35E-01	9.23E-01	0.15
Tl-208	11	4.43E-01	4.31E-01	4.61E-01	4.49E-01	9.23E-01	0.49
Tl-208	13	4.13E-01	4.11E-01	3.49E-01	3.81E-01	9.23E-01	0.41
Tl-208	14	3.08E-01	2.65E-01	2.96E-01	2.91E-01	9.23E-01	0.32
Tl-208	15	3.07E-01	3.10E-01	3.25E-01	3.17E-01	9.23E-01	0.34
Tl-208	16	3.22E-01	2.81E-01	3.06E-01	3.04E-01	9.23E-01	0.33
Tl-208	17	1.26E-01	1.14E-01	1.12E-01	1.16E-01	9.23E-01	0.13
Tl-208	18	3.69E-01	3.70E-01	3.74E-01	3.72E-01	9.23E-01	0.40
Tl-208	2	5.21E-01	5.28E-01	5.54E-01	5.39E-01	9.23E-01	0.58
Tl-208	3	5.10E-01	5.36E-01	5.77E-01	5.50E-01	9.23E-01	0.60
Tl-208	4	4.45E-01	4.65E-01	4.67E-01	4.61E-01	9.23E-01	0.50
Tl-208	5	5.20E-01	5.71E-01	4.78E-01	5.12E-01	9.23E-01	0.55
Tl-208	6	1.89E-01	2.57E-01	3.70E-01	2.97E-01	9.23E-01	0.32
Tl-208	8	2.76E-01	3.04E-01	2.78E-01	2.84E-01	9.23E-01	0.31
Tl-208	9	2.69E-01	2.71E-01	2.65E-01	2.68E-01	9.23E-01	0.29
U-232	18	**0.0143**	**-0.0315**	8.53E-02	3.84E-02	5.65E-02	0.68
U-233/234	1	9.69E-01	9.64E-01	9.77E-01	9.71E-01	1.87E+00	0.52

Table 5.4. Sample Results with Positive Detections, the Weighted Average Concentration, and Comparison of the Weighted Average Concentration with the BTV[a, b]

Radionuclide	Location[c]	0–3 cm (pCi g^{-1})	3–6 cm (pCi g^{-1})	6–12 cm (pCi g^{-1})	12-cm weighted average concentration (pCi g^{-1})	BTV (pCi g^{-1})	Ratio to BTV
U-233/234	10	1.54E+00	1.44E+00	1.63E+00	1.56E+00	1.87E+00	0.83
U-233/234	11	2.81E+00	3.13E+00	3.28E+00	3.13E+00	1.87E+00	1.67
U-233/234	13	9.64E-01	8.24E-01	1.01E+00	9.52E-01	1.87E+00	0.51
U-233/234	14	7.04E-01	8.31E-01	7.43E-01	7.55E-01	1.87E+00	0.40
U-233/234	15	6.41E-01	6.60E-01	6.12E-01	6.31E-01	1.87E+00	0.34
U-233/234	16	1.09E+00	1.05E+00	1.08E+00	1.08E+00	1.87E+00	0.57
U-233/234	17	2.98E-01	3.29E-01	2.47E-01	2.80E-01	1.87E+00	0.15
U-233/234	18	9.29E-01	9.24E-01	9.48E-01	9.37E-01	1.87E+00	0.50
U-233/234	2	1.02E+00	8.87E-01	7.82E-01	8.68E-01	1.87E+00	0.46
U-233/234	3	1.17E+00	1.39E+00	1.69E+00	1.49E+00	1.87E+00	0.79
U-233/234	4	1.03E+00	1.09E+00	9.29E-01	9.95E-01	1.87E+00	0.53
U-233/234	5	1.13E+00	9.17E-01	1.13E+00	1.08E+00	1.87E+00	0.58
U-233/234	6	5.47E-01	1.03E+00	9.08E-01	8.48E-01	1.87E+00	0.45
U-233/234	8	2.16E+00	2.10E+00	2.24E+00	2.19E+00	1.87E+00	1.17
U-233/234	9	7.88E-01	1.06E+00	1.09E+00	1.01E+00	1.87E+00	0.54
U-235/236	1	1.08E-01	7.08E-02	6.11E-02	7.53E-02	1.30E-01	0.58
U-235/236	10	1.50E-01	6.93E-02	1.33E-01	1.21E-01	1.30E-01	0.93
U-235/236	11	1.98E-01	1.85E-01	2.78E-01	2.35E-01	1.30E-01	1.81
U-235/236	13	6.55E-02	**0.0531**	**0.0346**	4.70E-02	1.30E-01	0.36
U-235/236	15	4.74E-02	4.65E-02	**0.0156**	3.13E-02	1.30E-01	0.24
U-235/236	16	2.44E-01	1.13E-01	2.25E-01	2.02E-01	1.30E-01	1.55
U-235/236	17	**0.0198**	2.78E-02	**0.0128**	1.83E-02	1.30E-01	0.14
U-235/236	18	4.28E-02	5.49E-02	**0.0432**	4.60E-02	1.30E-01	0.35
U-235/236	2	7.10E-02	5.44E-02	7.25E-02	6.76E-02	1.30E-01	0.52
U-235/236	3	8.32E-02	9.02E-02	1.80E-01	1.33E-01	1.30E-01	1.03
U-235/236	4	1.02E-01	1.64E-01	1.25E-01	1.29E-01	1.30E-01	0.99
U-235/236	5	8.49E-02	**0.0366**	**0.0546**	5.77E-02	1.30E-01	0.44
U-235/236	6	**0.018**	6.90E-02	5.32E-02	4.84E-02	1.30E-01	0.37
U-235/236	8	1.75E-01	2.38E-01	1.47E-01	1.77E-01	1.30E-01	1.36
U-235/236	9	8.20E-02	**0.0353**	1.36E-01	9.73E-02	1.30E-01	0.75
U-238	1	9.26E-01	1.02E+00	1.13E+00	1.05E+00	1.68E+00	0.63
U-238	10	1.43E+00	1.42E+00	1.74E+00	1.58E+00	1.68E+00	0.94
U-238	11	2.73E+00	3.01E+00	3.41E+00	3.14E+00	1.68E+00	1.87
U-238	13	1.00E+00	7.95E-01	1.09E+00	9.94E-01	1.68E+00	0.59
U-238	14	7.76E-01	6.91E-01	6.78E-01	7.06E-01	1.68E+00	0.42
U-238	15	6.21E-01	6.70E-01	6.25E-01	6.35E-01	1.68E+00	0.38
U-238	16	1.23E+00	1.28E+00	1.29E+00	1.27E+00	1.68E+00	0.76
U-238	17	3.23E-01	2.77E-01	3.15E-01	3.08E-01	1.68E+00	0.18
U-238	18	8.46E-01	9.01E-01	9.05E-01	8.89E-01	1.68E+00	0.53
U-238	2	9.20E-01	9.22E-01	9.62E-01	9.42E-01	1.68E+00	0.56
U-238	3	1.19E+00	1.50E+00	1.63E+00	1.49E+00	1.68E+00	0.89
U-238	4	9.11E-01	1.09E+00	8.95E-01	9.48E-01	1.68E+00	0.56
U-238	5	9.61E-01	1.18E+00	1.12E+00	1.10E+00	1.68E+00	0.65
U-238	6	4.82E-01	9.96E-01	9.66E-01	8.53E-01	1.68E+00	0.51
U-238	8	2.18E+00	2.37E+00	2.16E+00	2.22E+00	1.68E+00	1.32
U-238	9	7.90E-01	8.32E-01	1.07E+00	9.41E-01	1.68E+00	0.56

a. BTV ratios greater than 1.0 are shaded.

b. Non-detect values are identified in **bold**. A ***bold italic*** value represents the average of the primary sample and laboratory duplicate where either the primary or duplicate was a nondetect.

c. All sample results represent the average concentration reported in the primary sample and any laboratory duplicates. Concentrations for location 1 represent the average of the primary samples (1A, 1B, 1C) and the sample duplicate (1A-D, 1B-D, and 1C-D) including any laboratory duplicates.

5.3.1. Samples that Exceed the BTV

Sample locations with weighted average radionuclide concentrations that exceeded the BTV value were at locations inside the deposition plume, outside the deposition plume, and at background locations (Table 5-5). Analytical uncertainty was propagated through to the weighted average concentration using Equation 5-4 (Bevington and Robinson 1992)

$$\sigma_w = \sqrt{\frac{a^2\sigma_a^2 + b^2\sigma_b^2 + c^2\sigma_c^2}{(a+b+c)^2}} \tag{5-4}$$

where

σ_w	=	standard deviation of weighted mean concentration (pCi g^{-1})
σ_a	=	analytical uncertainty in the 0-3 cm layer (pCi g^{-1})
σ_b	=	analytical uncertainty in the 3-6 cm layer (pCi g^{-1})
σ_c	=	analytical uncertainty in the 6-12 cm layer (pCi g^{-1})
a, b, c	=	3 cm, 3 cm, and 12 cm, respectively.

Analytical uncertainties for each measurement are presented in Appendix B. A one-tailed *t*-test was performed to test whether the measured concentration was greater than the BTV value (α=0.025, df=∞, t=1.98). Thus, the null and alternative hypothesis and calculated *t* value are:

$$\begin{aligned} H_o &: \bar{X} \le BTV \\ H_a &: \bar{X} > BTV \\ t &= \frac{\bar{X} - BTV}{\sigma} \end{aligned} \tag{5-5}$$

Most sample/BTV ratios were less than 1.5. Many of the weighted average concentrations were not significantly higher than the BTV value and were taken in a geologic formation that differed from the formations sampled for the EPA background study (noted in Table 5.4). Thorium-229 had some of the highest BTV ratios, but weighted average concentrations were not significantly higher than the BTV value and these samples were taken at background location 1 (Rocky Peak north of SSFL). Background location 1 was outside the plume and upwind of the SSFL, therefore the concentrations cannot be attributed to the Woolsey Fire or SSFL operations.

Other radionuclides with a weighted-average concentration significantly greater than the BTV value were ^{226}Ra, ^{230}Th, and uranium isotopes, all of which are naturally occurring. Most of these samples were taken at either a background location, in a different geologic formation than the EPA background study, or outside the plume, except ^{226}Ra at location 13. Radium-226 at location 13 was only slightly above the BTV (BTV ratio of 1.14) and did show a decrease in concentration with depth; however, none of the other sample locations in that vicinity (14, 15, and 18) were above background or showed a decrease in concentration with depth. If the ^{226}Ra depth profile observed at location 13 was from plume deposition, then we would expect to see similar depth profiles at locations 14, 15, and 18, all of which were located less than a kilometer from one another. Moreover, ^{230}Th and ^{226}Ra had concentrations close to one another (2.30 and 2.35 pCi g^{-1}, respectively), as would be expected in the natural environment. Thorium-230 and ^{226}Ra are naturally occurring radionuclides and would exhibit natural variability in the environment. Given

the fact that BTV ratios were close to 1.0, we conclude that the ^{226}Ra detected at sample location 13 was from natural sources.

Table 5.5. Sample Results that have a Weighted Average Concentration Greater than the BTV

Radio-nuclide	Location	BTV (pCi/g)	12-cm weighted average with uncertainty (pCi g^{-1})	Ratio to BTV	Significant?[a]	In plume?	Notes
K-40	6	30.5	31.0±0.281	1.02	No	Yes	Natural background radionuclide
Pb-210	5	2.07	2.16±0.217	1.04	No	No	Background location and natural background radionuclide
Po-210	11	2.09	2.29±0.230	1.09	No	No	Different geologic formation than SSFL or EPA background formations
Ra-226	11	1.88	2.84±0.027	1.51	Yes	No	Different geologic formation than SSFL or EPA background formations
Ra-226	13	1.88	2.15±0.025	1.14	Yes	Yes	Natural background radionuclide – see discussion
Ra-226	8	1.88	2.07±0.031	1.10	Yes	Yes	Different geologic formation than SSFL or EPA background formations
Th-229	1	0.046	0.088±0.037	1.91	No	No	Background location
Th-229	4	0.046	0.070±0.017	1.50	No	No	Background location
Th-229	5	0.046	0.048±0.022	1.04	No	No	Background location
Th-230	11	2.04	2.85±0.246	1.40	Yes	No	Different geologic formation than SSFL or EPA background formations (Chatsworth and Santa Susana)
Th-230	13	2.04	2.24±0.141	1.10	No	Yes	Natural background radionuclide
Th-230	8	2.04	2.61±0.300	1.28	No	Yes	Different geologic formation than SSFL or EPA background formations (Chatsworth and Santa Susana)
Th-230	9	2.04	2.06±0.150	1.01	No	Yes	Different geologic formation than SSFL or EPA background formations (Chatsworth and Santa Susana)
Th-234	11	3.04	3.94±0.570	1.30	No	No	Different geologic formation than SSFL or EPA background formations. A short-lived progeny of U-238 and will not exist in nature without the presence of U-238
U-233/234	11	1.87	3.13±0.143	1.67	Yes	No	Different geologic formation than SSFL or EPA background formations (Chatsworth and Santa Susana)
U-233/234	8	1.87	2.19±0.106	1.17	Yes	Yes	Different geologic formation than SSFL or EPA background formations (Chatsworth and Santa Susana)
U-235/236	11	0.130	0.235±0.044	1.81	Yes	No	Different geologic formation than SSFL or EPA background formations (Chatsworth and Santa Susana)
U-235/236	16	0.130	0.202±0.035	1.55	Yes	Yes	Different geologic formation than SSFL or EPA background formations (Chatsworth and Santa Susana)

Radio-nuclide	Location	BTV (pCi/g)	12-cm weighted average with uncertainty (pCi g^{-1})	Ratio to BTV	Significant?[a]	In plume?	Notes
U-235/236	3	0.130	0.133±0.033	1.03	No	No	Natural background radionuclide
U-235/236	8	0.130	0.177±0.030	1.36	No	Yes	Different geologic formation than SSFL or EPA background formations (Chatsworth and Santa Susana)
U-238	11	1.68	3.14±0.144	1.87	Yes	No	Different geologic formation than SSFL or EPA background formations (Chatsworth and Santa Susana)
U-238	8	1.68	2.22±0.106	1.32	Yes	Yes	Different geologic formation than SSFL or EPA background formations (Chatsworth and Santa Susana)

a. The calculated *t*-value exceeded 1.98.

5.3.2. Results from TestAmerica Laboratory of Sample Split at Location 2

A split sample was taken at location 2, which was outside the plume and located about 500 m west of the EPA background location identified as Bridal Path. A complete tabulation of results including analytical uncertainty is provided in Appendix B. Table 5-6 shows the results that were positively detected according to the criteria in Section 5.2.3 and the BTV ratio. Uncertainty in the weighted average concentration was calculated using Equation 5-4. TestAmerica provided the analytical results for the primary and laboratory duplicate surface sample, and the values presented in Table 5-6 represent the average of the primary and laboratory duplicate sample. Table 5-7 shows a comparison of the TestAmerica results to those of GEL, where both the GEL and TestAmerica results were positively detected according to the criteria stated in Section 5.2.3. Analytical uncertainty was propagated using Equation 5-4 and a two-tailed t-test was performed using methods described in Appendix C. The ratio of the TestAmerica results to that of GEL ranged from 0.43 to 1.56, with an average ratio of 0.91. We conclude that for radionuclides that were positively detected, the TestAmerica results are comparable to the GEL results. Weighted-average concentrations of ^{228}Ac and ^{228}Ra were significantly different between GEL and TestAmerica at the p=0.05 level but not the p=0.025 level. All other weighted-average concentrations between GEL and Test America were not significantly different from one another at the p=0.05 level.

Table 5.6. Sample Results from TestAmerica with Positive Detections, the Weighted Average Concentration, and Comparison of the Weighted Average Concentration with the BTV

Radionuclide	0–3 cm (pCi g^{-1})[a]	3–6 cm (pCi g^{-1})	6–12 cm (pCi g^{-1})	Weighted average with uncertainty (pCi g^{-1})	Ratio to BTV	Significant?[b]
Ac-228	1.553	1.46	1.56	1.50±0.110	0.652	No
Bi-212	1.576	1.55	1.65	1.62±0.162	0.795	No
C-14	0.608	0.364	1.05	0.770±0.378	0.303	No
Cs-134	0.00391	0.08076	0.0948	0.058±0.013	1.94	Yes
Cs-137	0.0713	0.06322	0.0731	0.067±0.014	0.345	No

Radionuclide	0–3 cm (pCi g^{-1})[a]	3–6 cm (pCi g^{-1})	6–12 cm (pCi g^{-1})	Weighted average with uncertainty (pCi g^{-1})	Ratio to BTV	Significant?[b]
Eu-155	0.111	0.09216	0.138	0.12±0.033	0.588	No
K-40	20.5	21.19	21.1	20.7±1.440	0.677	No
Nb-94	0.00197	0.01615	-0.00464	0.004±0.012	0.222	No
Pb-210	1.29	1.435	1.35	1.33±0.383	0.642	No
Pb-212	1.59	1.602	1.71	1.62±0.120	0.608	No
Po-210	0.582	0.6302	0.494	0.54±0.058	0.258	No
Pu-241	1.65	1.382	0.125	0.85±0.577	2.45	No
Ra-226	1.38	1.338	1.42	1.37±0.100	0.7286	No
Ra-228	1.46	1.553	1.56	1.50±0.110	0.652	No
Th-228	1.38	1.316	1.36	1.34±0.117	0.366	No
Th-229	0.03	0.03028	-0.0104	0.002±0.012	0.0505	No
Th-230	1.00	1.331	0.859	0.96±0.094	0.471	No
Th-231	0.0748	0.1177	0.138	0.12±0.051	0.894	No
Th-232	1.35	1.217	1.17	1.21±0.107	0.411	No
Th-234	0.0748	0.9809	1.02	0.84±0.149	0.275	No
Tl-208	0.508	0.5015	0.539	0.52±0.040	0.563	No
U-238	2.12	1.038	0.844	1.08±0.127	0.642	No

a. Average of the sample and the laboratory duplicate
b. The calculated *t*-value exceeded 1.98.

Two radionuclides exceeded the BTV value in the TestAmerica results (Table 5-6): ^{134}Cs and ^{241}Pu but only ^{134}Cs was significantly different. These radionuclides are not priority-1 radionuclides. Location 2 is located 8.5 km west of the western edge of the SSFL site and is outside the Woolsey Fire particulate deposition plume area. Based on the annual wind rose (Figure 5-4), location 2 was very unlikely to have been impacted by the SSFL operations in the past. Winds would have had to come out of the east for any airborne contamination to impact location 2. Based on the annual wind rose, this occurs only 2% of the time. The EPA concluded in its background study that this location is unimpacted by the SSFL. These conclusions, along with the fact that the highest concentrations of ^{241}Pu and ^{134}Cs occurred at depth, means that ^{241}Pu and ^{134}Cs at location 2are not attributed to the Woolsey Fire or the SSFL operations in the past.

The detections of ^{134}Cs and ^{241}Pu are likely not accurate measurements for the reasons discussed below. First, ^{134}Cs was not detected in a reanalysis of the 0–3 cm surface sample, suggesting that the results for ^{134}Cs are questionable. Cesium-134 has a half-life of 2.0648 years, and in the 2011 EPA background study, almost all the ^{134}Cs samples were less than the MDC and were flagged as being subject to spectral interference. The ^{134}Cs MDC for the EPA background study was approximately 0.3 pCi g^{-1} and would have been adequate to detect the 0–12 cm weighted average concentration measured in this current study if the measured concentrations are accurate. Thus, if the ^{134}Cs measurement at sample location 2 was accurate, then it would have to have been deposited between the time of the EPA background study (2011) and the time of this study (2019).

As stated earlier in Section 4.2.1, it is possible ^{134}Cs could be attributed to the Fukushima accident, but if this were the case, then ^{137}Cs concentration would be higher than ^{134}Cs which was not the case. Thus, it seems likely that the ^{134}Cs measurement reflects spectral interference and is not accurate.

The ^{241}Pu sample was positively detected in the 0–3 cm and 0–6 cm layer but undetected in the 6–12 cm layer. Plutonium-241 would be associated with ^{239}Pu and, as discussed in Section 4.2.1, the ^{241}Pu/^{239}Pu activity ratio from weapons testing fallout accounting for decay would be approximately 0.93 in 2019. Thus, if the measurement were accurate and the activity was from weapons fallout origin, we would expect to see ^{239}Pu at roughly the same concentration as ^{241}Pu.

The ^{241}Pu measurements in the 2011 EPA background study were all flagged as non-detects with an MDC of approximately 0.6 pCi g^{-1}. The MDC for ^{241}Pu in the EPA background study would have been adequate to detect the 0–12 cm weighted average concentration measured in this current study if the measured concentrations are accurate. Because ^{239}Pu was undetected in the TestAmerica samples and EPA did not detect ^{241}Pu in their sampling performed in 2009, the ^{241}Pu activity cannot be attributed to past weapons fallout.

Thus, if the ^{241}Pu measurements at sample location 2 were accurate, then it would have had to have been deposited between the time of the EPA background study (2011) and time of this study (2019). As stated earlier in Section 4.2.1, it was not likely the ^{241}Pu could be attributed to the Fukushima accident. The measured concentration by TestAmerica exceeds the highest concentrations measured in Japan after the Fukushima accident (Yang et al. 2015). Plutonium-241 is a low-energy beta emitter with a mean beta energy (5.2 keV) that is close to that of ^{3}H (5.7 keV) (Browne and Firestone 1986). If the sample contained any ^{3}H, it would have been impossible to distinguish the ^{241}Pu beta from the ^{3}H beta. Thus, because it is possible that other beta interferences may be present in the sample and there is no conceivable source of the ^{241}Pu, it seems likely that the ^{241}Pu measurement is not accurate.

Table 5.7. Ratio of the TestAmerica Result to GEL for Radionuclides Positively Detected by TestAmerica and GEL

	Ratio of TestAmerica to GEL			TestAmerica weighted average with uncertainty (pCi g^{-1})	GEL weighted average with uncertainty (pCi g^{-1})
	0–3 cm	3–6 cm	6–12 cm		
Ac-228	0.88	0.80	0.89	1.50±0.11	1.74±0.06
Bi-212	0.85	0.79	0.99	1.62±0.16	1.81±0.15
Cs-137	1.11	0.74	1.56	0.07±0.01	0.06±0.01
K-40	0.95	0.95	0.94	20.8±1.44	22.0±0.28
Pb-210	1.34	1.01	0.56	1.33±0.38	1.78±0.08
Pb-212	0.65	0.89	0.99	1.50±0.12	1.71±0.02
Po-210	0.68	0.73	0.65	0.54±0.06	0.80±0.15
Ra-226	1.05	0.94	0.99	1.37±0.10	1.38±0.03
Ra-228	0.88	0.80	0.89	1.50±0.11	1.74±0.06
Th-228	1.14	1.02	1.05	1.34±0.12	1.27±0.13
Th-230	0.89	1.17	0.93	0.92±0.09	0.95±0.11
Th-232	0.81	1.05	0.91	1.21±0.11	1.33±0.12

	Ratio of TestAmerica to GEL			TestAmerica weighted average with uncertainty (pCi g^{-1})	GEL weighted average with uncertainty (pCi g^{-1})
	0–3 cm	3–6 cm	6–12 cm		
Th-234	0.69	0.55	0.43	0.96±0.15	1.91±0.85
Tl-208	0.97	0.94	0.97	0.52±0.04	0.54±0.02
U-238	1.12	1.14	0.88	0.94±0.13	0.94±0.07

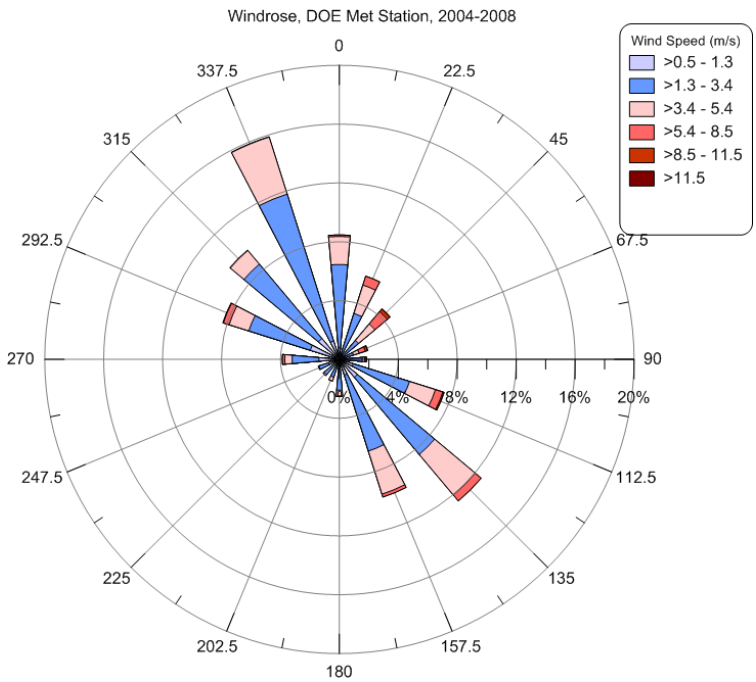

Figure 5-4. Annual wind rose measured at DOE meteorological tower from 2004 to 2008.

5.3.3. Radionuclide Concentration Cross Section across the Deposition Plume

Another way to view the results is to plot a cross section across the deposition plume. The cross-section line is illustrated in Figure 5-5. A cross section of the terrain and geology show the different geologic formations that are exposed on the surface (Figure 5-6) and was constructed from the geologic map provided in Yerks and Campbell (2005). Not shown in Figure 5-6 are the folds, faults, formation thickness, and other structural features. Thus, the geology shown in the figure is extremely simplified and does not show the structural complexity below the ground surface. The Cretaceous-age Chatsworth formation is the oldest formation and presumably underlies most of the region. It is overlain by the Tertiary-age Santa Susana formation, Modelo formation, and Towsley formation. In places, the Calabasas formation is unconformable above the Chatsworth formation in steeply dipping beds. Surface alluvium is present in drainage basins and in the western portion of the San Fernando valley between sample locations 10 and 11.

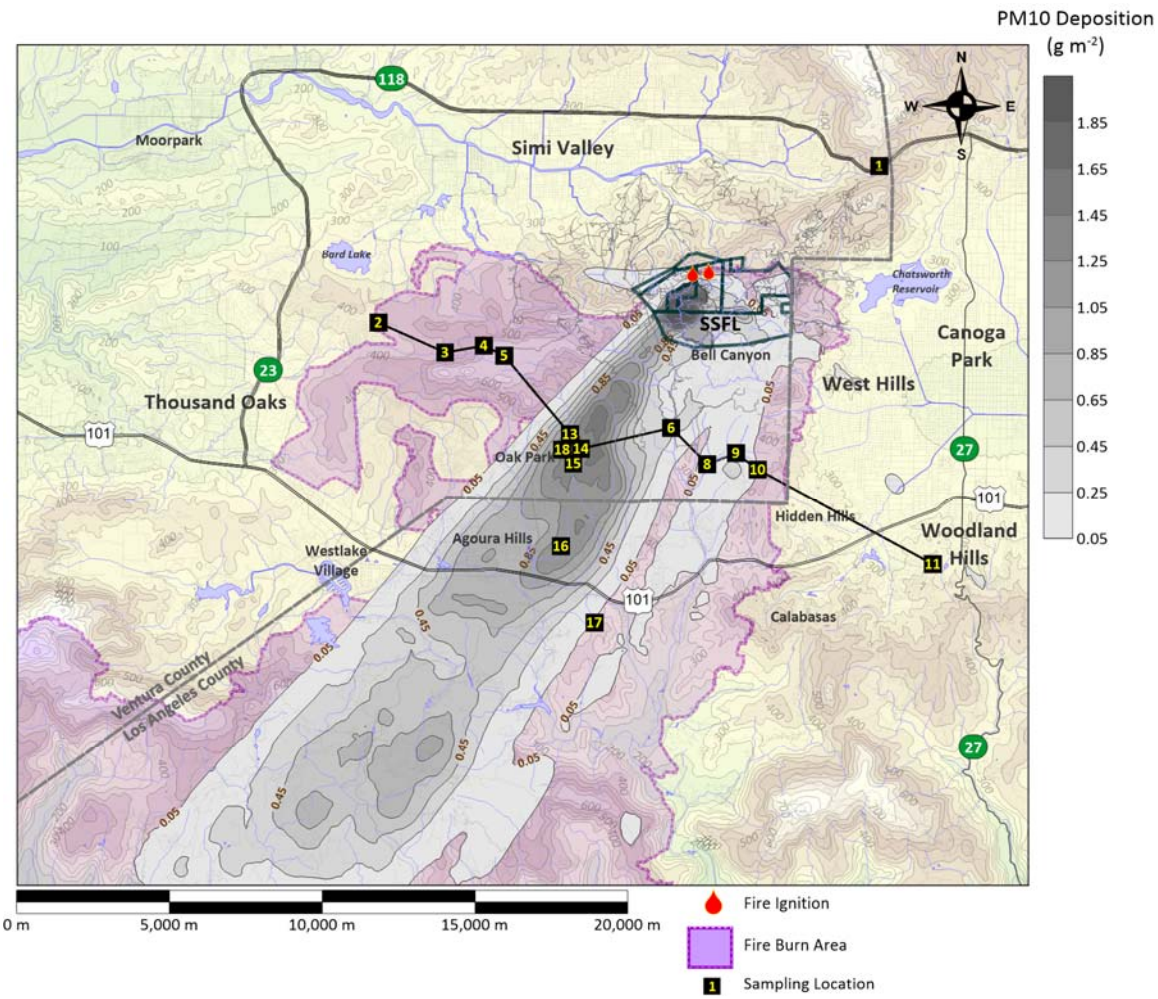

Figure 5-5. Plume deposition map showing cross-section line and terrain elevations. Cross-section line starts at sample location 2 and proceeds east to sample locations 3, 4, 5, 13, 14, 6, 8, 9, 10, and 11.

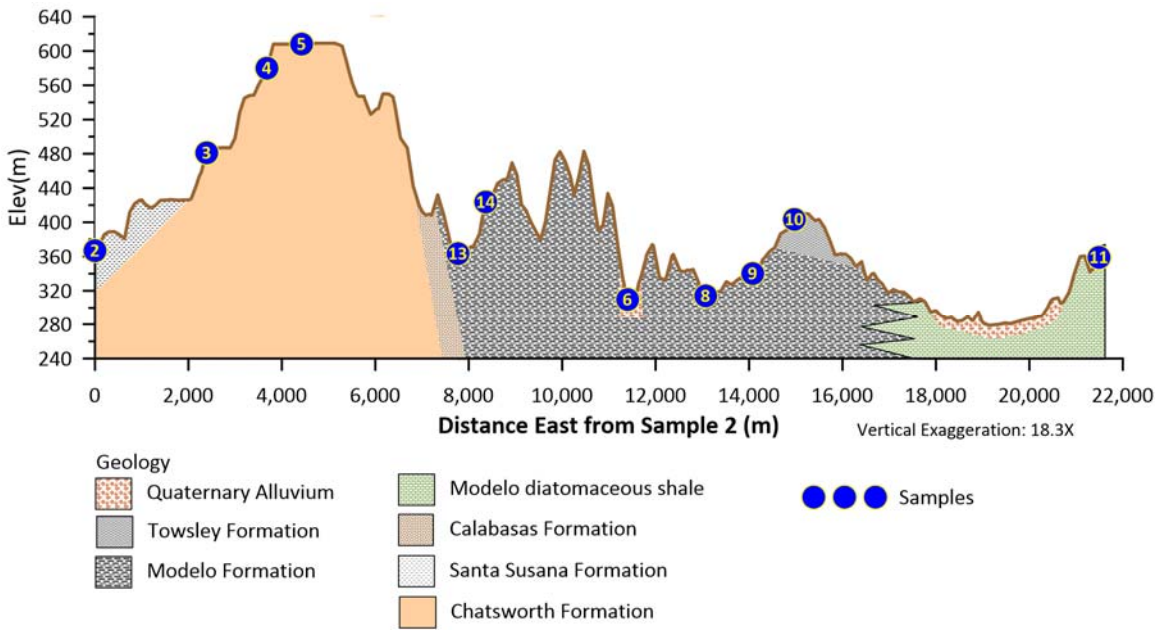

Figure 5-6. Terrain and simplified geologic cross section showing sample locations and geologic formations that are expressed on the surface. Folds, faults, and other structural features are not shown.

The deposition plume cross section and measured radionuclide concentrations in the 0–3 cm layer for priority-1 radionuclides that were positively detected at all locations in the cross section (Figure 5-7) show that (1) there are no discernable trends in anthropogenic radionuclide concentrations that would correspond to deposition from the plume and (2) concentrations for some naturally occurring radionuclides are related to the geology.

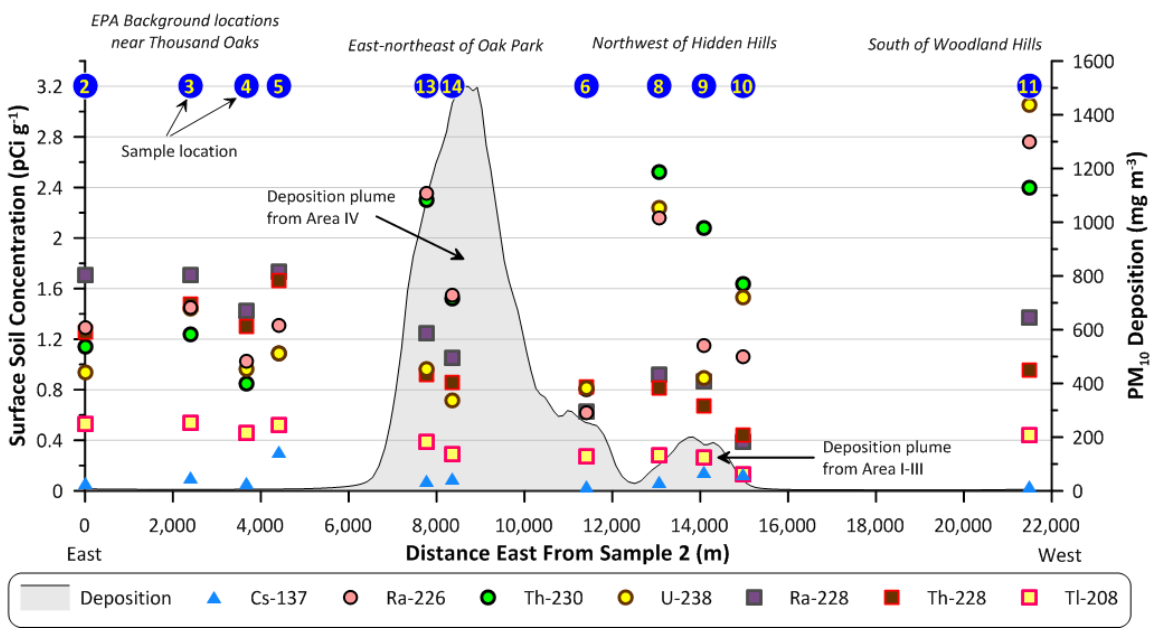

Figure 5-7. Deposition plume (gray-shaded region, right axis) and radionuclide concentrations (left axis) that were detected in 0–3 cm layer at all sample locations.

All sample results are generally within the range of expected natural background or fallout concentrations in the case of ^{137}Cs. Plutonium-239 was not detected in any of the surface or subsurface soils, and ^{90}Sr was only detected at location 5 which was outside the deposition plume. Sample 13, located in the center of the plume, is in the Modelo formation and exhibited higher ^{226}Ra and ^{230}Th concentrations compared to background locations 2, 3, 4, and 5. Radium-226 and ^{230}Th concentrations for sample 14 (located ~500 m SE of location 13) were nearly the same as the background values. Uranium concentrations were about the same as the background locations. As discussed earlier, the higher ^{226}Ra and ^{230}Th at location 13 was not attributed to deposition. Location 6 was in alluvium and exhibited the lowest concentrations of all the locations. The ^{137}Cs concentrations at location 6 show no discernable depth profile, and thus, the sediments have probably been reworked since weapons fallout.

Analysis of the depth profiles is important for understanding the source of the radionuclides measured in the soil sample. Radionuclides that deposit from the atmosphere and are relatively immobile in soil would be initially present only in the surface soil. Over time, (tens of years) leaching and physical processes will transport radionuclides deposited on the surface to deeper layers. If the soil is disturbed, then the depth profile will be altered and not show a clear decrease of concentration with depth. Figure 5-8 shows the depth profiles for ^{137}Cs and uranium decay series radionuclides (^{238}U, ^{230}Th, ^{226}Ra) at locations 5, 14, and 11. The depth profiles for ^{137}Cs show a clear decrease of concentration with depth (location 11 actually shows an increase in concentration in the 6–12 cm layer, but the concentration is not statistically different from the 3–6 cm layer [α = 0.05]). This is especially clear at location 5 where the concentration in the surface layer is almost a factor of 3 higher than in the 3–6 cm layer. A similar depth profile is observed if the radionuclide *inventories* in each layer are plotted instead of the concentration. The difference in the ^{137}Cs *inventory* in the surface and in the 3–6 cm layer in sample 5 is even greater (surface layer inventory is 3.7 times the inventory in the 3–6 cm layer). Thus, the ^{137}Cs profiles indicate atmospheric weapons testing fallout. The uranium series radionuclides have concentrations that vary within each of the layers but do not exhibit a consistent depth profile as observed with ^{137}Cs. These depth profiles and the fact that the relative proportion of the uranium series radionuclides remains the same with depth indicates a natural source.

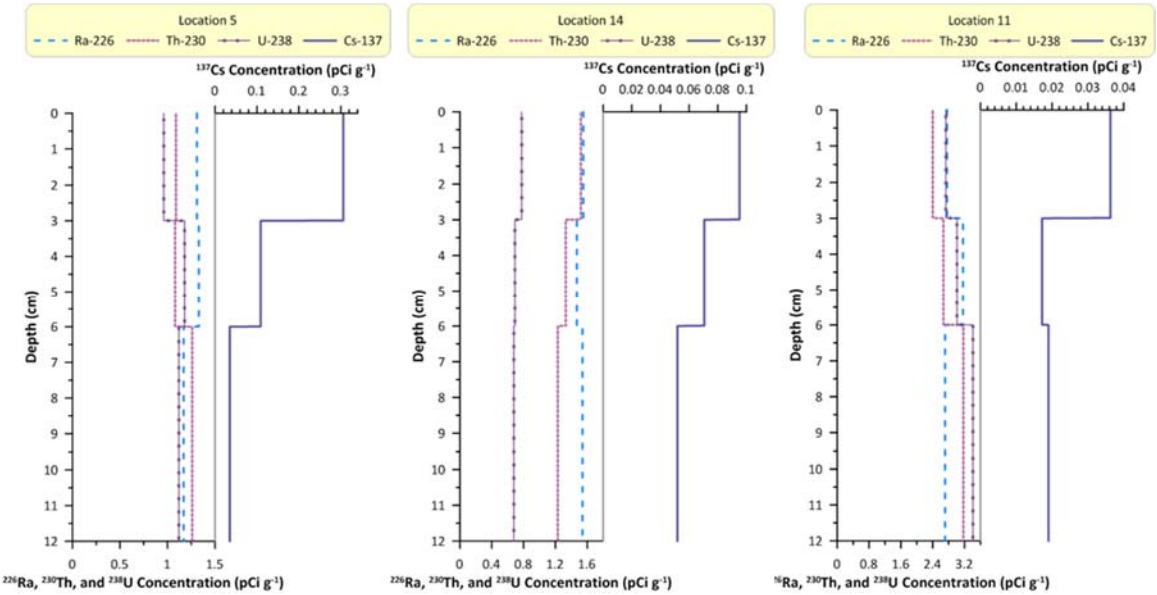

Figure 5-8. Depth profiles for ^{226}Ra, ^{230}Th, ^{238}U, and ^{137}Cs at locations 5 (background), 14 (center of plume), and 11 (east of plume). Cesium-137 soil concentrations are highest in the surface and generally decrease with depth, which is expected in undisturbed soil containing atmospheric fallout from weapons testing. Uranium decay-chain radionuclides exhibit a more-or-less uniform depth distribution, as would be expected for radionuclides of natural origin.

The highest uranium series concentrations were observed well outside the plume at location 11 in the diatomaceous shale member of the Modelo formation. The uranium and thorium series depth profiles at location 11 exhibit slightly higher concentrations at depth, and thus are of natural origin and not from any recent or past atmospheric source.

The highest thorium series concentrations were observed at background sampling locations 2, 3, 4, and 5, and outside the deposition plume. The highest ^{137}Cs concentration in the surface soil (0–3 cm) was observed outside the plume at background location 5.

Statistical tests (see Appendix D) were used to determine if a significant difference exists between mean radionuclide concentrations for background samples taken in the Chatsworth formation (samples 1, 3, 4, and 5) and those taken in the Modelo formation and within the deposition plume (samples 8, 9, 13, 14, 15, and 18). At the 95% confidence level ($\alpha = 0.05$), there was no significant difference between the mean ^{226}Ra concentrations in the 0–3 cm and 3–6 cm layer, but there was a significant difference in the 6–12 cm layer. For ^{230}Th, ^{234}U, and ^{238}U there was no significant difference between concentrations in the Chatsworth and Modelo formation in all layers, and thus no significant difference between sample locations in and outside the plume. For ^{232}Th, ^{228}Th, ^{228}Ra, and ^{208}Tl (thorium decay series), a significant difference was observed between the two formations in all layers.

A second analysis was performed for the thorium series radionuclides to test whether the concentrations were significantly higher in the Modelo formation. The results showed that thorium decay series radionuclide concentrations in the Modelo formation and within the plume were *lower* compared to the background samples taken outside the plume and in the Chatsworth formation ($p < 0.005$).

Overall, the cross-section and depth profiles show there is no evidence of radionuclides potentially from the SSFL in the deposition plume, and soil concentrations reflect natural variability and variability among the geologic formations, with the Modelo formation generally having lower thorium series concentrations compared to the Chatsworth formation that underlies most of the SSFL. If the plume from the Woolsey Fire deposited significant radionuclides of SSFL origin, then it would have been reflected in the surface soil concentrations. Thus, sample locations 13 and 14, which had the highest PM_{10} deposition would have been expected to have the highest concentration of radionuclides. But that was not the case. The highest concentrations were generally observed at location 8 and 11 for the uranium series radionuclides, locations 2, 3, 4, and 5 for the thorium series, and location 5 for ^{137}Cs. Cesium-137, in particular, would have shown the strongest deposition signature in the plume because it has the highest measured soil concentrations on the SSFL. Instead the measured ^{137}Cs concentrations in all soil samples reflect deposition amounts consistent with global weapons fallout.

5.3.4. Summary of Findings from Sampling Analysis

Radionuclides exist in the environment independent of SSFL operations, including those that occur naturally and those that may have been introduced as part of global weapons testing fallout. As a result, background concentrations of many radionuclides are expected to be found in soil samples collected anywhere. Because background levels can vary geographically, the EPA BTVs (background levels) developed for the geologic formations in the SSFL area were used to evaluate whether there was any indication of concentrations above what would normally be expected in the environment around SSFL. Sampling was conducted in geologic formations that were not sampled as part of the EPA background study and were shown to have background radionuclide concentrations that differed from those sampled by the EPA.

If SSFL-derived radionuclides were released from vegetation and surface soil during the fire, then they would be expected to follow the transport and deposition of similar particulate matter that is naturally emitted during the fire. Comparison of predicted and observed particulate matter concentrations at on-site sampling locations indicated that FEPS and CALPUFF provide a reliable model for the emission, transport, and deposition of particulate matter from the fire. The plume deposition footprint using the FEPS and CALPUFF model was about the same as the footprint published in the DTSC report for the Woolsey Fire, which provides a second check on the FEPS/CALPUFF modeling. Furthermore, measurements made by EPA and reported in the DTSC report also concluded that there was no evidence of radionuclides in off-site soil and sediment of SSFL origin in the Bell Canyon community.

In addition to making comparisons to background, two other observations are important to consider in determining whether there is any evidence of impacts from the fire on the surface soils in the region impacted by deposition plume from the Woolsey Fire burning on the SSFL. The first observation is an evaluation of the data spatially based on the sample locations and their proximity to the deposition footprint from the Woolsey Fire (see Figure 5-7). If the Woolsey Fire had resulted in measurable deposition of radionuclides specific to the SSFL at downwind locations, concentrations would be expected to be greater in the zones of maximum deposition. The data did not support this assertion. It was shown that a hypothetical release of ^{137}Cs, ^{90}Sr, or ^{239}Pu from the fire that would result in an annual dose of 0.1 mrem would be detected above background in the surface soil. No such concentrations were observed in the sampling. Furthermore, the highest

measured ^{137}Cs soil concentrations were observed *outside* the plume. All ^{137}Cs soil concentrations were below the EPA BTV. The second observation is an evaluation of the data by sample depth. If the Woolsey Fire had a measurable impact at downwind locations, concentrations would be expected to be greater in the 0–3 cm surface layer than in lower layers (i.e., 3–6 and 6–12 cm). For ^{137}Cs, higher concentrations are expected in the surface soil layer for locations undisturbed since global fallout occurred because ^{137}Cs was deposited on the surface and has limited mobility to migrate downward into the soil other than by mechanical disturbance (e.g., flooding, plowing, development). Likewise, radium, thorium, and—under reducing conditions—uranium have low mobility in soil. The highest concentrations of these radionuclides were observed at location 11 and well outside the plume. Sample depth profiles showed the concentration was roughly uniform with depth; thus, the higher concentrations reflect the geologic formation and not atmospheric deposition. The variability in naturally occurring radionuclides in the different geologic formations sampled was observed in the sampling.

6. Conclusions

We found no evidence of SSFL impact in off-site soils as a result of the Woolsey Fire. Computer modeling of the fire progression identified Oak Park as the area where the most particulate matter (PM_{10}) would have deposited while the Woolsey Fire burned on the SSFL. The community of Oak Park is located about 6 km southwest of the SSFL and there was no evidence of SSFL-derived radionuclides in the soils collected in this area. Any locations farther southwest toward the coast such as in the community of Malibu would have significantly less PM_{10} deposition from the Woolsey Fire burning on the SSFL (estimated to be about a factor of 5 less) because of atmospheric dilution, dispersion, and plume depletion, and thus lower impacts than those at Oak Park. We confirmed that the soil sampling analysis for our study had the ability to detect concentrations of radionuclides that would have resulted in doses to residents one thousand times smaller than the regulatory dose limits. Moreover, we found no impact on the off-site soils we sampled from past operations of the SSFL.

7. References

AI (Atomics International). 1960. Environmental Monitoring Annual Report for 1959. June.

Anderson, G.K., D.V. Sandberg, and R.A. Norheim. 2004. *Fire Emission Production Simulator (FEPS) User's Guide*. USDA Forest Service Pacific Northwest Research Station, Joint Fire Science Program (98-1-9-05). Available at http://www.fs.fed.us/pnw/fera/feps/.

Bevington, P.R. and D.K. Robinson. 1992. *Data Reduction and Error Analysis for the Physical Sciences.* New York: McGraw-Hill Inc.

Boeing. 2001. *Site Environmental Report for Calendar Year 2000, DOE Operations at The Boeing Company Rocketdyne Propulsion & Power*. RD01-152. September.

Boeing. 2005. *Site Environmental Report for Calendar Year 2004, DOE Operations at The Boeing Company Santa Susana Field Laboratory*. RD05-176. September.

Boeing. 2006. *Site Environmental Report for Calendar Year 2005, DOE Operations at The Boeing Company Santa Susana Field Laboratory*. September.

Boeing. 2008. *Site Environmental Report for Calendar Year 2007, DOE Operations at The Boeing Company Santa Susana Field Laboratory, Area IV*. September.

Boeing. 2018. Particulate Matter Monitoring Data. PMData-PostFire_20181120_Boeing.xlsx.

Browne, E. and R.B. Firestone. 1986. *Table of Radioactive Isotopes*. Edited by Virginia Shirley. New York: John Wiley & Sons, Inc.

CAL FIRE (California Department of Forestry and Fire Protection). 2019. Incident Report. Available at https://www.fire.ca.gov/incidents/2018/11/8/woolsey-fire/. Accessed August 21, 2019.

Chang, J.C. and S.R. Hanna. 2004. "Air Quality Model Performance Evaluation." *Meteorology and Atmospheric Physics* 87: 167–196.

Choppin, G.R. and J. Rydberg. 1983. *Nuclear Chemistry Theory and Application*. New York: Pergamon Press.

Citygate (Citygate Associates, LLC). 2019. *City of Los Angeles: After Action Review of the Woolsey Fire Incident*. Citygate Associates, LLC, Folsom, CA.

Deeming, J.E., R.E. Burgan, and J.D. Cohen. 1977. *The National Fire Danger Rating System-1978.* General Technical Report INT-39. USDA Forest Service, Intermountain Forest and Range Experiment Station, Ogden, UT.

DOE (U.S. Department of Energy). 2011a. *Derived Concentration Technical Standard*. DOE-Std-1196-2011. U.S. Department of Energy, Washington, D.C.

DOE. 2011b. *Radiation Protection of the Public and Environment*. DOE Order 458.1. U.S. Department of Energy, Washington, D.C. February.

DTSC (Department of Toxic Substance Control). 2018. *DTSC Interim Summary Report of Woolsey Fire*. California Environmental Protection Agency. December.

Efurd, D.W., G.W. Knobeloch, R.E. Perrin, and D.W. Barr. 1982. *Neptunium-237 Production from Atmospheric Nuclear Testing*. LA-9585-MS. Los Alamos National Laboratory, Los Alamos, NM.

Feely, H.W., I.K. Helfer, Z.R. Juzdan, C.S. Klusek, R.J. Larsen, R. Leifer, C.G. Sanderson, and M Dreicer. 1988. "Fallout in the New York Metropolitan Area Following the Chernobyl Accident." *Journal of Environmental Radioactivity* 7 (2): 177–191.

Grogan, H.A., J.W. Aanenson, P.D. McGavran, K.R. Meyer, H.J. Mohler, S. S. Mohler, J.R. Rocco, A.S. Rood, and J.E. Till. 2007. "Modeling of the Cerro Grande Fire at Los Alamos: An

Independent Analysis of Exposure, Health Risk, and Communication with the Public." In: T.M. Semkow, S.Pomme, S.M. Jerome, and D.J. Strom, Eds. *Applied Modeling and Computations in Nuclear Science*. ACS Symposium Series 945, American Chemical Society, Washington, D.C.

HydroGeologic (HydroGeologic, Inc.). 2011. *Final Radiological Background Study Report Santa Susana Field Laboratory Ventura County, California*. Prepared for U.S. Environmental Protection Agency Region 9. EPA Contract No: EP-S3-07-05. October.

HydroGeologic. 2012. *Final Technical Memorandum Look-Up Table Recommendations, Santa Susana Field Laboratory Area IV Radiological Study*. Technical Memorandum from L. Steven Vaughn, HGL Project Manager to Andrew Bain, EPA Region 9. November.

Ibrahim, S.A., S.B. Webb, and F.W. Whicker. 1997. "Contributions of Rocky Flats Releases to the Total Plutonium in Regional Soils." *Health Physics* 72 (1): 42–48.

Knoll, G.F. 2010. *Radiation Detection and Measurement*, 3rd edition. John Wiley & Sons, Inc.

LA County. 2019. Los Angeles County GIS Data Portal. Available at https://egis3.lacounty.gov/dataportal/2018/11/21/woolsey-fire-nov-2018-gis-data-applications/. Accessed June 19, 2019.

Lambert, G., M.F. Le Cloarec, B. Ardouin, and B. Bonsang. 1991. "Long-lived Radon Daughters Signature of Savanna Fires." In *Global Biomass Burning*. Edited by Joel S. Levine. Cambridge, MA: MIT Press. 181–184.

Le Cloarec, M.F., B. Ardouin, H. Cachier, C. Liousse, S. Neveu, and E.-Y. Nho. 1995. "^{210}Po in Savanna Burning Plumes." *Journal of Atmospheric Chemistry* 22: 111–122.

Moore, J.D. 1986. *Rocketdyne Division Environmental Monitoring Annual Report, De Soto and Santa Susana Field Laboratories Sites 1985*. Rockwell International. RI/RD86-140. April.

Moore, J.D. 1990. *Rocketdyne Division Environmental Monitoring Annual Report, De Soto and Santa Susana Field Laboratories Sites 1989*. Rockwell International. RI/RD90-132. May.

Nance, J.D., P.V. Hobbs, and L.F. Radke. 1993. "Airborne Measurements of Gases and Particles from an Alaskan Wildfire." *Journal of Geophysical Research* 98 (D8): 14,873–14,882.

NASA/Boeing/DOE. 2017. Baseline Air Monitoring Work Plan. Santa Susana Field Laboratory, Ventura County, CA. June.

NASA. 2019. Particulate Matter Monitoring Data. NASAPMFireData_20190208.xlsx.

NCRP (National Council on Radiation Protection and Measurements). 2009. *Ionizing Radiation Exposure of Population of the United States*. NCRP Report No. 160. National Council on Radiation Protection and Measurements, Bethesda, MD.

North Wind (North Wind, Inc.). 2015. *Annual Site Environmental Report for Calendar Year 2014, Department of Energy Operations at the Energy Technology Engineering Center – Area IV Santa Susana Field Laboratory*. North Wind, Inc., Idaho Falls, ID. May.

North Wind. 2018. *Annual Site Environmental Report for Calendar Year 2017, Department of Energy Operations at the Energy Technology Engineering Center – Area IV Santa Susana Field Laboratory.* North Wind, Inc., Idaho Falls, ID. March.

North Wind. 2019a. *Radioactive Particulate Air Sampling Results Associated with the Woolsey Fire.* North Wind, Inc., Idaho Falls, ID. January.

North Wind. 2019b. *Report on Quarterly Air Monitoring, Area IV, Third Quarter 2018-2019. Santa Susana Field Laboratory, Ventura County, California.* North Wind Inc., Idaho Falls, ID. June.

NRC (U.S. Nuclear Regulatory Commission). 2010. *Monitoring and Reporting Radioactive Materials in Liquid and Gaseous Effluents from Nuclear Fuel Cycle Facilities*. Regulatory Guide 4.16, Rev. 2. December.

Ornduff, R. 1974. *Introduction to California Plant Life*. University of California Press.

Piekarz, M., A. Komosa. 2014. "Rapid Method for Plutonium-241 Determination in Soil Samples." *Journal of Radioanalytical and Nuclear Chemistry* 299: 2019–2021.

Robinson, K.S. 1998. *Rocketdyne Propulsion & Power DOE Operations Annual Site Environmental Report 1997*. A4CM-ZR-0012. November.

Rockwell International. 1991. *Rocketdyne Division Environmental Monitoring Annual Report Santa Susana Field Laboratory, De Soto, and Canoga Sites 1990*. RI/RD91-136. June.

Rockwell International. 1992. *Rocketdyne Division Environmental Monitoring Annual Report Santa Susana Field Laboratory, De Soto, and Canoga Sites 1991*. RI/RD92-138. December.

Rockwell International. 1994. *Rocketdyne Division Environmental Monitoring Annual Report Santa Susana Field Laboratory, De Soto, and Canoga Sites 1993*. RI/RD94-126. October.

Rood, A.S., P.G. Voilleque, S.K. Rope, H.A. Grogan, and J.E. Till. 2008. "Reconstruction of Atmospheric Concentrations and Deposition of Uranium and Decay Products Released from the Former Uranium Mill at Uravan, Colorado." *Journal of Environmental Radioactivity* 99: 1258–1278.

Rutherford, P. 2019. Technical Memorandum: Boeing's Radiological Air Monitoring Data Associated with the Woolsey Fire. February 8.

Sapere Consulting and Boeing (Sapere Consulting, Inc., and The Boeing Company). 2005. *Historical Site Assessment of Area IV Santa Susana Field Laboratory Ventura County, California: Volume 1 – Methodology*. Prepared for the Department of Energy. May. https://www.etec.energy.gov/Library/Main/SSFLAreaIVHSAVolume%201.pdf.

Scire J.S., D.G. Strimaitis, and R.J. Yamartino. 2000. *A User's Guide for the CALPUFF Dispersion Model*. Earth Tech Inc., Concord, MA.

SSFL (Santa Susana Field Laboratory). 1996. Area IV Radiological Characterization Study, Final Report, Volume 1. A4CM-ZR-0011, Revision A. Rocketdyne Division, Rockwell International. August.

Turner, D.B. 1964. "A Diffusion Model for an Urban Area." *Journal of Applied Meteorology* 3: 83–91.

Webb, S.B. 1996. *The Spatial Distribution and Inventory of ^{239}Pu East of the Rocky Flats Plant*. Ph.D. dissertation. Colorado State University, Fort Collins, CO.

Wetherbee, G.A., T.M. Debey, M.A. Nilles, C.M.B. Lehmann, and D.A. Gay. 2011. Fission Products in National Atmospheric Deposition Program–Wet Deposition Samples Prior to and Following the Fukushima Dai-Ichi Nuclear Power Plant Incident, March 8–April 5, 2011. USGS Open File Report 2011-1277. United States Geologic Survey, Reston, VA.

Wetherbee, G.A., D.A. Gay, T.M. Debey, C.M.B. Lehmann, and M.A. Nilles. 2012. "Wet Deposition of Fission-Product Isotopes to North America from the Fukushima Dai-Ichi Incident March 2011." *Environmental Science & Technology* 46 (5): 2574–2582.

Whicker, F.W. and V. Shultz. 1982. *Radioecology: Nuclear Energy and the Environment*. Boca Raton, FL: CRC Press.

Wildfire Today. 2019. Woolsey Fire News. Available at https://wildfiretoday.com/?s=Woolsey+Fire&monthnum=11&year=2018&states_provinces=111&countries=&topics=. Accessed June 19, 2019.

Yang, G., J. Zheng, K Tagami, and S. Uchida. 2015. "Plutonium Concentration and Isotopic Ratio in Soil Samples from Central-Eastern Japan Collected Around the 1970s." *Scientific Reports* 5: 9636 DOI: 10.1038/srep09636.

Yerks, R.F. and R.H. Campbell. 2005. *Preliminary Geologic Map of the Los Angeles 30'×60' Quadrangle, Southern California.* USGS Open File Report 2005-1019. U.S. Department of the Interior, Geologic Survey, Washington, D.C.

Zheng, J., K. Tagami, Y. Watanabe, S. Uchida, T. Aono, N. Ishii, S. Yoshida, Y. Kubota, S. Fuma, and S. Ihara. 2012. "Isotopic Evidence of Plutonium Release into the Environment from the Fukushima DNPP Accident." *Scientific Reports* 2: 304 DOI: 10.1038/srep00304.

Appendix A. Sample Label and Collection Sheets

This appendix contains an example of the sample label affixed to each sample container, the completed original sample collection sheets, and the transcribed sample sheets.

Example of Sample Label

RAC SSFL Sampling Project

Sample ID: _____

Sample Type: _____

Sample Location Number:_____

Depth _____ (cm) Area _____ (cm^2)

Date/Time Collected _____

Sample Collected By: _____

_____

Figure A-1. Sample label that was affixed to each sample container.

Completed Sample Sheets

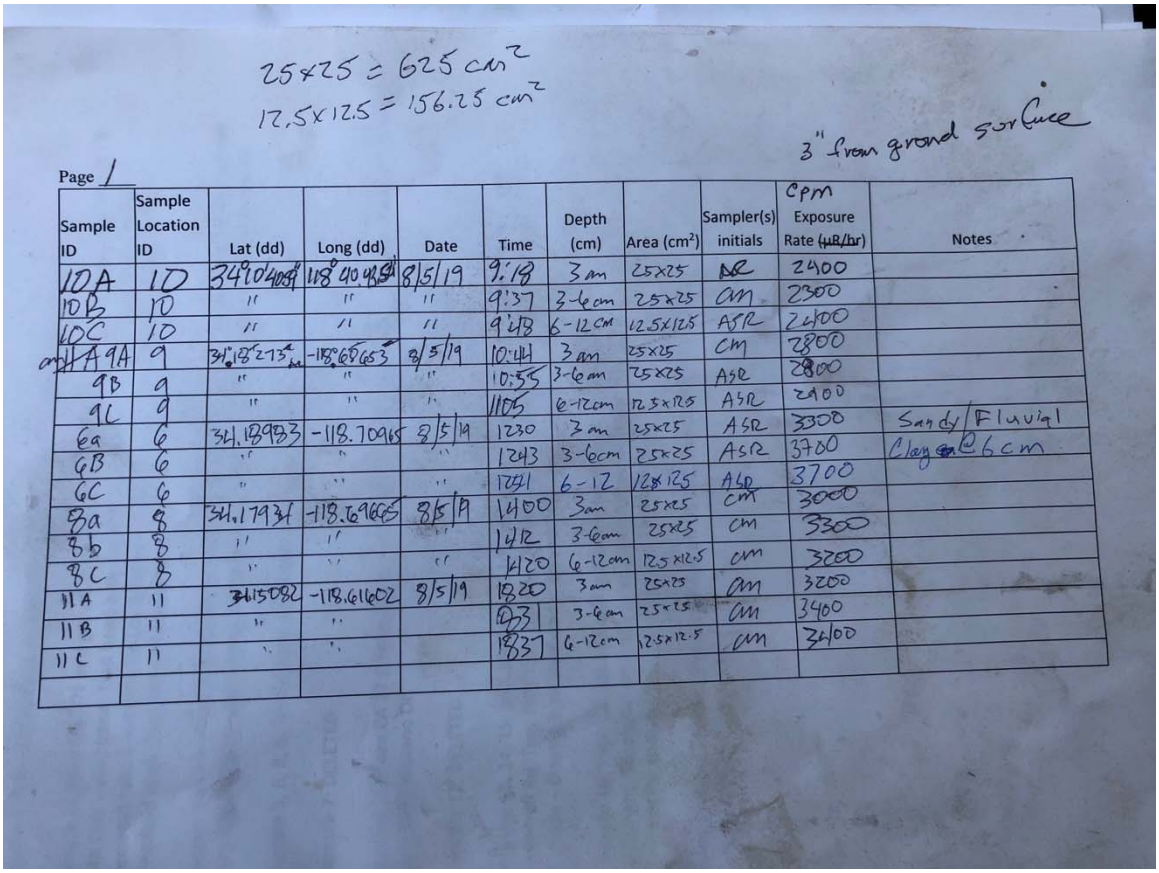

25x25 = 625 cm²
12.5x12.5 = 156.25 cm²

3" from ground surface

Page 1

Sample ID	Sample Location ID	Lat (dd)	Long (dd)	Date	Time	Depth (cm)	Area (cm²)	Sampler(s) initials	cpm Exposure Rate (μR/hr)	Notes
10A	10	34.04089	118.40.48	8/5/19	9:18	3 cm	25x25	AR	2400	
10B	10	"	"	"	9:37	3-6 cm	25x25	CM	2300	
10C	10	"	"	"	9:48	6-12 cm	12.5x12.5	ASR	2400	
9A	9	34.18273	-118.68653	8/5/19	10:44	3 cm	25x25	CM	2800	
9B	9	"	"	"	10:55	3-6 cm	25x25	ASR	2800	
9C	9	"	"	"	1105	6-12 cm	12.5x12.5	ASR	2400	
6a	6	34.18933	-118.70965	8/5/19	1230	3 cm	25x25	ASR	3300	Sandy Fluvial
6B	6	"	"	"	1243	3-6cm	25x25	ASR	3700	Clay @ 6cm
6C	6	"	"	"	1241	6-12	12.5x12.5	ASR	3700	
8a	8	34.17931	-118.69665	8/5/19	1400	3cm	25x25	CM	3000	
8b	8	"	"	"	1412	3-6cm	25x25	CM	3300	
8C	8	"	"	"	1420	6-12cm	12.5x12.5	CM	3200	
11A	11	34.15082	-118.61602	8/5/19	1820	3cm	25x25	CM	3200	
11B	11	"	"		1833	3-6cm	25x25	CM	3400	
11C	11	"	"		1837	6-12cm	12.5x12.5	CM	3400	

Figure A-2. Sample sheet for August 5, 2019.

Page 2

Sample ID	Sample Location ID	Lat (dd)	Long (dd)	Date	Time	Depth (cm)	Area (cm²)	Sampler(s) initials	CPM Exposure Rate (~~µR/hr~~)	Notes
17A	17	34.13194	-118.73577	8/5/19	1940	3	25x25	cm	2400	Poorly consolidate
17B	17	"	"	"	1950	3-6	25x25	cm	2000	Sandstone
17C	17	"	"	"	1957	6-12	12.5x12.5	cm	2200	
2A	2	34.2193	-118.81433	8/6/19	0730	3	25x25	cm	3600	
2B	2	"	"	8/6/19	0736	3-6	25x25	CM	3700	
2C	2	"	"	8/6/19	0742	6-12	12.5x12.5	cm	4000	
2A-S	2	"	"	8/6/19	0750	3	25x25	cm	3600	SPlit sample
2B-S	2	"	"	8/6/19	0754	3-6	25x25	cm	3700	4" apart
2C-S	2	"	"	8/6/19	0800	6-12	12.5x12.5	cm	4100	
3A	3	34.21086	-118.74044	8/6/19	0927	3	25x25	cm	3900	
3B	3	"	"	8/6/19	0933	3-6	25x25	cm	3500	
3C	3	"	"	8/6/19	0940	6-12	12.5x12.5	cm	3500	Very Rocky
4A	4	34.21306	-118.77671*	8/6/19	1020	3	25x25	cm	3200	
4B	4			8/6/19	1025	3-6	25x25	cm	3200	
4C	4			8/6/19	1030	6-12	12.5x12.5	cm	3300	

*-118.77671

Page 3

Sample ID	Sample Location ID	Lat (dd)	Long (dd)	Date	Time	Depth (cm)	Area (cm²)	Sampler(s) initials	Exposure Rate (µR/hr)	Notes
5A	5	34.21022	-118.76912	8/6/19	1104	3	25x25	cm	3400	
5B	5	"	"	8/6/19	1110	3-6	25x25	cm	3300	Rodent encountered @ corner of sample matrix
5C	5	"	"	8/6/19	1115	6-12	12.5x12.5	cm	3900	
1A	1	34.26509	-118.63730	8/6/19	1327	3	25x25	cm	3300	
1B	1	"	"	8/6/19	1333	3-6	25x25	cm	3500	
1C	1	"	"	8/6/19	1337	6-12	~~25x25~~ 12.5x12.5	cm	4000	
1A-D	1	"	"	8/6/19	1343	3	~~12.5x12.5~~ 25x25	cm	3400	
1B-D	1	"	"	8/6/19	1347	3-6	25x25	cm	3400	
1C-D	1	"	"	8/6/19	1351	6-12	12.5x12.5	cm	3400	
16-A	16	34.15430	-118.74819	8/6/19	1449	3	25x25	cm	2700	
16-B	16	"	"	8/6/19	1454	3-6	25x25	cm	2500	
16-C	16	"	"	8/6/19	1500	6-12	12.5x12.5	cm	2700	
13-A	13	34.18745	-118.74558	8/7/19	0712	3	25x25	cm	3200	mole activity throughout site
13-B	13	"	"	8/7/19	0715	3-6	25x25	cm	3300	no observable tracks in sample matrix
13-C	13	"	"	8/7/19	0719	6-12	12.5x12.5	cm	3400	

Page 4

Sample ID	Sample Location ID	Lat (dd)	Long (dd)	Date	Time	Depth (cm)	Area (cm²)	Sampler(s) initials	Exposure Rate (µR/hr)	Notes
15A	15	34.17887	-118.74424	8/7/19	0745	3	25x25	cm	3000	
15B	15	"	"	8/7/19	0751	3-6	25x25	cm	3000	
15C	15	"	"	8/7/19	0754	6-12	12.5x12.5	am	3400	
14A	14	34.18323	-118.74160	8/7/19	0830	3	25x25	cm	2500	
14B	14	"	"	8/7/19	0834	3-6	25x25	am	2400	
14C	14	"	"	8/7/19	0840	6-12	12.5x12.5	am	2500	
18A	18	34.18288	-118.74828	8/7/19	0907	3	25x25	am	2800	very loose soil
18B	18	"	"	8/7/19	0912	3-6	25x25	am	2700	
18C	18	"	"	8/7/19	0916	6-12	12.5x12.5	am	3000	

Transcribed Sample Sheets

Page 1

Sample ID	Sample Location ID	Lat (dd)	Long (dd)	Date	Time	Depth (cm)	Area (cm^2)	Sampler(s) initials	cpm	Notes
10A	10	34.17794167	-118.6787611	8/5/19	9:18	3	625		2400	Location coordinates converted to decimal degrees
10B	10	34.17794167	-118.6787611	8/5/19	9:37	3-6	625		2300	
10C	10	34.17794167	-118.6787611	8/5/19	9:48	6-12	312.5		2400	
9A	9	34.18273	-118.68653	8/5/19	10:44	3	625		2800	
9B	9	34.18273	-118.68653	8/5/19	10:55	3-6	625		2800	
9C	9	34.18273	-118.68653	8/5/19	11:05	6-12	312.5		2900	
6A	6	34.18983	-118.70965	8/5/19	12:30	3	625		3300	Sandy-fluvial
6B	6	34.18983	-118.70965	8/5/19	12:43	3-6	625		3700	Clay@6cm
6C	6	34.18983	-118.70965	8/5/19	12:51	6-12	312.5		3700	
8A	8	34.17931	-118.69665	8/5/19	14:00	3	625		3000	
8B	8	34.17931	-118.69665	8/5/19	14:12	3-6	625		3300	
8C	8	34.17931	-118.69665	8/5/19	14:20	6-12	312.5		3200	
11A	11	34.15082	-118.61602	8/5/19	18:20	3	625		3200	
11B	11	34.15082	-118.61602	8/5/19	18:31	3-6	625		3400	
11C	11	34.15082	-118.61602	8/5/19	18:37	6-12	312.5		3400	

Page 2

Sample ID	Sample Location ID	Lat (dd)	Long (dd)	Date	Time	Depth (cm)	Area (cm^2)	Sampler(s) initials	cpm	Notes
17A	17	34.13194	-118.73577	8/5/19	19:40	3	625		2400	poorly consolidated
17B	17	34.13194	-118.73577	8/5/19	19:50	3-6	625		2000	sandstone
17C	17	34.13194	-118.73577	8/5/19	19:57	6-12	312.5		2200	
2A	2	34.2193	-118.81433	8/6/19	07:30	3	625		3600	
2B	2	34.2193	-118.81433	8/6/19	07:36	3-6	625		3700	
2C	2	34.2193	-118.81433	8/6/19	07:42	6-12	312.5		4000	
2A-S	2	34.2193	-118.81433	8/6/19	07:50	3	625		3600	split sample taken 4 in apart
2B-S	2	34.2193	-118.81433	8/6/19	07:54	3-6	625		3700	
2C-S	2	34.2193	-118.81433	8/6/19	08:00	6-12	312.5		4100	
3A	3	34.21086	-118.79044	8/6/19	09:27	3	625		3900	
3B	3	34.21086	-118.79044	8/6/19	09:33	3-6	625		3500	
3C	3	34.21086	-118.79044	8/6/19	09:40	6-12	312.5		3500	very rocky
4A	4	34.21306	-118.77671	8/6/19	10:20	3	625		3200	
4B	4	34.21306	-118.77671	8/6/19	10:25	3-6	625		3200	
4C	4	34.21306	-118.77671	8/6/19	10:30	6-12	312.5		3300	

Page 3

Sample ID	Sample Location ID	Lat (dd)	Long (dd)	Date	Time	Depth (cm)	Area (cm^2)	Sampler(s) initials	cpm	Notes
5A	5	34.21022	-118.76942	8/6/19	11:04	3	625		3400	
5B	5	34.21022	-118.76942	8/6/19	11:10	3-6	625		3300	Rodent hole encountered @ corner of sample matrix
5C	5	34.21022	-118.76942	8/6/19	11:15	6-12	312.5		3900	
1A	1	34.26809	-118.63730	8/6/19	13:27	3	625		3300	
1B	1	34.26809	-118.63730	8/6/19	13:33	3-6	625		3500	
1C	1	34.26809	-118.63730	8/6/19	13:37	6-12	312.5		4000	
1A-D	1	34.26809	-118.63730	8/6/19	13:43	3	625		3400	
1B-D	1	34.26809	-118.63730	8/6/19	13:47	3-6	625		3400	
1C-D	1	34.26809	-118.63730	8/6/19	13:51	6-12	312.5		3400	
16A	16	34.15430	-118.74819	8/6/19	14:49	3	625		2700	
16B	16	34.15430	-118.74819	8/6/19	14:54	3-6	625		2500	
16C	16	34.15430	-118.74819	8/6/19	15:00	6-12	312.5		2700	
13A	13	34.18745	-118.74558	8/7/19	07:12	3	625		3200	mole activity throughout site but no observable trails in sample matrix
13B	13	34.18745	-118.74558	8/7/19	07:15	3-6	625		3300	
13C	13	34.18745	-118.74558	8/7/19	07:19	6-12	312.5		3400	

Page 4

Sample ID	Sample Location ID	Lat (dd)	Long (dd)	Date	Time	Depth (cm)	Area (cm^2)	Sampler(s) initials	cpm	Notes
15A	15	34.17887	-118.74424	8/7/19	07:45	3	625		3000	
15B	15	34.17887	-118.74424	8/7/19	07:51	3-6	625		3000	
15C	15	34.17887	-118.74424	8/7/19	07:56	6-12	312.5		3400	
14A	14	34.18323	-118.74160	8/7/19	08:30	3	625		2500	
14B	14	34.18323	-118.74160	8/7/19	08:34	3-6	625		2400	
14C	14	34.18323	-118.74160	8/7/19	08:40	6-12	312.5		2500	
18A	18	34.18288	-118.74828	8/7/19	09:07	3	625		2800	Very loose soil
18B	18	34.18288	-118.74828	8/7/19	09:12	3-6	625		2700	
18C	18	34.18288	-118.74828	8/7/19	09:16	6-12	312.5		3000	

Appendix B. Analytical Results from the Laboratories

This appendix contains the complete analytical results from GEL laboratories (Table B-1) and from Test America (Table B-3). Table B-2 provides the case narratives for GEL results with the "X" data qualifier.

Table B-1. Complete Results from the GEL Laboratory

Sample no.	Analysis date	Parameter	Result	Uncertainty	MDC[a]	Qualifier[b]	Units
1 A	09/26/19	Actinium-225	0.104	1.64	2.45	U	PCI/G
1 A	09/26/19	Actinium-227	0.0272	0.0531	0.0798	U	PCI/G
1 A	09/26/19	Actinium-228	1.59	0.0676	0.0359		PCI/G
1 A	09/26/19	Antimony-125	-0.00456	0.0166	0.0267	U	PCI/G
1 A	09/26/19	Barium-137m	0.0545	0.00843	0.00908		PCI/G
1 A	09/26/19	Bismuth-212	1.72	0.186	0.125		PCI/G
1 A	09/26/19	Bismuth-213	0.0198	0.0167	0.03	U	PCI/G
1 A	09/26/19	Bismuth-214	1.17	0.0346	0.0176		PCI/G
1 A	09/26/19	Cesium-134	0	0.0119	0.0163	UI	PCI/G
1 A	09/26/19	Cesium-137	0.0575	0.0089	0.0096		PCI/G
1 A	09/26/19	Cobalt-60	-0.00037	0.00554	0.0099	U	PCI/G
1 A	09/26/19	Europium-152	-0.0154	0.0162	0.0282	U	PCI/G
1 A	09/26/19	Europium-154	-0.00538	0.0196	0.0322	U	PCI/G
1 A	09/26/19	Europium-155	0	0.0439	0.0443	UI	PCI/G
1 A	09/26/19	Holmium-166m	-0.00091	0.00936	0.016	U	PCI/G
1 A	09/26/19	Lead-210	0.47	1.9	2.08	U	PCI/G
1 A	09/26/19	Lead-212	1.55	0.0277	0.0185		PCI/G
1 A	09/26/19	Lead-214	1.36	0.0403	0.0661		PCI/G
1 A	09/26/19	Neptunium-239	0.0986	0.0962	0.109	U	PCI/G
1 A	09/26/19	Niobium-94	0.0053	0.00522	0.00921	U	PCI/G
1 A	09/26/19	Potassium-40	23.7	0.361	0.0749		PCI/G
1 A	09/26/19	Promethium-147	-157	188	308	U	PCI/G
1 A	09/26/19	Protactinium-231	0	0.136	0.143	UI	PCI/G
1 A	09/26/19	Radium-226	1.17	0.0346	0.0176		PCI/G
1 A	09/26/19	Radium-228	1.59	0.0676	0.0359		PCI/G
1 A	09/26/19	Sodium-22	-0.00256	0.00706	0.0116	U	PCI/G
1 A	09/26/19	Tellurium-125m	1.98	4.01	6.22	U	PCI/G
1 A	09/26/19	Thallium-208	0.488	0.0186	0.00947		PCI/G
1 A	09/26/19	Thorium-231	0.0603	0.12	0.194	U	PCI/G
1 A	09/26/19	Thorium-234	1.05	0.619	0.673		PCI/G
1 A	09/26/19	Thulium-171	-5.28	6.2	10.4	U	PCI/G
1 A	09/26/19	Tin-126	0	0.034	0.0301	UI	PCI/G
1 A	09/26/19	Strontium-90	0.00143	0.00637	0.011	U	PCI/G
1 A	09/26/19	Yttrium-90	0.00143	0.00637	0.011	U	PCI/G
1 A	10/02/19	Nickel-59	-0.774	1.13	1.93	U	PCI/G
1 A	10/05/19	Americium-241	0.0167	0.0153	0.02	U	PCI/G
1 A	10/05/19	Americium-243	0.0128	0.0172	0.0279	U	PCI/G
1 A	10/05/19	Curium-243/244	0.0103	0.0134	0.0198	U	PCI/G
1 A	10/05/19	Curium-245/246	0	0.00831	0.0162	U	PCI/G
1 A	10/03/19	Polonium-210	1.36	0.236	0.121		PCI/G
1 A	10/03/19	Thorium-228	1.29	0.21	0.151		PCI/G
1 A	10/03/19	Thorium-229	0.0433	0.0824	0.143	U	PCI/G
1 A	10/03/19	Thorium-230	0.971	0.176	0.122		PCI/G
1 A	10/03/19	Thorium-232	1.16	0.186	0.103		PCI/G
1 A	10/01/19	Uranium-232	0.00352	0.053	0.0972	U	PCI/G
1 A	10/01/19	Uranium-233/234	0.878	0.111	0.0496		PCI/G
1 A	10/01/19	Uranium-235/236	0.0794	0.0364	0.0331		PCI/G
1 A	10/01/19	Uranium-238	0.895	0.113	0.061		PCI/G
1 A	10/01/19	Neptunium-236	-0.00373	0.00825	0.0203	U	PCI/G
1 A	10/01/19	Plutonium-236	-0.00373	0.00825	0.0203	U	PCI/G
1 A	10/01/19	Plutonium-239/240	0.00522	0.0111	0.0196	U	PCI/G
1 A	10/01/19	Plutonium-242	0.00269	0.0102	0.0194	U	PCI/G

Table B-1. Complete Results from the GEL Laboratory

Sample no.	Analysis date	Parameter	Result	Uncertainty	MDC[a]	Qualifier[b]	Units
1 A	10/01/19	Plutonium-244	0.00351	0.00754	0.0124	U	PCI/G
1 A	10/03/19	Neptunium-237	-0.00291	0.00879	0.0247	U	PCI/G
1 A	10/06/19	Plutonium-241	-1.09	1.52	2.66	U	PCI/G
1 A	09/25/19	Actinium-225	-2.36	1.67	2.8	U	PCI/G
1 A	09/25/19	Actinium-227	0.00182	0.0678	0.104	U	PCI/G
1 A	09/25/19	Actinium-228	1.62	0.0746	0.0449		PCI/G
1 A	09/25/19	Antimony-125	0.013	0.0202	0.0346	U	PCI/G
1 A	09/25/19	Barium-137m	0.0645	0.0125	0.0116		PCI/G
1 A	09/25/19	Bismuth-212	1.87	0.238	0.166		PCI/G
1 A	09/25/19	Bismuth-213	-0.000869	0.0223	0.0375	U	PCI/G
1 A	09/25/19	Bismuth-214	1.2	0.0411	0.0238		PCI/G
1 A	09/25/19	Cesium-134	0	0.0161	0.0194	UI	PCI/G
1 A	09/25/19	Cesium-137	0.0682	0.0132	0.0123		PCI/G
1 A	09/25/19	Cobalt-60	0.00177	0.00696	0.0123	U	PCI/G
1 A	09/25/19	Europium-152	0.00117	0.0222	0.0359	U	PCI/G
1 A	09/25/19	Europium-154	0.0191	0.0254	0.0402	U	PCI/G
1 A	09/25/19	Europium-155	0	0.0501	0.0624	UI	PCI/G
1 A	09/25/19	Holmium-166m	-0.00222	0.0115	0.0203	U	PCI/G
1 A	09/25/19	Lead-210	0	4.21	3.35	UI	PCI/G
1 A	09/25/19	Lead-212	1.5	0.0318	0.0233		PCI/G
1 A	09/25/19	Lead-214	1.33	0.0445	0.0265		PCI/G
1 A	09/25/19	Neptunium-239	-0.0425	0.086	0.149	U	PCI/G
1 A	09/25/19	Niobium-94	0.0107	0.0109	0.0118	U	PCI/G
1 A	09/25/19	Potassium-40	22.6	0.399	0.0956		PCI/G
1 A	09/25/19	Promethium-147	23.4	241	419	U	PCI/G
1 A	09/25/19	Protactinium-231	0	0.169	0.183	UI	PCI/G
1 A	09/25/19	Radium-226	1.2	0.0411	0.0238		PCI/G
1 A	09/25/19	Radium-228	1.62	0.0746	0.0449		PCI/G
1 A	09/25/19	Sodium-22	0.00673	0.00913	0.0144	U	PCI/G
1 A	09/25/19	Tellurium-125m	4.42	5.41	8.58	U	PCI/G
1 A	09/25/19	Thallium-208	0.493	0.0208	0.0125		PCI/G
1 A	09/25/19	Thorium-231	-0.106	0.164	0.243	U	PCI/G
1 A	09/25/19	Thorium-234	1.37	0.937	1.15		PCI/G
1 A	09/25/19	Thulium-171	-7.25	13.4	21.2	U	PCI/G
1 A	09/25/19	Tin-126	0	0.0449	0.0466	UI	PCI/G
1 A	09/28/19	Iodine-129	-0.0825	0.209	0.475	U	PCI/G
1 A	09/26/19	Iron-55	0.503	3.13	4.81	U	PCI/G
1 A	09/26/19	Nickel-63	-0.0338	0.456	0.783	U	PCI/G
1 A	09/25/19	Technetium-99	-0.109	0.293	0.502	U	PCI/G
1 A	09/27/19	Tritium	-1.17	2.13	3.99	U	PCI/G
1 A	09/28/19	Carbon-14	-0.123	1.46	2.57	U	PCI/G
1 A	10/03/19	Strontium-90	-0.0000586	0.00851	0.0149	U	PCI/G
1 A	10/03/19	Yttrium-90	-0.0000586	0.00851	0.0149	U	PCI/G
1 A	10/01/19	Nickel-59	-0.0055	0.633	1.04	U	PCI/G
1 A	10/05/19	Americium-241	0.00694	0.0136	0.0233	U	PCI/G
1 A	10/05/19	Americium-243	-2.81E-09	0.0155	0.0298	U	PCI/G
1 A	10/05/19	Curium-243/244	0.00344	0.00675	0.00516	U	PCI/G
1 A	10/05/19	Curium-245/246	0	0.00542	0.00586	U	PCI/G
1 A-D	09/25/19	Technetium-99	0.0246	0.429	0.729	U	PCI/G
1 A-D	09/27/19	Carbon-14	0.0723	1.71	2.96	U	PCI/G
1 A-D	09/27/19	Carbon-14	100	3.23	2.92		%
1 A-D	09/26/19	Actinium-225	-1.19	1.75	2.8	U	PCI/G
1 A-D	09/26/19	Actinium-227	0.0392	0.0632	0.0948	U	PCI/G
1 A-D	09/26/19	Actinium-228	1.58	0.0788	0.0425		PCI/G
1 A-D	09/26/19	Antimony-125	0.0171	0.0175	0.0313	U	PCI/G
1 A-D	09/26/19	Barium-137m	0.0969	0.0126	0.0111		PCI/G
1 A-D	09/26/19	Bismuth-212	1.81	0.253	0.145		PCI/G
1 A-D	09/26/19	Bismuth-213	0.00505	0.0194	0.034	U	PCI/G
1 A-D	09/26/19	Bismuth-214	1.1	0.043	0.0205		PCI/G
1 A-D	09/26/19	Cesium-134	0	0.0173	0.0188	UI	PCI/G

Table B-1. Complete Results from the GEL Laboratory

Sample no.	Analysis date	Parameter	Result	Uncertainty	MDC[a]	Qualifier[b]	Units
1 A-D	09/26/19	Cesium-137	0.102	0.0133	0.0118		PCI/G
1 A-D	09/26/19	Cobalt-60	0.00682	0.0069	0.0127	U	PCI/G
1 A-D	09/26/19	Europium-152	-0.0294	0.0202	0.0328	U	PCI/G
1 A-D	09/26/19	Europium-154	-0.022	0.0286	0.0393	U	PCI/G
1 A-D	09/26/19	Europium-155	0	0.0395	0.0492	UI	PCI/G
1 A-D	09/26/19	Holmium-166m	-0.00281	0.0113	0.019	U	PCI/G
1 A-D	09/26/19	Lead-210	2.57	3.09	3.54	U	PCI/G
1 A-D	09/26/19	Lead-212	1.55	0.0313	0.021		PCI/G
1 A-D	09/26/19	Lead-214	1.33	0.0435	0.0728		PCI/G
1 A-D	09/26/19	Neptunium-239	0	0.108	0.123	UI	PCI/G
1 A-D	09/26/19	Niobium-94	0.00745	0.00824	0.0107	U	PCI/G
1 A-D	09/26/19	Potassium-40	23	0.417	0.0935		PCI/G
1 A-D	09/26/19	Promethium-147	-117	210	347	U	PCI/G
1 A-D	09/26/19	Protactinium-231	0	0.155	0.161	UI	PCI/G
1 A-D	09/26/19	Radium-226	1.1	0.043	0.0205		PCI/G
1 A-D	09/26/19	Radium-228	1.58	0.0788	0.0425		PCI/G
1 A-D	09/26/19	Sodium-22	-0.00836	0.0103	0.0141	U	PCI/G
1 A-D	09/26/19	Tellurium-125m	3.21	4.14	6.99	U	PCI/G
1 A-D	09/26/19	Thallium-208	0.495	0.0206	0.011		PCI/G
1 A-D	09/26/19	Thorium-231	0.189	0.135	0.222	U	PCI/G
1 A-D	09/26/19	Thorium-234	1.21	0.863	0.804		PCI/G
1 A-D	09/26/19	Thulium-171	-0.557	8.84	15.1	U	PCI/G
1 A-D	09/26/19	Tin-126	0	0.0382	0.0351	UI	PCI/G
1 A-D	09/28/19	Iodine-129	-0.0647	0.198	0.46	U	PCI/G
1 A-D	10/01/19	Polonium-210	1.04	0.24	0.146		PCI/G
1 A-D	09/29/19	Thorium-228	1.42	0.208	0.136		PCI/G
1 A-D	09/29/19	Thorium-229	0.0333	0.0626	0.108	U	PCI/G
1 A-D	09/29/19	Thorium-230	1.22	0.18	0.0735		PCI/G
1 A-D	09/29/19	Thorium-232	1.25	0.179	0.0199		PCI/G
1 A-D	09/28/19	Uranium-232	-0.0347	0.0472	0.0976	U	PCI/G
1 A-D	09/28/19	Uranium-233/234	1.06	0.13	0.0443		PCI/G
1 A-D	09/28/19	Uranium-235/236	0.137	0.0498	0.0385		PCI/G
1 A-D	09/28/19	Uranium-238	0.957	0.123	0.0384		PCI/G
1 A-D	09/30/19	Neptunium-236	-0.0000679	0.00898	0.0189	U	PCI/G
1 A-D	09/30/19	Plutonium-236	-0.0000679	0.00898	0.0189	U	PCI/G
1 A-D	09/30/19	Plutonium-239/240	-0.0000654	0.00866	0.0182	U	PCI/G
1 A-D	09/30/19	Plutonium-242	0.00188	0.00724	0.0134	U	PCI/G
1 A-D	09/30/19	Plutonium-244	0.00489	0.0077	0.0115	U	PCI/G
1 A-D	10/01/19	Neptunium-237	0.00431	0.0135	0.0256	U	PCI/G
1 A-D	10/04/19	Plutonium-241	1.03	1.65	2.79	U	PCI/G
1 A-D	09/26/19	Iron-55	0.604	2.47	3.69	U	PCI/G
1 A-D	09/26/19	Nickel-63	0.0243	0.433	0.742	U	PCI/G
1 A-D	09/24/19	Technetium-99	-0.199	0.453	0.773	U	PCI/G
1 A-D	09/26/19	Tritium	-0.0587	2.15	3.82	U	PCI/G
1 A-D	09/27/19	Carbon-14	0.388	1.72	2.96	U	PCI/G
1 A-D	10/03/19	Strontium-90	-0.00175	0.00834	0.0149	U	PCI/G
1 A-D	10/03/19	Yttrium-90	-0.00175	0.00834	0.0149	U	PCI/G
1 A-D	10/02/19	Nickel-59	-0.000143	0.269	0.658	U	PCI/G
1 A-D	10/07/19	Americium-241	0.00948	0.0124	0.0194	U	PCI/G
1 A-D	10/07/19	Americium-243	0.00545	0.0128	0.0224	U	PCI/G
1 A-D	10/07/19	Curium-243/244	0.00157	0.00921	0.0173	U	PCI/G
1 A-D	10/07/19	Curium-245/246	0	0.00585	0.00633	U	PCI/G
1 B	10/02/19	Polonium-210	0.499	0.169	0.143		PCI/G
1 B	10/03/19	Thorium-228	1.66	0.345	0.292		PCI/G
1 B	10/03/19	Thorium-229	-0.0568	0.124	0.262	U	PCI/G
1 B	10/03/19	Thorium-230	1.71	0.318	0.174		PCI/G
1 B	10/03/19	Thorium-232	1.6	0.304	0.156		PCI/G
1 B	10/01/19	Uranium-232	-0.0293	0.0452	0.0893	U	PCI/G
1 B	10/01/19	Uranium-233/234	1.08	0.118	0.0557		PCI/G
1 B	10/01/19	Uranium-235/236	0.041	0.0321	0.0454	U	PCI/G
1 B	10/01/19	Uranium-238	1.17	0.121	0.0387		PCI/G
1 B	10/01/19	Neptunium-236	0.000831	0.00673	0.0136	U	PCI/G

Table B-1. Complete Results from the GEL Laboratory

Sample no.	Analysis date	Parameter	Result	Uncertainty	MDC[a]	Qualifier[b]	Units
1 B	10/01/19	Plutonium-236	0.000831	0.00673	0.0136	U	PCI/G
1 B	10/01/19	Plutonium-239/240	-0.0017	0.00707	0.0165	U	PCI/G
1 B	10/01/19	Plutonium-242	-0.00351	0.0162	0.0341	U	PCI/G
1 B	10/01/19	Plutonium-244	0.00163	0.00627	0.0116	U	PCI/G
1 B	10/05/19	Neptunium-237	-0.00243	0.00788	0.0182	U	PCI/G
1 B	10/06/19	Plutonium-241	0.32	1.66	2.84	U	PCI/G
1 B	09/25/19	Actinium-225	-0.99	1.59	2.55	U	PCI/G
1 B	09/25/19	Actinium-227	0.0504	0.0567	0.0926	U	PCI/G
1 B	09/25/19	Actinium-228	1.61	0.0755	0.0411		PCI/G
1 B	09/25/19	Antimony-125	0.00373	0.0175	0.0307	U	PCI/G
1 B	09/25/19	Barium-137m	0.0143	0.00808	0.0107		PCI/G
1 B	09/25/19	Bismuth-212	1.73	0.208	0.151		PCI/G
1 B	09/25/19	Bismuth-213	0	0.0331	0.031	UI	PCI/G
1 B	09/25/19	Bismuth-214	1.12	0.0367	0.0208		PCI/G
1 B	09/25/19	Cesium-134	0	0.0158	0.0181	UI	PCI/G
1 B	09/25/19	Cesium-137	0.0151	0.00854	0.0113		PCI/G
1 B	09/25/19	Cobalt-60	0.00571	0.00699	0.0128	U	PCI/G
1 B	09/25/19	Europium-152	0.00304	0.019	0.0321	U	PCI/G
1 B	09/25/19	Europium-154	0.0071	0.0228	0.0393	U	PCI/G
1 B	09/25/19	Europium-155	0	0.0486	0.0481	UI	PCI/G
1 B	09/25/19	Holmium-166m	-0.00101	0.0115	0.0174	U	PCI/G
1 B	09/25/19	Lead-210	1.17	2.11	3.62	U	PCI/G
1 B	09/25/19	Lead-212	1.57	0.0298	0.0212		PCI/G
1 B	09/25/19	Lead-214	1.3	0.0397	0.0722		PCI/G
1 B	09/25/19	Neptunium-239	0	0.106	0.12	UI	PCI/G
1 B	09/25/19	Niobium-94	0.00718	0.00625	0.0105	U	PCI/G
1 B	09/25/19	Potassium-40	23	0.409	0.0853		PCI/G
1 B	09/25/19	Promethium-147	-77.6	205	338	U	PCI/G
1 B	09/25/19	Protactinium-231	0	0.181	0.158	UI	PCI/G
1 B	09/25/19	Radium-226	1.12	0.0367	0.0208		PCI/G
1 B	09/25/19	Radium-228	1.61	0.0755	0.0411		PCI/G
1 B	09/25/19	Sodium-22	0.00268	0.00821	0.0141	U	PCI/G
1 B	09/25/19	Tellurium-125m	0	5.95	6.65	UI	PCI/G
1 B	09/25/19	Thallium-208	0.461	0.0194	0.011		PCI/G
1 B	09/25/19	Thorium-231	-0.16	0.138	0.212	U	PCI/G
1 B	09/25/19	Thorium-234	1.36	0.918	0.799		PCI/G
1 B	09/25/19	Thulium-171	-2.04	8.79	15	U	PCI/G
1 B	09/25/19	Tin-126	0	0.0348	0.0345	UI	PCI/G
1 B	09/28/19	Iodine-129	-0.221	0.369	0.567	U	PCI/G
1 B	09/26/19	Iron-55	-0.218	2.87	4.4	U	PCI/G
1 B	09/26/19	Nickel-63	-0.0743	0.348	0.599	U	PCI/G
1 B	09/25/19	Technetium-99	-0.133	0.3	0.514	U	PCI/G
1 B	09/27/19	Tritium	0.347	2.31	4.11	U	PCI/G
1 B	09/28/19	Carbon-14	-0.59	1.43	2.56	U	PCI/G
1 B	09/25/19	Strontium-90	0.00957	0.00798	0.0133	U	PCI/G
1 B	09/25/19	Yttrium-90	0.00957	0.00798	0.0133	U	PCI/G
1 B	10/01/19	Nickel-59	-0.00198	0.809	1.43	U	PCI/G
1 B	10/05/19	Americium-241	0.0112	0.0146	0.0215	U	PCI/G
1 B	10/05/19	Americium-243	0.00399	0.0207	0.0381	U	PCI/G
1 B	10/05/19	Curium-243/244	0.00222	0.00754	0.00667	U	PCI/G
1 B	10/05/19	Curium-245/246	3.86E-10	0.00908	0.0177	U	PCI/G
1 B-D	09/26/19	Iron-55	0.697	2.73	4.17	U	PCI/G
1 B-D	09/26/19	Nickel-63	0.0474	0.448	0.767	U	PCI/G
1 B-D	09/26/19	Actinium-225	0.519	1.6	2.63	U	PCI/G
1 B-D	09/26/19	Actinium-227	0.0151	0.0685	0.0897	U	PCI/G
1 B-D	09/26/19	Actinium-228	1.71	0.0708	0.0361		PCI/G
1 B-D	09/26/19	Antimony-125	-0.00393	0.0154	0.0267	U	PCI/G
1 B-D	09/26/19	Barium-137m	0.0593	0.0106	0.00949		PCI/G
1 B-D	09/26/19	Bismuth-212	1.75	0.179	0.134		PCI/G
1 B-D	09/26/19	Bismuth-213	0.00685	0.0173	0.0304	U	PCI/G

Table B-1. Complete Results from the GEL Laboratory

Sample no.	Analysis date	Parameter	Result	Uncertainty	MDC[a]	Qualifier[b]	Units
1 B-D	09/26/19	Bismuth-214	1.09	0.0334	0.0188		PCI/G
1 B-D	09/26/19	Cesium-134	0	0.0128	0.0159	UI	PCI/G
1 B-D	09/26/19	Cesium-137	0.0626	0.0112	0.01		PCI/G
1 B-D	09/26/19	Cobalt-60	-0.000558	0.00622	0.0108	U	PCI/G
1 B-D	09/26/19	Europium-152	0.000229	0.017	0.0301	U	PCI/G
1 B-D	09/26/19	Europium-154	-0.0128	0.0225	0.0355	U	PCI/G
1 B-D	09/26/19	Europium-155	0	0.0399	0.044	UI	PCI/G
1 B-D	09/26/19	Holmium-166m	-0.00599	0.00971	0.0161	U	PCI/G
1 B-D	09/26/19	Lead-210	1	1.66	2.89	U	PCI/G
1 B-D	09/26/19	Lead-212	1.71	0.03	0.0193		PCI/G
1 B-D	09/26/19	Lead-214	1.27	0.0414	0.0218		PCI/G
1 B-D	09/26/19	Neptunium-239	0.0146	0.0701	0.11	U	PCI/G
1 B-D	09/26/19	Niobium-94	0.00829	0.00815	0.00988	U	PCI/G
1 B-D	09/26/19	Potassium-40	24	0.386	0.084		PCI/G
1 B-D	09/26/19	Promethium-147	37.5	185	313	U	PCI/G
1 B-D	09/26/19	Protactinium-231	0	0.196	0.148	UI	PCI/G
1 B-D	09/26/19	Radium-226	1.09	0.0334	0.0188		PCI/G
1 B-D	09/26/19	Radium-228	1.71	0.0708	0.0361		PCI/G
1 B-D	09/26/19	Sodium-22	-0.0043	0.00809	0.0128	U	PCI/G
1 B-D	09/26/19	Tellurium-125m	4.46	3.94	6.28	U	PCI/G
1 B-D	09/26/19	Thallium-208	0.487	0.018	0.0097		PCI/G
1 B-D	09/26/19	Thorium-231	0.061	0.123	0.199	U	PCI/G
1 B-D	09/26/19	Thorium-234	0.969	0.722	0.671		PCI/G
1 B-D	09/26/19	Thulium-171	-1.35	6.9	12	U	PCI/G
1 B-D	09/26/19	Tin-126	0	0.0314	0.0304	UI	PCI/G
1 B-D	09/28/19	Iodine-129	0.14	0.394	0.727	U	PCI/G
1 B-D	10/01/19	Polonium-210	0.658	0.21	0.181		PCI/G
1 B-D	09/30/19	Thorium-228	1.46	0.198	0.105		PCI/G
1 B-D	09/30/19	Thorium-229	0.0494	0.0484	0.0683	U	PCI/G
1 B-D	09/30/19	Thorium-230	0.918	0.149	0.0471		PCI/G
1 B-D	09/30/19	Thorium-232	1.54	0.192	0.047		PCI/G
1 B-D	09/28/19	Uranium-232	-0.0583	0.0515	0.108	U	PCI/G
1 B-D	09/28/19	Uranium-233/234	0.847	0.125	0.0675		PCI/G
1 B-D	09/28/19	Uranium-235/236	0.0708	0.049	0.0677		PCI/G
1 B-D	09/28/19	Uranium-238	0.864	0.126	0.0713		PCI/G
1 B-D	09/30/19	Neptunium-236	-0.00101	0.00913	0.0201	U	PCI/G
1 B-D	09/30/19	Plutonium-236	-0.00101	0.00913	0.0201	U	PCI/G
1 B-D	09/30/19	Plutonium-239/240	0.00358	0.0109	0.0203	U	PCI/G
1 B-D	09/30/19	Plutonium-242	-0.00572	0.00886	0.0226	U	PCI/G
1 B-D	09/30/19	Plutonium-244	0.000905	0.00568	0.0107	U	PCI/G
1 B-D	10/01/19	Neptunium-237	-0.00168	0.00989	0.0235	U	PCI/G
1 B-D	10/04/19	Plutonium-241	1.01	2.03	3.46	U	PCI/G
1 B-D	09/26/19	Iron-55	-0.0739	2.44	3.68	U	PCI/G
1 B-D	09/26/19	Nickel-63	-0.117	0.442	0.763	U	PCI/G
1 B-D	09/24/19	Technetium-99	0.0916	0.4	0.678	U	PCI/G
1 B-D	09/26/19	Tritium	-1.53	2.21	4.11	U	PCI/G
1 B-D	09/27/19	Carbon-14	-0.907	1.62	2.89	U	PCI/G
1 B-D	09/28/19	Strontium-90	0.00683	0.00544	0.00899	U	PCI/G
1 B-D	09/28/19	Yttrium-90	0.00683	0.00544	0.00899	U	PCI/G
1 B-D	10/02/19	Nickel-59	-0.732	0.802	1.25	U	PCI/G
1 B-D	10/07/19	Americium-241	0.00597	0.0185	0.033	U	PCI/G
1 B-D	10/07/19	Americium-243	-0.00524	0.0157	0.0322	U	PCI/G
1 B-D	10/07/19	Curium-243/244	0.00296	0.013	0.0227	U	PCI/G
1 B-D	10/07/19	Curium-245/246	-0.00405	0.00795	0.0194	U	PCI/G
1 C	10/02/19	Polonium-210	0.813	0.209	0.139		PCI/G
1 C	10/02/19	Thorium-228	1.56	0.238	0.155		PCI/G
1 C	10/02/19	Thorium-229	0.0398	0.0749	0.129	U	PCI/G
1 C	10/02/19	Thorium-230	1.36	0.211	0.106		PCI/G
1 C	10/02/19	Thorium-232	1.4	0.209	0.0606		PCI/G
1 C	10/01/19	Uranium-232	-0.0295	0.0424	0.0852	U	PCI/G
1 C	10/01/19	Uranium-233/234	1.13	0.114	0.0323		PCI/G
1 C	10/01/19	Uranium-235/236	0.0556	0.0298	0.0324		PCI/G

Table B-1. Complete Results from the GEL Laboratory

Sample no.	Analysis date	Parameter	Result	Uncertainty	MDC[a]	Qualifier[b]	Units
1 C	10/01/19	Uranium-238	1.31	0.122	0.028		PCI/G
1 C	10/01/19	Neptunium-236	-0.000953	0.0063	0.0147	U	PCI/G
1 C	10/01/19	Plutonium-236	-0.000953	0.0063	0.0147	U	PCI/G
1 C	10/01/19	Plutonium-239/240	-0.00366	0.00912	0.0215	U	PCI/G
1 C	10/01/19	Plutonium-242	-0.01	0.013	0.0311	U	PCI/G
1 C	10/01/19	Plutonium-244	0.000847	0.00822	0.0168	U	PCI/G
1 C	10/06/19	Neptunium-237	-0.00636	0.0065	0.0154	U	PCI/G
1 C	10/06/19	Plutonium-241	0.296	1.55	2.66	U	PCI/G
1 C	09/25/19	Actinium-225	-0.0363	1.77	2.61	U	PCI/G
1 C	09/25/19	Actinium-227	-0.0369	0.0602	0.0947	U	PCI/G
1 C	09/25/19	Actinium-228	1.8	0.0709	0.0421		PCI/G
1 C	09/25/19	Antimony-125	0.00689	0.0178	0.031	U	PCI/G
1 C	09/25/19	Barium-137m	0.0122	0.012	0.0108		PCI/G
1 C	09/25/19	Bismuth-212	1.95	0.206	0.156		PCI/G
1 C	09/25/19	Bismuth-213	-0.00791	0.0217	0.033	U	PCI/G
1 C	09/25/19	Bismuth-214	1.2	0.0416	0.0208		PCI/G
1 C	09/25/19	Cesium-134	0	0.0179	0.0185	UI	PCI/G
1 C	09/25/19	Cesium-137	0.0129	0.0127	0.0115		PCI/G
1 C	09/25/19	Cobalt-60	0.0000183	0.00667	0.0115	U	PCI/G
1 C	09/25/19	Europium-152	0.0212	0.0252	0.0326	U	PCI/G
1 C	09/25/19	Europium-154	0.0316	0.0261	0.0416	U	PCI/G
1 C	09/25/19	Europium-155	0	0.044	0.0485	UI	PCI/G
1 C	09/25/19	Holmium-166m	-0.00749	0.0114	0.0186	U	PCI/G
1 C	09/25/19	Lead-210	0.296	1.58	2.71	U	PCI/G
1 C	09/25/19	Lead-212	1.76	0.0314	0.0208		PCI/G
1 C	09/25/19	Lead-214	1.34	0.0408	0.0717		PCI/G
1 C	09/25/19	Neptunium-239	0.046	0.0716	0.12	U	PCI/G
1 C	09/25/19	Niobium-94	0.00447	0.00651	0.0111	U	PCI/G
1 C	09/25/19	Potassium-40	22.9	0.398	0.0833		PCI/G
1 C	09/25/19	Promethium-147	-32.8	207	343	U	PCI/G
1 C	09/25/19	Protactinium-231	0	0.184	0.162	UI	PCI/G
1 C	09/25/19	Radium-226	1.2	0.0416	0.0208		PCI/G
1 C	09/25/19	Radium-228	1.8	0.0709	0.0421		PCI/G
1 C	09/25/19	Sodium-22	0.0113	0.00937	0.015	U	PCI/G
1 C	09/25/19	Tellurium-125m	4.1	5.97	6.7	U	PCI/G
1 C	09/25/19	Thallium-208	0.55	0.0206	0.011		PCI/G
1 C	09/25/19	Thorium-231	-0.0154	0.141	0.221	U	PCI/G
1 C	09/25/19	Thorium-234	1.22	0.696	0.742		PCI/G
1 C	09/25/19	Thulium-171	-1.94	7.27	12.5	U	PCI/G
1 C	09/25/19	Tin-126	0	0.0343	0.0338	UI	PCI/G
1 C	09/28/19	Iodine-129	0.552	0.543	1.07	U	PCI/G
1 C	09/26/19	Iron-55	-0.663	2.5	3.81	U	PCI/G
1 C	09/26/19	Nickel-63	0.0443	0.415	0.71	U	PCI/G
1 C	09/25/19	Technetium-99	-0.0897	0.322	0.55	U	PCI/G
1 C	09/27/19	Tritium	-0.0805	2.08	3.76	U	PCI/G
1 C	09/28/19	Carbon-14	-0.594	1.4	2.51	U	PCI/G
1 C	09/28/19	Strontium-90	-0.01	0.00793	0.0148	U	PCI/G
1 C	09/28/19	Yttrium-90	-0.01	0.00793	0.0148	U	PCI/G
1 C	10/02/19	Nickel-59	-0.898	0.911	1.41	U	PCI/G
1 C	10/07/19	Americium-241	0.0176	0.0149	0.0188	U	PCI/G
1 C	10/07/19	Americium-243	0.00448	0.0186	0.0343	U	PCI/G
1 C	10/07/19	Curium-243/244	0.0097	0.0114	0.0148	U	PCI/G
1 C	10/07/19	Curium-245/246	8.68E-10	0.0125	0.0249	U	PCI/G
1 C-D	09/26/19	Actinium-225	-0.745	1.47	2.36	U	PCI/G
1 C-D	09/26/19	Actinium-227	0.043	0.057	0.0793	U	PCI/G
1 C-D	09/26/19	Actinium-228	1.63	0.0708	0.0397		PCI/G
1 C-D	09/26/19	Antimony-125	0.0141	0.0158	0.0281	U	PCI/G
1 C-D	09/26/19	Barium-137m	0.0385	0.0109	0.0112		PCI/G
1 C-D	09/26/19	Bismuth-212	1.6	0.185	0.149		PCI/G
1 C-D	09/26/19	Bismuth-213	0.00175	0.02	0.0312	U	PCI/G

Table B-1. Complete Results from the GEL Laboratory

Sample no.	Analysis date	Parameter	Result	Uncertainty	MDC[a]	Qualifier[b]	Units
1 C-D	09/26/19	Bismuth-214	1.11	0.0363	0.0199		PCI/G
1 C-D	09/26/19	Cesium-134	0	0.0158	0.0182	UI	PCI/G
1 C-D	09/26/19	Cesium-137	0.0407	0.0115	0.0118		PCI/G
1 C-D	09/26/19	Cobalt-60	0.0037	0.00674	0.012	U	PCI/G
1 C-D	09/26/19	Europium-152	-0.0223	0.0165	0.0282	U	PCI/G
1 C-D	09/26/19	Europium-154	-0.00121	0.0224	0.036	U	PCI/G
1 C-D	09/26/19	Europium-155	0	0.0365	0.0357	UI	PCI/G
1 C-D	09/26/19	Holmium-166m	0.00593	0.0123	0.0188	U	PCI/G
1 C-D	09/26/19	Lead-210	1.02	0.243	0.221		PCI/G
1 C-D	09/26/19	Lead-212	1.61	0.0277	0.0173		PCI/G
1 C-D	09/26/19	Lead-214	1.26	0.0366	0.0658		PCI/G
1 C-D	09/26/19	Neptunium-239	-0.0211	0.0598	0.0922	U	PCI/G
1 C-D	09/26/19	Niobium-94	0.0103	0.00684	0.0109	U	PCI/G
1 C-D	09/26/19	Potassium-40	22.2	0.383	0.0826		PCI/G
1 C-D	09/26/19	Promethium-147	75.2	161	272	U	PCI/G
1 C-D	09/26/19	Protactinium-231	0	0.137	0.14	UI	PCI/G
1 C-D	09/26/19	Radium-226	1.11	0.0363	0.0199		PCI/G
1 C-D	09/26/19	Radium-228	1.63	0.0708	0.0397		PCI/G
1 C-D	09/26/19	Sodium-22	-0.000704	0.00853	0.013	U	PCI/G
1 C-D	09/26/19	Tellurium-125m	3.93	3.53	5.12	U	PCI/G
1 C-D	09/26/19	Thallium-208	0.528	0.0194	0.0101		PCI/G
1 C-D	09/26/19	Thorium-231	-0.0253	0.121	0.191	U	PCI/G
1 C-D	09/26/19	Thorium-234	1	0.327	0.273		PCI/G
1 C-D	09/26/19	Thulium-171	0	1.79	2.13	UI	PCI/G
1 C-D	09/26/19	Tin-126	0	0.0251	0.0219	UI	PCI/G
1 C-D	09/28/19	Iodine-129	0.284	0.421	0.815	U	PCI/G
1 C-D	10/01/19	Polonium-210	0.495	0.184	0.171		PCI/G
1 C-D	09/30/19	Thorium-228	1.22	0.181	0.12		PCI/G
1 C-D	09/30/19	Thorium-229	0.159	0.0739	0.0848		PCI/G
1 C-D	09/30/19	Thorium-230	0.869	0.145	0.0723		PCI/G
1 C-D	09/30/19	Thorium-232	0.884	0.146	0.0721		PCI/G
1 C-D	09/28/19	Uranium-232	-0.0165	0.0548	0.106	U	PCI/G
1 C-D	09/28/19	Uranium-233/234	0.823	0.107	0.0387		PCI/G
1 C-D	09/28/19	Uranium-235/236	0.0666	0.0344	0.0336		PCI/G
1 C-D	09/28/19	Uranium-238	0.954	0.114	0.0335		PCI/G
1 C-D	09/30/19	Neptunium-236	-0.00875	0.0106	0.0261	U	PCI/G
1 C-D	09/30/19	Plutonium-236	-0.00875	0.0106	0.0261	U	PCI/G
1 C-D	09/30/19	Plutonium-239/240	-0.00594	0.0106	0.0246	U	PCI/G
1 C-D	09/30/19	Plutonium-242	0.00263	0.00894	0.0168	U	PCI/G
1 C-D	09/30/19	Plutonium-244	0.00827	0.00905	0.0117	U	PCI/G
1 C-D	10/01/19	Neptunium-237	-0.000538	0.0125	0.0282	U	PCI/G
1 C-D	10/04/19	Plutonium-241	0.992	1.68	2.84	U	PCI/G
1 C-D	09/26/19	Iron-55	-1.39	2.34	3.57	U	PCI/G
1 C-D	09/26/19	Nickel-63	0.0293	0.461	0.789	U	PCI/G
1 C-D	09/24/19	Technetium-99	0.31	0.448	0.754	U	PCI/G
1 C-D	09/26/19	Tritium	-1.32	2.14	3.96	U	PCI/G
1 C-D	09/27/19	Carbon-14	1.61	1.75	2.94	U	PCI/G
1 C-D	10/03/19	Strontium-90	-0.00508	0.00808	0.0149	U	PCI/G
1 C-D	10/03/19	Yttrium-90	-0.00508	0.00808	0.0149	U	PCI/G
1 C-D	10/02/19	Nickel-59	0.881	0.993	1.91	U	PCI/G
1 C-D	10/05/19	Americium-241	0.011	0.0197	0.0338	U	PCI/G
1 C-D	10/05/19	Americium-243	-0.007	0.0145	0.031	U	PCI/G
1 C-D	10/05/19	Curium-243/244	-0.00728	0.0113	0.0262	U	PCI/G
1 C-D	10/05/19	Curium-245/246	0.00203	0.0069	0.00609	U	PCI/G
10 A	09/30/19	Polonium-210	1.79	0.337	0.127		PCI/G
10 A	09/29/19	Thorium-228	0.37	0.111	0.0995		PCI/G
10 A	09/29/19	Thorium-229	0.0452	0.0522	0.0794	U	PCI/G
10 A	09/29/19	Thorium-230	1.51	0.197	0.0712		PCI/G
10 A	09/29/19	Thorium-232	0.302	0.0899	0.0491		PCI/G
10 A	09/30/19	Uranium-232	-0.0416	0.0632	0.141	U	PCI/G
10 A	09/30/19	Uranium-233/234	1.55	0.173	0.0648		PCI/G
10 A	09/30/19	Uranium-235/236	0.0534	0.0436	0.0597	U	PCI/G

Table B-1. Complete Results from the GEL Laboratory

Sample no.	Analysis date	Parameter	Result	Uncertainty	MDC[a]	Qualifier[b]	Units
10 A	09/30/19	Uranium-238	1.43	0.165	0.0535		PCI/G
10 A	09/28/19	Neptunium-236	-0.00353	0.0109	0.0237	U	PCI/G
10 A	09/28/19	Plutonium-236	-0.00353	0.0109	0.0237	U	PCI/G
10 A	09/28/19	Plutonium-239/240	0.0017	0.0111	0.021	U	PCI/G
10 A	09/28/19	Plutonium-242	-0.00488	0.00789	0.0173	U	PCI/G
10 A	09/28/19	Plutonium-244	0.00851	0.01	0.013	U	PCI/G
10 A	09/30/19	Neptunium-237	0.0043	0.00901	0.0158	U	PCI/G
10 A	10/03/19	Plutonium-241	0.534	3.68	6.32	U	PCI/G
10 A	09/14/19	Actinium-225	-0.152	0.352	0.617	U	PCI/G
10 A	09/14/19	Actinium-227	0.0424	0.0349	0.0455	U	PCI/G
10 A	09/14/19	Actinium-228	0.409	0.0355	0.0234		PCI/G
10 A	09/14/19	Antimony-125	0.0124	0.0133	0.0156	U	PCI/G
10 A	09/14/19	Barium-137m	0.133	0.00655	0.00566		PCI/G
10 A	09/14/19	Bismuth-212	0.472	0.102	0.0791		PCI/G
10 A	09/14/19	Bismuth-213	0.0058	0.0115	0.0177	U	PCI/G
10 A	09/14/19	Bismuth-214	1.23	0.0219	0.0107		PCI/G
10 A	09/14/19	Cesium-134	0	0.00718	0.00675	UI	PCI/G
10 A	09/14/19	Cesium-137	0.14	0.00692	0.00598		PCI/G
10 A	09/14/19	Cobalt-60	-0.00408	0.00475	0.00671	U	PCI/G
10 A	09/14/19	Europium-152	-0.000471	0.00949	0.0163	U	PCI/G
10 A	09/14/19	Europium-154	0.00223	0.0136	0.0224	U	PCI/G
10 A	09/14/19	Europium-155	0	0.0166	0.0189	UI	PCI/G
10 A	09/14/19	Holmium-166m	0.000105	0.00565	0.01	U	PCI/G
10 A	09/14/19	Lead-210	1.43	0.163	0.13		PCI/G
10 A	09/14/19	Lead-212	0.388	0.011	0.0101		PCI/G
10 A	09/14/19	Lead-214	1.36	0.0238	0.0461		PCI/G
10 A	09/14/19	Neptunium-239	-0.0302	0.0305	0.0496	U	PCI/G
10 A	09/14/19	Niobium-94	0.00585	0.00644	0.00605	U	PCI/G
10 A	09/14/19	Potassium-40	12.4	0.204	0.0549		PCI/G
10 A	09/14/19	Promethium-147	-8.19	87.8	144	U	PCI/G
10 A	09/14/19	Protactinium-231	0	0.0714	0.0803	UI	PCI/G
10 A	09/14/19	Radium-226	1.23	0.0219	0.0107		PCI/G
10 A	09/14/19	Radium-228	0.409	0.0355	0.0234		PCI/G
10 A	09/14/19	Sodium-22	0.00147	0.00509	0.00805	U	PCI/G
10 A	09/14/19	Tellurium-125m	1.49	1.59	2.44	U	PCI/G
10 A	09/14/19	Thallium-208	0.118	0.00868	0.00618		PCI/G
10 A	09/14/19	Thorium-231	0.0285	0.0687	0.108	U	PCI/G
10 A	09/14/19	Thorium-234	1.47	0.177	0.149		PCI/G
10 A	09/14/19	Thulium-171	0	1.14	1.24	UI	PCI/G
10 A	09/14/19	Tin-126	0	0.0118	0.0115	UI	PCI/G
10 A	09/30/19	Iodine-129	0.468	0.337	0.83	U	PCI/G
10 A	09/30/19	Iodine-129	0.468	0.337	0.83	U	PCI/G
10 A	09/30/19	Iodine-129	88.1	1.99	0.902		%
10 A	09/30/19	Iodine-129	88.1	1.99	0.902		%
10 A	09/28/19	Strontium-90	0.00339	0.0082	0.0147	U	PCI/G
10 A	09/28/19	Yttrium-90	0.00339	0.0082	0.0147	U	PCI/G
10 A	09/28/19	Iron-55	-0.0571	2.79	4.11	U	PCI/G
10 A	09/28/19	Tritium	1.08	2.14	3.66	U	PCI/G
10 A	09/28/19	Tritium	85.7	4.26	3.86		%
10 A	09/26/19	Carbon-14	1.57	1.48	2.47	U	PCI/G
10 A	09/26/19	Carbon-14	101	3.12	2.46		%
10 A	09/27/19	Nickel-59	-0.043	0.904	1.62	U	PCI/G
10 A	10/03/19	Americium-241	-0.00757	0.0154	0.0371	U	PCI/G
10 A	10/03/19	Americium-243	-0.0228	0.0168	0.049	U	PCI/G
10 A	10/03/19	Curium-243/244	-0.0119	0.0126	0.0355	U	PCI/G
10 A	10/03/19	Curium-245/246	0.00403	0.0119	0.0121	U	PCI/G
10 A	10/02/19	Polonium-210	1.38	0.362	0.226		PCI/G
10 A	09/28/19	Thorium-228	0.416	0.117	0.0962		PCI/G
10 A	09/28/19	Thorium-229	0.0333	0.0506	0.0821	U	PCI/G
10 A	09/28/19	Thorium-230	1.64	0.208	0.0736		PCI/G

Table B-1. Complete Results from the GEL Laboratory

Sample no.	Analysis date	Parameter	Result	Uncertainty	MDC[a]	Qualifier[b]	Units
10 A	09/28/19	Thorium-232	0.378	0.102	0.0508		PCI/G
10 A	09/29/19	Uranium-232	-0.0278	0.0545	0.118	U	PCI/G
10 A	09/29/19	Uranium-233/234	1.54	0.153	0.0515		PCI/G
10 A	09/29/19	Uranium-235/236	0.15	0.0506	0.0369		PCI/G
10 A	09/29/19	Uranium-238	1.43	0.147	0.0425		PCI/G
10 A	09/28/19	Neptunium-236	0.00186	0.00365	0.00279	U	PCI/G
10 A	09/28/19	Plutonium-236	0.00186	0.00365	0.00279	U	PCI/G
10 A	09/28/19	Plutonium-239/240	0.00808	0.00767	0.011	U	PCI/G
10 A	09/28/19	Plutonium-242	0.00768	0.0128	0.0217	U	PCI/G
10 A	09/28/19	Plutonium-244	0.00808	0.00682	0.0086	U	PCI/G
10 A	09/30/19	Neptunium-237	0.000397	0.00755	0.0162	U	PCI/G
10 A	10/02/19	Plutonium-241	1.04	1.81	3.06	U	PCI/G
10 A	09/13/19	Actinium-225	-0.31	0.369	0.588	U	PCI/G
10 A	09/13/19	Actinium-227	0.0192	0.033	0.0464	U	PCI/G
10 A	09/13/19	Actinium-228	0.392	0.0306	0.0205		PCI/G
10 A	09/13/19	Antimony-125	0.00389	0.00957	0.0151	U	PCI/G
10 A	09/13/19	Barium-137m	0.124	0.00619	0.00484		PCI/G
10 A	09/13/19	Bismuth-212	0.375	0.0804	0.0692		PCI/G
10 A	09/13/19	Bismuth-213	-0.0000283	0.0103	0.0161	U	PCI/G
10 A	09/13/19	Bismuth-214	1.06	0.0194	0.00956		PCI/G
10 A	09/13/19	Cesium-134	0	0.00548	0.00551	UI	PCI/G
10 A	09/13/19	Cesium-137	0.131	0.00654	0.00511		PCI/G
10 A	09/13/19	Cobalt-60	0.00111	0.00327	0.00581	U	PCI/G
10 A	09/13/19	Europium-152	-0.00447	0.00998	0.0156	U	PCI/G
10 A	09/13/19	Europium-154	-0.00613	0.0123	0.0185	U	PCI/G
10 A	09/13/19	Europium-155	0	0.0202	0.0227	UI	PCI/G
10 A	09/13/19	Holmium-166m	-0.00145	0.00544	0.00814	U	PCI/G
10 A	09/13/19	Lead-210	2.23	1.59	1.67		PCI/G
10 A	09/13/19	Lead-212	0.373	0.0114	0.0102		PCI/G
10 A	09/13/19	Lead-214	1.24	0.0225	0.0119		PCI/G
10 A	09/13/19	Neptunium-239	-0.0291	0.034	0.0558	U	PCI/G
10 A	09/13/19	Niobium-94	0.00343	0.00418	0.00491	U	PCI/G
10 A	09/13/19	Potassium-40	12.5	0.194	0.0436		PCI/G
10 A	09/13/19	Promethium-147	24.8	96.1	160	U	PCI/G
10 A	09/13/19	Protactinium-231	0	0.0735	0.0763	UI	PCI/G
10 A	09/13/19	Radium-226	1.06	0.0194	0.00956		PCI/G
10 A	09/13/19	Radium-228	0.392	0.0306	0.0205		PCI/G
10 A	09/13/19	Sodium-22	-0.00219	0.00438	0.00661	U	PCI/G
10 A	09/13/19	Tellurium-125m	2.08	1.9	2.78	U	PCI/G
10 A	09/13/19	Thallium-208	0.117	0.00627	0.0055		PCI/G
10 A	09/13/19	Thorium-231	-0.00321	0.0674	0.107	U	PCI/G
10 A	09/13/19	Thorium-234	1.68	0.372	0.381		PCI/G
10 A	09/13/19	Thulium-171	-2.34	4.18	7.1	U	PCI/G
10 A	09/13/19	Tin-126	0	0.0148	0.0159	UI	PCI/G
10 A	09/30/19	Iodine-129	0.119	0.425	0.818	U	PCI/G
10 A	09/24/19	Technetium-99	-0.0227	0.41	0.699	U	PCI/G
10 A	09/28/19	Strontium-90	0.0114	0.00907	0.0146	U	PCI/G
10 A	09/28/19	Yttrium-90	0.0114	0.00907	0.0146	U	PCI/G
10 A	09/26/19	Nickel-63	0.148	0.238	0.402	U	PCI/G
10 A	09/27/19	Iron-55	1.58	3.34	4.95	U	PCI/G
10 A	09/27/19	Tritium	0.985	2.1	3.59	U	PCI/G
10 A	09/26/19	Carbon-14	0.183	1.43	2.48	U	PCI/G
10 A	09/26/19	Nickel-59	-0.0776	0.466	0.981	U	PCI/G
10 A	10/03/19	Americium-241	0.009	0.0142	0.0212	U	PCI/G
10 A	10/03/19	Americium-243	-0.0167	0.0199	0.0481	U	PCI/G
10 A	10/03/19	Curium-243/244	0.00148	0.00927	0.0175	U	PCI/G
10 A	10/03/19	Curium-245/246	0	0.0076	0.0104	U	PCI/G
10 B	09/29/19	Nickel-63	-0.0954	0.292	0.505	U	PCI/G
10 B	10/01/19	Polonium-210	1.09	0.302	0.198		PCI/G
10 B	09/28/19	Thorium-228	0.519	0.142	0.119		PCI/G
10 B	09/28/19	Thorium-229	0.118	0.0909	0.133	U	PCI/G
10 B	09/28/19	Thorium-230	1.82	0.244	0.133		PCI/G

Table B-1. Complete Results from the GEL Laboratory

Sample no.	Analysis date	Parameter	Result	Uncertainty	MDC[a]	Qualifier[b]	Units
10 B	09/28/19	Thorium-232	0.444	0.119	0.0597		PCI/G
10 B	09/29/19	Uranium-232	0.0218	0.0337	0.0521	U	PCI/G
10 B	09/29/19	Uranium-233/234	1.44	0.185	0.0931		PCI/G
10 B	09/29/19	Uranium-235/236	0.0693	0.0506	0.0639		PCI/G
10 B	09/29/19	Uranium-238	1.42	0.18	0.0552		PCI/G
10 B	09/28/19	Neptunium-236	-3.7E-10	0.00532	0.0106	U	PCI/G
10 B	09/28/19	Plutonium-236	-3.7E-10	0.00532	0.0106	U	PCI/G
10 B	09/28/19	Plutonium-239/240	0.00535	0.0096	0.0164	U	PCI/G
10 B	09/28/19	Plutonium-242	0.00269	0.0144	0.0266	U	PCI/G
10 B	09/28/19	Plutonium-244	0.00107	0.00469	0.00818	U	PCI/G
10 B	09/30/19	Neptunium-237	-0.000405	0.00982	0.0219	U	PCI/G
10 B	10/02/19	Plutonium-241	1.24	1.99	3.37	U	PCI/G
10 B	09/13/19	Actinium-225	0.0444	0.385	0.62	U	PCI/G
10 B	09/13/19	Actinium-227	0.04	0.0339	0.0489	U	PCI/G
10 B	09/13/19	Actinium-228	0.426	0.0328	0.0224		PCI/G
10 B	09/13/19	Antimony-125	0.00976	0.00884	0.0155	U	PCI/G
10 B	09/13/19	Barium-137m	0.115	0.00609	0.00517		PCI/G
10 B	09/13/19	Bismuth-212	0.476	0.0849	0.0746		PCI/G
10 B	09/13/19	Bismuth-213	0	0.0109	0.0175	UI	PCI/G
10 B	09/13/19	Bismuth-214	1.13	0.0224	0.0101		PCI/G
10 B	09/13/19	Cesium-134	0	0.00717	0.00746	UI	PCI/G
10 B	09/13/19	Cesium-137	0.122	0.00643	0.00546		PCI/G
10 B	09/13/19	Cobalt-60	-0.000592	0.00359	0.00611	U	PCI/G
10 B	09/13/19	Europium-152	-0.00748	0.00943	0.0162	U	PCI/G
10 B	09/13/19	Europium-154	-0.0044	0.0133	0.0196	U	PCI/G
10 B	09/13/19	Europium-155	0	0.0209	0.0235	UI	PCI/G
10 B	09/13/19	Holmium-166m	-0.0000237	0.00537	0.00892	U	PCI/G
10 B	09/13/19	Lead-210	0.554	1.05	1.35	U	PCI/G
10 B	09/13/19	Lead-212	0.423	0.0127	0.0108		PCI/G
10 B	09/13/19	Lead-214	1.32	0.0253	0.0453		PCI/G
10 B	09/13/19	Neptunium-239	0	0.0516	0.0577	UI	PCI/G
10 B	09/13/19	Niobium-94	0	0.00434	0.00527	UI	PCI/G
10 B	09/13/19	Potassium-40	13.5	0.201	0.0446		PCI/G
10 B	09/13/19	Promethium-147	19.5	101	168	U	PCI/G
10 B	09/13/19	Protactinium-231	0	0.0811	0.0816	UI	PCI/G
10 B	09/13/19	Radium-226	1.13	0.0224	0.0101		PCI/G
10 B	09/13/19	Radium-228	0.426	0.0328	0.0224		PCI/G
10 B	09/13/19	Sodium-22	-0.00132	0.00476	0.00704	U	PCI/G
10 B	09/13/19	Tellurium-125m	0.175	1.89	2.92	U	PCI/G
10 B	09/13/19	Thallium-208	0.121	0.00761	0.00559		PCI/G
10 B	09/13/19	Thorium-231	0.105	0.0856	0.11	U	PCI/G
10 B	09/13/19	Thorium-234	1.7	0.434	0.366		PCI/G
10 B	09/13/19	Thulium-171	-0.274	3.61	6.22	U	PCI/G
10 B	09/13/19	Tin-126	0	0.0169	0.0171	UI	PCI/G
10 B	09/30/19	Iodine-129	0.144	0.462	0.885	U	PCI/G
10 B	09/24/19	Technetium-99	-0.175	0.371	0.635	U	PCI/G
10 B	09/28/19	Strontium-90	-0.00321	0.00802	0.0148	U	PCI/G
10 B	09/28/19	Yttrium-90	-0.00321	0.00802	0.0148	U	PCI/G
10 B	09/29/19	Nickel-63	0.0397	0.327	0.559	U	PCI/G
10 B	09/29/19	Iron-55	3.35	2.23	3.24		PCI/G
10 B	09/27/19	Tritium	0.619	2.08	3.59	U	PCI/G
10 B	09/26/19	Carbon-14	0.776	1.41	2.4	U	PCI/G
10 B	09/26/19	Nickel-59	0.512	0.764	1.49	U	PCI/G
10 B	10/07/19	Americium-241	0.0107	0.0099	0.0117	U	PCI/G
10 B	10/07/19	Americium-243	-0.00462	0.0192	0.0449	U	PCI/G
10 B	10/07/19	Curium-243/244	0.00151	0.00662	0.0116	U	PCI/G
10 B	10/07/19	Curium-245/246	0.00521	0.0153	0.0156	U	PCI/G
10 C	09/28/19	Polonium-210	1.5	0.324	0.139		PCI/G
10 C	09/28/19	Thorium-228	0.377	0.118	0.123		PCI/G
10 C	09/28/19	Thorium-229	0.0649	0.0597	0.087	U	PCI/G

Table B-1. Complete Results from the GEL Laboratory

Sample no.	Analysis date	Parameter	Result	Uncertainty	MDC[a]	Qualifier[b]	Units
10 C	09/28/19	Thorium-230	1.42	0.197	0.115		PCI/G
10 C	09/28/19	Thorium-232	0.355	0.0988	0.0619		PCI/G
10 C	09/29/19	Uranium-232	0.0298	0.0338	0.0476	U	PCI/G
10 C	09/29/19	Uranium-233/234	1.63	0.172	0.0658		PCI/G
10 C	09/29/19	Uranium-235/236	0.133	0.0531	0.0439		PCI/G
10 C	09/29/19	Uranium-238	1.74	0.18	0.0809		PCI/G
10 C	09/30/19	Neptunium-236	-0.00533	0.00712	0.0195	U	PCI/G
10 C	09/30/19	Plutonium-236	-0.00533	0.00712	0.0195	U	PCI/G
10 C	09/30/19	Plutonium-239/240	-0.000118	0.0114	0.0232	U	PCI/G
10 C	09/30/19	Plutonium-242	0.0102	0.0117	0.0174	U	PCI/G
10 C	09/30/19	Plutonium-244	0.00928	0.00907	0.00991	U	PCI/G
10 C	09/30/19	Neptunium-237	0.00432	0.0102	0.0185	U	PCI/G
10 C	10/02/19	Plutonium-241	0.379	1.66	2.84	U	PCI/G
10 C	09/13/19	Actinium-225	-0.126	0.376	0.661	U	PCI/G
10 C	09/13/19	Actinium-227	0.04	0.0402	0.0504	U	PCI/G
10 C	09/13/19	Actinium-228	0.495	0.0415	0.0263		PCI/G
10 C	09/13/19	Antimony-125	0.00904	0.0109	0.0189	U	PCI/G
10 C	09/13/19	Barium-137m	0.1	0.00707	0.00663		PCI/G
10 C	09/13/19	Bismuth-212	0.486	0.106	0.0917		PCI/G
10 C	09/13/19	Bismuth-213	0	0.0214	0.0191	UI	PCI/G
10 C	09/13/19	Bismuth-214	1.25	0.0271	0.0126		PCI/G
10 C	09/13/19	Cesium-134	0	0.00925	0.00943	UI	PCI/G
10 C	09/13/19	Cesium-137	0.106	0.00747	0.007		PCI/G
10 C	09/13/19	Cobalt-60	0.00257	0.00455	0.00792	U	PCI/G
10 C	09/13/19	Europium-152	-0.0106	0.0108	0.0183	U	PCI/G
10 C	09/13/19	Europium-154	0.000951	0.015	0.0255	U	PCI/G
10 C	09/13/19	Europium-155	0	0.0192	0.0218	UI	PCI/G
10 C	09/13/19	Holmium-166m	0.00389	0.00635	0.0114	U	PCI/G
10 C	09/13/19	Lead-210	1.25	0.14	0.147		PCI/G
10 C	09/13/19	Lead-212	0.465	0.0126	0.0108		PCI/G
10 C	09/13/19	Lead-214	1.39	0.027	0.0522		PCI/G
10 C	09/13/19	Neptunium-239	-0.0382	0.0353	0.0573	U	PCI/G
10 C	09/13/19	Niobium-94	0.00177	0.00371	0.00665	U	PCI/G
10 C	09/13/19	Potassium-40	13.2	0.235	0.0578		PCI/G
10 C	09/13/19	Promethium-147	-1.21	101	166	U	PCI/G
10 C	09/13/19	Protactinium-231	0	0.0877	0.0924	UI	PCI/G
10 C	09/13/19	Radium-226	1.25	0.0271	0.0126		PCI/G
10 C	09/13/19	Radium-228	0.495	0.0415	0.0263		PCI/G
10 C	09/13/19	Sodium-22	0.00119	0.00551	0.00909	U	PCI/G
10 C	09/13/19	Tellurium-125m	1.32	2.1	2.8	U	PCI/G
10 C	09/13/19	Thallium-208	0.151	0.0104	0.00638		PCI/G
10 C	09/13/19	Thorium-231	0.068	0.105	0.123	U	PCI/G
10 C	09/13/19	Thorium-234	1.76	0.208	0.173		PCI/G
10 C	09/13/19	Thulium-171	0	1.31	1.46	UI	PCI/G
10 C	09/13/19	Tin-126	0	0.0138	0.0129	UI	PCI/G
10 C	09/30/19	Iodine-129	-0.201	0.575	0.985	U	PCI/G
10 C	09/24/19	Technetium-99	-0.262	0.366	0.63	U	PCI/G
10 C	09/28/19	Strontium-90	0.0105	0.00899	0.0148	U	PCI/G
10 C	09/28/19	Yttrium-90	0.0105	0.00899	0.0148	U	PCI/G
10 C	09/27/19	Nickel-63	0.103	0.277	0.47	U	PCI/G
10 C	09/29/19	Iron-55	4.17	2	2.84		PCI/G
10 C	09/27/19	Tritium	0.401	2.18	3.78	U	PCI/G
10 C	09/26/19	Carbon-14	0.244	1.4	2.42	U	PCI/G
10 C	09/26/19	Nickel-59	-0.376	1.39	2.4	U	PCI/G
10 C	10/07/19	Americium-241	0.00613	0.012	0.0196	U	PCI/G
10 C	10/07/19	Americium-243	-0.00682	0.0202	0.0453	U	PCI/G
10 C	10/07/19	Curium-243/244	0.0142	0.0143	0.0194	U	PCI/G
10 C	10/07/19	Curium-245/246	0	0.0084	0.0115	U	PCI/G
11 A	09/30/19	Polonium-210	2.85	0.47	0.172		PCI/G
11 A	10/01/19	Thorium-228	0.979	0.197	0.182		PCI/G
11 A	10/01/19	Thorium-229	0.0668	0.0756	0.12	U	PCI/G
11 A	10/01/19	Thorium-230	2.4	0.267	0.107		PCI/G

Table B-1. Complete Results from the GEL Laboratory

Sample no.	Analysis date	Parameter	Result	Uncertainty	MDC[a]	Qualifier[b]	Units
11 A	10/01/19	Thorium-232	0.709	0.156	0.125		PCI/G
11 A	09/30/19	Uranium-232	-0.00387	0.0448	0.0858	U	PCI/G
11 A	09/30/19	Uranium-233/234	2.81	0.196	0.0614		PCI/G
11 A	09/30/19	Uranium-235/236	0.198	0.0575	0.0501		PCI/G
11 A	09/30/19	Uranium-238	2.73	0.192	0.0427		PCI/G
11 A	09/30/19	Neptunium-236	0.0054	0.015	0.0275	U	PCI/G
11 A	09/30/19	Plutonium-236	0.0054	0.015	0.0275	U	PCI/G
11 A	09/30/19	Plutonium-239/240	0.0131	0.017	0.0265	U	PCI/G
11 A	09/30/19	Plutonium-242	0.00752	0.0104	0.0168	U	PCI/G
11 A	09/30/19	Plutonium-244	0.0118	0.0147	0.021	U	PCI/G
11 A	09/30/19	Neptunium-237	0.00425	0.00921	0.0154	U	PCI/G
11 A	10/03/19	Plutonium-241	-0.555	2.43	4.21	U	PCI/G
11 A	09/14/19	Actinium-225	0.0409	0.658	1.06	U	PCI/G
11 A	09/14/19	Actinium-227	0	0.0632	0.0744	UI	PCI/G
11 A	09/14/19	Actinium-228	1.37	0.0678	0.0409		PCI/G
11 A	09/14/19	Antimony-125	0.00863	0.0158	0.0269	U	PCI/G
11 A	09/14/19	Barium-137m	0.0344	0.0087	0.00934		PCI/G
11 A	09/14/19	Bismuth-212	1.31	0.181	0.132		PCI/G
11 A	09/14/19	Bismuth-213	0.021	0.0261	0.0289	U	PCI/G
11 A	09/14/19	Bismuth-214	2.76	0.0456	0.0179		PCI/G
11 A	09/14/19	Cesium-134	0	0.0148	0.0128	UI	PCI/G
11 A	09/14/19	Cesium-137	0.0363	0.00919	0.00986		PCI/G
11 A	09/14/19	Cobalt-60	0.00626	0.00663	0.0117	U	PCI/G
11 A	09/14/19	Europium-152	-0.00311	0.0169	0.0277	U	PCI/G
11 A	09/14/19	Europium-154	-0.00118	0.0247	0.0372	U	PCI/G
11 A	09/14/19	Europium-155	0	0.035	0.0369	UI	PCI/G
11 A	09/14/19	Holmium-166m	-0.00099	0.00935	0.0162	U	PCI/G
11 A	09/14/19	Lead-210	1.86	2.7	4.86	U	PCI/G
11 A	09/14/19	Lead-212	1.38	0.0246	0.018		PCI/G
11 A	09/14/19	Lead-214	3.32	0.046	0.0757		PCI/G
11 A	09/14/19	Neptunium-239	0.078	0.0785	0.0913	U	PCI/G
11 A	09/14/19	Niobium-94	0	0.00741	0.00946	UI	PCI/G
11 A	09/14/19	Potassium-40	22.6	0.363	0.107		PCI/G
11 A	09/14/19	Promethium-147	222	155	265	U	PCI/G
11 A	09/14/19	Protactinium-231	0	0.126	0.136	UI	PCI/G
11 A	09/14/19	Radium-226	2.76	0.0456	0.0179		PCI/G
11 A	09/14/19	Radium-228	1.37	0.0678	0.0409		PCI/G
11 A	09/14/19	Sodium-22	-0.000238	0.00884	0.0133	U	PCI/G
11 A	09/14/19	Tellurium-125m	1.76	4.41	4.59	U	PCI/G
11 A	09/14/19	Thallium-208	0.443	0.0183	0.0095		PCI/G
11 A	09/14/19	Thorium-231	0	0.159	0.181	UI	PCI/G
11 A	09/14/19	Thorium-234	3.99	0.997	0.765		PCI/G
11 A	09/14/19	Thulium-171	12.5	14.3	17.4	U	PCI/G
11 A	09/14/19	Tin-126	0	0.0302	0.0287	UI	PCI/G
11 A	09/30/19	Iodine-129	-0.0326	0.606	1.08	U	PCI/G
11 A	09/25/19	Technetium-99	-0.368	0.466	0.802	U	PCI/G
11 A	09/25/19	Strontium-90	-0.00633	0.00682	0.0124	U	PCI/G
11 A	09/25/19	Yttrium-90	-0.00633	0.00682	0.0124	U	PCI/G
11 A	09/28/19	Nickel-63	0.0289	0.279	0.477	U	PCI/G
11 A	09/30/19	Iron-55	0.711	2.42	3.64	U	PCI/G
11 A	09/28/19	Tritium	0.344	2.04	3.54	U	PCI/G
11 A	09/26/19	Carbon-14	0.786	1.45	2.47	U	PCI/G
11 A	09/27/19	Nickel-59	0.741	0.872	1.72	U	PCI/G
11 A	10/03/19	Americium-241	-0.0118	0.0213	0.0536	U	PCI/G
11 A	10/03/19	Americium-243	0.00829	0.0149	0.0254	U	PCI/G
11 A	10/03/19	Curium-243/244	-0.000275	0.0288	0.0593	U	PCI/G
11 A	10/03/19	Curium-245/246	0.00385	0.00924	0.0147	U	PCI/G
11 B	09/30/19	Polonium-210	2.55	0.382	0.145		PCI/G
11 B	10/01/19	Thorium-228	0.749	0.16	0.126		PCI/G
11 B	10/01/19	Thorium-229	0.042	0.0548	0.0861	U	PCI/G

Table B-1. Complete Results from the GEL Laboratory

Sample no.	Analysis date	Parameter	Result	Uncertainty	MDC[a]	Qualifier[b]	Units
11 B	10/01/19	Thorium-230	2.67	0.273	0.107		PCI/G
11 B	10/01/19	Thorium-232	0.744	0.145	0.0666		PCI/G
11 B	09/30/19	Uranium-232	0.0212	0.0361	0.0609	U	PCI/G
11 B	09/30/19	Uranium-233/234	3.13	0.187	0.0319		PCI/G
11 B	09/30/19	Uranium-235/236	0.185	0.0481	0.032		PCI/G
11 B	09/30/19	Uranium-238	3.01	0.183	0.0276		PCI/G
11 B	09/30/19	Neptunium-236	-0.00861	0.0115	0.0315	U	PCI/G
11 B	09/30/19	Plutonium-236	-0.00861	0.0115	0.0315	U	PCI/G
11 B	09/30/19	Plutonium-239/240	-0.00281	0.0117	0.0274	U	PCI/G
11 B	09/30/19	Plutonium-242	0.0126	0.0106	0.0134	U	PCI/G
11 B	09/30/19	Plutonium-244	0.00132	0.0107	0.0218	U	PCI/G
11 B	09/30/19	Neptunium-237	0.0106	0.015	0.0248	U	PCI/G
11 B	10/03/19	Plutonium-241	0.67	2.44	4.17	U	PCI/G
11 B	09/14/19	Actinium-225	-0.715	0.83	1.28	U	PCI/G
11 B	09/14/19	Actinium-227	0	0.0718	0.0965	UI	PCI/G
11 B	09/14/19	Actinium-228	1.51	0.0696	0.04		PCI/G
11 B	09/14/19	Antimony-125	0.00597	0.0185	0.0312	U	PCI/G
11 B	09/14/19	Barium-137m	0.0163	0.00865	0.0104		PCI/G
11 B	09/14/19	Bismuth-212	1.49	0.18	0.148		PCI/G
11 B	09/14/19	Bismuth-213	0.0294	0.0297	0.0327	U	PCI/G
11 B	09/14/19	Bismuth-214	3.16	0.0496	0.0193		PCI/G
11 B	09/14/19	Cesium-134	0	0.014	0.0158	UI	PCI/G
11 B	09/14/19	Cesium-137	0.0172	0.00914	0.011		PCI/G
11 B	09/14/19	Cobalt-60	0.00354	0.00714	0.0121	U	PCI/G
11 B	09/14/19	Europium-152	-0.00971	0.0195	0.0329	U	PCI/G
11 B	09/14/19	Europium-154	0	0.0435	0.0376	UI	PCI/G
11 B	09/14/19	Europium-155	0	0.0412	0.0481	UI	PCI/G
11 B	09/14/19	Holmium-166m	0.000985	0.0104	0.0182	U	PCI/G
11 B	09/14/19	Lead-210	0	4.31	5.15	UI	PCI/G
11 B	09/14/19	Lead-212	1.49	0.0276	0.0207		PCI/G
11 B	09/14/19	Lead-214	3.73	0.0514	0.0245		PCI/G
11 B	09/14/19	Neptunium-239	-0.0573	0.0735	0.118	U	PCI/G
11 B	09/14/19	Niobium-94	0.00825	0.00917	0.0106	U	PCI/G
11 B	09/14/19	Potassium-40	23.6	0.346	0.0973		PCI/G
11 B	09/14/19	Promethium-147	42.3	216	328	U	PCI/G
11 B	09/14/19	Protactinium-231	0	0.134	0.16	UI	PCI/G
11 B	09/14/19	Radium-226	3.16	0.0496	0.0193		PCI/G
11 B	09/14/19	Radium-228	1.51	0.0696	0.04		PCI/G
11 B	09/14/19	Sodium-22	0	0.0156	0.0133	UI	PCI/G
11 B	09/14/19	Tellurium-125m	5.22	4.52	6.04	U	PCI/G
11 B	09/14/19	Thallium-208	0.431	0.0181	0.0114		PCI/G
11 B	09/14/19	Thorium-231	0.0767	0.144	0.222	U	PCI/G
11 B	09/14/19	Thorium-234	4.43	1.11	0.965		PCI/G
11 B	09/14/19	Thulium-171	5.91	12.6	20.1	U	PCI/G
11 B	09/14/19	Tin-126	0	0.0424	0.0372	UI	PCI/G
11 B	09/30/19	Iodine-129	0.0672	0.319	0.68	U	PCI/G
11 B	09/25/19	Technetium-99	-0.224	0.392	0.672	U	PCI/G
11 B	10/05/19	Strontium-90	-0.00213	0.00814	0.0149	U	PCI/G
11 B	10/05/19	Yttrium-90	-0.00213	0.00814	0.0149	U	PCI/G
11 B	09/28/19	Nickel-63	-0.223	0.265	0.461	U	PCI/G
11 B	09/30/19	Iron-55	1.51	2.57	3.87	U	PCI/G
11 B	09/28/19	Tritium	1.37	2.16	3.66	U	PCI/G
11 B	09/26/19	Carbon-14	0.877	1.43	2.43	U	PCI/G
11 B	09/27/19	Nickel-59	-0.0835	0.442	0.948	U	PCI/G
11 B	10/03/19	Americium-241	0.00989	0.0176	0.029	U	PCI/G
11 B	10/03/19	Americium-243	0.0183	0.0259	0.0402	U	PCI/G
11 B	10/03/19	Curium-243/244	0.00645	0.0197	0.0366	U	PCI/G
11 B	10/03/19	Curium-245/246	0.00264	0.0166	0.0313	U	PCI/G
11 C	09/30/19	Polonium-210	1.87	0.346	0.159		PCI/G
11 C	09/30/19	Uranium-232	0.0269	0.0609	0.107	U	PCI/G
11 C	09/30/19	Uranium-233/234	3.28	0.251	0.0608		PCI/G
11 C	09/30/19	Uranium-235/236	0.278	0.0801	0.0664		PCI/G

Table B-1. Complete Results from the GEL Laboratory

Sample no.	Analysis date	Parameter	Result	Uncertainty	MDC[a]	Qualifier[b]	Units
11 C	09/30/19	Uranium-238	3.41	0.256	0.0547		PCI/G
11 C	09/30/19	Neptunium-236	-0.00305	0.00736	0.0188	U	PCI/G
11 C	09/30/19	Plutonium-236	-0.00305	0.00736	0.0188	U	PCI/G
11 C	09/30/19	Plutonium-239/240	0.00575	0.0102	0.0168	U	PCI/G
11 C	09/30/19	Plutonium-242	-0.0098	0.00898	0.0217	U	PCI/G
11 C	09/30/19	Plutonium-244	0.0125	0.011	0.0113	X	PCI/G
11 C	09/30/19	Neptunium-237	0.00513	0.00934	0.0152	U	PCI/G
11 C	10/03/19	Plutonium-241	-1.15	1.95	3.42	U	PCI/G
11 C	09/14/19	Actinium-225	0.283	0.695	1.22	U	PCI/G
11 C	09/14/19	Actinium-227	0	0.0744	0.0893	UI	PCI/G
11 C	09/14/19	Actinium-228	1.5	0.0619	0.0367		PCI/G
11 C	09/14/19	Antimony-125	0.0015	0.0166	0.0279	U	PCI/G
11 C	09/14/19	Barium-137m	0.018	0.00731	0.00951		PCI/G
11 C	09/14/19	Bismuth-212	1.52	0.153	0.135		PCI/G
11 C	09/14/19	Bismuth-213	-0.00162	0.0182	0.0305	U	PCI/G
11 C	09/14/19	Bismuth-214	2.71	0.041	0.0187		PCI/G
11 C	09/14/19	Cesium-134	0	0.0138	0.0146	UI	PCI/G
11 C	09/14/19	Cesium-137	0.019	0.00772	0.0101		PCI/G
11 C	09/14/19	Cobalt-60	0.00519	0.00659	0.0113	U	PCI/G
11 C	09/14/19	Europium-152	-0.0212	0.0177	0.0297	U	PCI/G
11 C	09/14/19	Europium-154	0.009	0.0239	0.0354	U	PCI/G
11 C	09/14/19	Europium-155	0	0.0368	0.0415	UI	PCI/G
11 C	09/14/19	Holmium-166m	0.000269	0.00956	0.0167	U	PCI/G
11 C	09/14/19	Lead-210	1.68	2.12	3.64	U	PCI/G
11 C	09/14/19	Lead-212	1.54	0.0249	0.0191		PCI/G
11 C	09/14/19	Lead-214	3.26	0.0479	0.0851		PCI/G
11 C	09/14/19	Neptunium-239	-0.0545	0.07	0.104	U	PCI/G
11 C	09/14/19	Niobium-94	0	0.0098	0.0102	UI	PCI/G
11 C	09/14/19	Potassium-40	23.3	0.328	0.0892		PCI/G
11 C	09/14/19	Promethium-147	85	183	300	U	PCI/G
11 C	09/14/19	Protactinium-231	0	0.15	0.149	UI	PCI/G
11 C	09/14/19	Radium-226	2.71	0.041	0.0187		PCI/G
11 C	09/14/19	Radium-228	1.5	0.0619	0.0367		PCI/G
11 C	09/14/19	Sodium-22	0.00651	0.00842	0.0127	U	PCI/G
11 C	09/14/19	Tellurium-125m	4.7	4.62	5.18	U	PCI/G
11 C	09/14/19	Thallium-208	0.461	0.0173	0.0098		PCI/G
11 C	09/14/19	Thorium-231	0.15	0.135	0.196	U	PCI/G
11 C	09/14/19	Thorium-234	3.67	0.862	0.736		PCI/G
11 C	09/14/19	Thulium-171	0	10.4	14.6	UI	PCI/G
11 C	09/14/19	Tin-126	0	0.0308	0.0313	UI	PCI/G
11 C	09/30/19	Iodine-129	-0.0153	0.228	0.474	U	PCI/G
11 C	09/25/19	Technetium-99	-0.371	0.374	0.646	U	PCI/G
11 C	09/25/19	Strontium-90	0.00403	0.00604	0.0102	U	PCI/G
11 C	09/25/19	Yttrium-90	0.00403	0.00604	0.0102	U	PCI/G
11 C	09/28/19	Nickel-63	0.0344	0.255	0.435	U	PCI/G
11 C	09/30/19	Iron-55	1.73	2.42	3.59	U	PCI/G
11 C	09/28/19	Tritium	0.724	2.12	3.64	U	PCI/G
11 C	09/26/19	Carbon-14	0.437	1.41	2.43	U	PCI/G
11 C	09/27/19	Nickel-59	-0.129	0.917	1.63	U	PCI/G
11 C	10/03/19	Americium-241	0.00839	0.0178	0.0315	U	PCI/G
11 C	10/03/19	Americium-243	-0.0034	0.0177	0.0391	U	PCI/G
11 C	10/03/19	Curium-243/244	0.00417	0.0123	0.0224	U	PCI/G
11 C	10/03/19	Curium-245/246	0.00559	0.0165	0.03	U	PCI/G
11 C	10/05/19	Thorium-228	1.14	0.331	0.365		PCI/G
11 C	10/05/19	Thorium-229	-0.0626	0.15	0.31	U	PCI/G
11 C	10/05/19	Thorium-230	3.17	0.453	0.239		PCI/G
11 C	10/05/19	Thorium-232	0.794	0.23	0.149		PCI/G
13 A	09/25/19	Actinium-225	-1.56	1.95	3.05	U	PCI/G
13 A	09/25/19	Actinium-227	0.105	0.0849	0.127	U	PCI/G
13 A	09/25/19	Actinium-228	1.21	0.115	0.0713		PCI/G

Table B-1. Complete Results from the GEL Laboratory

Sample no.	Analysis date	Parameter	Result	Uncertainty	MDC[a]	Qualifier[b]	Units
13 A	09/25/19	Antimony-125	0.00672	0.027	0.0465	U	PCI/G
13 A	09/25/19	Barium-137m	0.0971	0.0145	0.0162		PCI/G
13 A	09/25/19	Bismuth-212	1.54	0.231	0.238		PCI/G
13 A	09/25/19	Bismuth-213	-0.0085	0.0292	0.0494	U	PCI/G
13 A	09/25/19	Bismuth-214	2.46	0.0657	0.0326		PCI/G
13 A	09/25/19	Cesium-134	0	0.0194	0.0264	UI	PCI/G
13 A	09/25/19	Cesium-137	0.103	0.0153	0.0171		PCI/G
13 A	09/25/19	Cobalt-60	0.00491	0.0112	0.0197	U	PCI/G
13 A	09/25/19	Europium-152	-0.000493	0.0269	0.0465	U	PCI/G
13 A	09/25/19	Europium-154	-0.00984	0.0357	0.0604	U	PCI/G
13 A	09/25/19	Europium-155	0	0.0499	0.0511	UI	PCI/G
13 A	09/25/19	Holmium-166m	0.00333	0.0167	0.0299	U	PCI/G
13 A	09/25/19	Lead-210	2.65	0.416	0.347		PCI/G
13 A	09/25/19	Lead-212	1.24	0.0347	0.0288		PCI/G
13 A	09/25/19	Lead-214	2.68	0.0646	0.0341		PCI/G
13 A	09/25/19	Neptunium-239	-0.073	0.0819	0.133	U	PCI/G
13 A	09/25/19	Niobium-94	0.00974	0.0132	0.0158	U	PCI/G
13 A	09/25/19	Potassium-40	22.9	0.568	0.158		PCI/G
13 A	09/25/19	Promethium-147	39	236	390	U	PCI/G
13 A	09/25/19	Protactinium-231	0	0.22	0.221	UI	PCI/G
13 A	09/25/19	Radium-226	2.46	0.0657	0.0326		PCI/G
13 A	09/25/19	Radium-228	1.21	0.115	0.0713		PCI/G
13 A	09/25/19	Sodium-22	-0.00435	0.0133	0.0216	U	PCI/G
13 A	09/25/19	Tellurium-125m	6.92	6.22	7.02	U	PCI/G
13 A	09/25/19	Thallium-208	0.391	0.024	0.0162		PCI/G
13 A	09/25/19	Thorium-231	-0.0562	0.196	0.303	U	PCI/G
13 A	09/25/19	Thorium-234	1.14	0.431	0.41		PCI/G
13 A	09/25/19	Thulium-171	0	3	3.41	UI	PCI/G
13 A	09/25/19	Tin-126	0	0.0323	0.0311	UI	PCI/G
13 A	10/03/19	Polonium-210	1.52	0.348	0.193		PCI/G
13 A	10/03/19	Polonium-210	1.52	0.348	0.193		PCI/G
13 A	10/02/19	Thorium-228	0.936	0.184	0.106		PCI/G
13 A	10/02/19	Thorium-229	0.0571	0.0577	0.0782	U	PCI/G
13 A	10/02/19	Thorium-230	2.42	0.282	0.125		PCI/G
13 A	10/02/19	Thorium-232	0.804	0.163	0.0778		PCI/G
13 A	10/02/19	Thorium-228	0.936	0.184	0.106		PCI/G
13 A	10/02/19	Thorium-229	0.0571	0.0577	0.0782	U	PCI/G
13 A	10/02/19	Thorium-230	2.42	0.282	0.125		PCI/G
13 A	10/02/19	Thorium-232	0.804	0.163	0.0778		PCI/G
13 A	10/01/19	Uranium-232	-0.026	0.0318	0.0736	U	PCI/G
13 A	10/01/19	Uranium-233/234	1.01	0.121	0.0449		PCI/G
13 A	10/01/19	Uranium-235/236	0.0585	0.0321	0.028		PCI/G
13 A	10/01/19	Uranium-238	0.981	0.119	0.0349		PCI/G
13 A	10/01/19	Uranium-232	-0.026	0.0318	0.0736	U	PCI/G
13 A	10/01/19	Uranium-233/234	1.01	0.121	0.0449		PCI/G
13 A	10/01/19	Uranium-235/236	0.0585	0.0321	0.028		PCI/G
13 A	10/01/19	Uranium-238	0.981	0.119	0.0349		PCI/G
13 A	10/01/19	Neptunium-236	-0.00137	0.0109	0.0246	U	PCI/G
13 A	10/01/19	Plutonium-236	-0.00137	0.0109	0.0246	U	PCI/G
13 A	10/01/19	Plutonium-239/240	0.00247	0.0113	0.022	U	PCI/G
13 A	10/01/19	Plutonium-242	0.017	0.0166	0.0253	U	PCI/G
13 A	10/01/19	Plutonium-244	-0.00127	0.00606	0.0148	U	PCI/G
13 A	10/01/19	Neptunium-236	-0.00137	0.0109	0.0246	U	PCI/G
13 A	10/01/19	Plutonium-236	-0.00137	0.0109	0.0246	U	PCI/G
13 A	10/01/19	Plutonium-239/240	0.00247	0.0113	0.022	U	PCI/G
13 A	10/01/19	Plutonium-242	0.017	0.0166	0.0253	U	PCI/G
13 A	10/01/19	Plutonium-244	-0.00127	0.00606	0.0148	U	PCI/G
13 A	10/02/19	Americium-241	0.00528	0.0103	0.0178	U	PCI/G
13 A	10/02/19	Americium-243	0.00479	0.0115	0.0203	U	PCI/G
13 A	10/02/19	Curium-243/244	-0.0036	0.00795	0.0196	U	PCI/G
13 A	10/02/19	Curium-245/246	-0.00139	0.00609	0.0133	U	PCI/G
13 A	10/02/19	Americium-241	0.00528	0.0103	0.0178	U	PCI/G

Table B-1. Complete Results from the GEL Laboratory

Sample no.	Analysis date	Parameter	Result	Uncertainty	MDC[a]	Qualifier[b]	Units
13 A	10/02/19	Americium-243	0.00479	0.0115	0.0203	U	PCI/G
13 A	10/02/19	Curium-243/244	-0.0036	0.00795	0.0196	U	PCI/G
13 A	10/02/19	Curium-245/246	-0.00139	0.00609	0.0133	U	PCI/G
13 A	10/03/19	Neptunium-237	-0.00764	0.00961	0.0321	U	PCI/G
13 A	10/03/19	Neptunium-237	-0.00764	0.00961	0.0321	U	PCI/G
13 A	10/06/19	Plutonium-241	0.915	2.45	4.18	U	PCI/G
13 A	10/06/19	Plutonium-241	0.915	2.45	4.18	U	PCI/G
13 A	09/27/19	Nickel-63	0.284	0.405	0.684	U	PCI/G
13 A	09/26/19	Iron-55	-0.33	2.43	3.5	U	PCI/G
13 A	09/26/19	Technetium-99	-0.0267	0.35	0.596	U	PCI/G
13 A	09/26/19	Technetium-99	-0.0267	0.35	0.596	U	PCI/G
13 A	09/28/19	Tritium	0.257	2.26	4.02	U	PCI/G
13 A	09/28/19	Tritium	0.257	2.26	4.02	U	PCI/G
13 A	09/28/19	Tritium	83.6	24.9	13.3		%
13 A	09/28/19	Tritium	83.6	24.9	13.3		%
13 A	09/28/19	Carbon-14	-0.0804	1.46	2.57	U	PCI/G
13 A	09/28/19	Carbon-14	-0.0804	1.46	2.57	U	PCI/G
13 A	09/28/19	Carbon-14	91.5	3.02	2.5		%
13 A	09/28/19	Carbon-14	91.5	3.02	2.5		%
13 A	09/26/19	Nickel-59	0.219	0.87	1.59	U	PCI/G
13 A	09/25/19	Actinium-225	-1.7	1.99	3.45	U	PCI/G
13 A	09/25/19	Actinium-227	0	0.104	0.141	UI	PCI/G
13 A	09/25/19	Actinium-228	1.25	0.0901	0.063		PCI/G
13 A	09/25/19	Antimony-125	0.0221	0.0266	0.0462	U	PCI/G
13 A	09/25/19	Barium-137m	0.0766	0.0145	0.0157		PCI/G
13 A	09/25/19	Bismuth-212	1.34	0.243	0.215		PCI/G
13 A	09/25/19	Bismuth-213	0.0264	0.0288	0.05	U	PCI/G
13 A	09/25/19	Bismuth-214	2.35	0.0661	0.0293		PCI/G
13 A	09/25/19	Cesium-134	0	0.0196	0.0228	UI	PCI/G
13 A	09/25/19	Cesium-137	0.0809	0.0153	0.0166		PCI/G
13 A	09/25/19	Cobalt-60	-0.0062	0.0103	0.017	U	PCI/G
13 A	09/25/19	Europium-152	-0.0249	0.0276	0.0464	U	PCI/G
13 A	09/25/19	Europium-154	-0.00986	0.039	0.0569	U	PCI/G
13 A	09/25/19	Europium-155	0	0.0563	0.0642	UI	PCI/G
13 A	09/25/19	Holmium-166m	-0.00106	0.0151	0.0267	U	PCI/G
13 A	09/25/19	Lead-210	2.45	3.21	5.57	U	PCI/G
13 A	09/25/19	Lead-212	1.29	0.0376	0.03		PCI/G
13 A	09/25/19	Lead-214	2.73	0.068	0.0341		PCI/G
13 A	09/25/19	Neptunium-239	-0.0688	0.101	0.163	U	PCI/G
13 A	09/25/19	Niobium-94	0	0.0146	0.0154	UI	PCI/G
13 A	09/25/19	Potassium-40	23.4	0.525	0.14		PCI/G
13 A	09/25/19	Promethium-147	-45.2	278	454	U	PCI/G
13 A	09/25/19	Protactinium-231	0	0.224	0.229	UI	PCI/G
13 A	09/25/19	Radium-226	2.35	0.0661	0.0293		PCI/G
13 A	09/25/19	Radium-228	1.25	0.0901	0.063		PCI/G
13 A	09/25/19	Sodium-22	-0.00394	0.014	0.0204	U	PCI/G
13 A	09/25/19	Tellurium-125m	3.82	5.44	9.07	U	PCI/G
13 A	09/25/19	Thallium-208	0.413	0.0266	0.0156		PCI/G
13 A	09/25/19	Thorium-231	0.165	0.204	0.322	U	PCI/G
13 A	09/25/19	Thorium-234	1.47	1.43	1.12		PCI/G
13 A	09/25/19	Thulium-171	9.92	13.1	22.3	U	PCI/G
13 A	09/25/19	Tin-126	0	0.0492	0.0452	UI	PCI/G
13 A	10/02/19	Polonium-210	1.48	0.342	0.118		PCI/G
13 A	10/01/19	Thorium-228	0.987	0.177	0.132		PCI/G
13 A	10/01/19	Thorium-229	0.053	0.0779	0.131	U	PCI/G
13 A	10/01/19	Thorium-230	2.3	0.249	0.112		PCI/G
13 A	10/01/19	Thorium-232	0.883	0.157	0.0949		PCI/G
13 A	10/01/19	Uranium-232	-0.0346	0.0634	0.14	U	PCI/G
13 A	10/01/19	Uranium-233/234	0.964	0.108	0.0298		PCI/G
13 A	10/01/19	Uranium-235/236	0.0655	0.034	0.0384		PCI/G

Table B-1. Complete Results from the GEL Laboratory

Sample no.	Analysis date	Parameter	Result	Uncertainty	MDC[a]	Qualifier[b]	Units
13 A	10/01/19	Uranium-238	1	0.11	0.00933		PCI/G
13 A	10/01/19	Neptunium-236	-0.00206	0.0053	0.0144	U	PCI/G
13 A	10/01/19	Plutonium-236	-0.00206	0.0053	0.0144	U	PCI/G
13 A	10/01/19	Plutonium-239/240	-0.00105	0.00945	0.0208	U	PCI/G
13 A	10/01/19	Plutonium-242	0.000794	0.0154	0.0304	U	PCI/G
13 A	10/01/19	Plutonium-244	0.000971	0.00609	0.0115	U	PCI/G
13 A	10/02/19	Americium-241	0.00784	0.0103	0.0132	U	PCI/G
13 A	10/02/19	Americium-243	-0.00133	0.0106	0.0238	U	PCI/G
13 A	10/02/19	Curium-243/244	0.00548	0.0131	0.0236	U	PCI/G
13 A	10/02/19	Curium-245/246	0	0.00645	0.00882	U	PCI/G
13 A	10/02/19	Neptunium-237	-0.0000637	0.00844	0.0177	U	PCI/G
13 A	10/05/19	Plutonium-241	0.569	1.7	2.9	U	PCI/G
13 A	09/30/19	Iodine-129	0.411	0.405	0.936	U	PCI/G
13 A	09/26/19	Nickel-63	0.347	0.436	0.734	U	PCI/G
13 A	09/26/19	Iron-55	-0.538	2.31	3.31	U	PCI/G
13 A	09/24/19	Technetium-99	-0.22	0.364	0.626	U	PCI/G
13 A	09/26/19	Tritium	-1.24	2.44	4.55	U	PCI/G
13 A	09/28/19	Carbon-14	0.317	1.5	2.61	U	PCI/G
13 A	09/25/19	Nickel-59	0.36	1.14	2.12	U	PCI/G
13 A	10/07/19	Strontium-90	-0.00885	0.00704	0.0137	U	PCI/G
13 A	10/07/19	Yttrium-90	-0.00885	0.00704	0.0137	U	PCI/G
13 B	09/17/19	Actinium-225	-0.537	0.706	1.23	U	PCI/G
13 B	09/17/19	Actinium-227	0	0.0872	0.0808	UI	PCI/G
13 B	09/17/19	Actinium-228	1.18	0.0707	0.0436		PCI/G
13 B	09/17/19	Antimony-125	0.0129	0.0176	0.0303	U	PCI/G
13 B	09/17/19	Barium-137m	0.0782	0.0101	0.0106		PCI/G
13 B	09/17/19	Bismuth-212	1.37	0.185	0.153		PCI/G
13 B	09/17/19	Bismuth-213	0	0.0313	0.0308	UI	PCI/G
13 B	09/17/19	Bismuth-214	2.26	0.0435	0.0211		PCI/G
13 B	09/17/19	Cesium-134	0	0.0148	0.0174	UI	PCI/G
13 B	09/17/19	Cesium-137	0.0826	0.0107	0.0112		PCI/G
13 B	09/17/19	Cobalt-60	-0.00176	0.0074	0.0124	U	PCI/G
13 B	09/17/19	Europium-152	-0.00871	0.0179	0.0305	U	PCI/G
13 B	09/17/19	Europium-154	0.0104	0.0273	0.041	U	PCI/G
13 B	09/17/19	Europium-155	0	0.0338	0.0336	UI	PCI/G
13 B	09/17/19	Holmium-166m	0.00227	0.012	0.0189	U	PCI/G
13 B	09/17/19	Lead-210	1.93	0.287	0.235		PCI/G
13 B	09/17/19	Lead-212	1.28	0.0233	0.0181		PCI/G
13 B	09/17/19	Lead-214	2.51	0.0453	0.0224		PCI/G
13 B	09/17/19	Neptunium-239	0	0.0784	0.0902	UI	PCI/G
13 B	09/17/19	Niobium-94	0	0.00962	0.0115	UI	PCI/G
13 B	09/17/19	Potassium-40	22.3	0.369	0.0994		PCI/G
13 B	09/17/19	Promethium-147	8.06	157	257	U	PCI/G
13 B	09/17/19	Protactinium-231	0	0.159	0.146	UI	PCI/G
13 B	09/17/19	Radium-226	2.26	0.0435	0.0211		PCI/G
13 B	09/17/19	Radium-228	1.18	0.0707	0.0436		PCI/G
13 B	09/17/19	Sodium-22	0.0051	0.00967	0.0147	U	PCI/G
13 B	09/17/19	Tellurium-125m	0	3.78	4.32	UI	PCI/G
13 B	09/17/19	Thallium-208	0.411	0.0195	0.0108		PCI/G
13 B	09/17/19	Thorium-231	0.125	0.127	0.201	U	PCI/G
13 B	09/17/19	Thorium-234	1.24	0.292	0.276		PCI/G
13 B	09/17/19	Thulium-171	0	1.8	2.24	UI	PCI/G
13 B	09/17/19	Tin-126	0	0.0233	0.0201	UI	PCI/G
13 B	10/03/19	Polonium-210	1.35	0.302	0.18		PCI/G
13 B	10/02/19	Thorium-228	0.885	0.168	0.113		PCI/G
13 B	10/02/19	Thorium-229	0.0558	0.0546	0.0771	U	PCI/G
13 B	10/02/19	Thorium-230	2.37	0.253	0.0532		PCI/G
13 B	10/02/19	Thorium-232	0.832	0.151	0.053		PCI/G
13 B	10/01/19	Uranium-232	-0.0128	0.0344	0.0721	U	PCI/G
13 B	10/01/19	Uranium-233/234	0.824	0.19	0.101		PCI/G
13 B	10/01/19	Uranium-235/236	0.0531	0.0625	0.0813	U	PCI/G
13 B	10/01/19	Uranium-238	0.795	0.189	0.117		PCI/G

Table B-1. Complete Results from the GEL Laboratory

Sample no.	Analysis date	Parameter	Result	Uncertainty	MDC[a]	Qualifier[b]	Units
13 B	10/01/19	Neptunium-236	-0.00396	0.0058	0.0171	U	PCI/G
13 B	10/01/19	Plutonium-236	-0.00396	0.0058	0.0171	U	PCI/G
13 B	10/01/19	Plutonium-239/240	-0.00479	0.00744	0.02	U	PCI/G
13 B	10/01/19	Plutonium-242	0.00384	0.00741	0.0112	U	PCI/G
13 B	10/01/19	Plutonium-244	0.00565	0.00889	0.0133	U	PCI/G
13 B	10/02/19	Americium-241	0.00345	0.00741	0.0122	U	PCI/G
13 B	10/02/19	Americium-243	0.00312	0.0141	0.027	U	PCI/G
13 B	10/02/19	Curium-243/244	0.00512	0.00908	0.015	U	PCI/G
13 B	10/02/19	Curium-245/246	0.005	0.0107	0.0177	U	PCI/G
13 B	10/02/19	Neptunium-237	0.00213	0.0134	0.0253	U	PCI/G
13 B	10/05/19	Plutonium-241	0.184	1.73	2.97	U	PCI/G
13 B	09/30/19	Iodine-129	-0.151	0.196	0.34	U	PCI/G
13 B	09/26/19	Nickel-63	0.141	0.421	0.718	U	PCI/G
13 B	09/26/19	Iron-55	1.11	2.63	3.76	U	PCI/G
13 B	09/24/19	Technetium-99	0.104	0.352	0.596	U	PCI/G
13 B	09/30/19	Tritium	3.05	2.33	3.8	U	PCI/G
13 B	09/28/19	Carbon-14	-1.01	1.42	2.57	U	PCI/G
13 B	09/25/19	Nickel-59	-0.228	0.454	0.861	U	PCI/G
13 B	10/07/19	Strontium-90	-0.00313	0.00787	0.0143	U	PCI/G
13 B	10/07/19	Yttrium-90	-0.00313	0.00787	0.0143	U	PCI/G
13 C	09/28/19	Iodine-129	0.034	0.219	0.498	U	PCI/G
13 C	09/28/19	Iodine-129	0.034	0.219	0.498	U	PCI/G
13 C	09/28/19	Iodine-129	75.4	1.86	0.694		%
13 C	09/28/19	Iodine-129	75.4	1.86	0.694		%
13 C	09/18/19	Actinium-225	-0.348	0.6	0.885	U	PCI/G
13 C	09/18/19	Actinium-227	0.0495	0.0451	0.0562	U	PCI/G
13 C	09/18/19	Actinium-228	1.15	0.0518	0.0286		PCI/G
13 C	09/18/19	Antimony-125	0.00645	0.0113	0.0197	U	PCI/G
13 C	09/18/19	Barium-137m	0.0667	0.0069	0.00689		PCI/G
13 C	09/18/19	Bismuth-212	1.3	0.12	0.0976		PCI/G
13 C	09/18/19	Bismuth-213	0	0.0216	0.0208	UI	PCI/G
13 C	09/18/19	Bismuth-214	2	0.0309	0.0132		PCI/G
13 C	09/18/19	Cesium-134	0	0.0107	0.0112	UI	PCI/G
13 C	09/18/19	Cesium-137	0.0705	0.00729	0.00727		PCI/G
13 C	09/18/19	Cobalt-60	-0.00349	0.00535	0.00787	U	PCI/G
13 C	09/18/19	Europium-152	-0.00764	0.0118	0.0195	U	PCI/G
13 C	09/18/19	Europium-154	0.0124	0.0163	0.0266	U	PCI/G
13 C	09/18/19	Europium-155	0	0.0218	0.0237	UI	PCI/G
13 C	09/18/19	Holmium-166m	0.00272	0.00733	0.0124	U	PCI/G
13 C	09/18/19	Lead-210	1.63	0.174	0.149		PCI/G
13 C	09/18/19	Lead-212	1.06	0.017	0.0126		PCI/G
13 C	09/18/19	Lead-214	2.22	0.0298	0.0586		PCI/G
13 C	09/18/19	Neptunium-239	0.0428	0.0396	0.0619	U	PCI/G
13 C	09/18/19	Niobium-94	0.00545	0.00549	0.00719	U	PCI/G
13 C	09/18/19	Potassium-40	20.1	0.252	0.0604		PCI/G
13 C	09/18/19	Promethium-147	-67.3	108	178	U	PCI/G
13 C	09/18/19	Protactinium-231	0	0.101	0.0957	UI	PCI/G
13 C	09/18/19	Radium-226	2	0.0309	0.0132		PCI/G
13 C	09/18/19	Radium-228	1.15	0.0518	0.0286		PCI/G
13 C	09/18/19	Sodium-22	0.00314	0.0062	0.00953	U	PCI/G
13 C	09/18/19	Tellurium-125m	2.14	2.43	3.04	U	PCI/G
13 C	09/18/19	Thallium-208	0.349	0.0125	0.00706		PCI/G
13 C	09/18/19	Thorium-231	0.107	0.152	0.128	U	PCI/G
13 C	09/18/19	Thorium-234	1.04	0.223	0.185		PCI/G
13 C	09/18/19	Thulium-171	0	1.38	1.47	UI	PCI/G
13 C	09/18/19	Tin-126	0	0.0155	0.0139	UI	PCI/G
13 C	10/03/19	Polonium-210	1.66	0.315	0.107		PCI/G
13 C	10/02/19	Thorium-228	0.895	0.155	0.113		PCI/G
13 C	10/02/19	Thorium-229	0.0455	0.0523	0.0819	U	PCI/G
13 C	10/02/19	Thorium-230	2.15	0.219	0.0698		PCI/G

Table B-1. Complete Results from the GEL Laboratory

Sample no.	Analysis date	Parameter	Result	Uncertainty	MDC[a]	Qualifier[b]	Units
13 C	10/02/19	Thorium-232	0.848	0.14	0.0696		PCI/G
13 C	10/01/19	Uranium-232	0.00874	0.0402	0.0741	U	PCI/G
13 C	10/01/19	Uranium-233/234	1.01	0.14	0.0472		PCI/G
13 C	10/01/19	Uranium-235/236	0.0346	0.0399	0.0607	U	PCI/G
13 C	10/01/19	Uranium-238	1.09	0.148	0.066		PCI/G
13 C	10/01/19	Neptunium-236	0.00179	0.0112	0.0212	U	PCI/G
13 C	10/01/19	Plutonium-236	0.00179	0.0112	0.0212	U	PCI/G
13 C	10/01/19	Plutonium-239/240	0.00345	0.0133	0.0246	U	PCI/G
13 C	10/01/19	Plutonium-242	0.0032	0.0135	0.0254	U	PCI/G
13 C	10/01/19	Plutonium-244	0	0.00765	0.0105	U	PCI/G
13 C	10/02/19	Americium-241	0.00691	0.00769	0.00902	U	PCI/G
13 C	10/02/19	Americium-243	0.00196	0.0127	0.0249	U	PCI/G
13 C	10/02/19	Curium-243/244	0.00456	0.00717	0.0107	U	PCI/G
13 C	10/02/19	Curium-245/246	0.00598	0.00997	0.0141	U	PCI/G
13 C	10/02/19	Neptunium-237	-0.00163	0.0108	0.0252	U	PCI/G
13 C	10/05/19	Plutonium-241	-0.502	2.83	4.9	U	PCI/G
13 C	09/26/19	Nickel-63	0.377	0.474	0.798	U	PCI/G
13 C	09/28/19	Iodine-129	-0.172	0.431	0.689	U	PCI/G
13 C	09/26/19	Iron-55	1.24	2.55	3.63	U	PCI/G
13 C	09/24/19	Technetium-99	-0.122	0.36	0.616	U	PCI/G
13 C	09/26/19	Tritium	0.452	2.23	3.94	U	PCI/G
13 C	09/28/19	Carbon-14	-0.0153	1.45	2.54	U	PCI/G
13 C	09/26/19	Nickel-59	0	1.68	1.9	UI	PCI/G
13 C	10/07/19	Strontium-90	0.00767	0.00842	0.0141	U	PCI/G
13 C	10/07/19	Yttrium-90	0.00767	0.00842	0.0141	U	PCI/G
14 A	09/24/19	Actinium-225	-0.578	1.28	2.26	U	PCI/G
14 A	09/24/19	Actinium-227	0.0221	0.0616	0.0987	U	PCI/G
14 A	09/24/19	Actinium-228	1.05	0.0833	0.049		PCI/G
14 A	09/24/19	Antimony-125	0.00226	0.021	0.0361	U	PCI/G
14 A	09/24/19	Barium-137m	0.0901	0.0127	0.013		PCI/G
14 A	09/24/19	Bismuth-212	1.11	0.209	0.182		PCI/G
14 A	09/24/19	Bismuth-213	0.02	0.025	0.0396	U	PCI/G
14 A	09/24/19	Bismuth-214	1.55	0.0503	0.0259		PCI/G
14 A	09/24/19	Cesium-134	0	0.0177	0.021	UI	PCI/G
14 A	09/24/19	Cesium-137	0.0952	0.0134	0.0138		PCI/G
14 A	09/24/19	Cobalt-60	0.0003	0.00946	0.0144	U	PCI/G
14 A	09/24/19	Europium-152	0.0346	0.026	0.0368	U	PCI/G
14 A	09/24/19	Europium-154	-0.0079	0.029	0.0491	U	PCI/G
14 A	09/24/19	Europium-155	0	0.0356	0.0408	UI	PCI/G
14 A	09/24/19	Holmium-166m	-0.00996	0.0133	0.0231	U	PCI/G
14 A	09/24/19	Lead-210	1.48	0.329	0.27		PCI/G
14 A	09/24/19	Lead-212	0.912	0.0281	0.0233		PCI/G
14 A	09/24/19	Lead-214	1.67	0.051	0.0973		PCI/G
14 A	09/24/19	Neptunium-239	-0.0328	0.0639	0.105	U	PCI/G
14 A	09/24/19	Niobium-94	0.0131	0.0112	0.0134	U	PCI/G
14 A	09/24/19	Potassium-40	14.8	0.426	0.112		PCI/G
14 A	09/24/19	Promethium-147	-112	186	303	U	PCI/G
14 A	09/24/19	Protactinium-231	0	0.174	0.17	UI	PCI/G
14 A	09/24/19	Radium-226	1.55	0.0503	0.0259		PCI/G
14 A	09/24/19	Radium-228	1.05	0.0833	0.049		PCI/G
14 A	09/24/19	Sodium-22	-0.00182	0.0107	0.0176	U	PCI/G
14 A	09/24/19	Tellurium-125m	0	4.81	5.45	UI	PCI/G
14 A	09/24/19	Thallium-208	0.308	0.0189	0.0135		PCI/G
14 A	09/24/19	Thorium-231	0.0998	0.151	0.242	U	PCI/G
14 A	09/24/19	Thorium-234	1.27	0.399	0.312		PCI/G
14 A	09/24/19	Thulium-171	0	2.34	2.62	UI	PCI/G
14 A	09/24/19	Tin-126	0	0.0258	0.0253	UI	PCI/G
14 A	10/02/19	Polonium-210	1.26	0.286	0.141		PCI/G
14 A	10/02/19	Thorium-228	0.832	0.157	0.121		PCI/G
14 A	10/02/19	Thorium-229	-0.0123	0.0721	0.139	U	PCI/G
14 A	10/02/19	Thorium-230	1.52	0.193	0.0819		PCI/G
14 A	10/02/19	Thorium-232	0.829	0.147	0.0933		PCI/G

Table B-1. Complete Results from the GEL Laboratory

Sample no.	Analysis date	Parameter	Result	Uncertainty	MDC[a]	Qualifier[b]	Units
14 A	10/01/19	Uranium-232	-4.03E-09	0.0296	0.0581	U	PCI/G
14 A	10/01/19	Uranium-233/234	0.704	0.106	0.0703		PCI/G
14 A	10/01/19	Uranium-235/236	0.0221	0.0369	0.0626	U	PCI/G
14 A	10/01/19	Uranium-238	0.776	0.11	0.0624		PCI/G
14 A	10/01/19	Neptunium-236	-0.0000204	0.00665	0.0144	U	PCI/G
14 A	10/01/19	Plutonium-236	-0.0000204	0.00665	0.0144	U	PCI/G
14 A	10/01/19	Plutonium-239/240	-0.003	0.00724	0.0185	U	PCI/G
14 A	10/01/19	Plutonium-242	-0.00127	0.0101	0.0228	U	PCI/G
14 A	10/01/19	Plutonium-244	-0.000993	0.00474	0.0115	U	PCI/G
14 A	10/05/19	Americium-241	0.0134	0.0161	0.025	U	PCI/G
14 A	10/05/19	Americium-243	-0.0023	0.00958	0.0224	U	PCI/G
14 A	10/05/19	Curium-243/244	-0.00113	0.00537	0.0131	U	PCI/G
14 A	10/05/19	Curium-245/246	0	0.0057	0.00778	U	PCI/G
14 A	10/03/19	Neptunium-237	0.0021	0.0084	0.016	U	PCI/G
14 A	10/05/19	Plutonium-241	-0.791	1.9	3.31	U	PCI/G
14 A	09/26/19	Nickel-63	0.412	0.444	0.745	U	PCI/G
14 A	09/28/19	Iodine-129	0.103	0.172	0.613	U	PCI/G
14 A	09/26/19	Iron-55	1.91	2.46	3.48	U	PCI/G
14 A	09/24/19	Technetium-99	-0.0959	0.323	0.553	U	PCI/G
14 A	09/27/19	Tritium	0.372	2.18	3.88	U	PCI/G
14 A	09/28/19	Carbon-14	-1.38	1.4	2.57	U	PCI/G
14 A	09/26/19	Nickel-59	-0.263	0.847	1.48	U	PCI/G
14 A	10/07/19	Strontium-90	-0.00838	0.00757	0.0141	U	PCI/G
14 A	10/07/19	Yttrium-90	-0.00838	0.00757	0.0141	U	PCI/G
14 B	09/24/19	Actinium-225	-0.697	1.21	1.94	U	PCI/G
14 B	09/24/19	Actinium-227	0.0364	0.0826	0.084	U	PCI/G
14 B	09/24/19	Actinium-228	0.994	0.0591	0.0372		PCI/G
14 B	09/24/19	Antimony-125	-0.00542	0.0175	0.0272	U	PCI/G
14 B	09/24/19	Barium-137m	0.0668	0.00956	0.00898		PCI/G
14 B	09/24/19	Bismuth-212	0.984	0.147	0.125		PCI/G
14 B	09/24/19	Bismuth-213	0.00926	0.0172	0.0306	U	PCI/G
14 B	09/24/19	Bismuth-214	1.47	0.0416	0.0178		PCI/G
14 B	09/24/19	Cesium-134	0	0.0113	0.015	UI	PCI/G
14 B	09/24/19	Cesium-137	0.0706	0.0101	0.00949		PCI/G
14 B	09/24/19	Cobalt-60	-0.00188	0.00583	0.0104	U	PCI/G
14 B	09/24/19	Europium-152	0.0118	0.0162	0.0293	U	PCI/G
14 B	09/24/19	Europium-154	0.00595	0.0188	0.032	U	PCI/G
14 B	09/24/19	Europium-155	0	0.0377	0.0423	UI	PCI/G
14 B	09/24/19	Holmium-166m	-0.00389	0.00912	0.0155	U	PCI/G
14 B	09/24/19	Lead-210	0.777	1.27	2.15	U	PCI/G
14 B	09/24/19	Lead-212	0.976	0.0253	0.0184		PCI/G
14 B	09/24/19	Lead-214	1.69	0.043	0.0816		PCI/G
14 B	09/24/19	Neptunium-239	-0.0139	0.0681	0.104	U	PCI/G
14 B	09/24/19	Niobium-94	0.00305	0.0106	0.00912	U	PCI/G
14 B	09/24/19	Potassium-40	15.5	0.333	0.0773		PCI/G
14 B	09/24/19	Promethium-147	143	179	303	U	PCI/G
14 B	09/24/19	Protactinium-231	0	0.154	0.148	UI	PCI/G
14 B	09/24/19	Radium-226	1.47	0.0416	0.0178		PCI/G
14 B	09/24/19	Radium-228	0.994	0.0591	0.0372		PCI/G
14 B	09/24/19	Sodium-22	0.00197	0.00676	0.0115	U	PCI/G
14 B	09/24/19	Tellurium-125m	-1.76	3.77	5.75	U	PCI/G
14 B	09/24/19	Thallium-208	0.265	0.0155	0.00957		PCI/G
14 B	09/24/19	Thorium-231	-0.11	0.12	0.188	U	PCI/G
14 B	09/24/19	Thorium-234	0.656	0.616	0.658	U	PCI/G
14 B	09/24/19	Thulium-171	0.538	6.23	10.5	U	PCI/G
14 B	09/24/19	Tin-126	0	0.0305	0.03	UI	PCI/G
14 B	10/03/19	Polonium-210	1.04	0.307	0.242		PCI/G
14 B	10/02/19	Thorium-228	0.854	0.147	0.0846		PCI/G
14 B	10/02/19	Thorium-229	0.0341	0.0446	0.07	U	PCI/G
14 B	10/02/19	Thorium-230	1.33	0.173	0.0628		PCI/G

Table B-1. Complete Results from the GEL Laboratory

Sample no.	Analysis date	Parameter	Result	Uncertainty	MDC[a]	Qualifier[b]	Units
14 B	10/02/19	Thorium-232	0.73	0.128	0.0433		PCI/G
14 B	10/01/19	Uranium-232	0.00332	0.0427	0.079	U	PCI/G
14 B	10/01/19	Uranium-233/234	0.831	0.115	0.0688		PCI/G
14 B	10/01/19	Uranium-235/236	0.03	0.0389	0.0635	U	PCI/G
14 B	10/01/19	Uranium-238	0.691	0.105	0.0633		PCI/G
14 B	10/03/19	Neptunium-236	-0.00125	0.0066	0.0147	U	PCI/G
14 B	10/03/19	Plutonium-236	-0.00125	0.0066	0.0147	U	PCI/G
14 B	10/03/19	Plutonium-239/240	-0.0000549	0.00857	0.0174	U	PCI/G
14 B	10/03/19	Plutonium-242	0.0143	0.015	0.0209	U	PCI/G
14 B	10/03/19	Plutonium-244	-0.000604	0.00507	0.0112	U	PCI/G
14 B	10/02/19	Americium-241	0.00399	0.00706	0.00599	U	PCI/G
14 B	10/02/19	Americium-243	-0.00121	0.012	0.0258	U	PCI/G
14 B	10/02/19	Curium-243/244	0.00196	0.00753	0.014	U	PCI/G
14 B	10/02/19	Curium-245/246	0	0.00567	0.00775	U	PCI/G
14 B	10/03/19	Neptunium-237	-0.00723	0.00752	0.0222	U	PCI/G
14 B	10/05/19	Plutonium-241	-0.208	1.77	3.05	U	PCI/G
14 B	09/26/19	Nickel-63	0.232	0.446	0.756	U	PCI/G
14 B	09/28/19	Iodine-129	-0.101	0.483	0.795	U	PCI/G
14 B	09/26/19	Iron-55	1.76	2.08	2.91	U	PCI/G
14 B	09/24/19	Technetium-99	0.0292	0.332	0.565	U	PCI/G
14 B	09/27/19	Tritium	0.378	2.38	4.23	U	PCI/G
14 B	09/28/19	Carbon-14	-0.148	1.51	2.66	U	PCI/G
14 B	09/26/19	Nickel-59	0.0119	0.902	1.62	U	PCI/G
14 B	10/07/19	Strontium-90	-0.00125	0.00788	0.0142	U	PCI/G
14 B	10/07/19	Yttrium-90	-0.00125	0.00788	0.0142	U	PCI/G
14 C	09/24/19	Actinium-225	-0.336	1.49	2.4	U	PCI/G
14 C	09/24/19	Actinium-227	0.0467	0.0686	0.0997	U	PCI/G
14 C	09/24/19	Actinium-228	1.06	0.0717	0.0443		PCI/G
14 C	09/24/19	Antimony-125	0.00311	0.0188	0.0328	U	PCI/G
14 C	09/24/19	Barium-137m	0.049	0.0109	0.0111		PCI/G
14 C	09/24/19	Bismuth-212	1.14	0.227	0.164		PCI/G
14 C	09/24/19	Bismuth-213	0.0163	0.0208	0.0369	U	PCI/G
14 C	09/24/19	Bismuth-214	1.54	0.0474	0.0223		PCI/G
14 C	09/24/19	Cesium-134	0	0.0141	0.0181	UI	PCI/G
14 C	09/24/19	Cesium-137	0.0518	0.0115	0.0117		PCI/G
14 C	09/24/19	Cobalt-60	0.00515	0.0078	0.014	U	PCI/G
14 C	09/24/19	Europium-152	-0.00344	0.0201	0.035	U	PCI/G
14 C	09/24/19	Europium-154	-0.00195	0.0255	0.0408	U	PCI/G
14 C	09/24/19	Europium-155	0.0479	0.0486	0.0495	U	PCI/G
14 C	09/24/19	Holmium-166m	-0.00479	0.0114	0.0188	U	PCI/G
14 C	09/24/19	Lead-210	1.52	2.68	2.88	U	PCI/G
14 C	09/24/19	Lead-212	1.04	0.0299	0.0219		PCI/G
14 C	09/24/19	Lead-214	0	0.0526	0.0948	UI	PCI/G
14 C	09/24/19	Neptunium-239	0.00181	0.0712	0.119	U	PCI/G
14 C	09/24/19	Niobium-94	0	0.013	0.0119	UI	PCI/G
14 C	09/24/19	Potassium-40	15.9	0.388	0.102		PCI/G
14 C	09/24/19	Promethium-147	-101	224	341	U	PCI/G
14 C	09/24/19	Protactinium-231	0	0.175	0.17	UI	PCI/G
14 C	09/24/19	Radium-226	1.54	0.0474	0.0223		PCI/G
14 C	09/24/19	Radium-228	1.06	0.0717	0.0443		PCI/G
14 C	09/24/19	Sodium-22	-0.000483	0.00916	0.0147	U	PCI/G
14 C	09/24/19	Tellurium-125m	2.92	4.48	6.49	U	PCI/G
14 C	09/24/19	Thallium-208	0.296	0.0179	0.0117		PCI/G
14 C	09/24/19	Thorium-231	-0.0557	0.146	0.227	U	PCI/G
14 C	09/24/19	Thorium-234	1.1	0.807	0.758		PCI/G
14 C	09/24/19	Thulium-171	2.4	7.47	13	U	PCI/G
14 C	09/24/19	Tin-126	0.0333	0.0372	0.0394	U	PCI/G
14 C	10/02/19	Polonium-210	0.955	0.243	0.122		PCI/G
14 C	10/02/19	Thorium-228	0.875	0.149	0.0901		PCI/G
14 C	10/02/19	Thorium-229	0.0227	0.0545	0.0962	U	PCI/G
14 C	10/02/19	Thorium-230	1.23	0.171	0.096		PCI/G
14 C	10/02/19	Thorium-232	0.615	0.118	0.0432		PCI/G

Table B-1. Complete Results from the GEL Laboratory

Sample no.	Analysis date	Parameter	Result	Uncertainty	MDC[a]	Qualifier[b]	Units
14 C	10/01/19	Uranium-232	-0.00679	0.0421	0.0809	U	PCI/G
14 C	10/01/19	Uranium-233/234	0.743	0.111	0.0661		PCI/G
14 C	10/01/19	Uranium-235/236	0.0469	0.0419	0.0631	U	PCI/G
14 C	10/01/19	Uranium-238	0.678	0.106	0.0661		PCI/G
14 C	10/03/19	Neptunium-236	-0.000712	0.00598	0.0132	U	PCI/G
14 C	10/03/19	Plutonium-236	-0.000712	0.00598	0.0132	U	PCI/G
14 C	10/03/19	Plutonium-239/240	0.00555	0.0084	0.0128	U	PCI/G
14 C	10/03/19	Plutonium-242	0.00661	0.0161	0.0291	U	PCI/G
14 C	10/03/19	Plutonium-244	0.00243	0.0072	0.0128	U	PCI/G
14 C	10/02/19	Americium-241	-0.0000244	0.00795	0.0172	U	PCI/G
14 C	10/02/19	Americium-243	0.00741	0.0175	0.0314	U	PCI/G
14 C	10/02/19	Curium-243/244	-0.00122	0.00582	0.0142	U	PCI/G
14 C	10/02/19	Curium-245/246	-0.00114	0.00754	0.0176	U	PCI/G
14 C	10/03/19	Neptunium-237	0.000244	0.00904	0.0193	U	PCI/G
14 C	10/05/19	Plutonium-241	-0.32	2.06	3.56	U	PCI/G
14 C	09/26/19	Nickel-63	0.646	0.439	0.725	U	PCI/G
14 C	09/28/19	Iodine-129	0.283	0.478	0.93	U	PCI/G
14 C	09/26/19	Iron-55	-0.166	2.35	3.38	U	PCI/G
14 C	09/25/19	Technetium-99	0.125	0.324	0.549	U	PCI/G
14 C	09/27/19	Tritium	2.42	2.46	4.1	U	PCI/G
14 C	09/28/19	Carbon-14	-0.214	1.48	2.62	U	PCI/G
14 C	09/26/19	Nickel-59	-0.351	1.22	2.14	U	PCI/G
14 C	10/08/19	Strontium-90	0.0137	0.0089	0.0146	U	PCI/G
14 C	10/08/19	Yttrium-90	0.0137	0.0089	0.0146	U	PCI/G
15 A	10/07/19	Strontium-90	0.00254	0.00819	0.0143	U	PCI/G
15 A	10/07/19	Yttrium-90	0.00254	0.00819	0.0143	U	PCI/G
15 A	10/07/19	Strontium-90	0.00254	0.00819	0.0143	U	PCI/G
15 A	10/07/19	Yttrium-90	0.00254	0.00819	0.0143	U	PCI/G
15 A	09/24/19	Actinium-225	0.369	1.44	2.35	U	PCI/G
15 A	09/24/19	Actinium-227	0.0782	0.0633	0.0972	U	PCI/G
15 A	09/24/19	Actinium-228	1.02	0.0723	0.0471		PCI/G
15 A	09/24/19	Antimony-125	0.00927	0.0181	0.0321	U	PCI/G
15 A	09/24/19	Barium-137m	0.0806	0.0149	0.0115		PCI/G
15 A	09/24/19	Bismuth-212	1.23	0.19	0.158		PCI/G
15 A	09/24/19	Bismuth-213	0.01	0.02	0.0354	U	PCI/G
15 A	09/24/19	Bismuth-214	1.27	0.0427	0.0217		PCI/G
15 A	09/24/19	Cesium-134	0	0.0173	0.0177	UI	PCI/G
15 A	09/24/19	Cesium-137	0.0852	0.0158	0.0122		PCI/G
15 A	09/24/19	Cobalt-60	0.00315	0.00748	0.0135	U	PCI/G
15 A	09/24/19	Europium-152	-0.0064	0.0193	0.0338	U	PCI/G
15 A	09/24/19	Europium-154	-0.00324	0.0268	0.0435	U	PCI/G
15 A	09/24/19	Europium-155	0.0474	0.0488	0.0493	U	PCI/G
15 A	09/24/19	Holmium-166m	0.0108	0.0115	0.0203	U	PCI/G
15 A	09/24/19	Lead-210	0	3.38	3.52	UI	PCI/G
15 A	09/24/19	Lead-212	1.07	0.0291	0.0217		PCI/G
15 A	09/24/19	Lead-214	1.54	0.0488	0.0838		PCI/G
15 A	09/24/19	Neptunium-239	-0.0227	0.0724	0.12	U	PCI/G
15 A	09/24/19	Niobium-94	0.0033	0.00989	0.0116	U	PCI/G
15 A	09/24/19	Potassium-40	25.5	0.465	0.0977		PCI/G
15 A	09/24/19	Promethium-147	172	260	337	U	PCI/G
15 A	09/24/19	Protactinium-231	0	0.16	0.167	UI	PCI/G
15 A	09/24/19	Radium-226	1.27	0.0427	0.0217		PCI/G
15 A	09/24/19	Radium-228	1.02	0.0723	0.0471		PCI/G
15 A	09/24/19	Sodium-22	-0.000766	0.00962	0.0157	U	PCI/G
15 A	09/24/19	Tellurium-125m	0.226	4.33	6.69	U	PCI/G
15 A	09/24/19	Thallium-208	0.307	0.0175	0.0121		PCI/G
15 A	09/24/19	Thorium-231	0.0465	0.141	0.227	U	PCI/G
15 A	09/24/19	Thorium-234	0.65	0.752	0.805	U	PCI/G
15 A	09/24/19	Thulium-171	-1.36	8.76	15	U	PCI/G
15 A	09/24/19	Tin-126	0	0.0349	0.0347	UI	PCI/G

Table B-1. Complete Results from the GEL Laboratory

Sample no.	Analysis date	Parameter	Result	Uncertainty	MDC[a]	Qualifier[b]	Units
15 A	10/02/19	Polonium-210	1.2	0.263	0.174		PCI/G
15 A	10/02/19	Thorium-228	0.747	0.15	0.117		PCI/G
15 A	10/02/19	Thorium-229	0.0802	0.0605	0.0827	U	PCI/G
15 A	10/02/19	Thorium-230	0.911	0.157	0.109		PCI/G
15 A	10/02/19	Thorium-232	0.699	0.132	0.0588		PCI/G
15 A	10/01/19	Uranium-232	-0.0325	0.0476	0.0952	U	PCI/G
15 A	10/01/19	Uranium-233/234	0.641	0.0993	0.0587		PCI/G
15 A	10/01/19	Uranium-235/236	0.0474	0.0342	0.0448		PCI/G
15 A	10/01/19	Uranium-238	0.621	0.0979	0.0587		PCI/G
15 A	10/01/19	Neptunium-236	-0.00402	0.00755	0.0198	U	PCI/G
15 A	10/01/19	Plutonium-236	-0.00402	0.00755	0.0198	U	PCI/G
15 A	10/01/19	Plutonium-239/240	0.00374	0.0114	0.0212	U	PCI/G
15 A	10/01/19	Plutonium-242	-0.00195	0.011	0.0238	U	PCI/G
15 A	10/01/19	Plutonium-244	0.00476	0.00794	0.0112	U	PCI/G
15 A	10/02/19	Americium-241	0.00476	0.00793	0.0112	U	PCI/G
15 A	10/02/19	Americium-243	-0.00746	0.0133	0.0308	U	PCI/G
15 A	10/02/19	Curium-243/244	0.00187	0.00718	0.0133	U	PCI/G
15 A	10/02/19	Curium-245/246	0.00359	0.0106	0.0192	U	PCI/G
15 A	10/03/19	Neptunium-237	-0.000708	0.00433	0.0104	U	PCI/G
15 A	10/05/19	Plutonium-241	-2.03	1.8	3.19	U	PCI/G
15 A	09/26/19	Nickel-63	0.335	0.369	0.619	U	PCI/G
15 A	09/28/19	Iodine-129	-0.134	0.385	0.674	U	PCI/G
15 A	09/26/19	Iron-55	-0.512	2.32	3.35	U	PCI/G
15 A	09/25/19	Technetium-99	-0.00452	0.372	0.634	U	PCI/G
15 A	09/27/19	Tritium	-0.716	2.12	3.91	U	PCI/G
15 A	09/28/19	Carbon-14	-0.128	1.45	2.55	U	PCI/G
15 A	09/26/19	Nickel-59	-0.447	0.819	1.39	U	PCI/G
15 A	10/07/19	Strontium-90	-0.0078	0.00766	0.0142	U	PCI/G
15 A	10/07/19	Yttrium-90	-0.0078	0.00766	0.0142	U	PCI/G
15 B	09/24/19	Actinium-225	-1.02	1.39	2.36	U	PCI/G
15 B	09/24/19	Actinium-227	0.0161	0.0572	0.0982	U	PCI/G
15 B	09/24/19	Actinium-228	1.01	0.0679	0.0422		PCI/G
15 B	09/24/19	Antimony-125	0.0108	0.0188	0.0321	U	PCI/G
15 B	09/24/19	Barium-137m	0.0793	0.0123	0.0112		PCI/G
15 B	09/24/19	Bismuth-212	1.14	0.223	0.153		PCI/G
15 B	09/24/19	Bismuth-213	0.0171	0.0208	0.0358	U	PCI/G
15 B	09/24/19	Bismuth-214	1.23	0.0433	0.0219		PCI/G
15 B	09/24/19	Cesium-134	0	0.0149	0.0177	UI	PCI/G
15 B	09/24/19	Cesium-137	0.0838	0.013	0.0119		PCI/G
15 B	09/24/19	Cobalt-60	0.00184	0.00709	0.0125	U	PCI/G
15 B	09/24/19	Europium-152	-0.00686	0.0208	0.0349	U	PCI/G
15 B	09/24/19	Europium-154	-0.0196	0.0228	0.0383	U	PCI/G
15 B	09/24/19	Europium-155	0.0311	0.034	0.06	U	PCI/G
15 B	09/24/19	Holmium-166m	0.00335	0.0107	0.0192	U	PCI/G
15 B	09/24/19	Lead-210	0	4.62	3.04	UI	PCI/G
15 B	09/24/19	Lead-212	0.936	0.0289	0.0217		PCI/G
15 B	09/24/19	Lead-214	1.44	0.0481	0.0775		PCI/G
15 B	09/24/19	Neptunium-239	0.132	0.11	0.139	U	PCI/G
15 B	09/24/19	Niobium-94	0.00967	0.00618	0.0115	U	PCI/G
15 B	09/24/19	Potassium-40	23.2	0.415	0.0913		PCI/G
15 B	09/24/19	Promethium-147	53.3	225	394	U	PCI/G
15 B	09/24/19	Protactinium-231	0	0.142	0.169	UI	PCI/G
15 B	09/24/19	Radium-226	1.23	0.0433	0.0219		PCI/G
15 B	09/24/19	Radium-228	1.01	0.0679	0.0422		PCI/G
15 B	09/24/19	Sodium-22	-0.00727	0.00819	0.0137	U	PCI/G
15 B	09/24/19	Tellurium-125m	-2.41	4.47	7.74	U	PCI/G
15 B	09/24/19	Thallium-208	0.31	0.0199	0.0116		PCI/G
15 B	09/24/19	Thorium-231	0.00524	0.156	0.236	U	PCI/G
15 B	09/24/19	Thorium-234	1.91	1.08	1.06		PCI/G
15 B	09/24/19	Thulium-171	2.26	12.3	19.7	U	PCI/G
15 B	09/24/19	Tin-126	0	0.0466	0.0431	UI	PCI/G
15 B	10/03/19	Polonium-210	1.02	0.243	0.173		PCI/G

Table B-1. Complete Results from the GEL Laboratory

Sample no.	Analysis date	Parameter	Result	Uncertainty	MDC[a]	Qualifier[b]	Units
15 B	10/02/19	Thorium-228	0.934	0.172	0.134		PCI/G
15 B	10/02/19	Thorium-229	0.0525	0.0656	0.106	U	PCI/G
15 B	10/02/19	Thorium-230	1.12	0.172	0.0724		PCI/G
15 B	10/02/19	Thorium-232	0.764	0.14	0.0196		PCI/G
15 B	10/01/19	Uranium-232	-0.0818	0.0652	0.133	U	PCI/G
15 B	10/01/19	Uranium-233/234	0.66	0.0909	0.0414		PCI/G
15 B	10/01/19	Uranium-235/236	0.0465	0.0278	0.0297		PCI/G
15 B	10/01/19	Uranium-238	0.67	0.0908	0.0341		PCI/G
15 B	10/01/19	Neptunium-236	-0.0085	0.00823	0.0233	U	PCI/G
15 B	10/01/19	Plutonium-236	-0.0085	0.00823	0.0233	U	PCI/G
15 B	10/01/19	Plutonium-239/240	-0.00103	0.0123	0.0254	U	PCI/G
15 B	10/01/19	Plutonium-242	-0.000842	0.00895	0.019	U	PCI/G
15 B	10/01/19	Plutonium-244	0.00449	0.00749	0.0106	U	PCI/G
15 B	10/02/19	Americium-241	-0.0018	0.00748	0.0175	U	PCI/G
15 B	10/02/19	Americium-243	0.00694	0.00962	0.0155	U	PCI/G
15 B	10/02/19	Curium-243/244	-0.00175	0.0045	0.0122	U	PCI/G
15 B	10/02/19	Curium-245/246	0.00134	0.00589	0.0103	U	PCI/G
15 B	10/03/19	Neptunium-237	-0.00241	0.00539	0.0156	U	PCI/G
15 B	10/06/19	Plutonium-241	0.0357	1.64	2.83	U	PCI/G
15 B	09/26/19	Nickel-63	0.0724	0.394	0.676	U	PCI/G
15 B	09/28/19	Iodine-129	-0.0738	0.237	0.468	U	PCI/G
15 B	09/26/19	Iron-55	1.55	2.37	3.32	U	PCI/G
15 B	09/25/19	Technetium-99	-0.285	0.306	0.528	U	PCI/G
15 B	09/27/19	Tritium	0.811	2.46	4.32	U	PCI/G
15 B	09/28/19	Carbon-14	0.331	1.5	2.59	U	PCI/G
15 B	09/26/19	Nickel-59	0.407	0.435	1.13	U	PCI/G
15 B	10/09/19	Strontium-90	0.00517	0.00849	0.0147	U	PCI/G
15 B	10/09/19	Yttrium-90	0.00517	0.00849	0.0147	U	PCI/G
15 C	09/25/19	Actinium-225	-0.465	1.42	2.28	U	PCI/G
15 C	09/25/19	Actinium-227	0.00377	0.0551	0.088	U	PCI/G
15 C	09/25/19	Actinium-228	1.08	0.0683	0.0416		PCI/G
15 C	09/25/19	Antimony-125	-0.00611	0.0168	0.0287	U	PCI/G
15 C	09/25/19	Barium-137m	0.0652	0.0098	0.0103		PCI/G
15 C	09/25/19	Bismuth-212	1.13	0.169	0.14		PCI/G
15 C	09/25/19	Bismuth-213	-0.00262	0.0191	0.0327	U	PCI/G
15 C	09/25/19	Bismuth-214	1.33	0.041	0.0201		PCI/G
15 C	09/25/19	Cesium-134	0	0.014	0.0167	UI	PCI/G
15 C	09/25/19	Cesium-137	0.0689	0.0104	0.0109		PCI/G
15 C	09/25/19	Cobalt-60	-0.00266	0.00701	0.0119	U	PCI/G
15 C	09/25/19	Europium-152	-0.014	0.0189	0.031	U	PCI/G
15 C	09/25/19	Europium-154	-0.0116	0.025	0.039	U	PCI/G
15 C	09/25/19	Europium-155	0	0.0496	0.0446	UI	PCI/G
15 C	09/25/19	Holmium-166m	-0.00623	0.011	0.0181	U	PCI/G
15 C	09/25/19	Lead-210	0.485	1.87	2.58	U	PCI/G
15 C	09/25/19	Lead-212	1.06	0.0268	0.0197		PCI/G
15 C	09/25/19	Lead-214	1.48	0.0435	0.0233		PCI/G
15 C	09/25/19	Neptunium-239	0.0803	0.0848	0.112	U	PCI/G
15 C	09/25/19	Niobium-94	0.00566	0.00874	0.0106	U	PCI/G
15 C	09/25/19	Potassium-40	24.8	0.418	0.0858		PCI/G
15 C	09/25/19	Promethium-147	209	201	315	U	PCI/G
15 C	09/25/19	Protactinium-231	0	0.158	0.157	UI	PCI/G
15 C	09/25/19	Radium-226	1.33	0.041	0.0201		PCI/G
15 C	09/25/19	Radium-228	1.08	0.0683	0.0416		PCI/G
15 C	09/25/19	Sodium-22	-0.00388	0.009	0.014	U	PCI/G
15 C	09/25/19	Tellurium-125m	0.385	4.49	6.11	U	PCI/G
15 C	09/25/19	Thallium-208	0.325	0.0142	0.0104		PCI/G
15 C	09/25/19	Thorium-231	0.00183	0.132	0.208	U	PCI/G
15 C	09/25/19	Thorium-234	0.558	0.586	0.681	U	PCI/G
15 C	09/25/19	Thulium-171	6.91	10.1	11.8	U	PCI/G
15 C	09/25/19	Tin-126	0	0.0342	0.0305	UI	PCI/G

Table B-1. Complete Results from the GEL Laboratory

Sample no.	Analysis date	Parameter	Result	Uncertainty	MDC[a]	Qualifier[b]	Units
15 C	10/03/19	Polonium-210	0.642	0.198	0.162		PCI/G
15 C	10/02/19	Thorium-228	0.715	0.161	0.156		PCI/G
15 C	10/02/19	Thorium-229	0.0597	0.0675	0.107	U	PCI/G
15 C	10/02/19	Thorium-230	1.1	0.174	0.0953		PCI/G
15 C	10/02/19	Thorium-232	0.726	0.147	0.112		PCI/G
15 C	10/01/19	Uranium-232	-0.0573	0.0476	0.102	U	PCI/G
15 C	10/01/19	Uranium-233/234	0.612	0.0893	0.0502		PCI/G
15 C	10/01/19	Uranium-235/236	0.0156	0.022	0.0345	U	PCI/G
15 C	10/01/19	Uranium-238	0.625	0.0876	0.0298		PCI/G
15 C	10/01/19	Neptunium-236	-0.00394	0.00577	0.0171	U	PCI/G
15 C	10/01/19	Plutonium-236	-0.00394	0.00577	0.0171	U	PCI/G
15 C	10/01/19	Plutonium-239/240	0.00844	0.0104	0.015	U	PCI/G
15 C	10/01/19	Plutonium-242	-0.0000842	0.0098	0.0203	U	PCI/G
15 C	10/01/19	Plutonium-244	0	0.00413	0.00565	U	PCI/G
15 C	10/02/19	Americium-241	0.00178	0.0115	0.0227	U	PCI/G
15 C	10/02/19	Americium-243	0.0131	0.0148	0.0221	U	PCI/G
15 C	10/02/19	Curium-243/244	0.00368	0.00913	0.0162	U	PCI/G
15 C	10/02/19	Curium-245/246	0	0.00561	0.00766	U	PCI/G
15 C	10/03/19	Neptunium-237	-0.00553	0.00892	0.0284	U	PCI/G
15 C	10/06/19	Plutonium-241	-0.16	1.62	2.79	U	PCI/G
15 C	09/26/19	Nickel-63	0.121	0.401	0.685	U	PCI/G
15 C	09/28/19	Iodine-129	-0.128	0.229	0.398	U	PCI/G
15 C	09/26/19	Iron-55	0.792	2.27	3.21	U	PCI/G
15 C	09/25/19	Technetium-99	-0.0977	0.287	0.491	U	PCI/G
15 C	09/27/19	Tritium	0.565	2.44	4.31	U	PCI/G
15 C	09/28/19	Carbon-14	-0.126	1.47	2.59	U	PCI/G
15 C	09/26/19	Nickel-59	0.162	0.85	1.53	U	PCI/G
15 C	10/07/19	Strontium-90	0.00397	0.00827	0.0142	U	PCI/G
15 C	10/07/19	Yttrium-90	0.00397	0.00827	0.0142	U	PCI/G
16 A	10/05/19	Strontium-90	0.00146	0.00843	0.0149	U	PCI/G
16 A	10/05/19	Yttrium-90	0.00146	0.00843	0.0149	U	PCI/G
16 A	09/27/19	Actinium-225	-1.41	1.87	3.17	U	PCI/G
16 A	09/27/19	Actinium-227	0.0285	0.0853	0.105	U	PCI/G
16 A	09/27/19	Actinium-228	1.03	0.074	0.0428		PCI/G
16 A	09/27/19	Antimony-125	-0.00311	0.0198	0.0333	U	PCI/G
16 A	09/27/19	Barium-137m	0.0707	0.0117	0.0116		PCI/G
16 A	09/27/19	Bismuth-212	1.02	0.187	0.161		PCI/G
16 A	09/27/19	Bismuth-213	0.0114	0.0224	0.0382	U	PCI/G
16 A	09/27/19	Bismuth-214	1.68	0.0479	0.0224		PCI/G
16 A	09/27/19	Cesium-134	0	0.0194	0.0181	UI	PCI/G
16 A	09/27/19	Cesium-137	0.0747	0.0123	0.0122		PCI/G
16 A	09/27/19	Cobalt-60	0.0045	0.0071	0.0128	U	PCI/G
16 A	09/27/19	Europium-152	-0.0291	0.0215	0.0353	U	PCI/G
16 A	09/27/19	Europium-154	-0.00651	0.0251	0.04	U	PCI/G
16 A	09/27/19	Europium-155	0.0415	0.0356	0.0631	U	PCI/G
16 A	09/27/19	Holmium-166m	0.0046	0.0111	0.02	U	PCI/G
16 A	09/27/19	Lead-210	0	4.42	3.35	UI	PCI/G
16 A	09/27/19	Lead-212	0.977	0.029	0.0231		PCI/G
16 A	09/27/19	Lead-214	1.93	0.053	0.0902		PCI/G
16 A	09/27/19	Neptunium-239	0.0214	0.0839	0.147	U	PCI/G
16 A	09/27/19	Niobium-94	0	0.0149	0.012	UI	PCI/G
16 A	09/27/19	Potassium-40	18.4	0.385	0.0992		PCI/G
16 A	09/27/19	Promethium-147	123	236	413	U	PCI/G
16 A	09/27/19	Protactinium-231	0	0.178	0.175	UI	PCI/G
16 A	09/27/19	Radium-226	1.68	0.0479	0.0224		PCI/G
16 A	09/27/19	Radium-228	1.03	0.074	0.0428		PCI/G
16 A	09/27/19	Sodium-22	-0.00227	0.00904	0.0144	U	PCI/G
16 A	09/27/19	Tellurium-125m	-1.11	4.89	8.5	U	PCI/G
16 A	09/27/19	Thallium-208	0.322	0.0188	0.0125		PCI/G
16 A	09/27/19	Thorium-231	0.0609	0.163	0.248	U	PCI/G
16 A	09/27/19	Thorium-234	1.2	0.834	1.16		PCI/G
16 A	09/27/19	Thulium-171	-2.79	12.2	21.5	U	PCI/G

Table B-1. Complete Results from the GEL Laboratory

Sample no.	Analysis date	Parameter	Result	Uncertainty	MDC[a]	Qualifier[b]	Units
16 A	09/27/19	Tin-126	0	0.0483	0.0464	UI	PCI/G
16 A	09/29/19	Iodine-129	-0.0745	0.416	0.694	U	PCI/G
16 A	10/01/19	Polonium-210	0.96	0.276	0.116		PCI/G
16 A	09/30/19	Thorium-228	0.936	0.171	0.137		PCI/G
16 A	09/30/19	Thorium-229	0.07	0.0738	0.117	U	PCI/G
16 A	09/30/19	Thorium-230	1.71	0.208	0.0782		PCI/G
16 A	09/30/19	Thorium-232	0.861	0.149	0.07		PCI/G
16 A	09/28/19	Uranium-232	-0.00341	0.0428	0.0813	U	PCI/G
16 A	09/28/19	Uranium-233/234	1.09	0.123	0.0553		PCI/G
16 A	09/28/19	Uranium-235/236	0.244	0.0605	0.0422		PCI/G
16 A	09/28/19	Uranium-238	1.23	0.131	0.0553		PCI/G
16 A	10/01/19	Neptunium-236	-0.00101	0.00481	0.0117	U	PCI/G
16 A	10/01/19	Plutonium-236	-0.00101	0.00481	0.0117	U	PCI/G
16 A	10/01/19	Plutonium-239/240	0.000934	0.00757	0.0153	U	PCI/G
16 A	10/01/19	Plutonium-242	-0.00675	0.0102	0.0253	U	PCI/G
16 A	10/01/19	Plutonium-244	0.00385	0.00681	0.00578	U	PCI/G
16 A	10/01/19	Neptunium-237	0.00575	0.0114	0.0186	U	PCI/G
16 A	10/04/19	Plutonium-241	0.834	1.9	3.25	U	PCI/G
16 A	09/30/19	Iron-55	-0.728	2.93	4.38	U	PCI/G
16 A	09/28/19	Nickel-63	0.061	0.451	0.773	U	PCI/G
16 A	09/25/19	Technetium-99	0.231	0.433	0.73	U	PCI/G
16 A	09/27/19	Tritium	-1.8	2.36	4.56	U	PCI/G
16 A	09/27/19	Carbon-14	-1.06	1.68	3	U	PCI/G
16 A	09/30/19	Nickel-59	0.452	1.06	1.97	U	PCI/G
16 A	10/05/19	Strontium-90	0.00209	0.00844	0.0149	U	PCI/G
16 A	10/05/19	Yttrium-90	0.00209	0.00844	0.0149	U	PCI/G
16 A	10/06/19	Americium-241	0.00465	0.017	0.0311	U	PCI/G
16 A	10/06/19	Americium-243	0.00678	0.0194	0.0346	U	PCI/G
16 A	10/06/19	Curium-243/244	0.0023	0.00782	0.00691	U	PCI/G
16 A	10/06/19	Curium-245/246	0	0.00945	0.0188	U	PCI/G
16 B	09/30/19	Nickel-59	-0.267	0.715	1.2	U	PCI/G
16 B	09/27/19	Actinium-225	-1.11	1.72	2.75	U	PCI/G
16 B	09/27/19	Actinium-227	0.00645	0.0599	0.0888	U	PCI/G
16 B	09/27/19	Actinium-228	0.922	0.0631	0.0386		PCI/G
16 B	09/27/19	Antimony-125	0.00246	0.0166	0.0291	U	PCI/G
16 B	09/27/19	Barium-137m	0.0554	0.00979	0.00981		PCI/G
16 B	09/27/19	Bismuth-212	1.06	0.183	0.138		PCI/G
16 B	09/27/19	Bismuth-213	0.0003	0.0181	0.0317	U	PCI/G
16 B	09/27/19	Bismuth-214	1.53	0.0416	0.019		PCI/G
16 B	09/27/19	Cesium-134	0	0.0123	0.016	UI	PCI/G
16 B	09/27/19	Cesium-137	0.0586	0.0103	0.0104		PCI/G
16 B	09/27/19	Cobalt-60	0.00112	0.00642	0.0115	U	PCI/G
16 B	09/27/19	Europium-152	0.00475	0.018	0.0319	U	PCI/G
16 B	09/27/19	Europium-154	0.0312	0.0237	0.0395	U	PCI/G
16 B	09/27/19	Europium-155	0	0.0451	0.0455	UI	PCI/G
16 B	09/27/19	Holmium-166m	0.00677	0.01	0.0175	U	PCI/G
16 B	09/27/19	Lead-210	0	3.01	3.24	UI	PCI/G
16 B	09/27/19	Lead-212	0.956	0.0261	0.0198		PCI/G
16 B	09/27/19	Lead-214	1.76	0.0446	0.0233		PCI/G
16 B	09/27/19	Neptunium-239	-0.0828	0.067	0.109	U	PCI/G
16 B	09/27/19	Niobium-94	0.00691	0.00554	0.00975	U	PCI/G
16 B	09/27/19	Potassium-40	18.1	0.364	0.095		PCI/G
16 B	09/27/19	Promethium-147	-63.5	195	323	U	PCI/G
16 B	09/27/19	Protactinium-231	0	0.197	0.152	UI	PCI/G
16 B	09/27/19	Radium-226	1.53	0.0416	0.019		PCI/G
16 B	09/27/19	Radium-228	0.922	0.0631	0.0386		PCI/G
16 B	09/27/19	Sodium-22	0.011	0.00852	0.0142	U	PCI/G
16 B	09/27/19	Tellurium-125m	1.08	4.19	6.5	U	PCI/G
16 B	09/27/19	Thallium-208	0.281	0.0149	0.0107		PCI/G
16 B	09/27/19	Thorium-231	0.0432	0.131	0.21	U	PCI/G

Table B-1. Complete Results from the GEL Laboratory

Sample no.	Analysis date	Parameter	Result	Uncertainty	MDC[a]	Qualifier[b]	Units
16 B	09/27/19	Thorium-234	1.03	0.63	0.753		PCI/G
16 B	09/27/19	Thulium-171	-0.207	8.43	14.5	U	PCI/G
16 B	09/27/19	Tin-126	0	0.0326	0.0327	UI	PCI/G
16 B	09/29/19	Iodine-129	-0.128	0.306	0.56	U	PCI/G
16 B	10/03/19	Polonium-210	0.977	0.274	0.181		PCI/G
16 B	09/30/19	Thorium-228	0.896	0.148	0.107		PCI/G
16 B	09/30/19	Thorium-229	0.0622	0.0557	0.0838	U	PCI/G
16 B	09/30/19	Thorium-230	1.63	0.183	0.0694		PCI/G
16 B	09/30/19	Thorium-232	0.722	0.121	0.0395		PCI/G
16 B	09/28/19	Uranium-232	0.00979	0.0532	0.0957	U	PCI/G
16 B	09/28/19	Uranium-233/234	1.05	0.122	0.0473		PCI/G
16 B	09/28/19	Uranium-235/236	0.113	0.0428	0.0339		PCI/G
16 B	09/28/19	Uranium-238	1.28	0.133	0.0391		PCI/G
16 B	10/01/19	Neptunium-236	0	0.0047	0.00642	U	PCI/G
16 B	10/01/19	Plutonium-236	0	0.0047	0.00642	U	PCI/G
16 B	10/01/19	Plutonium-239/240	0.00515	0.00859	0.0121	U	PCI/G
16 B	10/01/19	Plutonium-242	-0.000179	0.015	0.0302	U	PCI/G
16 B	10/01/19	Plutonium-244	-0.00208	0.00538	0.0146	U	PCI/G
16 B	10/01/19	Neptunium-237	-0.0055	0.00951	0.027	U	PCI/G
16 B	10/04/19	Plutonium-241	0.182	1.76	3.04	U	PCI/G
16 B	09/30/19	Iron-55	-0.191	2.78	4.06	U	PCI/G
16 B	09/28/19	Nickel-63	-0.0248	0.409	0.704	U	PCI/G
16 B	09/25/19	Technetium-99	0.143	0.415	0.701	U	PCI/G
16 B	09/27/19	Tritium	-0.865	2.29	4.28	U	PCI/G
16 B	09/27/19	Carbon-14	0.575	1.73	2.97	U	PCI/G
16 B	09/30/19	Nickel-59	-0.264	0.259	0.194	U	PCI/G
16 B	10/05/19	Strontium-90	0.00422	0.00847	0.0147	U	PCI/G
16 B	10/05/19	Yttrium-90	0.00422	0.00847	0.0147	U	PCI/G
16 B	10/06/19	Americium-241	2.18E-09	0.0136	0.0264	U	PCI/G
16 B	10/06/19	Americium-243	-0.0163	0.0181	0.0388	U	PCI/G
16 B	10/06/19	Curium-243/244	-0.00162	0.00841	0.0179	U	PCI/G
16 B	10/06/19	Curium-245/246	0.00568	0.0083	0.00568	X	PCI/G
16 C	09/27/19	Actinium-225	-3.09	1.97	3.07	U	PCI/G
16 C	09/27/19	Actinium-227	0.0509	0.0695	0.101	U	PCI/G
16 C	09/27/19	Actinium-228	0.961	0.0751	0.0493		PCI/G
16 C	09/27/19	Antimony-125	0.0119	0.0195	0.0338	U	PCI/G
16 C	09/27/19	Barium-137m	0.0392	0.0124	0.0114		PCI/G
16 C	09/27/19	Bismuth-212	0.889	0.193	0.171		PCI/G
16 C	09/27/19	Bismuth-213	-0.00631	0.0217	0.0356	U	PCI/G
16 C	09/27/19	Bismuth-214	1.52	0.0444	0.0223		PCI/G
16 C	09/27/19	Cesium-134	0	0.0189	0.0165	UI	PCI/G
16 C	09/27/19	Cesium-137	0.0414	0.0132	0.012		PCI/G
16 C	09/27/19	Cobalt-60	-0.00475	0.00831	0.0138	U	PCI/G
16 C	09/27/19	Europium-152	-0.0123	0.0204	0.035	U	PCI/G
16 C	09/27/19	Europium-154	0.00061	0.0301	0.0461	U	PCI/G
16 C	09/27/19	Europium-155	0	0.0407	0.0489	UI	PCI/G
16 C	09/27/19	Holmium-166m	-0.00183	0.0117	0.0204	U	PCI/G
16 C	09/27/19	Lead-210	0.575	3.29	5.95	U	PCI/G
16 C	09/27/19	Lead-212	0.989	0.0282	0.0222		PCI/G
16 C	09/27/19	Lead-214	1.82	0.0471	0.0897		PCI/G
16 C	09/27/19	Neptunium-239	-0.0354	0.0712	0.12	U	PCI/G
16 C	09/27/19	Niobium-94	0.0104	0.00669	0.0122	U	PCI/G
16 C	09/27/19	Potassium-40	18.1	0.403	0.113		PCI/G
16 C	09/27/19	Promethium-147	-174	204	342	U	PCI/G
16 C	09/27/19	Protactinium-231	0	0.145	0.17	UI	PCI/G
16 C	09/27/19	Radium-226	1.52	0.0444	0.0223		PCI/G
16 C	09/27/19	Radium-228	0.961	0.0751	0.0493		PCI/G
16 C	09/27/19	Sodium-22	0.000112	0.0108	0.0165	U	PCI/G
16 C	09/27/19	Tellurium-125m	0.958	4.13	7.02	U	PCI/G
16 C	09/27/19	Thallium-208	0.306	0.0211	0.0115		PCI/G
16 C	09/27/19	Thorium-231	0.0659	0.15	0.235	U	PCI/G
16 C	09/27/19	Thorium-234	1.63	1.18	0.941		PCI/G

Table B-1. Complete Results from the GEL Laboratory

Sample no.	Analysis date	Parameter	Result	Uncertainty	MDC[a]	Qualifier[b]	Units
16 C	09/27/19	Thulium-171	7.67	12.1	21.9	U	PCI/G
16 C	09/27/19	Tin-126	0	0.0369	0.035	UI	PCI/G
16 C	09/29/19	Iodine-129	-0.0645	0.453	0.811	U	PCI/G
16 C	10/02/19	Polonium-210	0.988	0.301	0.243		PCI/G
16 C	09/30/19	Thorium-228	0.891	0.177	0.164		PCI/G
16 C	09/30/19	Thorium-229	-0.0653	0.0868	0.178	U	PCI/G
16 C	09/30/19	Thorium-230	1.57	0.213	0.145		PCI/G
16 C	09/30/19	Thorium-232	0.767	0.152	0.12		PCI/G
16 C	09/28/19	Uranium-232	-0.153	0.122	0.249	U	PCI/G
16 C	09/28/19	Uranium-233/234	1.08	0.125	0.0574		PCI/G
16 C	09/28/19	Uranium-235/236	0.225	0.0589	0.0394		PCI/G
16 C	09/28/19	Uranium-238	1.29	0.134	0.0341		PCI/G
16 C	10/01/19	Neptunium-236	-0.00114	0.0103	0.0226	U	PCI/G
16 C	10/01/19	Plutonium-236	-0.00114	0.0103	0.0226	U	PCI/G
16 C	10/01/19	Plutonium-239/240	-0.00106	0.00702	0.0164	U	PCI/G
16 C	10/01/19	Plutonium-242	-0.0175	0.0126	0.034	U	PCI/G
16 C	10/01/19	Plutonium-244	-0.0000206	0.00671	0.0145	U	PCI/G
16 C	10/01/19	Neptunium-237	-0.00692	0.00973	0.0285	U	PCI/G
16 C	10/04/19	Plutonium-241	0.636	1.72	2.94	U	PCI/G
16 C	09/30/19	Iron-55	-2.37	2.77	4.18	U	PCI/G
16 C	09/28/19	Nickel-63	0.132	0.395	0.674	U	PCI/G
16 C	09/25/19	Technetium-99	0.511	0.423	0.707	U	PCI/G
16 C	09/27/19	Tritium	0.0122	2.21	3.99	U	PCI/G
16 C	09/27/19	Carbon-14	0.504	1.66	2.85	U	PCI/G
16 C	09/30/19	Nickel-59	-0.257	0.36	0.629	U	PCI/G
16 C	10/08/19	Strontium-90	0.0133	0.00923	0.0147	U	PCI/G
16 C	10/08/19	Yttrium-90	0.0133	0.00923	0.0147	U	PCI/G
16 C	10/06/19	Americium-241	0.0152	0.0128	0.0162	U	PCI/G
16 C	10/06/19	Americium-243	0	0.0157	0.0303	U	PCI/G
16 C	10/06/19	Curium-243/244	2.79E-10	0.00657	0.0128	U	PCI/G
16 C	10/06/19	Curium-245/246	0.00794	0.00953	0.00596	X	PCI/G
17 A	09/30/19	Polonium-210	0.417	0.16	0.145		PCI/G
17 A	10/05/19	Thorium-228	0.226	0.129	0.182		PCI/G
17 A	10/05/19	Thorium-229	0.0246	0.0532	0.0905	U	PCI/G
17 A	10/05/19	Thorium-230	0.506	0.136	0.1		PCI/G
17 A	10/05/19	Thorium-232	0.366	0.114	0.078		PCI/G
17 A	09/30/19	Uranium-232	-0.0463	0.0513	0.11	U	PCI/G
17 A	09/30/19	Uranium-233/234	0.298	0.0715	0.0485		PCI/G
17 A	09/30/19	Uranium-235/236	0.0198	0.0279	0.0437	U	PCI/G
17 A	09/30/19	Uranium-238	0.323	0.0716	0.0301		PCI/G
17 A	09/28/19	Neptunium-236	-0.00166	0.00609	0.0127	U	PCI/G
17 A	09/28/19	Plutonium-236	-0.00166	0.00609	0.0127	U	PCI/G
17 A	09/28/19	Plutonium-239/240	-0.0008	0.00647	0.0129	U	PCI/G
17 A	09/28/19	Plutonium-242	-0.00339	0.00665	0.0152	U	PCI/G
17 A	09/28/19	Plutonium-244	0.004	0.00471	0.00613	U	PCI/G
17 A	09/30/19	Neptunium-237	-0.00661	0.00825	0.0238	U	PCI/G
17 A	10/03/19	Plutonium-241	0.252	1.74	2.98	U	PCI/G
17 A	09/14/19	Actinium-225	-0.164	0.318	0.51	U	PCI/G
17 A	09/14/19	Actinium-227	0.0049	0.0231	0.0372	U	PCI/G
17 A	09/14/19	Actinium-228	0.389	0.029	0.0201		PCI/G
17 A	09/14/19	Antimony-125	0.00508	0.00678	0.012	U	PCI/G
17 A	09/14/19	Barium-137m	0.0507	0.00521	0.00474		PCI/G
17 A	09/14/19	Bismuth-212	0.406	0.065	0.0628		PCI/G
17 A	09/14/19	Bismuth-213	0	0.0118	0.0138	UI	PCI/G
17 A	09/14/19	Bismuth-214	0.362	0.0141	0.00867		PCI/G
17 A	09/14/19	Cesium-134	0	0.00597	0.00676	UI	PCI/G
17 A	09/14/19	Cesium-137	0.0535	0.0055	0.00501		PCI/G
17 A	09/14/19	Cobalt-60	-0.00167	0.00397	0.00598	U	PCI/G
17 A	09/14/19	Europium-152	0.000735	0.00737	0.013	U	PCI/G
17 A	09/14/19	Europium-154	0.000928	0.0118	0.0206	U	PCI/G

Table B-1. Complete Results from the GEL Laboratory

Sample no.	Analysis date	Parameter	Result	Uncertainty	MDC[a]	Qualifier[b]	Units
17 A	09/14/19	Europium-155	0.0139	0.0169	0.0187	U	PCI/G
17 A	09/14/19	Holmium-166m	0.00197	0.00476	0.00812	U	PCI/G
17 A	09/14/19	Lead-210	0	1.3	1.35	UI	PCI/G
17 A	09/14/19	Lead-212	0.387	0.0104	0.00825		PCI/G
17 A	09/14/19	Lead-214	0.412	0.0149	0.0246		PCI/G
17 A	09/14/19	Neptunium-239	-0.0000417	0.0277	0.0459	U	PCI/G
17 A	09/14/19	Niobium-94	0.00315	0.00259	0.00452	U	PCI/G
17 A	09/14/19	Potassium-40	23.9	0.238	0.0347		PCI/G
17 A	09/14/19	Promethium-147	-33.2	77.9	129	U	PCI/G
17 A	09/14/19	Protactinium-231	0	0.0686	0.0634	UI	PCI/G
17 A	09/14/19	Radium-226	0.362	0.0141	0.00867		PCI/G
17 A	09/14/19	Radium-228	0.389	0.029	0.0201		PCI/G
17 A	09/14/19	Sodium-22	0.000378	0.00423	0.00737	U	PCI/G
17 A	09/14/19	Tellurium-125m	0.128	1.5	2.32	U	PCI/G
17 A	09/14/19	Thallium-208	0.126	0.00777	0.00439		PCI/G
17 A	09/14/19	Thorium-231	-0.0107	0.0555	0.0875	U	PCI/G
17 A	09/14/19	Thorium-234	0.417	0.263	0.307		PCI/G
17 A	09/14/19	Thulium-171	4.81	4.02	5.71	U	PCI/G
17 A	09/14/19	Tin-126	0	0.0153	0.0134	UI	PCI/G
17 A	09/30/19	Iodine-129	-0.166	0.18	0.274	U	PCI/G
17 A	09/25/19	Technetium-99	-0.345	0.297	0.515	U	PCI/G
17 A	09/25/19	Strontium-90	-0.00266	0.00784	0.0139	U	PCI/G
17 A	09/25/19	Yttrium-90	-0.00266	0.00784	0.0139	U	PCI/G
17 A	09/28/19	Nickel-63	0.127	0.298	0.505	U	PCI/G
17 A	09/28/19	Iron-55	2.28	2.3	3.22	U	PCI/G
17 A	09/28/19	Tritium	1.46	2.11	3.57	U	PCI/G
17 A	09/26/19	Carbon-14	0.126	1.41	2.45	U	PCI/G
17 A	09/27/19	Nickel-59	0.0566	0.339	0.775	U	PCI/G
17 A	10/03/19	Americium-241	-0.000119	0.0188	0.0399	U	PCI/G
17 A	10/03/19	Americium-243	0.00678	0.0256	0.0482	U	PCI/G
17 A	10/03/19	Curium-243/244	-0.012	0.016	0.0439	U	PCI/G
17 A	10/03/19	Curium-245/246	0	0.00895	0.0122	U	PCI/G
17 B	09/30/19	Polonium-210	0.378	0.144	0.092		PCI/G
17 B	09/29/19	Thorium-228	0.401	0.132	0.149		PCI/G
17 B	09/29/19	Thorium-229	-0.0347	0.0592	0.128	U	PCI/G
17 B	09/29/19	Thorium-230	0.353	0.106	0.0851		PCI/G
17 B	09/29/19	Thorium-232	0.393	0.109	0.0763		PCI/G
17 B	09/30/19	Uranium-232	0.0254	0.0536	0.0931	U	PCI/G
17 B	09/30/19	Uranium-233/234	0.329	0.0668	0.0471		PCI/G
17 B	09/30/19	Uranium-235/236	0.0278	0.0201	0.00926		PCI/G
17 B	09/30/19	Uranium-238	0.277	0.0609	0.0412		PCI/G
17 B	09/28/19	Neptunium-236	-0.00578	0.0107	0.0219	U	PCI/G
17 B	09/28/19	Plutonium-236	-0.00578	0.0107	0.0219	U	PCI/G
17 B	09/28/19	Plutonium-239/240	0.00093	0.0111	0.0206	U	PCI/G
17 B	09/28/19	Plutonium-242	0.00269	0.00646	0.0103	U	PCI/G
17 B	09/28/19	Plutonium-244	0.00186	0.00515	0.00891	U	PCI/G
17 B	09/30/19	Neptunium-237	0.0029	0.0113	0.0216	U	PCI/G
17 B	10/03/19	Plutonium-241	1.24	1.82	3.08	U	PCI/G
17 B	09/14/19	Actinium-225	-0.222	0.311	0.494	U	PCI/G
17 B	09/14/19	Actinium-227	-0.00843	0.0228	0.036	U	PCI/G
17 B	09/14/19	Actinium-228	0.372	0.0315	0.02		PCI/G
17 B	09/14/19	Antimony-125	-0.00163	0.00688	0.0118	U	PCI/G
17 B	09/14/19	Barium-137m	0.0288	0.00459	0.00453		PCI/G
17 B	09/14/19	Bismuth-212	0.385	0.0738	0.0643		PCI/G
17 B	09/14/19	Bismuth-213	0.0135	0.00874	0.014	U	PCI/G
17 B	09/14/19	Bismuth-214	0.348	0.0142	0.00825		PCI/G
17 B	09/14/19	Cesium-134	0	0.00703	0.00664	UI	PCI/G
17 B	09/14/19	Cesium-137	0.0305	0.00485	0.00478		PCI/G
17 B	09/14/19	Cobalt-60	-0.000589	0.00397	0.00588	U	PCI/G
17 B	09/14/19	Europium-152	-0.00682	0.00733	0.0125	U	PCI/G
17 B	09/14/19	Europium-154	-0.00223	0.0119	0.0201	U	PCI/G
17 B	09/14/19	Europium-155	0.0112	0.0109	0.0184	U	PCI/G

Table B-1. Complete Results from the GEL Laboratory

Sample no.	Analysis date	Parameter	Result	Uncertainty	MDC[a]	Qualifier[b]	Units
17 B	09/14/19	Holmium-166m	-0.00105	0.0047	0.00775	U	PCI/G
17 B	09/14/19	Lead-210	0.545	0.957	0.992	U	PCI/G
17 B	09/14/19	Lead-212	0.369	0.00987	0.00798		PCI/G
17 B	09/14/19	Lead-214	0.387	0.0149	0.00937		PCI/G
17 B	09/14/19	Neptunium-239	0.0126	0.0269	0.045	U	PCI/G
17 B	09/14/19	Niobium-94	0.00376	0.004	0.00449	U	PCI/G
17 B	09/14/19	Potassium-40	24.4	0.23	0.0349		PCI/G
17 B	09/14/19	Promethium-147	-13.6	75.9	126	U	PCI/G
17 B	09/14/19	Protactinium-231	0	0.0632	0.0632	UI	PCI/G
17 B	09/14/19	Radium-226	0.348	0.0142	0.00825		PCI/G
17 B	09/14/19	Radium-228	0.372	0.0315	0.02		PCI/G
17 B	09/14/19	Sodium-22	-0.000892	0.00424	0.00718	U	PCI/G
17 B	09/14/19	Tellurium-125m	0.232	1.34	2.23	U	PCI/G
17 B	09/14/19	Thallium-208	0.114	0.00701	0.00445		PCI/G
17 B	09/14/19	Thorium-231	-0.0108	0.0545	0.0851	U	PCI/G
17 B	09/14/19	Thorium-234	0.182	0.295	0.27	U	PCI/G
17 B	09/14/19	Thulium-171	-2.13	2.66	4.54	U	PCI/G
17 B	09/14/19	Tin-126	0	0.0123	0.0126	UI	PCI/G
17 B	09/30/19	Iodine-129	-0.279	0.769	1.13	U	PCI/G
17 B	09/25/19	Technetium-99	-0.158	0.307	0.527	U	PCI/G
17 B	10/05/19	Strontium-90	-0.00289	0.00815	0.015	U	PCI/G
17 B	10/05/19	Yttrium-90	-0.00289	0.00815	0.015	U	PCI/G
17 B	09/28/19	Nickel-63	-0.0389	0.3	0.515	U	PCI/G
17 B	09/28/19	Iron-55	1.17	2.02	2.86	U	PCI/G
17 B	09/28/19	Tritium	1.09	2.12	3.62	U	PCI/G
17 B	09/26/19	Carbon-14	1.22	1.45	2.44	U	PCI/G
17 B	09/27/19	Nickel-59	0.657	0.801	1.19	U	PCI/G
17 B	10/03/19	Americium-241	0.00192	0.0215	0.0438	U	PCI/G
17 B	10/03/19	Americium-243	0.00305	0.0127	0.0234	U	PCI/G
17 B	10/03/19	Curium-243/244	-0.00419	0.0146	0.0359	U	PCI/G
17 B	10/03/19	Curium-245/246	0	0.00851	0.017	U	PCI/G
17 C	09/26/19	Technetium-99	0.166	0.306	0.516	U	PCI/G
17 C	09/30/19	Polonium-210	0.203	0.122	0.127		PCI/G
17 C	09/29/19	Thorium-228	0.311	0.119	0.141		PCI/G
17 C	09/29/19	Thorium-229	9.37E-09	0.0584	0.114	U	PCI/G
17 C	09/29/19	Thorium-230	0.4	0.114	0.094		PCI/G
17 C	09/29/19	Thorium-232	0.328	0.0978	0.0535		PCI/G
17 C	09/30/19	Uranium-232	-0.0283	0.0434	0.0933	U	PCI/G
17 C	09/30/19	Uranium-233/234	0.247	0.0689	0.0525		PCI/G
17 C	09/30/19	Uranium-235/236	0.0128	0.0222	0.0327	U	PCI/G
17 C	09/30/19	Uranium-238	0.315	0.0747	0.0408		PCI/G
17 C	09/28/19	Neptunium-236	0.000896	0.0068	0.0129	U	PCI/G
17 C	09/28/19	Plutonium-236	0.000896	0.0068	0.0129	U	PCI/G
17 C	09/28/19	Plutonium-239/240	0.00346	0.00719	0.0124	U	PCI/G
17 C	09/28/19	Plutonium-242	0	0.00588	0.0117	U	PCI/G
17 C	09/28/19	Plutonium-244	0.00518	0.00634	0.00956	U	PCI/G
17 C	09/30/19	Neptunium-237	-0.00119	0.00902	0.0203	U	PCI/G
17 C	10/03/19	Plutonium-241	-0.337	1.61	2.79	U	PCI/G
17 C	09/14/19	Actinium-225	0.000927	0.309	0.503	U	PCI/G
17 C	09/14/19	Actinium-227	0.00703	0.0229	0.0371	U	PCI/G
17 C	09/14/19	Actinium-228	0.407	0.0267	0.0197		PCI/G
17 C	09/14/19	Antimony-125	0.00773	0.01	0.012	U	PCI/G
17 C	09/14/19	Barium-137m	0.0236	0.00418	0.0043		PCI/G
17 C	09/14/19	Bismuth-212	0.343	0.0699	0.0627		PCI/G
17 C	09/14/19	Bismuth-213	0.00804	0.00842	0.0135	U	PCI/G
17 C	09/14/19	Bismuth-214	0.341	0.015	0.00824		PCI/G
17 C	09/14/19	Cesium-134	0	0.00334	0.00598	UI	PCI/G
17 C	09/14/19	Cesium-137	0.025	0.00441	0.00454		PCI/G
17 C	09/14/19	Cobalt-60	-0.000674	0.00337	0.0058	U	PCI/G
17 C	09/14/19	Europium-152	-0.00156	0.00714	0.0125	U	PCI/G

Table B-1. Complete Results from the GEL Laboratory

Sample no.	Analysis date	Parameter	Result	Uncertainty	MDC[a]	Qualifier[b]	Units
17 C	09/14/19	Europium-154	0.000929	0.0131	0.0199	U	PCI/G
17 C	09/14/19	Europium-155	0.0175	0.0144	0.0178	U	PCI/G
17 C	09/14/19	Holmium-166m	-0.0031	0.00443	0.00733	U	PCI/G
17 C	09/14/19	Lead-210	0.893	1.19	1.12	U	PCI/G
17 C	09/14/19	Lead-212	0.397	0.0105	0.00831		PCI/G
17 C	09/14/19	Lead-214	0.404	0.0142	0.00946		PCI/G
17 C	09/14/19	Neptunium-239	0.0116	0.0264	0.0447	U	PCI/G
17 C	09/14/19	Niobium-94	0.00136	0.00254	0.00433	U	PCI/G
17 C	09/14/19	Potassium-40	27	0.241	0.0371		PCI/G
17 C	09/14/19	Promethium-147	-18.8	74.7	125	U	PCI/G
17 C	09/14/19	Protactinium-231	0	0.0642	0.0624	UI	PCI/G
17 C	09/14/19	Radium-226	0.341	0.015	0.00824		PCI/G
17 C	09/14/19	Radium-228	0.407	0.0267	0.0197		PCI/G
17 C	09/14/19	Sodium-22	0.000165	0.00468	0.00712	U	PCI/G
17 C	09/14/19	Tellurium-125m	1.26	1.29	2.21	U	PCI/G
17 C	09/14/19	Thallium-208	0.112	0.00608	0.00433		PCI/G
17 C	09/14/19	Thorium-231	0.0731	0.0532	0.0872	U	PCI/G
17 C	09/14/19	Thorium-234	0	0.272	0.27	UI	PCI/G
17 C	09/14/19	Thulium-171	0.863	2.79	4.89	U	PCI/G
17 C	09/14/19	Tin-126	0	0.0136	0.0123	UI	PCI/G
17 C	09/30/19	Iodine-129	-0.0703	0.225	0.455	U	PCI/G
17 C	09/25/19	Technetium-99	-0.106	0.311	0.532	U	PCI/G
17 C	10/07/19	Strontium-90	0.00429	0.00837	0.0146	U	PCI/G
17 C	10/07/19	Yttrium-90	0.00429	0.00837	0.0146	U	PCI/G
17 C	09/28/19	Nickel-63	-0.0753	0.296	0.509	U	PCI/G
17 C	09/28/19	Iron-55	-0.166	2.13	3.09	U	PCI/G
17 C	09/28/19	Tritium	1.13	2.11	3.6	U	PCI/G
17 C	09/26/19	Carbon-14	-0.0546	1.39	2.43	U	PCI/G
17 C	09/27/19	Nickel-59	0.45	0.889	1.67	U	PCI/G
17 C	10/03/19	Americium-241	0.00628	0.0186	0.0337	U	PCI/G
17 C	10/03/19	Americium-243	-0.0142	0.0151	0.0424	U	PCI/G
17 C	10/03/19	Curium-243/244	-0.0000838	0.017	0.0366	U	PCI/G
17 C	10/03/19	Curium-245/246	-0.00206	0.00981	0.0239	U	PCI/G
18 A	09/18/19	Actinium-225	-0.911	0.693	1.1	U	PCI/G
18 A	09/18/19	Actinium-227	0.0535	0.0415	0.0676	U	PCI/G
18 A	09/18/19	Actinium-228	1.22	0.0522	0.0292		PCI/G
18 A	09/18/19	Antimony-125	0.00807	0.0126	0.0221	U	PCI/G
18 A	09/18/19	Barium-137m	0.0794	0.00777	0.00749		PCI/G
18 A	09/18/19	Bismuth-212	1.34	0.131	0.105		PCI/G
18 A	09/18/19	Bismuth-213	0.0094	0.0152	0.024	U	PCI/G
18 A	09/18/19	Bismuth-214	1.79	0.0327	0.0145		PCI/G
18 A	09/18/19	Cesium-134	0	0.011	0.0127	UI	PCI/G
18 A	09/18/19	Cesium-137	0.0839	0.00821	0.00791		PCI/G
18 A	09/18/19	Cobalt-60	-0.00164	0.00489	0.00846	U	PCI/G
18 A	09/18/19	Europium-152	-0.00144	0.014	0.0234	U	PCI/G
18 A	09/18/19	Europium-154	0.000169	0.0161	0.0261	U	PCI/G
18 A	09/18/19	Europium-155	0	0.0301	0.0334	UI	PCI/G
18 A	09/18/19	Holmium-166m	0.00358	0.00767	0.0131	U	PCI/G
18 A	09/18/19	Lead-210	0.355	2.31	2.51	U	PCI/G
18 A	09/18/19	Lead-212	1.23	0.0207	0.0157		PCI/G
18 A	09/18/19	Lead-214	2.06	0.0347	0.0658		PCI/G
18 A	09/18/19	Neptunium-239	0	0.0738	0.0835	UI	PCI/G
18 A	09/18/19	Niobium-94	0	0.00645	0.00786	UI	PCI/G
18 A	09/18/19	Potassium-40	15.3	0.252	0.0699		PCI/G
18 A	09/18/19	Promethium-147	-87.5	147	234	U	PCI/G
18 A	09/18/19	Protactinium-231	0	0.11	0.114	UI	PCI/G
18 A	09/18/19	Radium-226	1.79	0.0327	0.0145		PCI/G
18 A	09/18/19	Radium-228	1.22	0.0522	0.0292		PCI/G
18 A	09/18/19	Sodium-22	0.000281	0.00576	0.00938	U	PCI/G
18 A	09/18/19	Tellurium-125m	0	2.89	4.21	UI	PCI/G
18 A	09/18/19	Thallium-208	0.369	0.0141	0.00784		PCI/G
18 A	09/18/19	Thorium-231	-0.0801	0.102	0.158	U	PCI/G

Table B-1. Complete Results from the GEL Laboratory

Sample no.	Analysis date	Parameter	Result	Uncertainty	MDC[a]	Qualifier[b]	Units
18 A	09/18/19	Thorium-234	1.19	0.497	0.586		PCI/G
18 A	09/18/19	Thulium-171	5.47	8.22	11	U	PCI/G
18 A	09/18/19	Tin-126	0	0.0247	0.0237	UI	PCI/G
18 A	10/03/19	Polonium-210	1.25	0.301	0.19		PCI/G
18 A	10/03/19	Thorium-228	0.883	0.158	0.108		PCI/G
18 A	10/03/19	Thorium-229	0.0368	0.048	0.0754	U	PCI/G
18 A	10/03/19	Thorium-230	1.86	0.215	0.0936		PCI/G
18 A	10/03/19	Thorium-232	0.914	0.149	0.0584		PCI/G
18 A	10/01/19	Uranium-232	0.0143	0.0429	0.0771	U	PCI/G
18 A	10/01/19	Uranium-233/234	0.929	0.114	0.0393		PCI/G
18 A	10/01/19	Uranium-235/236	0.0428	0.0313	0.0394		PCI/G
18 A	10/01/19	Uranium-238	0.846	0.11	0.0476		PCI/G
18 A	10/01/19	Neptunium-236	-0.00176	0.00455	0.0123	U	PCI/G
18 A	10/01/19	Plutonium-236	-0.00176	0.00455	0.0123	U	PCI/G
18 A	10/01/19	Plutonium-239/240	0.00669	0.00948	0.0147	U	PCI/G
18 A	10/01/19	Plutonium-242	0.00527	0.0103	0.0168	U	PCI/G
18 A	10/01/19	Plutonium-244	0.000832	0.00522	0.00987	U	PCI/G
18 A	10/05/19	Americium-241	0.00932	0.0132	0.0205	U	PCI/G
18 A	10/05/19	Americium-243	0.0112	0.0139	0.0217	U	PCI/G
18 A	10/05/19	Curium-243/244	-0.0000464	0.00941	0.0203	U	PCI/G
18 A	10/05/19	Curium-245/246	0	0.00522	0.00714	U	PCI/G
18 A	10/02/19	Neptunium-237	-0.000824	0.00545	0.0127	U	PCI/G
18 A	10/05/19	Plutonium-241	-0.49	1.64	2.85	U	PCI/G
18 A	09/26/19	Nickel-63	0.146	0.429	0.732	U	PCI/G
18 A	09/28/19	Iodine-129	-0.246	0.613	1.04	U	PCI/G
18 A	09/26/19	Iron-55	0.872	2.71	3.9	U	PCI/G
18 A	09/24/19	Technetium-99	-0.0394	0.322	0.55	U	PCI/G
18 A	09/26/19	Tritium	-1.8	2.33	4.44	U	PCI/G
18 A	09/28/19	Carbon-14	-0.482	1.46	2.6	U	PCI/G
18 A	09/26/19	Nickel-59	-0.0682	1.33	2.33	U	PCI/G
18 A	10/08/19	Strontium-90	0.012	0.00894	0.0147	U	PCI/G
18 A	10/08/19	Yttrium-90	0.012	0.00894	0.0147	U	PCI/G
18 B	09/18/19	Actinium-225	0.077	0.662	1.06	U	PCI/G
18 B	09/18/19	Actinium-227	0.0462	0.0523	0.0647	U	PCI/G
18 B	09/18/19	Actinium-228	1.24	0.0539	0.0278		PCI/G
18 B	09/18/19	Antimony-125	0.00532	0.0125	0.0215	U	PCI/G
18 B	09/18/19	Barium-137m	0.0828	0.00753	0.00713		PCI/G
18 B	09/18/19	Bismuth-212	1.24	0.152	0.0971		PCI/G
18 B	09/18/19	Bismuth-213	0.000476	0.0133	0.0227	U	PCI/G
18 B	09/18/19	Bismuth-214	1.76	0.0323	0.0137		PCI/G
18 B	09/18/19	Cesium-134	0	0.0111	0.0117	UI	PCI/G
18 B	09/18/19	Cesium-137	0.0875	0.00795	0.00754		PCI/G
18 B	09/18/19	Cobalt-60	-0.00145	0.00453	0.00766	U	PCI/G
18 B	09/18/19	Europium-152	-0.0131	0.013	0.0222	U	PCI/G
18 B	09/18/19	Europium-154	0.0121	0.0167	0.0258	U	PCI/G
18 B	09/18/19	Europium-155	0	0.0319	0.0318	UI	PCI/G
18 B	09/18/19	Holmium-166m	-0.00332	0.00759	0.0124	U	PCI/G
18 B	09/18/19	Lead-210	0.431	1.15	1.88	U	PCI/G
18 B	09/18/19	Lead-212	1.24	0.0201	0.0141		PCI/G
18 B	09/18/19	Lead-214	2.04	0.0346	0.0622		PCI/G
18 B	09/18/19	Neptunium-239	0	0.0622	0.0788	UI	PCI/G
18 B	09/18/19	Niobium-94	0	0.00603	0.00758	UI	PCI/G
18 B	09/18/19	Potassium-40	15.3	0.243	0.0672		PCI/G
18 B	09/18/19	Promethium-147	-3.65	134	222	U	PCI/G
18 B	09/18/19	Protactinium-231	0	0.117	0.115	UI	PCI/G
18 B	09/18/19	Radium-226	1.76	0.0323	0.0137		PCI/G
18 B	09/18/19	Radium-228	1.24	0.0539	0.0278		PCI/G
18 B	09/18/19	Sodium-22	0.00414	0.00599	0.00922	U	PCI/G
18 B	09/18/19	Tellurium-125m	2.86	3.19	3.92	U	PCI/G
18 B	09/18/19	Thallium-208	0.37	0.0134	0.00734		PCI/G

Table B-1. Complete Results from the GEL Laboratory

Sample no.	Analysis date	Parameter	Result	Uncertainty	MDC[a]	Qualifier[b]	Units
18 B	09/18/19	Thorium-231	0.0963	0.103	0.15	U	PCI/G
18 B	09/18/19	Thorium-234	1.65	0.53	0.492		PCI/G
18 B	09/18/19	Thulium-171	4.98	6.67	8.43	U	PCI/G
18 B	09/18/19	Tin-126	0	0.0229	0.0219	UI	PCI/G
18 B	10/02/19	Polonium-210	0.929	0.261	0.188		PCI/G
18 B	10/02/19	Thorium-228	0.82	0.162	0.121		PCI/G
18 B	10/02/19	Thorium-229	0.0201	0.0707	0.128	U	PCI/G
18 B	10/02/19	Thorium-230	1.82	0.218	0.064		PCI/G
18 B	10/02/19	Thorium-232	0.772	0.149	0.0959		PCI/G
18 B	10/01/19	Uranium-232	-0.0315	0.0488	0.0996	U	PCI/G
18 B	10/01/19	Uranium-233/234	0.924	0.117	0.0558		PCI/G
18 B	10/01/19	Uranium-235/236	0.0549	0.0358	0.045		PCI/G
18 B	10/01/19	Uranium-238	0.901	0.115	0.0489		PCI/G
18 B	10/01/19	Neptunium-236	0.000849	0.00533	0.0101	U	PCI/G
18 B	10/01/19	Plutonium-236	0.000849	0.00533	0.0101	U	PCI/G
18 B	10/01/19	Plutonium-239/240	0.00162	0.00744	0.0144	U	PCI/G
18 B	10/01/19	Plutonium-242	-0.00498	0.00642	0.0178	U	PCI/G
18 B	10/01/19	Plutonium-244	0.000818	0.00513	0.00969	U	PCI/G
18 B	10/02/19	Americium-241	-0.00223	0.00775	0.0191	U	PCI/G
18 B	10/02/19	Americium-243	-0.00423	0.0126	0.0281	U	PCI/G
18 B	10/02/19	Curium-243/244	0.00324	0.00795	0.0127	U	PCI/G
18 B	10/02/19	Curium-245/246	-0.0012	0.00572	0.0139	U	PCI/G
18 B	10/02/19	Neptunium-237	-0.00995	0.00827	0.0239	U	PCI/G
18 B	10/05/19	Plutonium-241	-1.18	1.66	2.9	U	PCI/G
18 B	09/26/19	Nickel-63	0.118	0.41	0.7	U	PCI/G
18 B	09/28/19	Iodine-129	0	0.366	0.409	UI	PCI/G
18 B	09/26/19	Iron-55	-0.22	2.63	3.81	U	PCI/G
18 B	09/24/19	Technetium-99	0.0127	0.328	0.558	U	PCI/G
18 B	09/30/19	Tritium	1.91	2.18	3.66	U	PCI/G
18 B	09/28/19	Carbon-14	-1.02	1.44	2.6	U	PCI/G
18 B	09/26/19	Nickel-59	-0.244	0.981	1.72	U	PCI/G
18 B	10/07/19	Strontium-90	0.00911	0.0085	0.0141	U	PCI/G
18 B	10/07/19	Yttrium-90	0.00911	0.0085	0.0141	U	PCI/G
18 C	09/24/19	Actinium-225	0.658	1.56	2.69	U	PCI/G
18 C	09/24/19	Actinium-227	-0.00484	0.0742	0.113	U	PCI/G
18 C	09/24/19	Actinium-228	1.26	0.0746	0.0456		PCI/G
18 C	09/24/19	Antimony-125	0	0.0256	0.0374	UI	PCI/G
18 C	09/24/19	Barium-137m	0.0786	0.0127	0.0119		PCI/G
18 C	09/24/19	Bismuth-212	1.46	0.255	0.158		PCI/G
18 C	09/24/19	Bismuth-213	-0.0000433	0.0232	0.0392	U	PCI/G
18 C	09/24/19	Bismuth-214	1.88	0.057	0.0246		PCI/G
18 C	09/24/19	Cesium-134	0	0.016	0.0193	UI	PCI/G
18 C	09/24/19	Cesium-137	0.083	0.0134	0.0126		PCI/G
18 C	09/24/19	Cobalt-60	-0.000606	0.00708	0.0124	U	PCI/G
18 C	09/24/19	Europium-152	-0.0186	0.0231	0.0385	U	PCI/G
18 C	09/24/19	Europium-154	-0.00718	0.0226	0.0375	U	PCI/G
18 C	09/24/19	Europium-155	0	0.0518	0.0657	UI	PCI/G
18 C	09/24/19	Holmium-166m	-0.0107	0.0114	0.0197	U	PCI/G
18 C	09/24/19	Lead-210	0	4.22	3.56	UI	PCI/G
18 C	09/24/19	Lead-212	1.16	0.0342	0.0254		PCI/G
18 C	09/24/19	Lead-214	2.17	0.0568	0.1		PCI/G
18 C	09/24/19	Neptunium-239	-0.0143	0.0951	0.158	U	PCI/G
18 C	09/24/19	Niobium-94	0.00764	0.00691	0.0127	U	PCI/G
18 C	09/24/19	Potassium-40	14.2	0.374	0.104		PCI/G
18 C	09/24/19	Promethium-147	-163	253	437	U	PCI/G
18 C	09/24/19	Protactinium-231	0	0.17	0.189	UI	PCI/G
18 C	09/24/19	Radium-226	1.88	0.057	0.0246		PCI/G
18 C	09/24/19	Radium-228	1.26	0.0746	0.0456		PCI/G
18 C	09/24/19	Sodium-22	-0.00289	0.00808	0.0134	U	PCI/G
18 C	09/24/19	Tellurium-125m	3.53	6.88	8.52	U	PCI/G
18 C	09/24/19	Thallium-208	0.374	0.0247	0.0129		PCI/G
18 C	09/24/19	Thorium-231	-0.0668	0.178	0.264	U	PCI/G

Table B-1. Complete Results from the GEL Laboratory

Sample no.	Analysis date	Parameter	Result	Uncertainty	MDC[a]	Qualifier[b]	Units
18 C	09/24/19	Thorium-234	1.63	1.24	1.24		PCI/G
18 C	09/24/19	Thulium-171	-7.14	13.5	22.7	U	PCI/G
18 C	09/24/19	Tin-126	0	0.0524	0.0494	UI	PCI/G
18 C	10/03/19	Polonium-210	0.992	0.272	0.209		PCI/G
18 C	10/03/19	Thorium-228	0.786	0.204	0.194		PCI/G
18 C	10/03/19	Thorium-229	-0.0493	0.127	0.25	U	PCI/G
18 C	10/03/19	Thorium-230	2.12	0.3	0.188		PCI/G
18 C	10/03/19	Thorium-232	0.864	0.221	0.239		PCI/G
18 C	10/01/19	Uranium-232	0.0853	0.0527	0.0741		PCI/G
18 C	10/01/19	Uranium-233/234	0.948	0.112	0.0408		PCI/G
18 C	10/01/19	Uranium-235/236	0.0432	0.0326	0.0446	U	PCI/G
18 C	10/01/19	Uranium-238	0.905	0.11	0.0507		PCI/G
18 C	10/03/19	Neptunium-236	-0.00249	0.00541	0.0141	U	PCI/G
18 C	10/03/19	Plutonium-236	-0.00249	0.00541	0.0141	U	PCI/G
18 C	10/03/19	Plutonium-239/240	-0.00506	0.00872	0.0211	U	PCI/G
18 C	10/03/19	Plutonium-242	0.00344	0.0143	0.0275	U	PCI/G
18 C	10/03/19	Plutonium-244	0.000466	0.00569	0.0111	U	PCI/G
18 C	10/02/19	Americium-241	-0.000936	0.00843	0.0185	U	PCI/G
18 C	10/02/19	Americium-243	0.00386	0.0115	0.0208	U	PCI/G
18 C	10/02/19	Curium-243/244	0.00431	0.00834	0.0138	U	PCI/G
18 C	10/02/19	Curium-245/246	0	0.00716	0.0143	U	PCI/G
18 C	10/03/19	Neptunium-237	-0.00426	0.0079	0.0215	U	PCI/G
18 C	10/05/19	Plutonium-241	0.45	2.02	3.45	U	PCI/G
18 C	09/26/19	Nickel-63	0.411	0.425	0.712	U	PCI/G
18 C	09/28/19	Iodine-129	0.295	0.372	0.847	U	PCI/G
18 C	09/26/19	Iron-55	0.372	2.42	3.49	U	PCI/G
18 C	09/24/19	Technetium-99	0.154	0.335	0.566	U	PCI/G
18 C	09/27/19	Tritium	-0.793	2.5	4.6	U	PCI/G
18 C	09/28/19	Carbon-14	-0.492	1.5	2.66	U	PCI/G
18 C	09/26/19	Nickel-59	-0.654	1.35	2.35	U	PCI/G
18 C	10/07/19	Strontium-90	0.00754	0.00842	0.0141	U	PCI/G
18 C	10/07/19	Yttrium-90	0.00754	0.00842	0.0141	U	PCI/G
2 A	10/03/19	Polonium-210	0.891	0.222	0.0424		PCI/G
2 A	10/03/19	Thorium-228	1.18	0.234	0.186		PCI/G
2 A	10/03/19	Thorium-229	-0.0567	0.0641	0.153	U	PCI/G
2 A	10/03/19	Thorium-230	1.14	0.213	0.126		PCI/G
2 A	10/03/19	Thorium-232	1.59	0.242	0.0719		PCI/G
2 A	10/01/19	Uranium-232	-0.0233	0.06	0.118	U	PCI/G
2 A	10/01/19	Uranium-233/234	1.02	0.123	0.0458		PCI/G
2 A	10/01/19	Uranium-235/236	0.071	0.0408	0.0501		PCI/G
2 A	10/01/19	Uranium-238	0.92	0.117	0.0412		PCI/G
2 A	10/01/19	Neptunium-236	-0.00599	0.00579	0.0179	U	PCI/G
2 A	10/01/19	Plutonium-236	-0.00599	0.00579	0.0179	U	PCI/G
2 A	10/01/19	Plutonium-239/240	-0.00333	0.00736	0.0181	U	PCI/G
2 A	10/01/19	Plutonium-242	-0.00866	0.0145	0.0334	U	PCI/G
2 A	10/01/19	Plutonium-244	0.000808	0.00507	0.00958	U	PCI/G
2 A	10/02/19	Neptunium-237	-0.00352	0.00778	0.0192	U	PCI/G
2 A	10/06/19	Plutonium-241	-1.07	1.63	2.86	U	PCI/G
2 A	09/25/19	Actinium-225	-1.53	1.62	2.59	U	PCI/G
2 A	09/25/19	Actinium-227	0.0444	0.061	0.0924	U	PCI/G
2 A	09/25/19	Actinium-228	1.71	0.0751	0.0373		PCI/G
2 A	09/25/19	Antimony-125	0.000315	0.019	0.0304	U	PCI/G
2 A	09/25/19	Barium-137m	0.0575	0.0106	0.0108		PCI/G
2 A	09/25/19	Bismuth-212	1.83	0.194	0.147		PCI/G
2 A	09/25/19	Bismuth-213	0.0242	0.0284	0.0325	U	PCI/G
2 A	09/25/19	Bismuth-214	1.29	0.04	0.0201		PCI/G
2 A	09/25/19	Cesium-134	0	0.0152	0.0189	UI	PCI/G
2 A	09/25/19	Cesium-137	0.0608	0.0112	0.0114		PCI/G
2 A	09/25/19	Cobalt-60	-0.000308	0.00637	0.0114	U	PCI/G
2 A	09/25/19	Europium-152	-0.00365	0.0181	0.0319	U	PCI/G

Table B-1. Complete Results from the GEL Laboratory

Sample no.	Analysis date	Parameter	Result	Uncertainty	MDC[a]	Qualifier[b]	Units
2 A	09/25/19	Europium-154	0.00229	0.022	0.0369	U	PCI/G
2 A	09/25/19	Europium-155	0	0.048	0.048	UI	PCI/G
2 A	09/25/19	Holmium-166m	-0.0023	0.0108	0.0185	U	PCI/G
2 A	09/25/19	Lead-210	1.02	1.98	2.38	U	PCI/G
2 A	09/25/19	Lead-212	1.69	0.032	0.0212		PCI/G
2 A	09/25/19	Lead-214	1.54	0.0458	0.0779		PCI/G
2 A	09/25/19	Neptunium-239	0	0.119	0.12	UI	PCI/G
2 A	09/25/19	Niobium-94	0.00253	0.00598	0.0104	U	PCI/G
2 A	09/25/19	Potassium-40	22.4	0.399	0.0913		PCI/G
2 A	09/25/19	Promethium-147	-76.7	205	339	U	PCI/G
2 A	09/25/19	Protactinium-231	0	0.171	0.164	UI	PCI/G
2 A	09/25/19	Radium-226	1.29	0.04	0.0201		PCI/G
2 A	09/25/19	Radium-228	1.71	0.0751	0.0373		PCI/G
2 A	09/25/19	Sodium-22	-0.000594	0.00798	0.0133	U	PCI/G
2 A	09/25/19	Tellurium-125m	6.46	5.93	6.52	U	PCI/G
2 A	09/25/19	Thallium-208	0.521	0.0203	0.0109		PCI/G
2 A	09/25/19	Thorium-231	-0.0909	0.137	0.215	U	PCI/G
2 A	09/25/19	Thorium-234	1.51	0.699	0.756		PCI/G
2 A	09/25/19	Thulium-171	-4.7	7.69	11.9	U	PCI/G
2 A	09/25/19	Tin-126	0	0.0342	0.0339	UI	PCI/G
2 A	09/28/19	Iodine-129	-0.256	0.411	0.685	U	PCI/G
2 A	09/26/19	Iron-55	0.396	2.85	4.36	U	PCI/G
2 A	09/26/19	Nickel-63	-0.00601	0.471	0.809	U	PCI/G
2 A	09/25/19	Technetium-99	-0.0689	0.33	0.563	U	PCI/G
2 A	09/27/19	Tritium	0.428	2.59	4.6	U	PCI/G
2 A	09/28/19	Carbon-14	-1.71	1.42	2.64	U	PCI/G
2 A	10/03/19	Strontium-90	-0.00132	0.00845	0.0149	U	PCI/G
2 A	10/03/19	Yttrium-90	-0.00132	0.00845	0.0149	U	PCI/G
2 A	10/02/19	Nickel-59	-0.289	1.32	2.33	U	PCI/G
2 A	10/05/19	Americium-241	0.0131	0.016	0.0241	U	PCI/G
2 A	10/05/19	Americium-243	0.00579	0.0217	0.0394	U	PCI/G
2 A	10/05/19	Curium-243/244	0	0.006	0.00649	U	PCI/G
2 A	10/05/19	Curium-245/246	7.47E-10	0.0108	0.0215	U	PCI/G
2 B	09/27/19	Tritium	-1	2.38	4.47	U	PCI/G
2 B	09/27/19	Tritium	91.7	17.7	8.38		%
2 B	10/03/19	Polonium-210	0.775	0.205	0.0415		PCI/G
2 B	10/03/19	Thorium-228	1.28	0.233	0.203		PCI/G
2 B	10/03/19	Thorium-229	-0.146	0.0983	0.221	U	PCI/G
2 B	10/03/19	Thorium-230	0.82	0.186	0.18		PCI/G
2 B	10/03/19	Thorium-232	1.17	0.206	0.149		PCI/G
2 B	10/01/19	Uranium-232	-0.0649	0.0566	0.117	U	PCI/G
2 B	10/01/19	Uranium-233/234	0.887	0.113	0.0445		PCI/G
2 B	10/01/19	Uranium-235/236	0.0544	0.0341	0.0401		PCI/G
2 B	10/01/19	Uranium-238	0.922	0.114	0.0277		PCI/G
2 B	10/01/19	Neptunium-236	-0.0116	0.00897	0.0248	U	PCI/G
2 B	10/01/19	Plutonium-236	-0.0116	0.00897	0.0248	U	PCI/G
2 B	10/01/19	Plutonium-239/240	-0.00249	0.0109	0.0233	U	PCI/G
2 B	10/01/19	Plutonium-242	-0.00457	0.00669	0.0198	U	PCI/G
2 B	10/01/19	Plutonium-244	0.00628	0.00802	0.0111	U	PCI/G
2 B	10/03/19	Neptunium-237	-0.0032	0.00966	0.0271	U	PCI/G
2 B	10/06/19	Plutonium-241	0.14	1.4	2.4	U	PCI/G
2 B	09/25/19	Actinium-225	0.112	1.64	2.91	U	PCI/G
2 B	09/25/19	Actinium-227	0.0559	0.0819	0.106	U	PCI/G
2 B	09/25/19	Actinium-228	1.72	0.0943	0.0541		PCI/G
2 B	09/25/19	Antimony-125	0.0196	0.0218	0.0382	U	PCI/G
2 B	09/25/19	Barium-137m	0.068	0.0141	0.0144		PCI/G
2 B	09/25/19	Bismuth-212	2.06	0.255	0.199		PCI/G
2 B	09/25/19	Bismuth-213	0.0207	0.0245	0.0428	U	PCI/G
2 B	09/25/19	Bismuth-214	1.36	0.0507	0.0271		PCI/G
2 B	09/25/19	Cesium-134	0	0.0183	0.0241	UI	PCI/G
2 B	09/25/19	Cesium-137	0.0718	0.0149	0.0153		PCI/G
2 B	09/25/19	Cobalt-60	-0.00618	0.01	0.0143	U	PCI/G

Table B-1. Complete Results from the GEL Laboratory

Sample no.	Analysis date	Parameter	Result	Uncertainty	MDC[a]	Qualifier[b]	Units
2 B	09/25/19	Europium-152	-0.0265	0.0225	0.0379	U	PCI/G
2 B	09/25/19	Europium-154	0.0271	0.03	0.0535	U	PCI/G
2 B	09/25/19	Europium-155	0	0.0444	0.0453	UI	PCI/G
2 B	09/25/19	Holmium-166m	-0.0023	0.0139	0.0246	U	PCI/G
2 B	09/25/19	Lead-210	1.24	0.321	0.296		PCI/G
2 B	09/25/19	Lead-212	1.67	0.0336	0.023		PCI/G
2 B	09/25/19	Lead-214	1.5	0.0528	0.0893		PCI/G
2 B	09/25/19	Neptunium-239	0.0572	0.0764	0.118	U	PCI/G
2 B	09/25/19	Niobium-94	0.00777	0.00793	0.0145	U	PCI/G
2 B	09/25/19	Potassium-40	20.6	0.463	0.112		PCI/G
2 B	09/25/19	Promethium-147	99	203	337	U	PCI/G
2 B	09/25/19	Protactinium-231	0	0.192	0.188	UI	PCI/G
2 B	09/25/19	Radium-226	1.36	0.0507	0.0271		PCI/G
2 B	09/25/19	Radium-228	1.72	0.0943	0.0541		PCI/G
2 B	09/25/19	Sodium-22	0.00821	0.0109	0.0193	U	PCI/G
2 B	09/25/19	Tellurium-125m	3.97	4.27	6.54	U	PCI/G
2 B	09/25/19	Thallium-208	0.528	0.024	0.014		PCI/G
2 B	09/25/19	Thorium-231	-0.0217	0.165	0.256	U	PCI/G
2 B	09/25/19	Thorium-234	1.42	0.34	0.354		PCI/G
2 B	09/25/19	Thulium-171	2.7	2.58	2.88	U	PCI/G
2 B	09/25/19	Tin-126	0	0.028	0.0275	UI	PCI/G
2 B	09/28/19	Iodine-129	0.0335	0.29	0.591	U	PCI/G
2 B	09/26/19	Iron-55	-0.205	2.91	4.5	U	PCI/G
2 B	09/26/19	Nickel-63	-0.0721	0.382	0.658	U	PCI/G
2 B	09/25/19	Technetium-99	-0.175	0.317	0.545	U	PCI/G
2 B	09/26/19	Tritium	0.347	2.27	4	U	PCI/G
2 B	09/28/19	Carbon-14	-0.952	1.42	2.56	U	PCI/G
2 B	09/28/19	Strontium-90	0.00628	0.00853	0.0144	U	PCI/G
2 B	09/28/19	Yttrium-90	0.00628	0.00853	0.0144	U	PCI/G
2 B	10/02/19	Nickel-59	-0.759	0.892	1.41	U	PCI/G
2 B	10/07/19	Americium-241	0.0149	0.0126	0.0142		PCI/G
2 B	10/07/19	Americium-243	-0.0197	0.0219	0.047	U	PCI/G
2 B	10/07/19	Curium-243/244	0.00184	0.00626	0.00553	U	PCI/G
2 B	10/07/19	Curium-245/246	0.00229	0.00778	0.00687	U	PCI/G
2 C	10/03/19	Polonium-210	0.554	0.177	0.145		PCI/G
2 C	09/30/19	Thorium-228	1.24	0.225	0.174		PCI/G
2 C	09/30/19	Thorium-229	0.0254	0.0759	0.137	U	PCI/G
2 C	09/30/19	Thorium-230	0.877	0.175	0.0933		PCI/G
2 C	09/30/19	Thorium-232	1.14	0.193	0.0252		PCI/G
2 C	09/28/19	Uranium-232	0.0236	0.0733	0.13	U	PCI/G
2 C	09/28/19	Uranium-233/234	0.896	0.114	0.0612		PCI/G
2 C	09/28/19	Uranium-235/236	0.104	0.0451	0.0499		PCI/G
2 C	09/28/19	Uranium-238	1.03	0.119	0.0425		PCI/G
2 C	10/01/19	Neptunium-236	-0.000023	0.00751	0.0162	U	PCI/G
2 C	10/01/19	Plutonium-236	-0.000023	0.00751	0.0162	U	PCI/G
2 C	10/01/19	Plutonium-239/240	-0.00224	0.00578	0.0157	U	PCI/G
2 C	10/01/19	Plutonium-242	0.00589	0.0105	0.0173	U	PCI/G
2 C	10/01/19	Plutonium-244	0.0011	0.00689	0.013	U	PCI/G
2 C	10/01/19	Neptunium-237	-0.00874	0.00844	0.0296	U	PCI/G
2 C	10/04/19	Plutonium-241	0.155	2.15	3.7	U	PCI/G
2 C	09/26/19	Actinium-225	-1.12	2.1	3.57	U	PCI/G
2 C	09/26/19	Actinium-227	0.0541	0.0692	0.12	U	PCI/G
2 C	09/26/19	Actinium-228	1.76	0.0968	0.0537		PCI/G
2 C	09/26/19	Antimony-125	0.00552	0.0235	0.0398	U	PCI/G
2 C	09/26/19	Barium-137m	0.0444	0.0147	0.014		PCI/G
2 C	09/26/19	Bismuth-212	1.67	0.264	0.196		PCI/G
2 C	09/26/19	Bismuth-213	-0.005	0.0256	0.0428	U	PCI/G
2 C	09/26/19	Bismuth-214	1.43	0.0588	0.0261		PCI/G
2 C	09/26/19	Cesium-134	0	0.0196	0.0237	UI	PCI/G
2 C	09/26/19	Cesium-137	0.0469	0.0156	0.0148		PCI/G

Table B-1. Complete Results from the GEL Laboratory

Sample no.	Analysis date	Parameter	Result	Uncertainty	MDC[a]	Qualifier[b]	Units
2 C	09/26/19	Cobalt-60	0.00102	0.00884	0.0137	U	PCI/G
2 C	09/26/19	Europium-152	-0.0211	0.026	0.0412	U	PCI/G
2 C	09/26/19	Europium-154	-0.00953	0.0303	0.0453	U	PCI/G
2 C	09/26/19	Europium-155	0.0632	0.0418	0.0743	U	PCI/G
2 C	09/26/19	Holmium-166m	0.00911	0.0134	0.0243	U	PCI/G
2 C	09/26/19	Lead-210	2.43	3.96	5.42	U	PCI/G
2 C	09/26/19	Lead-212	1.73	0.0395	0.027		PCI/G
2 C	09/26/19	Lead-214	1.62	0.0621	0.0888		PCI/G
2 C	09/26/19	Neptunium-239	0.089	0.151	0.17	U	PCI/G
2 C	09/26/19	Niobium-94	0.00102	0.00733	0.0131	U	PCI/G
2 C	09/26/19	Potassium-40	22.5	0.474	0.112		PCI/G
2 C	09/26/19	Promethium-147	-298	271	466	U	PCI/G
2 C	09/26/19	Protactinium-231	0	0.203	0.206	UI	PCI/G
2 C	09/26/19	Radium-226	1.43	0.0588	0.0261		PCI/G
2 C	09/26/19	Radium-228	1.76	0.0968	0.0537		PCI/G
2 C	09/26/19	Sodium-22	-0.00322	0.0109	0.0163	U	PCI/G
2 C	09/26/19	Tellurium-125m	-3.46	5.71	9.89	U	PCI/G
2 C	09/26/19	Thallium-208	0.554	0.0269	0.0144		PCI/G
2 C	09/26/19	Thorium-231	-0.126	0.189	0.279	U	PCI/G
2 C	09/26/19	Thorium-234	2.36	1.66	1.35		PCI/G
2 C	09/26/19	Thulium-171	-9.29	14	24.5	U	PCI/G
2 C	09/26/19	Tin-126	0	0.0621	0.0531	UI	PCI/G
2 C	09/28/19	Iodine-129	0.0624	0.394	0.798	U	PCI/G
2 C	10/01/19	Polonium-210	0.763	0.25	0.208		PCI/G
2 C	09/29/19	Thorium-228	1.3	0.188	0.116		PCI/G
2 C	09/29/19	Thorium-229	0.0606	0.0557	0.0812	U	PCI/G
2 C	09/29/19	Thorium-230	0.925	0.157	0.107		PCI/G
2 C	09/29/19	Thorium-232	1.28	0.175	0.0577		PCI/G
2 C	09/28/19	Uranium-232	0.0351	0.0523	0.0886	U	PCI/G
2 C	09/28/19	Uranium-233/234	0.782	0.109	0.0468		PCI/G
2 C	09/28/19	Uranium-235/236	0.0725	0.0403	0.0469		PCI/G
2 C	09/28/19	Uranium-238	0.962	0.119	0.0291		PCI/G
2 C	09/30/19	Neptunium-236	0.00275	0.0124	0.0238	U	PCI/G
2 C	09/30/19	Plutonium-236	0.00275	0.0124	0.0238	U	PCI/G
2 C	09/30/19	Plutonium-239/240	-0.00287	0.0111	0.0245	U	PCI/G
2 C	09/30/19	Plutonium-242	0.000834	0.00809	0.0165	U	PCI/G
2 C	09/30/19	Plutonium-244	0.00275	0.00674	0.0108	U	PCI/G
2 C	10/01/19	Neptunium-237	0.00112	0.0134	0.0279	U	PCI/G
2 C	10/04/19	Plutonium-241	1.17	1.76	2.98	U	PCI/G
2 C	09/26/19	Iron-55	-0.738	2.57	3.93	U	PCI/G
2 C	09/26/19	Nickel-63	0.275	0.447	0.756	U	PCI/G
2 C	09/25/19	Technetium-99	-0.0629	0.287	0.49	U	PCI/G
2 C	09/26/19	Tritium	0.0726	2.03	3.6	U	PCI/G
2 C	09/28/19	Carbon-14	-0.259	1.44	2.54	U	PCI/G
2 C	09/28/19	Strontium-90	0.00637	0.0076	0.0128	U	PCI/G
2 C	09/28/19	Yttrium-90	0.00637	0.0076	0.0128	U	PCI/G
2 C	10/02/19	Nickel-59	-1.17	1.19	1.98	U	PCI/G
2 C	10/05/19	Americium-241	0.00726	0.0159	0.0278	U	PCI/G
2 C	10/05/19	Americium-243	-0.00593	0.0102	0.0243	U	PCI/G
2 C	10/05/19	Curium-243/244	-0.0126	0.0137	0.0319	U	PCI/G
2 C	10/05/19	Curium-245/246	0.0023	0.00779	0.00689	U	PCI/G
3 A	09/26/19	Actinium-225	-0.0316	2.01	2.98	U	PCI/G
3 A	09/26/19	Actinium-227	0.0693	0.0624	0.102	U	PCI/G
3 A	09/26/19	Actinium-228	1.71	0.0796	0.044		PCI/G
3 A	09/26/19	Antimony-125	0.00134	0.0192	0.0332	U	PCI/G
3 A	09/26/19	Barium-137m	0.1	0.012	0.0121		PCI/G
3 A	09/26/19	Bismuth-212	1.8	0.207	0.16		PCI/G
3 A	09/26/19	Bismuth-213	0.0154	0.0233	0.0366	U	PCI/G
3 A	09/26/19	Bismuth-214	1.45	0.0428	0.0231		PCI/G
3 A	09/26/19	Cesium-134	0	0.0164	0.0194	UI	PCI/G
3 A	09/26/19	Cesium-137	0.106	0.0126	0.0128		PCI/G
3 A	09/26/19	Cobalt-60	0.00108	0.00762	0.0132	U	PCI/G

Table B-1. Complete Results from the GEL Laboratory

Sample no.	Analysis date	Parameter	Result	Uncertainty	MDC[a]	Qualifier[b]	Units
3 A	09/26/19	Europium-152	-0.00569	0.0204	0.0354	U	PCI/G
3 A	09/26/19	Europium-154	-0.00224	0.0257	0.0425	U	PCI/G
3 A	09/26/19	Europium-155	0	0.0458	0.0507	UI	PCI/G
3 A	09/26/19	Holmium-166m	0.0072	0.0118	0.0201	U	PCI/G
3 A	09/26/19	Lead-210	2.32	2.83	2.9	U	PCI/G
3 A	09/26/19	Lead-212	1.67	0.0329	0.0237		PCI/G
3 A	09/26/19	Lead-214	1.7	0.0453	0.0823		PCI/G
3 A	09/26/19	Neptunium-239	-0.0277	0.0755	0.125	U	PCI/G
3 A	09/26/19	Niobium-94	0.00325	0.00679	0.0115	U	PCI/G
3 A	09/26/19	Potassium-40	26.3	0.438	0.101		PCI/G
3 A	09/26/19	Promethium-147	-17	215	356	U	PCI/G
3 A	09/26/19	Protactinium-231	0	0.197	0.177	UI	PCI/G
3 A	09/26/19	Radium-226	1.45	0.0428	0.0231		PCI/G
3 A	09/26/19	Radium-228	1.71	0.0796	0.044		PCI/G
3 A	09/26/19	Sodium-22	-0.00064	0.00924	0.0153	U	PCI/G
3 A	09/26/19	Tellurium-125m	3.14	4.34	7.32	U	PCI/G
3 A	09/26/19	Thallium-208	0.51	0.0212	0.0118		PCI/G
3 A	09/26/19	Thorium-231	0.0186	0.151	0.238	U	PCI/G
3 A	09/26/19	Thorium-234	2.07	0.743	0.777		PCI/G
3 A	09/26/19	Thulium-171	1.53	7.68	13.3	U	PCI/G
3 A	09/26/19	Tin-126	0	0.0391	0.0358	UI	PCI/G
3 A	09/28/19	Iodine-129	-0.218	0.76	1.34	U	PCI/G
3 A	10/01/19	Polonium-210	1.75	0.298	0.102		PCI/G
3 A	09/30/19	Thorium-228	1.53	0.214	0.128		PCI/G
3 A	09/30/19	Thorium-229	0.0536	0.067	0.108	U	PCI/G
3 A	09/30/19	Thorium-230	1.24	0.183	0.0823		PCI/G
3 A	09/30/19	Thorium-232	1.32	0.187	0.0737		PCI/G
3 A	10/01/19	Uranium-232	-0.0473	0.0524	0.109	U	PCI/G
3 A	10/01/19	Uranium-233/234	1.17	0.132	0.0464		PCI/G
3 A	10/01/19	Uranium-235/236	0.0832	0.0419	0.0465		PCI/G
3 A	10/01/19	Uranium-238	1.19	0.132	0.0288		PCI/G
3 A	09/30/19	Neptunium-236	-0.0000264	0.0086	0.0186	U	PCI/G
3 A	09/30/19	Plutonium-236	-0.0000264	0.0086	0.0186	U	PCI/G
3 A	09/30/19	Plutonium-239/240	0.00118	0.0132	0.0269	U	PCI/G
3 A	09/30/19	Plutonium-242	-0.000911	0.00434	0.0106	U	PCI/G
3 A	09/30/19	Plutonium-244	0.00763	0.0103	0.00763	X	PCI/G
3 A	10/01/19	Neptunium-237	0.00027	0.0124	0.0273	U	PCI/G
3 A	10/04/19	Plutonium-241	1.83	2.61	4.4	U	PCI/G
3 A	09/26/19	Iron-55	0.158	2.72	4.14	U	PCI/G
3 A	09/26/19	Nickel-63	-0.013	0.473	0.812	U	PCI/G
3 A	09/24/19	Technetium-99	0.379	0.427	0.717	U	PCI/G
3 A	09/27/19	Tritium	0.0247	2.16	3.84	U	PCI/G
3 A	09/27/19	Carbon-14	0.263	1.72	2.97	U	PCI/G
3 A	09/28/19	Strontium-90	0.0114	0.00735	0.012	U	PCI/G
3 A	09/28/19	Yttrium-90	0.0114	0.00735	0.012	U	PCI/G
3 A	10/02/19	Nickel-59	-0.434	0.452	0.707	U	PCI/G
3 A	10/05/19	Americium-241	0.00487	0.0139	0.0249	U	PCI/G
3 A	10/05/19	Americium-243	0.0114	0.0139	0.021	U	PCI/G
3 A	10/05/19	Curium-243/244	0.00161	0.0151	0.0285	U	PCI/G
3 A	10/05/19	Curium-245/246	0	0.00611	0.00662	U	PCI/G
3 B	09/29/19	Iodine-129	0.0496	0.316	0.67	U	PCI/G
3 B	09/29/19	Iodine-129	92.4	2.61	0.907		%
3 B	10/01/19	Iron-55	-0.135	2.73	4.07	U	PCI/G
3 B	09/29/19	Nickel-63	0.0211	0.439	0.754	U	PCI/G
3 B	09/26/19	Actinium-225	-1.89	2.77	4.58	U	PCI/G
3 B	09/26/19	Actinium-227	0.017	0.0917	0.154	U	PCI/G
3 B	09/26/19	Actinium-228	1.86	0.146	0.074		PCI/G
3 B	09/26/19	Antimony-125	0.049	0.0559	0.0557	U	PCI/G
3 B	09/26/19	Barium-137m	0.0479	0.0199	0.0213		PCI/G
3 B	09/26/19	Bismuth-212	1.86	0.453	0.283		PCI/G

Table B-1. Complete Results from the GEL Laboratory

Sample no.	Analysis date	Parameter	Result	Uncertainty	MDC[a]	Qualifier[b]	Units
3 B	09/26/19	Bismuth-213	0.00224	0.034	0.0611	U	PCI/G
3 B	09/26/19	Bismuth-214	1.39	0.0758	0.0388		PCI/G
3 B	09/26/19	Cesium-134	0	0.0229	0.0325	UI	PCI/G
3 B	09/26/19	Cesium-137	0.0506	0.0211	0.0225		PCI/G
3 B	09/26/19	Cobalt-60	0.000699	0.0122	0.022	U	PCI/G
3 B	09/26/19	Europium-152	0.0291	0.0365	0.0576	U	PCI/G
3 B	09/26/19	Europium-154	-0.00958	0.0448	0.0694	U	PCI/G
3 B	09/26/19	Europium-155	0	0.062	0.0634	UI	PCI/G
3 B	09/26/19	Holmium-166m	0.00574	0.0205	0.0362	U	PCI/G
3 B	09/26/19	Lead-210	1.62	0.602	0.447		PCI/G
3 B	09/26/19	Lead-212	1.73	0.0554	0.0348		PCI/G
3 B	09/26/19	Lead-214	1.62	0.082	0.135		PCI/G
3 B	09/26/19	Neptunium-239	-0.0541	0.0963	0.166	U	PCI/G
3 B	09/26/19	Niobium-94	0.00396	0.0122	0.0214	U	PCI/G
3 B	09/26/19	Potassium-40	26.4	0.745	0.18		PCI/G
3 B	09/26/19	Promethium-147	108	280	494	U	PCI/G
3 B	09/26/19	Protactinium-231	0	0.308	0.285	UI	PCI/G
3 B	09/26/19	Radium-226	1.39	0.0758	0.0388		PCI/G
3 B	09/26/19	Radium-228	1.86	0.146	0.074		PCI/G
3 B	09/26/19	Sodium-22	-0.00382	0.0161	0.0249	U	PCI/G
3 B	09/26/19	Tellurium-125m	4.08	5.29	9.43	U	PCI/G
3 B	09/26/19	Thallium-208	0.536	0.0379	0.0209		PCI/G
3 B	09/26/19	Thorium-231	0.0802	0.261	0.401	U	PCI/G
3 B	09/26/19	Thorium-234	1.55	0.573	0.483		PCI/G
3 B	09/26/19	Thulium-171	2.14	4.48	3.93	U	PCI/G
3 B	09/26/19	Tin-126	0	0.0488	0.0397	UI	PCI/G
3 B	09/28/19	Iodine-129	-0.282	0.45	0.687	U	PCI/G
3 B	10/01/19	Polonium-210	1.74	0.322	0.174		PCI/G
3 B	09/30/19	Thorium-228	1.47	0.22	0.134		PCI/G
3 B	09/30/19	Thorium-229	0.0441	0.0814	0.14	U	PCI/G
3 B	09/30/19	Thorium-230	1.3	0.194	0.0702		PCI/G
3 B	09/30/19	Thorium-232	1.25	0.195	0.105		PCI/G
3 B	09/28/19	Uranium-232	-0.031	0.0572	0.117	U	PCI/G
3 B	09/28/19	Uranium-233/234	1.39	0.14	0.0345		PCI/G
3 B	09/28/19	Uranium-235/236	0.0902	0.0381	0.0276		PCI/G
3 B	09/28/19	Uranium-238	1.5	0.145	0.0398		PCI/G
3 B	09/30/19	Neptunium-236	-0.00667	0.00906	0.0235	U	PCI/G
3 B	09/30/19	Plutonium-236	-0.00667	0.00906	0.0235	U	PCI/G
3 B	09/30/19	Plutonium-239/240	0.00258	0.0133	0.0255	U	PCI/G
3 B	09/30/19	Plutonium-242	-0.0000187	0.00608	0.0132	U	PCI/G
3 B	09/30/19	Plutonium-244	0.0108	0.0105	0.0128	U	PCI/G
3 B	10/01/19	Neptunium-237	-0.0029	0.00876	0.0246	U	PCI/G
3 B	10/04/19	Plutonium-241	-0.534	1.84	3.2	U	PCI/G
3 B	09/30/19	Iron-55	-1.51	3.3	4.99	U	PCI/G
3 B	09/28/19	Nickel-63	0.0836	0.436	0.745	U	PCI/G
3 B	09/24/19	Technetium-99	0.413	0.428	0.717	U	PCI/G
3 B	09/27/19	Tritium	-1.72	2.18	4.07	U	PCI/G
3 B	09/27/19	Carbon-14	-0.586	1.67	2.95	U	PCI/G
3 B	09/28/19	Nickel-59	-0.157	0.885	1.57	U	PCI/G
3 B	09/28/19	Strontium-90	0.013	0.00839	0.0138	U	PCI/G
3 B	09/28/19	Yttrium-90	0.013	0.00839	0.0138	U	PCI/G
3 B	10/05/19	Americium-241	0.0126	0.0191	0.031	U	PCI/G
3 B	10/05/19	Americium-243	0.00896	0.0206	0.0362	U	PCI/G
3 B	10/05/19	Curium-243/244	0.00998	0.0155	0.0239	U	PCI/G
3 B	10/05/19	Curium-245/246	0	0.0125	0.0249	U	PCI/G
3 C	09/26/19	Actinium-225	0.385	1.8	3.13	U	PCI/G
3 C	09/26/19	Actinium-227	0.05	0.0877	0.104	U	PCI/G
3 C	09/26/19	Actinium-228	1.91	0.0729	0.0418		PCI/G
3 C	09/26/19	Antimony-125	0.00973	0.0203	0.0345	U	PCI/G
3 C	09/26/19	Barium-137m	0.0113	0.011	0.0118	U	PCI/G
3 C	09/26/19	Bismuth-212	1.81	0.209	0.165		PCI/G
3 C	09/26/19	Bismuth-213	0	0.0456	0.0351	UI	PCI/G

Table B-1. Complete Results from the GEL Laboratory

Sample no.	Analysis date	Parameter	Result	Uncertainty	MDC[a]	Qualifier[b]	Units
3 C	09/26/19	Bismuth-214	1.5	0.041	0.0231		PCI/G
3 C	09/26/19	Cesium-134	0	0.0173	0.0182	UI	PCI/G
3 C	09/26/19	Cesium-137	0.012	0.0116	0.0125	U	PCI/G
3 C	09/26/19	Cobalt-60	-0.00384	0.00835	0.0122	U	PCI/G
3 C	09/26/19	Europium-152	-0.00408	0.0212	0.0361	U	PCI/G
3 C	09/26/19	Europium-154	0.0118	0.0288	0.0406	U	PCI/G
3 C	09/26/19	Europium-155	0	0.0457	0.0483	UI	PCI/G
3 C	09/26/19	Holmium-166m	-0.00966	0.0117	0.0203	U	PCI/G
3 C	09/26/19	Lead-210	2.14	2.16	2.27	U	PCI/G
3 C	09/26/19	Lead-212	1.91	0.0321	0.023		PCI/G
3 C	09/26/19	Lead-214	1.81	0.0447	0.0774		PCI/G
3 C	09/26/19	Neptunium-239	-0.0515	0.0761	0.121	U	PCI/G
3 C	09/26/19	Niobium-94	0.00844	0.012	0.0116	U	PCI/G
3 C	09/26/19	Potassium-40	28.1	0.398	0.0962		PCI/G
3 C	09/26/19	Promethium-147	-93.9	217	347	U	PCI/G
3 C	09/26/19	Protactinium-231	0	0.162	0.177	UI	PCI/G
3 C	09/26/19	Radium-226	1.5	0.041	0.0231		PCI/G
3 C	09/26/19	Radium-228	1.91	0.0729	0.0418		PCI/G
3 C	09/26/19	Sodium-22	0.00445	0.0103	0.0146	U	PCI/G
3 C	09/26/19	Tellurium-125m	4.6	5.05	6.82	U	PCI/G
3 C	09/26/19	Thallium-208	0.577	0.0209	0.0116		PCI/G
3 C	09/26/19	Thorium-231	0.186	0.157	0.245	U	PCI/G
3 C	09/26/19	Thorium-234	2.09	0.69	0.671		PCI/G
3 C	09/26/19	Thulium-171	9.23	9.21	11.2	U	PCI/G
3 C	09/26/19	Tin-126	0	0.0317	0.0328	UI	PCI/G
3 C	09/28/19	Iodine-129	-0.0971	0.693	1.24	U	PCI/G
3 C	10/01/19	Polonium-210	1.3	0.319	0.0599		PCI/G
3 C	09/30/19	Thorium-228	1.43	0.19	0.0966		PCI/G
3 C	09/30/19	Thorium-229	0.0523	0.0693	0.115	U	PCI/G
3 C	09/30/19	Thorium-230	1.44	0.182	0.0641		PCI/G
3 C	09/30/19	Thorium-232	1.25	0.168	0.0442		PCI/G
3 C	09/28/19	Uranium-232	0.00919	0.0637	0.116	U	PCI/G
3 C	09/28/19	Uranium-233/234	1.69	0.167	0.0409		PCI/G
3 C	09/28/19	Uranium-235/236	0.18	0.0605	0.0527		PCI/G
3 C	09/28/19	Uranium-238	1.63	0.166	0.0572		PCI/G
3 C	09/30/19	Neptunium-236	-0.0118	0.00838	0.0265	U	PCI/G
3 C	09/30/19	Plutonium-236	-0.0118	0.00838	0.0265	U	PCI/G
3 C	09/30/19	Plutonium-239/240	-0.0114	0.0107	0.0289	U	PCI/G
3 C	09/30/19	Plutonium-242	-0.00534	0.0109	0.0261	U	PCI/G
3 C	09/30/19	Plutonium-244	0.0133	0.0117	0.012	X	PCI/G
3 C	10/01/19	Neptunium-237	-0.00492	0.00694	0.0227	U	PCI/G
3 C	10/04/19	Plutonium-241	1.08	2.03	3.46	U	PCI/G
3 C	10/01/19	Iron-55	-2.1	2.58	3.93	U	PCI/G
3 C	09/28/19	Nickel-63	-0.137	0.474	0.821	U	PCI/G
3 C	09/24/19	Technetium-99	0.406	0.466	0.783	U	PCI/G
3 C	09/27/19	Tritium	0.44	2.42	4.31	U	PCI/G
3 C	09/27/19	Carbon-14	0.859	1.77	3.03	U	PCI/G
3 C	09/28/19	Nickel-59	-0.548	1.02	1.76	U	PCI/G
3 C	09/25/19	Strontium-90	0.00595	0.008	0.0136	U	PCI/G
3 C	09/25/19	Yttrium-90	0.00595	0.008	0.0136	U	PCI/G
3 C	10/05/19	Americium-241	-0.00212	0.0138	0.0284	U	PCI/G
3 C	10/05/19	Americium-243	0.00837	0.0116	0.016	U	PCI/G
3 C	10/05/19	Curium-243/244	-0.0126	0.0193	0.0416	U	PCI/G
3 C	10/05/19	Curium-245/246	0.00243	0.00825	0.00729	U	PCI/G
4 A	09/27/19	Actinium-225	-1.04	1.71	2.71	U	PCI/G
4 A	09/27/19	Actinium-227	0.022	0.0663	0.0855	U	PCI/G
4 A	09/27/19	Actinium-228	1.4	0.0753	0.0393		PCI/G
4 A	09/27/19	Antimony-125	0.00644	0.0159	0.0276	U	PCI/G
4 A	09/27/19	Barium-137m	0.0561	0.00962	0.0101		PCI/G
4 A	09/27/19	Bismuth-212	1.54	0.198	0.141		PCI/G

Table B-1. Complete Results from the GEL Laboratory

Sample no.	Analysis date	Parameter	Result	Uncertainty	MDC[a]	Qualifier[b]	Units
4 A	09/27/19	Bismuth-213	0.0123	0.0179	0.0313	U	PCI/G
4 A	09/27/19	Bismuth-214	1.06	0.0354	0.0187		PCI/G
4 A	09/27/19	Cesium-134	0	0.0132	0.0164	UI	PCI/G
4 A	09/27/19	Cesium-137	0.0593	0.0102	0.0106		PCI/G
4 A	09/27/19	Cobalt-60	-0.00422	0.00668	0.0112	U	PCI/G
4 A	09/27/19	Europium-152	0.00761	0.0172	0.0303	U	PCI/G
4 A	09/27/19	Europium-154	0.0123	0.0252	0.0387	U	PCI/G
4 A	09/27/19	Europium-155	0	0.0398	0.0442	UI	PCI/G
4 A	09/27/19	Holmium-166m	-0.00505	0.0105	0.0172	U	PCI/G
4 A	09/27/19	Lead-210	0	2.59	2.37	UI	PCI/G
4 A	09/27/19	Lead-212	1.36	0.0274	0.0193		PCI/G
4 A	09/27/19	Lead-214	1.22	0.0387	0.0218		PCI/G
4 A	09/27/19	Neptunium-239	0.0698	0.0856	0.109	U	PCI/G
4 A	09/27/19	Niobium-94	0.00438	0.00576	0.00982	U	PCI/G
4 A	09/27/19	Potassium-40	23.3	0.387	0.0812		PCI/G
4 A	09/27/19	Promethium-147	158	185	312	U	PCI/G
4 A	09/27/19	Protactinium-231	0	0.151	0.147	UI	PCI/G
4 A	09/27/19	Radium-226	1.06	0.0354	0.0187		PCI/G
4 A	09/27/19	Radium-228	1.4	0.0753	0.0393		PCI/G
4 A	09/27/19	Sodium-22	0.00444	0.00906	0.0139	U	PCI/G
4 A	09/27/19	Tellurium-125m	4.14	5.49	6.17	U	PCI/G
4 A	09/27/19	Thallium-208	0.415	0.0178	0.0103		PCI/G
4 A	09/27/19	Thorium-231	0.0693	0.128	0.204	U	PCI/G
4 A	09/27/19	Thorium-234	1.12	0.683	0.648		PCI/G
4 A	09/27/19	Thulium-171	-2.23	6.49	11.2	U	PCI/G
4 A	09/27/19	Tin-126	0	0.0305	0.0304	UI	PCI/G
4 A	09/26/19	Actinium-225	-0.712	1.72	2.92	U	PCI/G
4 A	09/26/19	Actinium-227	0.0022	0.0621	0.095	U	PCI/G
4 A	09/26/19	Actinium-228	1.42	0.0712	0.0421		PCI/G
4 A	09/26/19	Antimony-125	-0.00427	0.0189	0.0317	U	PCI/G
4 A	09/26/19	Barium-137m	0.0566	0.0113	0.0114		PCI/G
4 A	09/26/19	Bismuth-212	1.5	0.172	0.15		PCI/G
4 A	09/26/19	Bismuth-213	0.0318	0.0273	0.0333	U	PCI/G
4 A	09/26/19	Bismuth-214	1.03	0.0324	0.0212		PCI/G
4 A	09/26/19	Cesium-134	0	0.0141	0.0127	UI	PCI/G
4 A	09/26/19	Cesium-137	0.0598	0.012	0.012		PCI/G
4 A	09/26/19	Cobalt-60	0.00351	0.0065	0.0116	U	PCI/G
4 A	09/26/19	Europium-152	-0.0108	0.0209	0.0333	U	PCI/G
4 A	09/26/19	Europium-154	0.00674	0.0227	0.0369	U	PCI/G
4 A	09/26/19	Europium-155	0.0474	0.0357	0.0605	U	PCI/G
4 A	09/26/19	Holmium-166m	-0.00407	0.0106	0.0187	U	PCI/G
4 A	09/26/19	Lead-210	0	3.23	2.61	UI	PCI/G
4 A	09/26/19	Lead-212	1.3	0.0296	0.0218		PCI/G
4 A	09/26/19	Lead-214	1.18	0.0427	0.0251		PCI/G
4 A	09/26/19	Neptunium-239	-0.00554	0.0807	0.14	U	PCI/G
4 A	09/26/19	Niobium-94	0	0.00962	0.0112	UI	PCI/G
4 A	09/26/19	Potassium-40	22	0.381	0.0904		PCI/G
4 A	09/26/19	Promethium-147	-142	227	391	U	PCI/G
4 A	09/26/19	Protactinium-231	0	0.185	0.17	UI	PCI/G
4 A	09/26/19	Radium-226	1.03	0.0324	0.0212		PCI/G
4 A	09/26/19	Radium-228	1.42	0.0712	0.0421		PCI/G
4 A	09/26/19	Sodium-22	0.00288	0.00817	0.0133	U	PCI/G
4 A	09/26/19	Tellurium-125m	5.99	7.11	8.13	U	PCI/G
4 A	09/26/19	Thallium-208	0.445	0.0199	0.0114		PCI/G
4 A	09/26/19	Thorium-231	-0.00201	0.149	0.224	U	PCI/G
4 A	09/26/19	Thorium-234	1.29	0.867	1.07		PCI/G
4 A	09/26/19	Thulium-171	-0.431	12.3	19.6	U	PCI/G
4 A	09/26/19	Tin-126	0	0.0455	0.0435	UI	PCI/G
4 A	09/29/19	Iodine-129	0.031	0.39	0.691	U	PCI/G
4 A	10/01/19	Polonium-210	1.32	0.255	0.0879		PCI/G
4 A	09/30/19	Thorium-228	1.27	0.175	0.11		PCI/G
4 A	09/30/19	Thorium-229	0.0107	0.0663	0.122	U	PCI/G

Table B-1. Complete Results from the GEL Laboratory

Sample no.	Analysis date	Parameter	Result	Uncertainty	MDC[a]	Qualifier[b]	Units
4 A	09/30/19	Thorium-230	0.849	0.137	0.0715		PCI/G
4 A	09/30/19	Thorium-232	1.12	0.157	0.0815		PCI/G
4 A	09/28/19	Uranium-232	0.0549	0.0459	0.07	U	PCI/G
4 A	09/28/19	Uranium-233/234	1.03	0.117	0.0376		PCI/G
4 A	09/28/19	Uranium-235/236	0.102	0.0412	0.0377		PCI/G
4 A	09/28/19	Uranium-238	0.911	0.111	0.0455		PCI/G
4 A	10/01/19	Neptunium-236	0.00231	0.00887	0.0165	U	PCI/G
4 A	10/01/19	Plutonium-236	0.00231	0.00887	0.0165	U	PCI/G
4 A	10/01/19	Plutonium-239/240	0.00663	0.0151	0.0271	U	PCI/G
4 A	10/01/19	Plutonium-242	-0.00502	0.00777	0.0199	U	PCI/G
4 A	10/01/19	Plutonium-244	0.0135	0.0119	0.00674	X	PCI/G
4 A	10/01/19	Neptunium-237	-0.0011	0.0132	0.0297	U	PCI/G
4 A	10/04/19	Plutonium-241	0.763	1.98	3.37	U	PCI/G
4 A	09/30/19	Iron-55	-2.83	3.12	4.85	U	PCI/G
4 A	09/28/19	Nickel-63	-0.217	0.467	0.811	U	PCI/G
4 A	09/24/19	Technetium-99	0.101	0.464	0.786	U	PCI/G
4 A	09/27/19	Tritium	-1.63	2.25	4.33	U	PCI/G
4 A	09/27/19	Carbon-14	-1.09	1.68	3	U	PCI/G
4 A	09/28/19	Nickel-59	0.217	0.328	0.913	U	PCI/G
4 A	10/05/19	Strontium-90	0.0000923	0.00817	0.0147	U	PCI/G
4 A	10/05/19	Yttrium-90	0.0000923	0.00817	0.0147	U	PCI/G
4 A	10/05/19	Americium-241	-0.0124	0.0188	0.042	U	PCI/G
4 A	10/05/19	Americium-243	0.0163	0.0128	0.0139	X	PCI/G
4 A	10/05/19	Curium-243/244	-0.0123	0.0198	0.0435	U	PCI/G
4 A	10/05/19	Curium-245/246	0.00211	0.00715	0.00632	U	PCI/G
4 B	09/26/19	Actinium-225	-0.927	1.75	2.8	U	PCI/G
4 B	09/26/19	Actinium-227	-0.0223	0.0622	0.091	U	PCI/G
4 B	09/26/19	Actinium-228	1.5	0.0729	0.0444		PCI/G
4 B	09/26/19	Antimony-125	0.0164	0.025	0.0307	U	PCI/G
4 B	09/26/19	Barium-137m	0.0263	0.0081	0.0107		PCI/G
4 B	09/26/19	Bismuth-212	1.53	0.177	0.148		PCI/G
4 B	09/26/19	Bismuth-213	-0.00581	0.0188	0.0326	U	PCI/G
4 B	09/26/19	Bismuth-214	1.1	0.0409	0.02		PCI/G
4 B	09/26/19	Cesium-134	0	0.0147	0.0178	UI	PCI/G
4 B	09/26/19	Cesium-137	0.0278	0.00856	0.0113		PCI/G
4 B	09/26/19	Cobalt-60	8.61E-06	0.00662	0.0117	U	PCI/G
4 B	09/26/19	Europium-152	-0.00775	0.0179	0.0312	U	PCI/G
4 B	09/26/19	Europium-154	-0.0167	0.0229	0.0391	U	PCI/G
4 B	09/26/19	Europium-155	0	0.0433	0.0487	UI	PCI/G
4 B	09/26/19	Holmium-166m	-0.00478	0.0105	0.0176	U	PCI/G
4 B	09/26/19	Lead-210	-0.154	2.05	3.49	U	PCI/G
4 B	09/26/19	Lead-212	1.48	0.0289	0.0206		PCI/G
4 B	09/26/19	Lead-214	1.27	0.042	0.0706		PCI/G
4 B	09/26/19	Neptunium-239	0.109	0.0934	0.117	U	PCI/G
4 B	09/26/19	Niobium-94	0.00972	0.00874	0.0108	U	PCI/G
4 B	09/26/19	Potassium-40	24.6	0.423	0.0883		PCI/G
4 B	09/26/19	Promethium-147	34.7	204	340	U	PCI/G
4 B	09/26/19	Protactinium-231	0	0.179	0.157	UI	PCI/G
4 B	09/26/19	Radium-226	1.1	0.0409	0.02		PCI/G
4 B	09/26/19	Radium-228	1.5	0.0729	0.0444		PCI/G
4 B	09/26/19	Sodium-22	-0.00561	0.00823	0.0141	U	PCI/G
4 B	09/26/19	Tellurium-125m	2.85	4.41	6.87	U	PCI/G
4 B	09/26/19	Thallium-208	0.465	0.019	0.0106		PCI/G
4 B	09/26/19	Thorium-231	0.0204	0.136	0.216	U	PCI/G
4 B	09/26/19	Thorium-234	0.903	0.749	0.79		PCI/G
4 B	09/26/19	Thulium-171	-1.63	8.71	14.9	U	PCI/G
4 B	09/26/19	Tin-126	0	0.0311	0.0346	UI	PCI/G
4 B	09/29/19	Iodine-129	0.255	0.344	0.712	U	PCI/G
4 B	10/01/19	Polonium-210	0.934	0.237	0.0459		PCI/G
4 B	09/30/19	Thorium-228	1.31	0.193	0.11		PCI/G

Table B-1. Complete Results from the GEL Laboratory

Sample no.	Analysis date	Parameter	Result	Uncertainty	MDC[a]	Qualifier[b]	Units
4 B	09/30/19	Thorium-229	0.128	0.0689	0.079		PCI/G
4 B	09/30/19	Thorium-230	1.01	0.166	0.0981		PCI/G
4 B	09/30/19	Thorium-232	1.25	0.177	0.0612		PCI/G
4 B	09/28/19	Uranium-232	-0.0527	0.0484	0.105	U	PCI/G
4 B	09/28/19	Uranium-233/234	1.09	0.142	0.0695		PCI/G
4 B	09/28/19	Uranium-235/236	0.164	0.0605	0.056		PCI/G
4 B	09/28/19	Uranium-238	1.09	0.141	0.0608		PCI/G
4 B	10/01/19	Neptunium-236	0.00438	0.00941	0.0155	U	PCI/G
4 B	10/01/19	Plutonium-236	0.00438	0.00941	0.0155	U	PCI/G
4 B	10/01/19	Plutonium-239/240	-0.00111	0.00884	0.02	U	PCI/G
4 B	10/01/19	Plutonium-242	-0.00105	0.00948	0.0208	U	PCI/G
4 B	10/01/19	Plutonium-244	0.00422	0.00907	0.015	U	PCI/G
4 B	10/01/19	Neptunium-237	-0.00366	0.0104	0.0262	U	PCI/G
4 B	10/04/19	Plutonium-241	0.0399	1.65	2.86	U	PCI/G
4 B	09/30/19	Iron-55	-3.02	2.9	4.45	U	PCI/G
4 B	09/28/19	Nickel-63	-0.079	0.408	0.704	U	PCI/G
4 B	09/24/19	Technetium-99	0.493	0.407	0.681	U	PCI/G
4 B	09/27/19	Tritium	-1.22	2.28	4.32	U	PCI/G
4 B	09/27/19	Carbon-14	-0.0924	1.68	2.93	U	PCI/G
4 B	09/29/19	Nickel-59	0.213	0.868	1.61	U	PCI/G
4 B	10/03/19	Strontium-90	-0.00186	0.00842	0.0146	U	PCI/G
4 B	10/03/19	Yttrium-90	-0.00186	0.00842	0.0146	U	PCI/G
4 B	10/05/19	Americium-241	0.00844	0.00993	0.0129	U	PCI/G
4 B	10/05/19	Americium-243	0.00673	0.0198	0.0354	U	PCI/G
4 B	10/05/19	Curium-243/244	0.00837	0.0118	0.0185	U	PCI/G
4 B	10/05/19	Curium-245/246	0.0117	0.0108	0.00586	X	PCI/G
4 C	09/26/19	Actinium-225	-0.214	2.02	2.65	U	PCI/G
4 C	09/26/19	Actinium-227	0.000144	0.053	0.0858	U	PCI/G
4 C	09/26/19	Actinium-228	1.6	0.0676	0.0359		PCI/G
4 C	09/26/19	Antimony-125	0.00293	0.0156	0.0273	U	PCI/G
4 C	09/26/19	Barium-137m	0.0118	0.0103	0.00941		PCI/G
4 C	09/26/19	Bismuth-212	1.59	0.188	0.131		PCI/G
4 C	09/26/19	Bismuth-213	0	0.0254	0.03	UI	PCI/G
4 C	09/26/19	Bismuth-214	1.12	0.0374	0.0179		PCI/G
4 C	09/26/19	Cesium-134	0	0.014	0.0157	UI	PCI/G
4 C	09/26/19	Cesium-137	0.0125	0.0109	0.00994		PCI/G
4 C	09/26/19	Cobalt-60	-0.00452	0.00595	0.0101	U	PCI/G
4 C	09/26/19	Europium-152	-0.012	0.017	0.0297	U	PCI/G
4 C	09/26/19	Europium-154	-0.000789	0.0217	0.0366	U	PCI/G
4 C	09/26/19	Europium-155	0	0.0499	0.0438	UI	PCI/G
4 C	09/26/19	Holmium-166m	0.017	0.0128	0.0175	U	PCI/G
4 C	09/26/19	Lead-210	1.14	1.65	2.88	U	PCI/G
4 C	09/26/19	Lead-212	1.61	0.0297	0.0197		PCI/G
4 C	09/26/19	Lead-214	1.33	0.0409	0.0221		PCI/G
4 C	09/26/19	Neptunium-239	0.0944	0.0868	0.108	U	PCI/G
4 C	09/26/19	Niobium-94	0.00425	0.00539	0.00935	U	PCI/G
4 C	09/26/19	Potassium-40	24.5	0.394	0.079		PCI/G
4 C	09/26/19	Promethium-147	111	185	315	U	PCI/G
4 C	09/26/19	Protactinium-231	0	0.132	0.148	UI	PCI/G
4 C	09/26/19	Radium-226	1.12	0.0374	0.0179		PCI/G
4 C	09/26/19	Radium-228	1.6	0.0676	0.0359		PCI/G
4 C	09/26/19	Sodium-22	6.47E-06	0.00782	0.0132	U	PCI/G
4 C	09/26/19	Tellurium-125m	2.6	4.99	6.13	U	PCI/G
4 C	09/26/19	Thallium-208	0.467	0.0186	0.00992		PCI/G
4 C	09/26/19	Thorium-231	-0.0644	0.126	0.199	U	PCI/G
4 C	09/26/19	Thorium-234	1.05	0.562	0.665		PCI/G
4 C	09/26/19	Thulium-171	10.7	10.6	12.1	U	PCI/G
4 C	09/26/19	Tin-126	0	0.0339	0.0301	UI	PCI/G
4 C	09/29/19	Iodine-129	0.062	0.674	1.21	U	PCI/G
4 C	10/01/19	Polonium-210	0.848	0.215	0.0417		PCI/G
4 C	09/30/19	Thorium-228	1.31	0.218	0.192		PCI/G
4 C	09/30/19	Thorium-229	0.0697	0.104	0.177	U	PCI/G

Table B-1. Complete Results from the GEL Laboratory

Sample no.	Analysis date	Parameter	Result	Uncertainty	MDC[a]	Qualifier[b]	Units
4 C	09/30/19	Thorium-230	1.06	0.181	0.128		PCI/G
4 C	09/30/19	Thorium-232	1.18	0.199	0.169		PCI/G
4 C	09/28/19	Uranium-232	-0.037	0.0352	0.0765	U	PCI/G
4 C	09/28/19	Uranium-233/234	0.929	0.108	0.0392		PCI/G
4 C	09/28/19	Uranium-235/236	0.125	0.0447	0.0428		PCI/G
4 C	09/28/19	Uranium-238	0.895	0.108	0.0488		PCI/G
4 C	10/01/19	Neptunium-236	-0.00219	0.00761	0.0187	U	PCI/G
4 C	10/01/19	Plutonium-236	-0.00219	0.00761	0.0187	U	PCI/G
4 C	10/01/19	Plutonium-239/240	-0.00941	0.00911	0.0259	U	PCI/G
4 C	10/01/19	Plutonium-242	-0.00119	0.00949	0.0214	U	PCI/G
4 C	10/01/19	Plutonium-244	-0.0000207	0.00673	0.0146	U	PCI/G
4 C	10/01/19	Neptunium-237	-0.00232	0.0103	0.0268	U	PCI/G
4 C	10/04/19	Plutonium-241	0.196	1.8	3.11	U	PCI/G
4 C	09/30/19	Iron-55	-0.435	3.02	4.49	U	PCI/G
4 C	09/28/19	Nickel-63	0.209	0.437	0.743	U	PCI/G
4 C	09/25/19	Technetium-99	0.37	0.395	0.663	U	PCI/G
4 C	09/27/19	Tritium	-0.223	2.45	4.47	U	PCI/G
4 C	09/27/19	Carbon-14	-1.15	1.63	2.92	U	PCI/G
4 C	09/29/19	Nickel-59	0.374	1.22	2.24	U	PCI/G
4 C	09/26/19	Strontium-90	0.00113	0.00741	0.0128	U	PCI/G
4 C	09/26/19	Yttrium-90	0.00113	0.00741	0.0128	U	PCI/G
4 C	10/05/19	Americium-241	-0.00693	0.0127	0.028	U	PCI/G
4 C	10/05/19	Americium-243	-0.014	0.0174	0.0377	U	PCI/G
4 C	10/05/19	Curium-243/244	-0.00687	0.00952	0.023	U	PCI/G
4 C	10/05/19	Curium-245/246	3.38E-10	0.00795	0.0155	U	PCI/G
5 A	10/08/19	Strontium-90	0.0163	0.00605	0.00937		PCI/G
5 A	10/08/19	Yttrium-90	0.0163	0.00605	0.00937		PCI/G
5 A	09/27/19	Actinium-225	-1.73	2	3.48	U	PCI/G
5 A	09/27/19	Actinium-227	0.0889	0.0952	0.114	U	PCI/G
5 A	09/27/19	Actinium-228	1.73	0.0823	0.0489		PCI/G
5 A	09/27/19	Antimony-125	0.00342	0.0204	0.0348	U	PCI/G
5 A	09/27/19	Barium-137m	0.29	0.0154	0.0124		PCI/G
5 A	09/27/19	Bismuth-212	1.86	0.22	0.168		PCI/G
5 A	09/27/19	Bismuth-213	0.0068	0.0239	0.0406	U	PCI/G
5 A	09/27/19	Bismuth-214	1.31	0.0394	0.024		PCI/G
5 A	09/27/19	Cesium-134	0	0.0167	0.0202	UI	PCI/G
5 A	09/27/19	Cesium-137	0.306	0.0163	0.013		PCI/G
5 A	09/27/19	Cobalt-60	-0.0028	0.00796	0.0133	U	PCI/G
5 A	09/27/19	Europium-152	0.00411	0.0247	0.038	U	PCI/G
5 A	09/27/19	Europium-154	-0.00805	0.0272	0.0454	U	PCI/G
5 A	09/27/19	Europium-155	0	0.0487	0.0546	UI	PCI/G
5 A	09/27/19	Holmium-166m	0.00762	0.0121	0.0217	U	PCI/G
5 A	09/27/19	Lead-210	4.22	3.67	4.4	U	PCI/G
5 A	09/27/19	Lead-212	1.75	0.0344	0.0248		PCI/G
5 A	09/27/19	Lead-214	1.51	0.0499	0.0806		PCI/G
5 A	09/27/19	Neptunium-239	0.0213	0.09	0.136	U	PCI/G
5 A	09/27/19	Niobium-94	0.00482	0.00697	0.0125	U	PCI/G
5 A	09/27/19	Potassium-40	25.6	0.452	0.1		PCI/G
5 A	09/27/19	Promethium-147	36.2	239	392	U	PCI/G
5 A	09/27/19	Protactinium-231	0	0.187	0.188	UI	PCI/G
5 A	09/27/19	Radium-226	1.31	0.0394	0.024		PCI/G
5 A	09/27/19	Radium-228	1.73	0.0823	0.0489		PCI/G
5 A	09/27/19	Sodium-22	0.00122	0.00963	0.0163	U	PCI/G
5 A	09/27/19	Tellurium-125m	0	6.75	7.72	UI	PCI/G
5 A	09/27/19	Thallium-208	0.52	0.0218	0.0127		PCI/G
5 A	09/27/19	Thorium-231	0.0482	0.168	0.261	U	PCI/G
5 A	09/27/19	Thorium-234	2.11	1.03	0.899		PCI/G
5 A	09/27/19	Thulium-171	0.29	10.7	18.1	U	PCI/G
5 A	09/27/19	Tin-126	0	0.0457	0.0391	UI	PCI/G
5 A	09/29/19	Iodine-129	0.221	0.267	0.663	U	PCI/G

Table B-1. Complete Results from the GEL Laboratory

Sample no.	Analysis date	Parameter	Result	Uncertainty	MDC[a]	Qualifier[b]	Units
5 A	10/01/19	Polonium-210	1.58	0.307	0.147		PCI/G
5 A	10/02/19	Thorium-228	1.54	0.21	0.156		PCI/G
5 A	10/02/19	Thorium-229	2.68E-08	0.0874	0.162	U	PCI/G
5 A	10/02/19	Thorium-230	1.09	0.172	0.132		PCI/G
5 A	10/02/19	Thorium-232	1.3	0.181	0.109		PCI/G
5 A	09/28/19	Uranium-232	0.011	0.0447	0.081	U	PCI/G
5 A	09/28/19	Uranium-233/234	1.13	0.142	0.0809		PCI/G
5 A	09/28/19	Uranium-235/236	0.0849	0.0526	0.072		PCI/G
5 A	09/28/19	Uranium-238	0.961	0.13	0.0718		PCI/G
5 A	10/02/19	Neptunium-236	-0.00501	0.00619	0.0187	U	PCI/G
5 A	10/02/19	Plutonium-236	-0.00501	0.00619	0.0187	U	PCI/G
5 A	10/02/19	Plutonium-239/240	0.0104	0.013	0.0202	U	PCI/G
5 A	10/02/19	Plutonium-242	-0.00666	0.00904	0.0234	U	PCI/G
5 A	10/02/19	Plutonium-244	0.00574	0.00773	0.00574	X	PCI/G
5 A	10/01/19	Neptunium-237	0.00475	0.0149	0.0279	U	PCI/G
5 A	10/04/19	Plutonium-241	0.00663	1.83	3.16	U	PCI/G
5 A	09/30/19	Iron-55	2.38	3.23	4.71	U	PCI/G
5 A	09/28/19	Nickel-63	0.14	0.436	0.743	U	PCI/G
5 A	09/25/19	Technetium-99	0.0796	0.441	0.748	U	PCI/G
5 A	09/27/19	Tritium	-0.954	2.39	4.47	U	PCI/G
5 A	09/27/19	Carbon-14	-1.03	1.6	2.85	U	PCI/G
5 A	09/29/19	Nickel-59	0.214	0.381	0.981	U	PCI/G
5 A	10/05/19	Americium-241	1.91E-09	0.014	0.0276	U	PCI/G
5 A	10/05/19	Americium-243	-0.0237	0.0217	0.047	U	PCI/G
5 A	10/05/19	Curium-243/244	0.00949	0.0144	0.0234	U	PCI/G
5 A	10/05/19	Curium-245/246	0.00635	0.0125	0.0203	U	PCI/G
5 A	10/08/19	Strontium-90	0.0248	0.00693	0.0103		PCI/G
5 A	10/08/19	Yttrium-90	0.0248	0.00693	0.0103		PCI/G
5 B	10/06/19	Americium-241	0.0018	0.0106	0.0199	U	PCI/G
5 B	10/06/19	Americium-243	0.00466	0.0133	0.0238	U	PCI/G
5 B	10/06/19	Curium-243/244	0.00358	0.00701	0.00536	U	PCI/G
5 B	10/06/19	Curium-245/246	0.00361	0.00867	0.0138	U	PCI/G
5 B	09/27/19	Actinium-225	0.0901	1.99	3.24	U	PCI/G
5 B	09/27/19	Actinium-227	0.06	0.0661	0.101	U	PCI/G
5 B	09/27/19	Actinium-228	1.99	0.0841	0.0401		PCI/G
5 B	09/27/19	Antimony-125	-0.00292	0.018	0.0312	U	PCI/G
5 B	09/27/19	Barium-137m	0.104	0.0116	0.0111		PCI/G
5 B	09/27/19	Bismuth-212	1.93	0.194	0.162		PCI/G
5 B	09/27/19	Bismuth-213	0.0221	0.0199	0.0355	U	PCI/G
5 B	09/27/19	Bismuth-214	1.33	0.0406	0.021		PCI/G
5 B	09/27/19	Cesium-134	0	0.0142	0.0185	UI	PCI/G
5 B	09/27/19	Cesium-137	0.109	0.0122	0.0117		PCI/G
5 B	09/27/19	Cobalt-60	0.0017	0.00714	0.0126	U	PCI/G
5 B	09/27/19	Europium-152	-0.00267	0.0197	0.0347	U	PCI/G
5 B	09/27/19	Europium-154	-0.0174	0.0275	0.0409	U	PCI/G
5 B	09/27/19	Europium-155	0	0.0514	0.0501	UI	PCI/G
5 B	09/27/19	Holmium-166m	0.00545	0.0113	0.0194	U	PCI/G
5 B	09/27/19	Lead-210	2.41	2.68	3.22	U	PCI/G
5 B	09/27/19	Lead-212	2.02	0.0349	0.0227		PCI/G
5 B	09/27/19	Lead-214	1.65	0.0453	0.0253		PCI/G
5 B	09/27/19	Neptunium-239	0.0318	0.0747	0.127	U	PCI/G
5 B	09/27/19	Niobium-94	0	0.00923	0.0112	UI	PCI/G
5 B	09/27/19	Potassium-40	27.8	0.44	0.0885		PCI/G
5 B	09/27/19	Promethium-147	97.8	210	356	U	PCI/G
5 B	09/27/19	Protactinium-231	0	0.156	0.173	UI	PCI/G
5 B	09/27/19	Radium-226	1.33	0.0406	0.021		PCI/G
5 B	09/27/19	Radium-228	1.99	0.0841	0.0401		PCI/G
5 B	09/27/19	Sodium-22	-0.00653	0.00987	0.0147	U	PCI/G
5 B	09/27/19	Tellurium-125m	4.83	4.56	7.25	U	PCI/G
5 B	09/27/19	Thallium-208	0.571	0.0209	0.0117		PCI/G
5 B	09/27/19	Thorium-231	0.0524	0.146	0.235	U	PCI/G
5 B	09/27/19	Thorium-234	1.27	0.815	0.768		PCI/G

Table B-1. Complete Results from the GEL Laboratory

Sample no.	Analysis date	Parameter	Result	Uncertainty	MDC[a]	Qualifier[b]	Units
5 B	09/27/19	Thulium-171	1.96	7.97	14	U	PCI/G
5 B	09/27/19	Tin-126	0	0.0398	0.0347	UI	PCI/G
5 B	09/29/19	Iodine-129	0.0399	0.309	0.64	U	PCI/G
5 B	10/01/19	Polonium-210	0.692	0.205	0.134		PCI/G
5 B	09/30/19	Thorium-228	1.9	0.233	0.134		PCI/G
5 B	09/30/19	Thorium-229	0.129	0.0873	0.127		PCI/G
5 B	09/30/19	Thorium-230	1.08	0.173	0.109		PCI/G
5 B	09/30/19	Thorium-232	1.33	0.187	0.092		PCI/G
5 B	10/01/19	Uranium-232	0.0505	0.0374	0.0519	U	PCI/G
5 B	10/01/19	Uranium-233/234	0.917	0.129	0.0504		PCI/G
5 B	10/01/19	Uranium-235/236	0.0366	0.0335	0.0438	U	PCI/G
5 B	10/01/19	Uranium-238	1.18	0.145	0.0437		PCI/G
5 B	10/01/19	Neptunium-236	-0.00319	0.00769	0.0197	U	PCI/G
5 B	10/01/19	Plutonium-236	-0.00319	0.00769	0.0197	U	PCI/G
5 B	10/01/19	Plutonium-239/240	0.00295	0.0112	0.0213	U	PCI/G
5 B	10/01/19	Plutonium-242	-0.0174	0.0121	0.0339	U	PCI/G
5 B	10/01/19	Plutonium-244	0.00403	0.00712	0.00604	U	PCI/G
5 B	10/01/19	Neptunium-237	0.00185	0.013	0.0268	U	PCI/G
5 B	10/04/19	Plutonium-241	1.15	2.01	3.4	U	PCI/G
5 B	10/01/19	Iron-55	-2.35	2.56	3.81	U	PCI/G
5 B	09/28/19	Nickel-63	0.51	0.481	0.805	U	PCI/G
5 B	09/25/19	Technetium-99	0.629	0.411	0.685	U	PCI/G
5 B	09/27/19	Tritium	-1.11	2.45	4.6	U	PCI/G
5 B	09/27/19	Carbon-14	-0.445	1.69	2.97	U	PCI/G
5 B	09/30/19	Nickel-59	-0.193	1.1	1.96	U	PCI/G
5 B	10/03/19	Strontium-90	0.0122	0.00909	0.015	U	PCI/G
5 B	10/03/19	Yttrium-90	0.0122	0.00909	0.015	U	PCI/G
5 B	10/05/19	Americium-241	0.0126	0.0175	0.029	U	PCI/G
5 B	10/05/19	Americium-243	-0.0204	0.0202	0.0442	U	PCI/G
5 B	10/05/19	Curium-243/244	0.00312	0.0137	0.0252	U	PCI/G
5 B	10/05/19	Curium-245/246	7.18E-10	0.0103	0.0206	U	PCI/G
5 C	09/26/19	Actinium-225	-0.637	2.09	3.64	U	PCI/G
5 C	09/26/19	Actinium-227	0.0215	0.075	0.131	U	PCI/G
5 C	09/26/19	Actinium-228	1.55	0.16	0.0736		PCI/G
5 C	09/26/19	Antimony-125	0.0011	0.0298	0.0495	U	PCI/G
5 C	09/26/19	Barium-137m	0.0336	0.0199	0.0196		PCI/G
5 C	09/26/19	Bismuth-212	1.97	0.405	0.27		PCI/G
5 C	09/26/19	Bismuth-213	0.0182	0.0344	0.0583	U	PCI/G
5 C	09/26/19	Bismuth-214	1.17	0.0705	0.0377		PCI/G
5 C	09/26/19	Cesium-134	0	0.0293	0.0367	UI	PCI/G
5 C	09/26/19	Cesium-137	0.0355	0.0211	0.0207		PCI/G
5 C	09/26/19	Cobalt-60	-0.00535	0.0132	0.023	U	PCI/G
5 C	09/26/19	Europium-152	-0.00213	0.0301	0.0508	U	PCI/G
5 C	09/26/19	Europium-154	-0.0114	0.0447	0.0788	U	PCI/G
5 C	09/26/19	Europium-155	0	0.0505	0.0469	UI	PCI/G
5 C	09/26/19	Holmium-166m	-0.0099	0.0204	0.035	U	PCI/G
5 C	09/26/19	Lead-210	1.01	0.434	0.344		PCI/G
5 C	09/26/19	Lead-212	1.46	0.0431	0.029		PCI/G
5 C	09/26/19	Lead-214	1.15	0.0642	0.0376		PCI/G
5 C	09/26/19	Neptunium-239	0	0.148	0.124	UI	PCI/G
5 C	09/26/19	Niobium-94	0.0131	0.0112	0.0208	U	PCI/G
5 C	09/26/19	Potassium-40	20	0.708	0.184		PCI/G
5 C	09/26/19	Promethium-147	5.91	235	362	U	PCI/G
5 C	09/26/19	Protactinium-231	0	0.286	0.223	UI	PCI/G
5 C	09/26/19	Radium-226	1.17	0.0705	0.0377		PCI/G
5 C	09/26/19	Radium-228	1.55	0.16	0.0736		PCI/G
5 C	09/26/19	Sodium-22	-0.00376	0.0161	0.0284	U	PCI/G
5 C	09/26/19	Tellurium-125m	4.63	6.42	6.6	U	PCI/G
5 C	09/26/19	Thallium-208	0.478	0.0329	0.0196		PCI/G
5 C	09/26/19	Thorium-231	0.0283	0.207	0.327	U	PCI/G

Table B-1. Complete Results from the GEL Laboratory

Sample no.	Analysis date	Parameter	Result	Uncertainty	MDC[a]	Qualifier[b]	Units
5 C	09/26/19	Thorium-234	1.2	0.458	0.341		PCI/G
5 C	09/26/19	Thulium-171	0	2.68	2.91	UI	PCI/G
5 C	09/26/19	Tin-126	0	0.0314	0.0252	UI	PCI/G
5 C	09/29/19	Iodine-129	0.0919	0.206	0.606	U	PCI/G
5 C	10/01/19	Polonium-210	0.797	0.223	0.131		PCI/G
5 C	09/30/19	Thorium-228	1.55	0.204	0.0904		PCI/G
5 C	09/30/19	Thorium-229	0.0316	0.0541	0.0911	U	PCI/G
5 C	09/30/19	Thorium-230	1.26	0.179	0.0777		PCI/G
5 C	09/30/19	Thorium-232	1.33	0.184	0.0775		PCI/G
5 C	10/01/19	Uranium-232	0.0128	0.0426	0.0763	U	PCI/G
5 C	10/01/19	Uranium-233/234	1.13	0.152	0.0757		PCI/G
5 C	10/01/19	Uranium-235/236	0.0546	0.0505	0.0759	U	PCI/G
5 C	10/01/19	Uranium-238	1.12	0.152	0.0799		PCI/G
5 C	10/01/19	Neptunium-236	-0.00487	0.00601	0.0182	U	PCI/G
5 C	10/01/19	Plutonium-236	-0.00487	0.00601	0.0182	U	PCI/G
5 C	10/01/19	Plutonium-239/240	0.0102	0.00999	0.0109	U	PCI/G
5 C	10/01/19	Plutonium-242	0.00083	0.0161	0.0318	U	PCI/G
5 C	10/01/19	Plutonium-244	0.00744	0.00836	0.00558	X	PCI/G
5 C	10/01/19	Neptunium-237	-0.00259	0.0111	0.0271	U	PCI/G
5 C	10/04/19	Plutonium-241	0.28	1.86	3.21	U	PCI/G
5 C	09/30/19	Iron-55	-1.65	3.17	4.85	U	PCI/G
5 C	09/28/19	Nickel-63	0.018	0.468	0.804	U	PCI/G
5 C	09/25/19	Technetium-99	0.396	0.423	0.711	U	PCI/G
5 C	09/27/19	Tritium	-1.31	2.4	4.54	U	PCI/G
5 C	09/27/19	Carbon-14	1.5	1.75	2.94	U	PCI/G
5 C	09/30/19	Nickel-59	0.137	0.476	1.08	U	PCI/G
5 C	10/05/19	Americium-241	-0.00885	0.0159	0.0339	U	PCI/G
5 C	10/05/19	Americium-243	0.0092	0.0247	0.044	U	PCI/G
5 C	10/05/19	Curium-243/244	-0.00527	0.015	0.0311	U	PCI/G
5 C	10/05/19	Curium-245/246	0.00267	0.0117	0.0204	U	PCI/G
5 C	10/08/19	Strontium-90	0.0167	0.00802	0.0129		PCI/G
5 C	10/08/19	Yttrium-90	0.0167	0.00802	0.0129		PCI/G
6 A	09/30/19	Polonium-210	1.85	0.329	0.0452		PCI/G
6 A	10/01/19	Thorium-228	0.64	0.149	0.135		PCI/G
6 A	10/01/19	Thorium-229	0.0527	0.0578	0.0884	U	PCI/G
6 A	10/01/19	Thorium-230	0.802	0.155	0.117		PCI/G
6 A	10/01/19	Thorium-232	0.492	0.116	0.0628		PCI/G
6 A	09/29/19	Uranium-232	0.0582	0.0487	0.0741	U	PCI/G
6 A	09/29/19	Uranium-233/234	0.547	0.0903	0.0482		PCI/G
6 A	09/29/19	Uranium-235/236	0.018	0.0274	0.0444	U	PCI/G
6 A	09/29/19	Uranium-238	0.482	0.0868	0.0581		PCI/G
6 A	09/28/19	Neptunium-236	-0.00377	0.00691	0.0152	U	PCI/G
6 A	09/28/19	Plutonium-236	-0.00377	0.00691	0.0152	U	PCI/G
6 A	09/28/19	Plutonium-239/240	0.00273	0.00735	0.0131	U	PCI/G
6 A	09/28/19	Plutonium-242	0.00518	0.0095	0.0159	U	PCI/G
6 A	09/28/19	Plutonium-244	0.00364	0.00617	0.0101	U	PCI/G
6 A	09/30/19	Neptunium-237	-0.00346	0.00642	0.0175	U	PCI/G
6 A	10/03/19	Plutonium-241	1.38	1.66	2.79	U	PCI/G
6 A	09/14/19	Actinium-225	-0.294	0.581	0.936	U	PCI/G
6 A	09/14/19	Actinium-227	0.0302	0.0454	0.0688	U	PCI/G
6 A	09/14/19	Actinium-228	0.631	0.0493	0.0347		PCI/G
6 A	09/14/19	Antimony-125	0.00232	0.0125	0.0221	U	PCI/G
6 A	09/14/19	Barium-137m	0.0299	0.00797	0.00834		PCI/G
6 A	09/14/19	Bismuth-212	0.568	0.134	0.115		PCI/G
6 A	09/14/19	Bismuth-213	0.0122	0.0152	0.0248	U	PCI/G
6 A	09/14/19	Bismuth-214	0.617	0.0279	0.0155		PCI/G
6 A	09/14/19	Cesium-134	0	0.00706	0.0121	UI	PCI/G
6 A	09/14/19	Cesium-137	0.0316	0.00842	0.00881		PCI/G
6 A	09/14/19	Cobalt-60	0.0000405	0.00534	0.00961	U	PCI/G
6 A	09/14/19	Europium-152	0.00186	0.0138	0.0235	U	PCI/G
6 A	09/14/19	Europium-154	-0.00194	0.0208	0.0344	U	PCI/G
6 A	09/14/19	Europium-155	0	0.0317	0.036	UI	PCI/G

Table B-1. Complete Results from the GEL Laboratory

Sample no.	Analysis date	Parameter	Result	Uncertainty	MDC[a]	Qualifier[b]	Units
6 A	09/14/19	Holmium-166m	-0.00541	0.00833	0.0141	U	PCI/G
6 A	09/14/19	Lead-210	0.839	1.39	1.69	U	PCI/G
6 A	09/14/19	Lead-212	0.603	0.0193	0.0152		PCI/G
6 A	09/14/19	Lead-214	0.707	0.0284	0.0176		PCI/G
6 A	09/14/19	Neptunium-239	-0.0288	0.0529	0.0873	U	PCI/G
6 A	09/14/19	Niobium-94	0.000819	0.00464	0.00805	U	PCI/G
6 A	09/14/19	Potassium-40	32	0.422	0.0691		PCI/G
6 A	09/14/19	Promethium-147	-4.46	150	249	U	PCI/G
6 A	09/14/19	Protactinium-231	0	0.13	0.111	UI	PCI/G
6 A	09/14/19	Radium-226	0.617	0.0279	0.0155		PCI/G
6 A	09/14/19	Radium-228	0.631	0.0493	0.0347		PCI/G
6 A	09/14/19	Sodium-22	-0.00299	0.0075	0.0123	U	PCI/G
6 A	09/14/19	Tellurium-125m	1.55	2.85	4.44	U	PCI/G
6 A	09/14/19	Thallium-208	0.189	0.0139	0.00812		PCI/G
6 A	09/14/19	Thorium-231	-0.0673	0.0982	0.155	U	PCI/G
6 A	09/14/19	Thorium-234	0	0.543	0.523	UI	PCI/G
6 A	09/14/19	Thulium-171	0.501	5.05	8.51	U	PCI/G
6 A	09/14/19	Tin-126	0	0.0243	0.0251	UI	PCI/G
6 A	09/30/19	Iodine-129	0.214	0.458	0.527	U	PCI/G
6 A	09/25/19	Technetium-99	-0.0394	0.289	0.493	U	PCI/G
6 A	09/28/19	Strontium-90	0.00545	0.00871	0.0148	U	PCI/G
6 A	09/28/19	Yttrium-90	0.00545	0.00871	0.0148	U	PCI/G
6 A	09/27/19	Nickel-63	-0.0179	0.305	0.522	U	PCI/G
6 A	09/28/19	Iron-55	1.23	2.75	3.96	U	PCI/G
6 A	09/28/19	Tritium	-0.296	2.06	3.62	U	PCI/G
6 A	09/26/19	Carbon-14	0.974	1.41	2.39	U	PCI/G
6 A	09/26/19	Nickel-59	0.0341	0.281	0.594	U	PCI/G
6 A	10/03/19	Americium-241	0.0122	0.02	0.0329	U	PCI/G
6 A	10/03/19	Americium-243	-0.00751	0.0289	0.0604	U	PCI/G
6 A	10/03/19	Curium-243/244	0.00343	0.0132	0.0245	U	PCI/G
6 A	10/03/19	Curium-245/246	0.00407	0.0156	0.029	U	PCI/G
6 B	09/30/19	Polonium-210	1.24	0.28	0.154		PCI/G
6 B	10/01/19	Thorium-228	1.05	0.201	0.165		PCI/G
6 B	10/01/19	Thorium-229	0.0772	0.0801	0.125	U	PCI/G
6 B	10/01/19	Thorium-230	1.25	0.197	0.0852		PCI/G
6 B	10/01/19	Thorium-232	0.906	0.165	0.023		PCI/G
6 B	09/30/19	Uranium-232	-0.0377	0.0379	0.0809	U	PCI/G
6 B	09/30/19	Uranium-233/234	1.03	0.117	0.053		PCI/G
6 B	09/30/19	Uranium-235/236	0.069	0.0359	0.0404		PCI/G
6 B	09/30/19	Uranium-238	0.996	0.115	0.053		PCI/G
6 B	09/28/19	Neptunium-236	-0.00426	0.0059	0.0143	U	PCI/G
6 B	09/28/19	Plutonium-236	-0.00426	0.0059	0.0143	U	PCI/G
6 B	09/28/19	Plutonium-239/240	0.00308	0.00668	0.0114	U	PCI/G
6 B	09/28/19	Plutonium-242	0.00105	0.0107	0.0201	U	PCI/G
6 B	09/28/19	Plutonium-244	0.00616	0.00637	0.00786	U	PCI/G
6 B	09/30/19	Neptunium-237	0.00304	0.00655	0.00981	U	PCI/G
6 B	10/03/19	Plutonium-241	-0.141	2.03	3.5	U	PCI/G
6 B	09/18/19	Actinium-225	-0.169	0.735	1.08	U	PCI/G
6 B	09/18/19	Actinium-227	-0.00883	0.0377	0.0597	U	PCI/G
6 B	09/18/19	Actinium-228	0.896	0.0481	0.0327		PCI/G
6 B	09/18/19	Antimony-125	0.0142	0.012	0.0207	U	PCI/G
6 B	09/18/19	Barium-137m	0.0618	0.00841	0.00746		PCI/G
6 B	09/18/19	Bismuth-212	0.897	0.121	0.108		PCI/G
6 B	09/18/19	Bismuth-213	0.0186	0.0148	0.023	U	PCI/G
6 B	09/18/19	Bismuth-214	0.942	0.0255	0.014		PCI/G
6 B	09/18/19	Cesium-134	0	0.0119	0.011	UI	PCI/G
6 B	09/18/19	Cesium-137	0.0653	0.00888	0.00788		PCI/G
6 B	09/18/19	Cobalt-60	0.00293	0.00573	0.0101	U	PCI/G
6 B	09/18/19	Europium-152	-0.00506	0.0123	0.0211	U	PCI/G
6 B	09/18/19	Europium-154	0.000275	0.0213	0.0336	U	PCI/G

Table B-1. Complete Results from the GEL Laboratory

Sample no.	Analysis date	Parameter	Result	Uncertainty	MDC[a]	Qualifier[b]	Units
6 B	09/18/19	Europium-155	0	0.0275	0.0291	UI	PCI/G
6 B	09/18/19	Holmium-166m	-0.00186	0.00772	0.0133	U	PCI/G
6 B	09/18/19	Lead-210	2.17	1.94	3.53	U	PCI/G
6 B	09/18/19	Lead-212	0.886	0.0171	0.0133		PCI/G
6 B	09/18/19	Lead-214	1.11	0.0269	0.0452		PCI/G
6 B	09/18/19	Neptunium-239	0	0.0656	0.072	UI	PCI/G
6 B	09/18/19	Niobium-94	0.00483	0.00425	0.00753	U	PCI/G
6 B	09/18/19	Potassium-40	32.3	0.332	0.0646		PCI/G
6 B	09/18/19	Promethium-147	17.9	120	202	U	PCI/G
6 B	09/18/19	Protactinium-231	0	0.106	0.104	UI	PCI/G
6 B	09/18/19	Radium-226	0.942	0.0255	0.014		PCI/G
6 B	09/18/19	Radium-228	0.896	0.0481	0.0327		PCI/G
6 B	09/18/19	Sodium-22	-0.00332	0.00773	0.012	U	PCI/G
6 B	09/18/19	Tellurium-125m	0.836	2.21	3.77	U	PCI/G
6 B	09/18/19	Thallium-208	0.257	0.0125	0.00768		PCI/G
6 B	09/18/19	Thorium-231	0.0658	0.0913	0.144	U	PCI/G
6 B	09/18/19	Thorium-234	0.979	0.655	0.562		PCI/G
6 B	09/18/19	Thulium-171	-2.21	7.09	12.6	U	PCI/G
6 B	09/18/19	Tin-126	0	0.0225	0.0222	UI	PCI/G
6 B	09/30/19	Iodine-129	0.115	0.297	0.665	U	PCI/G
6 B	09/25/19	Technetium-99	-0.0799	0.319	0.545	U	PCI/G
6 B	09/28/19	Strontium-90	0.00139	0.00843	0.0148	U	PCI/G
6 B	09/28/19	Yttrium-90	0.00139	0.00843	0.0148	U	PCI/G
6 B	09/27/19	Nickel-63	-0.0188	0.266	0.456	U	PCI/G
6 B	09/28/19	Iron-55	2.34	2.71	3.86	U	PCI/G
6 B	09/28/19	Tritium	1.22	2.11	3.6	U	PCI/G
6 B	09/26/19	Carbon-14	0.976	1.46	2.49	U	PCI/G
6 B	09/27/19	Nickel-59	0.574	0.782	1.53	U	PCI/G
6 B	10/03/19	Americium-241	-0.000194	0.0257	0.0538	U	PCI/G
6 B	10/03/19	Americium-243	0.00308	0.028	0.0542	U	PCI/G
6 B	10/03/19	Curium-243/244	-0.0000961	0.0195	0.042	U	PCI/G
6 B	10/03/19	Curium-245/246	0.00394	0.0151	0.0281	U	PCI/G
6 C	09/30/19	Polonium-210	1.49	0.31	0.15		PCI/G
6 C	09/29/19	Thorium-228	0.783	0.154	0.112		PCI/G
6 C	09/29/19	Thorium-229	0.0714	0.0583	0.0799	U	PCI/G
6 C	09/29/19	Thorium-230	1.07	0.171	0.0992		PCI/G
6 C	09/29/19	Thorium-232	0.6	0.126	0.0619		PCI/G
6 C	09/30/19	Uranium-232	-0.0044	0.0579	0.109	U	PCI/G
6 C	09/30/19	Uranium-233/234	0.908	0.118	0.0546		PCI/G
6 C	09/30/19	Uranium-235/236	0.0532	0.0333	0.0364		PCI/G
6 C	09/30/19	Uranium-238	0.966	0.124	0.0671		PCI/G
6 C	09/30/19	Neptunium-236	0.000811	0.00657	0.0133	U	PCI/G
6 C	09/30/19	Plutonium-236	0.000811	0.00657	0.0133	U	PCI/G
6 C	09/30/19	Plutonium-239/240	0.0112	0.0119	0.0179	U	PCI/G
6 C	09/30/19	Plutonium-242	-0.00499	0.00896	0.0191	U	PCI/G
6 C	09/30/19	Plutonium-244	0.00321	0.0069	0.0114	U	PCI/G
6 C	09/30/19	Neptunium-237	0.00417	0.00904	0.0152	U	PCI/G
6 C	10/03/19	Plutonium-241	0.751	1.68	2.87	U	PCI/G
6 C	09/14/19	Actinium-225	0.103	0.723	1.18	U	PCI/G
6 C	09/14/19	Actinium-227	-0.0214	0.0542	0.0867	U	PCI/G
6 C	09/14/19	Actinium-228	1.19	0.0775	0.0477		PCI/G
6 C	09/14/19	Antimony-125	0.00725	0.0187	0.0297	U	PCI/G
6 C	09/14/19	Barium-137m	0.083	0.0142	0.0121		PCI/G
6 C	09/14/19	Bismuth-212	1.36	0.23	0.162		PCI/G
6 C	09/14/19	Bismuth-213	0.014	0.0208	0.0334	U	PCI/G
6 C	09/14/19	Bismuth-214	1.05	0.0431	0.0219		PCI/G
6 C	09/14/19	Cesium-134	0	0.0152	0.0188	UI	PCI/G
6 C	09/14/19	Cesium-137	0.0877	0.015	0.0128		PCI/G
6 C	09/14/19	Cobalt-60	-0.00104	0.00794	0.0138	U	PCI/G
6 C	09/14/19	Europium-152	-0.00931	0.0182	0.0303	U	PCI/G
6 C	09/14/19	Europium-154	-0.0198	0.0268	0.0453	U	PCI/G
6 C	09/14/19	Europium-155	0	0.034	0.0368	UI	PCI/G

Table B-1. Complete Results from the GEL Laboratory

Sample no.	Analysis date	Parameter	Result	Uncertainty	MDC[a]	Qualifier[b]	Units
6 C	09/14/19	Holmium-166m	-0.00761	0.0119	0.0197	U	PCI/G
6 C	09/14/19	Lead-210	1.26	0.25	0.247		PCI/G
6 C	09/14/19	Lead-212	1.16	0.0268	0.0196		PCI/G
6 C	09/14/19	Lead-214	1.19	0.0389	0.072		PCI/G
6 C	09/14/19	Neptunium-239	-0.0213	0.0581	0.0971	U	PCI/G
6 C	09/14/19	Niobium-94	0.00328	0.00671	0.0115	U	PCI/G
6 C	09/14/19	Potassium-40	29.8	0.494	0.0989		PCI/G
6 C	09/14/19	Promethium-147	-153	164	272	U	PCI/G
6 C	09/14/19	Protactinium-231	0	0.146	0.15	UI	PCI/G
6 C	09/14/19	Radium-226	1.05	0.0431	0.0219		PCI/G
6 C	09/14/19	Radium-228	1.19	0.0775	0.0477		PCI/G
6 C	09/14/19	Sodium-22	-0.00417	0.00986	0.0163	U	PCI/G
6 C	09/14/19	Tellurium-125m	1.97	3.22	4.62	U	PCI/G
6 C	09/14/19	Thallium-208	0.37	0.0198	0.0112		PCI/G
6 C	09/14/19	Thorium-231	-0.0696	0.129	0.202	U	PCI/G
6 C	09/14/19	Thorium-234	1.12	0.344	0.288		PCI/G
6 C	09/14/19	Thulium-171	0	2.17	2.16	UI	PCI/G
6 C	09/14/19	Tin-126	0	0.0255	0.0218	UI	PCI/G
6 C	09/30/19	Iodine-129	0.0379	0.261	0.659	U	PCI/G
6 C	09/25/19	Technetium-99	-0.256	0.376	0.647	U	PCI/G
6 C	09/28/19	Strontium-90	-0.00055	0.00835	0.0148	U	PCI/G
6 C	09/28/19	Yttrium-90	-0.00055	0.00835	0.0148	U	PCI/G
6 C	09/27/19	Nickel-63	0.0501	0.239	0.408	U	PCI/G
6 C	09/30/19	Iron-55	6.63	1.94	2.65		PCI/G
6 C	09/28/19	Tritium	-0.0908	2.06	3.61	U	PCI/G
6 C	09/26/19	Carbon-14	2.32	1.47	2.4	U	PCI/G
6 C	09/27/19	Nickel-59	0.189	0.38	0.931	U	PCI/G
6 C	10/03/19	Americium-241	-0.00332	0.0157	0.0355	U	PCI/G
6 C	10/03/19	Americium-243	0.00196	0.0158	0.03	U	PCI/G
6 C	10/03/19	Curium-243/244	0.00787	0.0152	0.0252	U	PCI/G
6 C	10/03/19	Curium-245/246	-0.00228	0.00998	0.0218	U	PCI/G
8 A	09/30/19	Polonium-210	2.54	0.386	0.176		PCI/G
8 A	09/29/19	Thorium-228	0.832	0.174	0.145		PCI/G
8 A	09/29/19	Thorium-229	0.0942	0.0738	0.104	U	PCI/G
8 A	09/29/19	Thorium-230	2.52	0.268	0.089		PCI/G
8 A	09/29/19	Thorium-232	0.771	0.153	0.0887		PCI/G
8 A	09/29/19	Uranium-232	0	0.0246	0.0491	U	PCI/G
8 A	09/29/19	Uranium-233/234	2.16	0.183	0.0488		PCI/G
8 A	09/29/19	Uranium-235/236	0.175	0.0563	0.044		PCI/G
8 A	09/29/19	Uranium-238	2.18	0.183	0.0304		PCI/G
8 A	09/28/19	Neptunium-236	-0.00279	0.0128	0.0257	U	PCI/G
8 A	09/28/19	Plutonium-236	-0.00279	0.0128	0.0257	U	PCI/G
8 A	09/28/19	Plutonium-239/240	0.00135	0.0142	0.0266	U	PCI/G
8 A	09/28/19	Plutonium-242	0.0113	0.0104	0.0151	U	PCI/G
8 A	09/28/19	Plutonium-244	0.00673	0.00791	0.0103	U	PCI/G
8 A	09/30/19	Neptunium-237	-0.0038	0.00705	0.0192	U	PCI/G
8 A	10/02/19	Plutonium-241	0.649	2.4	4.11	U	PCI/G
8 A	09/14/19	Actinium-225	-0.601	0.907	1.45	U	PCI/G
8 A	09/14/19	Actinium-227	0.0551	0.0745	0.113	U	PCI/G
8 A	09/14/19	Actinium-228	0.921	0.0724	0.0464		PCI/G
8 A	09/14/19	Antimony-125	0.00392	0.0206	0.0362	U	PCI/G
8 A	09/14/19	Barium-137m	0.0624	0.012	0.0112		PCI/G
8 A	09/14/19	Bismuth-212	0.995	0.188	0.166		PCI/G
8 A	09/14/19	Bismuth-213	0.0113	0.0217	0.0384	U	PCI/G
8 A	09/14/19	Bismuth-214	2.16	0.0537	0.0231		PCI/G
8 A	09/14/19	Cesium-134	0	0.0165	0.0183	UI	PCI/G
8 A	09/14/19	Cesium-137	0.066	0.0127	0.0118		PCI/G
8 A	09/14/19	Cobalt-60	-0.00236	0.00755	0.0132	U	PCI/G
8 A	09/14/19	Europium-152	-0.00469	0.0215	0.0378	U	PCI/G
8 A	09/14/19	Europium-154	0.00131	0.0253	0.0434	U	PCI/G

Table B-1. Complete Results from the GEL Laboratory

Sample no.	Analysis date	Parameter	Result	Uncertainty	MDC[a]	Qualifier[b]	Units
8 A	09/14/19	Europium-155	0.0122	0.0329	0.0555	U	PCI/G
8 A	09/14/19	Holmium-166m	-0.000469	0.0119	0.0203	U	PCI/G
8 A	09/14/19	Lead-210	2.36	3.9	4.16	U	PCI/G
8 A	09/14/19	Lead-212	1	0.0304	0.0235		PCI/G
8 A	09/14/19	Lead-214	2.54	0.0603	0.0275		PCI/G
8 A	09/14/19	Neptunium-239	-0.00531	0.0824	0.137	U	PCI/G
8 A	09/14/19	Niobium-94	0	0.0114	0.0126	UI	PCI/G
8 A	09/14/19	Potassium-40	16.4	0.407	0.111		PCI/G
8 A	09/14/19	Promethium-147	188	230	388	U	PCI/G
8 A	09/14/19	Protactinium-231	0	0.196	0.19	UI	PCI/G
8 A	09/14/19	Radium-226	2.16	0.0537	0.0231		PCI/G
8 A	09/14/19	Radium-228	0.921	0.0724	0.0464		PCI/G
8 A	09/14/19	Sodium-22	0.000205	0.00902	0.0155	U	PCI/G
8 A	09/14/19	Tellurium-125m	6.12	5.14	6.66	U	PCI/G
8 A	09/14/19	Thallium-208	0.276	0.0201	0.0125		PCI/G
8 A	09/14/19	Thorium-231	0	0.258	0.248	UI	PCI/G
8 A	09/14/19	Thorium-234	2.43	0.877	0.945		PCI/G
8 A	09/14/19	Thulium-171	1.7	10.3	17.7	U	PCI/G
8 A	09/14/19	Tin-126	0	0.0401	0.0398	UI	PCI/G
8 A	09/30/19	Iodine-129	0.217	0.271	0.679	U	PCI/G
8 A	09/24/19	Technetium-99	-0.195	0.398	0.683	U	PCI/G
8 A	10/05/19	Strontium-90	-0.0101	0.00843	0.015	U	PCI/G
8 A	10/05/19	Yttrium-90	-0.0101	0.00843	0.015	U	PCI/G
8 A	09/27/19	Nickel-63	-0.0597	0.272	0.467	U	PCI/G
8 A	09/29/19	Iron-55	1.61	2.12	3.09	U	PCI/G
8 A	09/27/19	Tritium	0.184	2.06	3.58	U	PCI/G
8 A	09/26/19	Carbon-14	0.0117	1.42	2.49	U	PCI/G
8 A	09/26/19	Nickel-59	0.438	0.55	1.33	U	PCI/G
8 A	10/03/19	Americium-241	0.0043	0.0106	0.0169	U	PCI/G
8 A	10/03/19	Americium-243	0.012	0.0185	0.0303	U	PCI/G
8 A	10/03/19	Curium-243/244	-0.0000285	0.00929	0.0201	U	PCI/G
8 A	10/03/19	Curium-245/246	0.00351	0.0103	0.0105	U	PCI/G
8 B	10/01/19	Polonium-210	2.33	0.396	0.199		PCI/G
8 B	10/01/19	Thorium-228	0.792	0.152	0.105		PCI/G
8 B	10/01/19	Thorium-229	0.0754	0.0578	0.0773	U	PCI/G
8 B	10/01/19	Thorium-230	2.63	0.254	0.0693		PCI/G
8 B	10/01/19	Thorium-232	0.687	0.131	0.0478		PCI/G
8 B	09/29/19	Uranium-232	-0.0164	0.0368	0.0744	U	PCI/G
8 B	09/29/19	Uranium-233/234	2.1	0.166	0.0512		PCI/G
8 B	09/29/19	Uranium-235/236	0.238	0.0562	0.0101		PCI/G
8 B	09/29/19	Uranium-238	2.37	0.176	0.0448		PCI/G
8 B	09/28/19	Neptunium-236	-0.00235	0.00923	0.019	U	PCI/G
8 B	09/28/19	Plutonium-236	-0.00235	0.00923	0.019	U	PCI/G
8 B	09/28/19	Plutonium-239/240	0.00454	0.00943	0.0163	U	PCI/G
8 B	09/28/19	Plutonium-242	0.0154	0.0145	0.0193	U	PCI/G
8 B	09/28/19	Plutonium-244	0.0034	0.00588	0.00868	U	PCI/G
8 B	09/30/19	Neptunium-237	0.00665	0.0105	0.0159	U	PCI/G
8 B	10/02/19	Plutonium-241	0.092	2.25	3.87	U	PCI/G
8 B	09/14/19	Actinium-225	0.278	0.868	1.41	U	PCI/G
8 B	09/14/19	Actinium-227	0.0437	0.0651	0.107	U	PCI/G
8 B	09/14/19	Actinium-228	0.961	0.0709	0.0465		PCI/G
8 B	09/14/19	Antimony-125	0.0284	0.0198	0.0354	U	PCI/G
8 B	09/14/19	Barium-137m	0.0436	0.0108	0.011		PCI/G
8 B	09/14/19	Bismuth-212	1.08	0.185	0.16		PCI/G
8 B	09/14/19	Bismuth-213	0.0149	0.021	0.0369	U	PCI/G
8 B	09/14/19	Bismuth-214	2.02	0.0529	0.0233		PCI/G
8 B	09/14/19	Cesium-134	0	0.0157	0.0185	UI	PCI/G
8 B	09/14/19	Cesium-137	0.0461	0.0114	0.0116		PCI/G
8 B	09/14/19	Cobalt-60	-0.00464	0.00767	0.0129	U	PCI/G
8 B	09/14/19	Europium-152	-0.00963	0.0207	0.0358	U	PCI/G
8 B	09/14/19	Europium-154	-0.0078	0.025	0.0411	U	PCI/G
8 B	09/14/19	Europium-155	0	0.0464	0.0506	UI	PCI/G

Table B-1. Complete Results from the GEL Laboratory

Sample no.	Analysis date	Parameter	Result	Uncertainty	MDC[a]	Qualifier[b]	Units
8 B	09/14/19	Holmium-166m	-0.0018	0.0114	0.019	U	PCI/G
8 B	09/14/19	Lead-210	2.61	2.59	3.01	U	PCI/G
8 B	09/14/19	Lead-212	0.942	0.03	0.0243		PCI/G
8 B	09/14/19	Lead-214	2.44	0.0571	0.0263		PCI/G
8 B	09/14/19	Neptunium-239	-0.0145	0.0779	0.13	U	PCI/G
8 B	09/14/19	Niobium-94	0	0.012	0.0123	UI	PCI/G
8 B	09/14/19	Potassium-40	16.3	0.385	0.107		PCI/G
8 B	09/14/19	Promethium-147	-11.1	221	368	U	PCI/G
8 B	09/14/19	Protactinium-231	0	0.162	0.172	UI	PCI/G
8 B	09/14/19	Radium-226	2.02	0.0529	0.0233		PCI/G
8 B	09/14/19	Radium-228	0.961	0.0709	0.0465		PCI/G
8 B	09/14/19	Sodium-22	-0.00291	0.00893	0.0147	U	PCI/G
8 B	09/14/19	Tellurium-125m	4.62	5	6.3	U	PCI/G
8 B	09/14/19	Thallium-208	0.304	0.0198	0.0114		PCI/G
8 B	09/14/19	Thorium-231	0.0811	0.21	0.249	U	PCI/G
8 B	09/14/19	Thorium-234	2.25	0.778	0.815		PCI/G
8 B	09/14/19	Thulium-171	1.65	8.19	14.2	U	PCI/G
8 B	09/14/19	Tin-126	0	0.0408	0.0375	UI	PCI/G
8 B	09/30/19	Iodine-129	-0.0222	0.199	0.517	U	PCI/G
8 B	09/24/19	Technetium-99	-0.393	0.41	0.708	U	PCI/G
8 B	09/25/19	Strontium-90	-0.00703	0.00581	0.0107	U	PCI/G
8 B	09/25/19	Yttrium-90	-0.00703	0.00581	0.0107	U	PCI/G
8 B	09/27/19	Nickel-63	0.145	0.281	0.476	U	PCI/G
8 B	09/29/19	Iron-55	5.64	2.28	3.25		PCI/G
8 B	09/27/19	Tritium	-0.671	2.06	3.66	U	PCI/G
8 B	09/26/19	Carbon-14	1.15	1.46	2.46	U	PCI/G
8 B	09/26/19	Nickel-59	0.00272	0.598	1.05	U	PCI/G
8 B	10/03/19	Americium-241	-0.0000945	0.0148	0.0316	U	PCI/G
8 B	10/03/19	Americium-243	0.00707	0.0222	0.0411	U	PCI/G
8 B	10/03/19	Curium-243/244	0.00933	0.0147	0.022	U	PCI/G
8 B	10/03/19	Curium-245/246	0.00339	0.00997	0.0102	U	PCI/G
8 C	10/05/19	Thorium-228	0.896	0.251	0.172		PCI/G
8 C	10/05/19	Thorium-229	0.0457	0.13	0.233	U	PCI/G
8 C	10/05/19	Thorium-230	2.64	0.411	0.233		PCI/G
8 C	10/05/19	Thorium-232	0.667	0.222	0.203		PCI/G
8 C	09/30/19	Polonium-210	0.545	0.162	0.0837		PCI/G
8 C	09/29/19	Uranium-232	0	0.0576	0.107	U	PCI/G
8 C	09/29/19	Uranium-233/234	2.24	0.173	0.0419		PCI/G
8 C	09/29/19	Uranium-235/236	0.147	0.0459	0.0262		PCI/G
8 C	09/29/19	Uranium-238	2.16	0.169	0.0326		PCI/G
8 C	09/28/19	Neptunium-236	0.00876	0.00858	0.0121	U	PCI/G
8 C	09/28/19	Plutonium-236	0.00876	0.00858	0.0121	U	PCI/G
8 C	09/28/19	Plutonium-239/240	0.00739	0.0103	0.0171	U	PCI/G
8 C	09/28/19	Plutonium-242	0.0143	0.0126	0.0145	U	PCI/G
8 C	09/28/19	Plutonium-244	0.00844	0.00774	0.0101	U	PCI/G
8 C	09/30/19	Neptunium-237	-0.00153	0.0115	0.0253	U	PCI/G
8 C	10/03/19	Plutonium-241	1.62	2.18	3.68	U	PCI/G
8 C	09/14/19	Actinium-225	0.72	0.841	1.4	U	PCI/G
8 C	09/14/19	Actinium-227	0.044	0.0835	0.105	U	PCI/G
8 C	09/14/19	Actinium-228	1.07	0.0676	0.0431		PCI/G
8 C	09/14/19	Antimony-125	0.00729	0.018	0.0319	U	PCI/G
8 C	09/14/19	Barium-137m	0.0308	0.0112	0.0108		PCI/G
8 C	09/14/19	Bismuth-212	1.05	0.178	0.147		PCI/G
8 C	09/14/19	Bismuth-213	-0.00538	0.0203	0.0353	U	PCI/G
8 C	09/14/19	Bismuth-214	2.05	0.0491	0.0202		PCI/G
8 C	09/14/19	Cesium-134	0	0.00894	0.0153	UI	PCI/G
8 C	09/14/19	Cesium-137	0.0325	0.0119	0.0114		PCI/G
8 C	09/14/19	Cobalt-60	0.00417	0.00705	0.0128	U	PCI/G
8 C	09/14/19	Europium-152	0.00294	0.0195	0.0347	U	PCI/G
8 C	09/14/19	Europium-154	0.0132	0.024	0.0384	U	PCI/G

Table B-1. Complete Results from the GEL Laboratory

Sample no.	Analysis date	Parameter	Result	Uncertainty	MDC[a]	Qualifier[b]	Units
8 C	09/14/19	Europium-155	0	0.0495	0.0491	UI	PCI/G
8 C	09/14/19	Holmium-166m	0.00181	0.0106	0.0181	U	PCI/G
8 C	09/14/19	Lead-210	-0.173	1.99	3.38	U	PCI/G
8 C	09/14/19	Lead-212	1.04	0.0306	0.0241		PCI/G
8 C	09/14/19	Lead-214	2.45	0.0568	0.0253		PCI/G
8 C	09/14/19	Neptunium-239	-0.00446	0.0786	0.123	U	PCI/G
8 C	09/14/19	Niobium-94	0.00622	0.01	0.0109	U	PCI/G
8 C	09/14/19	Potassium-40	16.9	0.376	0.103		PCI/G
8 C	09/14/19	Promethium-147	-139	207	345	U	PCI/G
8 C	09/14/19	Protactinium-231	0	0.147	0.176	UI	PCI/G
8 C	09/14/19	Radium-226	2.05	0.0491	0.0202		PCI/G
8 C	09/14/19	Radium-228	1.07	0.0676	0.0431		PCI/G
8 C	09/14/19	Sodium-22	0.00459	0.00858	0.0137	U	PCI/G
8 C	09/14/19	Tellurium-125m	1.15	3.89	6.14	U	PCI/G
8 C	09/14/19	Thallium-208	0.278	0.018	0.0114		PCI/G
8 C	09/14/19	Thorium-231	0.107	0.14	0.231	U	PCI/G
8 C	09/14/19	Thorium-234	2.89	0.766	0.781		PCI/G
8 C	09/14/19	Thulium-171	-3.58	7.97	13.8	U	PCI/G
8 C	09/14/19	Tin-126	0	0.039	0.0355	UI	PCI/G
8 C	09/30/19	Iodine-129	0.262	0.507	0.971	U	PCI/G
8 C	09/25/19	Technetium-99	-0.03	0.388	0.662	U	PCI/G
8 C	09/25/19	Strontium-90	0.00539	0.00715	0.0121	U	PCI/G
8 C	09/25/19	Yttrium-90	0.00539	0.00715	0.0121	U	PCI/G
8 C	09/27/19	Nickel-63	0.334	0.291	0.487	U	PCI/G
8 C	09/30/19	Iron-55	3.35	2.04	2.94		PCI/G
8 C	09/28/19	Tritium	1.68	2.16	3.65	U	PCI/G
8 C	09/26/19	Carbon-14	1.21	1.35	2.28	U	PCI/G
8 C	09/26/19	Nickel-59	0.468	0.816	1.49	U	PCI/G
8 C	10/03/19	Americium-241	0.0149	0.022	0.0364	U	PCI/G
8 C	10/03/19	Americium-243	-0.0149	0.0304	0.0699	U	PCI/G
8 C	10/03/19	Curium-243/244	-0.00604	0.00885	0.0261	U	PCI/G
8 C	10/03/19	Curium-245/246	0.00839	0.0206	0.0329	U	PCI/G
8 C	10/05/19	Thorium-228	0.527	0.379	0.55	U	PCI/G
8 C	10/05/19	Thorium-229	0	0.139	0.277	U	PCI/G
8 C	10/05/19	Thorium-230	2.65	0.571	0.355		PCI/G
8 C	10/05/19	Thorium-232	0.834	0.324	0.22		PCI/G
9 A	09/28/19	Polonium-210	1.44	0.324	0.145		PCI/G
9 A	09/28/19	Thorium-228	0.735	0.15	0.126		PCI/G
9 A	09/28/19	Thorium-229	0.0675	0.0648	0.0992	U	PCI/G
9 A	09/28/19	Thorium-230	2.08	0.224	0.0677		PCI/G
9 A	09/28/19	Thorium-232	0.782	0.136	0.0183		PCI/G
9 A	09/29/19	Uranium-232	0	0.0418	0.0797	U	PCI/G
9 A	09/29/19	Uranium-233/234	0.788	0.138	0.0965		PCI/G
9 A	09/29/19	Uranium-235/236	0.082	0.0577	0.0787		PCI/G
9 A	09/29/19	Uranium-238	0.79	0.133	0.067		PCI/G
9 A	09/30/19	Neptunium-236	-0.00576	0.0077	0.0211	U	PCI/G
9 A	09/30/19	Plutonium-236	-0.00576	0.0077	0.0211	U	PCI/G
9 A	09/30/19	Plutonium-239/240	0.00908	0.0118	0.0183	U	PCI/G
9 A	09/30/19	Plutonium-242	-0.00338	0.0134	0.0262	U	PCI/G
9 A	09/30/19	Plutonium-244	0.00456	0.00761	0.0107	U	PCI/G
9 A	09/30/19	Neptunium-237	0.00356	0.0116	0.0219	U	PCI/G
9 A	10/02/19	Plutonium-241	0.704	1.86	3.18	U	PCI/G
9 A	09/13/19	Actinium-225	-0.175	0.48	0.769	U	PCI/G
9 A	09/13/19	Actinium-227	0.0446	0.0365	0.0569	U	PCI/G
9 A	09/13/19	Actinium-228	0.866	0.0434	0.0277		PCI/G
9 A	09/13/19	Antimony-125	0.00156	0.0114	0.0194	U	PCI/G
9 A	09/13/19	Barium-137m	0.138	0.00781	0.00658		PCI/G
9 A	09/13/19	Bismuth-212	0.942	0.114	0.0897		PCI/G
9 A	09/13/19	Bismuth-213	-0.00376	0.0126	0.0212	U	PCI/G
9 A	09/13/19	Bismuth-214	1.15	0.025	0.0134		PCI/G
9 A	09/13/19	Cesium-134	0	0.00789	0.00908	UI	PCI/G
9 A	09/13/19	Cesium-137	0.145	0.00825	0.00695		PCI/G

Table B-1. Complete Results from the GEL Laboratory

Sample no.	Analysis date	Parameter	Result	Uncertainty	MDC[a]	Qualifier[b]	Units
9 A	09/13/19	Cobalt-60	0.00126	0.00456	0.00802	U	PCI/G
9 A	09/13/19	Europium-152	-0.00988	0.0118	0.0201	U	PCI/G
9 A	09/13/19	Europium-154	-0.00349	0.017	0.0255	U	PCI/G
9 A	09/13/19	Europium-155	0	0.0242	0.0287	UI	PCI/G
9 A	09/13/19	Holmium-166m	0.000962	0.00666	0.0116	U	PCI/G
9 A	09/13/19	Lead-210	0.551	1.93	3.49	U	PCI/G
9 A	09/13/19	Lead-212	0.829	0.0164	0.0133		PCI/G
9 A	09/13/19	Lead-214	1.35	0.0291	0.0493		PCI/G
9 A	09/13/19	Neptunium-239	-0.00989	0.0419	0.0707	U	PCI/G
9 A	09/13/19	Niobium-94	0.0044	0.0063	0.00672	U	PCI/G
9 A	09/13/19	Potassium-40	13.6	0.236	0.0623		PCI/G
9 A	09/13/19	Promethium-147	-56	118	198	U	PCI/G
9 A	09/13/19	Protactinium-231	0	0.0977	0.102	UI	PCI/G
9 A	09/13/19	Radium-226	1.15	0.025	0.0134		PCI/G
9 A	09/13/19	Radium-228	0.866	0.0434	0.0277		PCI/G
9 A	09/13/19	Sodium-22	-0.0012	0.00607	0.00912	U	PCI/G
9 A	09/13/19	Tellurium-125m	0.694	2.14	3.55	U	PCI/G
9 A	09/13/19	Thallium-208	0.269	0.0125	0.00658		PCI/G
9 A	09/13/19	Thorium-231	-0.0298	0.0883	0.136	U	PCI/G
9 A	09/13/19	Thorium-234	0	0.583	0.555	UI	PCI/G
9 A	09/13/19	Thulium-171	-6.49	6.95	12.3	U	PCI/G
9 A	09/13/19	Tin-126	0	0.0241	0.0205	UI	PCI/G
9 A	09/30/19	Iodine-129	-0.108	0.15	0.193	U	PCI/G
9 A	09/24/19	Technetium-99	-0.374	0.437	0.753	U	PCI/G
9 A	10/05/19	Strontium-90	0.00565	0.00739	0.0126	U	PCI/G
9 A	10/05/19	Yttrium-90	0.00565	0.00739	0.0126	U	PCI/G
9 A	09/27/19	Nickel-63	0.34	0.411	0.691	U	PCI/G
9 A	09/29/19	Iron-55	2.72	2.25	3.27	U	PCI/G
9 A	09/27/19	Tritium	0.192	2.01	3.5	U	PCI/G
9 A	09/26/19	Carbon-14	0.31	1.43	2.48	U	PCI/G
9 A	09/26/19	Nickel-59	0.306	0.487	1.2	U	PCI/G
9 A	10/03/19	Americium-241	0.00176	0.011	0.0208	U	PCI/G
9 A	10/03/19	Americium-243	-0.006	0.0133	0.0327	U	PCI/G
9 A	10/03/19	Curium-243/244	0.00516	0.0196	0.0373	U	PCI/G
9 A	10/03/19	Curium-245/246	0.00342	0.0101	0.0102	U	PCI/G
9 B	09/30/19	Polonium-210	0.736	0.241	0.0597		PCI/G
9 B	09/28/19	Thorium-228	0.618	0.179	0.197		PCI/G
9 B	09/28/19	Thorium-229	0.0594	0.0831	0.137	U	PCI/G
9 B	09/28/19	Thorium-230	2.05	0.265	0.122		PCI/G
9 B	09/28/19	Thorium-232	0.641	0.162	0.143		PCI/G
9 B	10/03/19	Uranium-232	0.0144	0.0431	0.0776	U	PCI/G
9 B	10/03/19	Uranium-233/234	1.06	0.167	0.12		PCI/G
9 B	10/03/19	Uranium-235/236	0.0353	0.0431	0.065	U	PCI/G
9 B	10/03/19	Uranium-238	0.832	0.145	0.0947		PCI/G
9 B	09/30/19	Neptunium-236	0.00241	0.00928	0.0172	U	PCI/G
9 B	09/30/19	Plutonium-236	0.00241	0.00928	0.0172	U	PCI/G
9 B	09/30/19	Plutonium-239/240	0.00347	0.0118	0.0221	U	PCI/G
9 B	09/30/19	Plutonium-242	0.00739	0.0103	0.0171	U	PCI/G
9 B	09/30/19	Plutonium-244	0.00352	0.00864	0.0138	U	PCI/G
9 B	09/30/19	Neptunium-237	0.000649	0.0111	0.0229	U	PCI/G
9 B	10/02/19	Plutonium-241	-0.303	2.45	4.24	U	PCI/G
9 B	09/14/19	Actinium-225	-0.592	0.759	1.31	U	PCI/G
9 B	09/14/19	Actinium-227	-0.00633	0.056	0.097	U	PCI/G
9 B	09/14/19	Actinium-228	0.955	0.0727	0.0412		PCI/G
9 B	09/14/19	Antimony-125	0.00243	0.018	0.0306	U	PCI/G
9 B	09/14/19	Barium-137m	0.081	0.0117	0.0104		PCI/G
9 B	09/14/19	Bismuth-212	1.18	0.17	0.144		PCI/G
9 B	09/14/19	Bismuth-213	0.0212	0.0201	0.035	U	PCI/G
9 B	09/14/19	Bismuth-214	1.29	0.0441	0.0212		PCI/G
9 B	09/14/19	Cesium-134	0	0.0133	0.0162	UI	PCI/G

Table B-1. Complete Results from the GEL Laboratory

Sample no.	Analysis date	Parameter	Result	Uncertainty	MDC[a]	Qualifier[b]	Units
9 B	09/14/19	Cesium-137	0.0855	0.0124	0.011		PCI/G
9 B	09/14/19	Cobalt-60	0.00012	0.00743	0.0127	U	PCI/G
9 B	09/14/19	Europium-152	-0.0125	0.0203	0.0326	U	PCI/G
9 B	09/14/19	Europium-154	0.0256	0.0303	0.036	U	PCI/G
9 B	09/14/19	Europium-155	0.0491	0.0384	0.0531	U	PCI/G
9 B	09/14/19	Holmium-166m	-0.00037	0.0105	0.0186	U	PCI/G
9 B	09/14/19	Lead-210	1.68	2.98	5.12	U	PCI/G
9 B	09/14/19	Lead-212	0.932	0.0293	0.0207		PCI/G
9 B	09/14/19	Lead-214	1.52	0.0497	0.0246		PCI/G
9 B	09/14/19	Neptunium-239	0.00423	0.0756	0.123	U	PCI/G
9 B	09/14/19	Niobium-94	0.00262	0.0059	0.0106	U	PCI/G
9 B	09/14/19	Potassium-40	13.9	0.337	0.0968		PCI/G
9 B	09/14/19	Promethium-147	10.6	214	348	U	PCI/G
9 B	09/14/19	Protactinium-231	0	0.148	0.163	UI	PCI/G
9 B	09/14/19	Radium-226	1.29	0.0441	0.0212		PCI/G
9 B	09/14/19	Radium-228	0.955	0.0727	0.0412		PCI/G
9 B	09/14/19	Sodium-22	-0.00166	0.0123	0.0128	U	PCI/G
9 B	09/14/19	Tellurium-125m	2.61	4.71	6.29	U	PCI/G
9 B	09/14/19	Thallium-208	0.271	0.0164	0.0113		PCI/G
9 B	09/14/19	Thorium-231	-0.00496	0.146	0.224	U	PCI/G
9 B	09/14/19	Thorium-234	1.04	0.979	0.957		PCI/G
9 B	09/14/19	Thulium-171	5.28	12	20.4	U	PCI/G
9 B	09/14/19	Tin-126	0	0.0424	0.0477	UI	PCI/G
9 B	09/30/19	Iodine-129	0.0232	0.448	0.827	U	PCI/G
9 B	09/24/19	Technetium-99	-0.203	0.375	0.644	U	PCI/G
9 B	09/24/19	Strontium-90	0.00735	0.00646	0.0107	U	PCI/G
9 B	09/24/19	Yttrium-90	0.00735	0.00646	0.0107	U	PCI/G
9 B	09/27/19	Nickel-63	0.0642	0.299	0.509	U	PCI/G
9 B	09/29/19	Iron-55	3.08	2.47	3.62	U	PCI/G
9 B	09/27/19	Tritium	0.698	2.08	3.58	U	PCI/G
9 B	09/26/19	Carbon-14	0.716	1.44	2.47	U	PCI/G
9 B	09/26/19	Nickel-59	0.431	0.906	1.72	U	PCI/G
9 B	10/03/19	Americium-241	0.0185	0.0203	0.0262	U	PCI/G
9 B	10/03/19	Americium-243	-0.0131	0.0232	0.0524	U	PCI/G
9 B	10/03/19	Curium-243/244	-0.0000736	0.0149	0.0322	U	PCI/G
9 B	10/03/19	Curium-245/246	0.00366	0.0141	0.0261	U	PCI/G
9 C	09/30/19	Polonium-210	0.885	0.27	0.159		PCI/G
9 C	09/29/19	Thorium-228	0.671	0.157	0.126		PCI/G
9 C	09/29/19	Thorium-229	0.0603	0.0591	0.0833	U	PCI/G
9 C	09/29/19	Thorium-230	2.05	0.245	0.0575		PCI/G
9 C	09/29/19	Thorium-232	0.607	0.135	0.0574		PCI/G
9 C	09/29/19	Uranium-232	-0.00448	0.0362	0.0724	U	PCI/G
9 C	09/29/19	Uranium-233/234	1.09	0.124	0.0438		PCI/G
9 C	09/29/19	Uranium-235/236	0.136	0.0494	0.0478		PCI/G
9 C	09/29/19	Uranium-238	1.07	0.122	0.0393		PCI/G
9 C	09/30/19	Neptunium-236	-0.00485	0.00911	0.024	U	PCI/G
9 C	09/30/19	Plutonium-236	-0.00485	0.00911	0.024	U	PCI/G
9 C	09/30/19	Plutonium-239/240	0.0137	0.0165	0.0256	U	PCI/G
9 C	09/30/19	Plutonium-242	-0.00506	0.0111	0.0233	U	PCI/G
9 C	09/30/19	Plutonium-244	0.00575	0.00959	0.0135	U	PCI/G
9 C	09/30/19	Neptunium-237	-0.007	0.00641	0.0214	U	PCI/G
9 C	10/02/19	Plutonium-241	0.0484	2.43	4.18	U	PCI/G
9 C	09/14/19	Actinium-225	-0.265	0.779	1.36	U	PCI/G
9 C	09/14/19	Actinium-227	0.0973	0.0754	0.101	U	PCI/G
9 C	09/14/19	Actinium-228	0.938	0.0674	0.0429		PCI/G
9 C	09/14/19	Antimony-125	0.0233	0.0188	0.0331	U	PCI/G
9 C	09/14/19	Barium-137m	0.0565	0.011	0.0107		PCI/G
9 C	09/14/19	Bismuth-212	0.89	0.181	0.149		PCI/G
9 C	09/14/19	Bismuth-213	0.012	0.0202	0.0349	U	PCI/G
9 C	09/14/19	Bismuth-214	1.34	0.0432	0.0207		PCI/G
9 C	09/14/19	Cesium-134	0	0.012	0.0161	UI	PCI/G
9 C	09/14/19	Cesium-137	0.0597	0.0116	0.0113		PCI/G

Table B-1. Complete Results from the GEL Laboratory

Sample no.	Analysis date	Parameter	Result	Uncertainty	MDC[a]	Qualifier[b]	Units
9 C	09/14/19	Cobalt-60	0.00835	0.0114	0.0122	U	PCI/G
9 C	09/14/19	Europium-152	0.00345	0.0196	0.0339	U	PCI/G
9 C	09/14/19	Europium-154	-0.00803	0.0264	0.0385	U	PCI/G
9 C	09/14/19	Europium-155	0	0.045	0.0476	UI	PCI/G
9 C	09/14/19	Holmium-166m	0.00208	0.0103	0.0184	U	PCI/G
9 C	09/14/19	Lead-210	2.9	2.29	4.01	U	PCI/G
9 C	09/14/19	Lead-212	0.924	0.0276	0.022		PCI/G
9 C	09/14/19	Lead-214	1.6	0.0492	0.0857		PCI/G
9 C	09/14/19	Neptunium-239	0.0629	0.0901	0.119	U	PCI/G
9 C	09/14/19	Niobium-94	0.000356	0.00601	0.0107	U	PCI/G
9 C	09/14/19	Potassium-40	13.5	0.35	0.101		PCI/G
9 C	09/14/19	Promethium-147	-45.5	210	343	U	PCI/G
9 C	09/14/19	Protactinium-231	0	0.151	0.168	UI	PCI/G
9 C	09/14/19	Radium-226	1.34	0.0432	0.0207		PCI/G
9 C	09/14/19	Radium-228	0.938	0.0674	0.0429		PCI/G
9 C	09/14/19	Sodium-22	-0.00476	0.00956	0.0137	U	PCI/G
9 C	09/14/19	Tellurium-125m	1.8	3.98	6.02	U	PCI/G
9 C	09/14/19	Thallium-208	0.265	0.0175	0.0118		PCI/G
9 C	09/14/19	Thorium-231	0.105	0.15	0.238	U	PCI/G
9 C	09/14/19	Thorium-234	1.29	0.757	0.824		PCI/G
9 C	09/14/19	Thulium-171	-3.39	9.34	15.8	U	PCI/G
9 C	09/14/19	Tin-126	0	0.0334	0.0342	UI	PCI/G
9 C	09/30/19	Iodine-129	0	0.236	0.503	U	PCI/G
9 C	09/24/19	Technetium-99	-0.319	0.358	0.617	U	PCI/G
9 C	09/25/19	Strontium-90	-0.00217	0.00679	0.0119	U	PCI/G
9 C	09/25/19	Yttrium-90	-0.00217	0.00679	0.0119	U	PCI/G
9 C	09/27/19	Nickel-63	-0.0256	0.276	0.473	U	PCI/G
9 C	09/29/19	Iron-55	1.32	2.28	3.38	U	PCI/G
9 C	09/27/19	Tritium	0.682	2.06	3.54	U	PCI/G
9 C	09/26/19	Carbon-14	1.04	1.43	2.42	U	PCI/G
9 C	09/26/19	Nickel-59	-0.41	1.23	2.11	U	PCI/G
9 C	10/03/19	Americium-241	0.0111	0.0146	0.0186	U	PCI/G
9 C	10/03/19	Americium-243	0.00674	0.0255	0.048	U	PCI/G
9 C	10/03/19	Curium-243/244	0.00624	0.0134	0.0221	U	PCI/G
9 C	10/03/19	Curium-245/246	0.00812	0.0143	0.0122	U	PCI/G
LCS	09/25/19	Americium-241	108	2.06	1.22		%
LCS	09/25/19	Cesium-137	113	0.332	0.101		%
LCS	09/25/19	Cobalt-60	107	0.28	0.0542		%
LCS	09/30/19	Polonium-210	109	1.29	0.22		%
LCS	09/29/19	Thorium-230	94.3	0.406	0.0938		%
LCS	09/30/19	Uranium-238	95.9	0.266	0.011		%
LCS	09/28/19	Plutonium-239/240	101	0.0547	0.00958		%
LCS	09/30/19	Neptunium-237	116	0.168	0.0471		%
LCS	10/03/19	Plutonium-241	106	3.45	3.03		%
LCS	10/02/19	Polonium-210	88.7	0.708	0.0809		%
LCS	10/02/19	Polonium-210	88.7	0.708	0.0809		%
LCS	10/02/19	Thorium-230	90.4	0.465	0.116		%
LCS	10/02/19	Thorium-230	90.4	0.465	0.116		%
LCS	10/01/19	Uranium-238	98.3	0.249	0.0497		%
LCS	10/01/19	Uranium-238	98.3	0.249	0.0497		%
LCS	10/01/19	Plutonium-239/240	123	0.0922	0.0129		%
LCS	10/01/19	Plutonium-239/240	123	0.0922	0.0129		%
LCS	10/02/19	Americium-241	91.6	0.0684	0.0145		%
LCS	10/02/19	Curium-243/244	97.6	0.076	0.0118		%
LCS	10/02/19	Americium-241	91.6	0.0684	0.0145		%
LCS	10/02/19	Curium-243/244	97.6	0.076	0.0118		%
LCS	10/03/19	Neptunium-237	109	0.198	0.0379		%
LCS	10/03/19	Neptunium-237	109	0.198	0.0379		%
LCS	10/06/19	Plutonium-241	90.2	2.7	2.38		%
LCS	10/06/19	Plutonium-241	90.2	2.7	2.38		%

Table B-1. Complete Results from the GEL Laboratory

Sample no.	Analysis date	Parameter	Result	Uncertainty	MDC[a]	Qualifier[b]	Units
LCS	09/14/19	Americium-241	105	0.61	0.326		%
LCS	09/14/19	Cesium-137	111	0.317	0.0862		%
LCS	09/14/19	Cobalt-60	104	0.275	0.0419		%
LCS	09/30/19	Iodine-129	84.8	2.26	1.01		%
LCS	09/30/19	Iodine-129	84.8	2.26	1.01		%
LCS	09/26/19	Technetium-99	97	1.43	1.12		%
LCS	09/25/19	Strontium-90	110	0.0694	0.0257		%
LCS	09/25/19	Yttrium-90	110	0.0694	0.0257		%
LCS	09/28/19	Nickel-63	88.7	1.91	1.03		%
LCS	09/27/19	Nickel-63	88.9	1.02	0.7		%
LCS	09/25/19	Americium-241	110	2.01	1.27		%
LCS	09/25/19	Cesium-137	113	0.327	0.0952		%
LCS	09/25/19	Cobalt-60	112	0.282	0.0585		%
LCS	09/27/19	Americium-241	113	0.697	0.364		%
LCS	09/27/19	Cesium-137	114	0.353	0.0925		%
LCS	09/27/19	Cobalt-60	111	0.315	0.0647		%
LCS	09/28/19	Iodine-129	90.8	2.08	1.06		%
LCS	09/28/19	Iodine-129	90.8	2.08	1.06		%
LCS	09/29/19	Iodine-129	86.7	1.65	1.18		%
LCS	10/02/19	Polonium-210	94.6	0.628	0.0934		%
LCS	09/30/19	Thorium-230	91.5	0.392	0.0856		%
LCS	09/28/19	Uranium-238	100	0.228	0.0259		%
LCS	09/30/19	Plutonium-239/240	107	0.082	0.0102		%
LCS	10/01/19	Neptunium-237	117	0.168	0.0382		%
LCS	10/04/19	Plutonium-241	103	3.29	2.71		%
LCS	09/28/19	Iron-55	107	2.83	2.68		%
LCS	09/26/19	Iron-55	92.2	2.12	1.99		%
LCS	10/01/19	Iron-55	97.1	2.73	2.6		%
LCS	09/26/19	Iron-55	101	2.13	1.99		%
LCS	09/26/19	Nickel-63	89.7	1.8	1.12		%
LCS	09/29/19	Nickel-63	84.7	0.991	0.739		%
LCS	09/26/19	Technetium-99	81	1.16	0.884		%
LCS	09/26/19	Technetium-99	81	1.16	0.884		%
LCS	09/25/19	Technetium-99	107	0.647	0.602		%
LCS	09/28/19	Tritium	85.2	4.16	3.74		%
LCS	09/28/19	Tritium	94.1	20.8	9		%
LCS	09/28/19	Tritium	94.1	20.8	9		%
LCS	09/27/19	Tritium	82.1	14.9	7.21		%
LCS	09/26/19	Carbon-14	97.1	2.85	2.27		%
LCS	09/28/19	Carbon-14	92.2	3.04	2.51		%
LCS	09/28/19	Carbon-14	92.2	3.04	2.51		%
LCS	09/27/19	Carbon-14	98	3.15	2.87		%
LCS	09/27/19	Nickel-59	76.8	3.38	2.12		%
LCS	09/26/19	Nickel-59	107	3.37	1.61		%
LCS	09/30/19	Nickel-59	76.8	3.23	2		%
LCS	09/26/19	Strontium-90	103	0.0626	0.0175		%
LCS	09/26/19	Yttrium-90	103	0.0626	0.0175		%
LCS	10/02/19	Nickel-59	88.4	3.38	1.11		%
LCS	10/03/19	Strontium-90	113	0.081	0.0294		%
LCS	10/03/19	Yttrium-90	113	0.081	0.0294		%
LCS	10/03/19	Americium-241	96	0.152	0.0328		%
LCS	10/03/19	Curium-243/244	96.5	0.165	0.0303		%
LCS	10/09/19	Strontium-90	86.6	0.0569	0.0166		%
LCS	10/09/19	Yttrium-90	86.6	0.0569	0.0166		%
LCS	10/09/19	Strontium-90	86.6	0.0569	0.0166		%
LCS	10/09/19	Yttrium-90	86.6	0.0569	0.0166		%
LCS	10/05/19	Thorium-230	89.3	0.414	0.101		%
LCS	10/06/19	Americium-241	89.3	0.0932	0.0171		%
LCS	10/06/19	Curium-243/244	97.5	0.105	0.0183		%
LCS	10/05/19	Americium-241	103	0.115	0.0133		%
LCS	10/05/19	Curium-243/244	101	0.124	0.0263		%
LCS	10/08/19	Strontium-90	91.5	0.0697	0.0354		%

Table B-1. Complete Results from the GEL Laboratory

Sample no.	Analysis date	Parameter	Result	Uncertainty	MDC[a]	Qualifier[b]	Units
LCS	10/08/19	Yttrium-90	91.5	0.0697	0.0354		%
MB	09/25/19	Actinium-225	0.00925	0.0215	0.0377	U	PCI/G
MB	09/25/19	Actinium-227	0.00101	0.0113	0.0193	U	PCI/G
MB	09/25/19	Actinium-228	0.00536	0.0102	0.0121	U	PCI/G
MB	09/25/19	Antimony-125	-0.00873	0.00748	0.00662	U	PCI/G
MB	09/25/19	Barium-137m	-0.000666	0.00128	0.00223	U	PCI/G
MB	09/25/19	Bismuth-212	0	0.04	0.037	UI	PCI/G
MB	09/25/19	Bismuth-213	0.00129	0.00435	0.00823	U	PCI/G
MB	09/25/19	Bismuth-214	-0.00119	0.00411	0.00662	U	PCI/G
MB	09/25/19	Cesium-134	0.000455	0.00144	0.00277	U	PCI/G
MB	09/25/19	Cesium-137	-0.000704	0.00135	0.00235	U	PCI/G
MB	09/25/19	Cobalt-60	0.000398	0.0014	0.00287	U	PCI/G
MB	09/25/19	Europium-152	0.00167	0.00353	0.00685	U	PCI/G
MB	09/25/19	Europium-154	-0.000618	0.00325	0.00527	U	PCI/G
MB	09/25/19	Europium-155	0.000391	0.00455	0.00799	U	PCI/G
MB	09/25/19	Holmium-166m	0.00134	0.00226	0.00444	U	PCI/G
MB	09/25/19	Lead-210	0.145	0.395	0.423	U	PCI/G
MB	09/25/19	Lead-212	0.00115	0.00428	0.00517	U	PCI/G
MB	09/25/19	Lead-214	0.00145	0.00607	0.00683	U	PCI/G
MB	09/25/19	Neptunium-239	0.00073	0.0117	0.0204	U	PCI/G
MB	09/25/19	Niobium-94	0.000681	0.0014	0.00267	U	PCI/G
MB	09/25/19	Potassium-40	0.017	0.0262	0.0236	U	PCI/G
MB	09/25/19	Promethium-147	-3.66	32.4	55.8	U	PCI/G
MB	09/25/19	Protactinium-231	-0.00381	0.0188	0.0346	U	PCI/G
MB	09/25/19	Radium-226	-0.00119	0.00411	0.00662	U	PCI/G
MB	09/25/19	Radium-228	0.00536	0.0102	0.0121	U	PCI/G
MB	09/25/19	Sodium-22	-0.000434	0.00122	0.00186	U	PCI/G
MB	09/25/19	Tellurium-125m	-0.0882	0.433	0.741	U	PCI/G
MB	09/25/19	Thallium-208	-0.00098	0.00199	0.00268	U	PCI/G
MB	09/25/19	Thorium-231	0.00915	0.0243	0.0466	U	PCI/G
MB	09/25/19	Thorium-234	0.149	0.145	0.166	U	PCI/G
MB	09/25/19	Thulium-171	-0.268	1.35	2.04	U	PCI/G
MB	09/25/19	Tin-126	0.00136	0.00364	0.00605	U	PCI/G
MB	09/30/19	Polonium-210	-0.124	0.151	0.397	U	PCI/G
MB	09/29/19	Thorium-228	-0.00489	0.0899	0.17	U	PCI/G
MB	09/29/19	Thorium-229	-0.115	0.0888	0.195	U	PCI/G
MB	09/29/19	Thorium-230	-0.0929	0.0672	0.159	U	PCI/G
MB	09/29/19	Thorium-232	-0.0356	0.0609	0.131	U	PCI/G
MB	09/30/19	Uranium-232	-0.0154	0.0455	0.0876	U	PCI/G
MB	09/30/19	Uranium-233/234	0.0032	0.019	0.0358	U	PCI/G
MB	09/30/19	Uranium-235/236	0.0187	0.0216	0.0329	U	PCI/G
MB	09/30/19	Uranium-238	0.008	0.024	0.0431	U	PCI/G
MB	09/30/19	Neptunium-236	-0.00286	0.00691	0.0177	U	PCI/G
MB	09/30/19	Plutonium-236	-0.00286	0.00691	0.0177	U	PCI/G
MB	09/30/19	Plutonium-239/240	0.00839	0.0104	0.0149	U	PCI/G
MB	09/30/19	Plutonium-242	-0.00182	0.00837	0.0168	U	PCI/G
MB	09/30/19	Plutonium-244	0.0103	0.01	0.011	U	PCI/G
MB	09/30/19	Neptunium-237	-0.00474	0.00867	0.0224	U	PCI/G
MB	10/03/19	Plutonium-241	0.743	1.9	3.24	U	PCI/G
MB	10/02/19	Polonium-210	-0.0858	0.0577	0.183	U	PCI/G
MB	10/02/19	Polonium-210	-0.0858	0.0577	0.183	U	PCI/G
MB	10/02/19	Thorium-228	0.0713	0.0744	0.119	U	PCI/G
MB	10/02/19	Thorium-229	0.0243	0.0673	0.12	U	PCI/G
MB	10/02/19	Thorium-230	-0.0121	0.0503	0.103	U	PCI/G
MB	10/02/19	Thorium-232	-0.0241	0.0374	0.0869	U	PCI/G
MB	10/02/19	Thorium-228	0.0713	0.0744	0.119	U	PCI/G
MB	10/02/19	Thorium-229	0.0243	0.0673	0.12	U	PCI/G
MB	10/02/19	Thorium-230	-0.0121	0.0503	0.103	U	PCI/G
MB	10/02/19	Thorium-232	-0.0241	0.0374	0.0869	U	PCI/G
MB	10/01/19	Uranium-232	-0.0288	0.0349	0.0745	U	PCI/G

Table B-1. Complete Results from the GEL Laboratory

Sample no.	Analysis date	Parameter	Result	Uncertainty	MDC[a]	Qualifier[b]	Units
MB	10/01/19	Uranium-233/234	0.0128	0.0254	0.0438	U	PCI/G
MB	10/01/19	Uranium-235/236	0.0373	0.0218	0.0086		PCI/G
MB	10/01/19	Uranium-238	0.00286	0.0202	0.0383	U	PCI/G
MB	10/01/19	Uranium-232	-0.0288	0.0349	0.0745	U	PCI/G
MB	10/01/19	Uranium-233/234	0.0128	0.0254	0.0438	U	PCI/G
MB	10/01/19	Uranium-235/236	0.0373	0.0218	0.0086		PCI/G
MB	10/01/19	Uranium-238	0.00286	0.0202	0.0383	U	PCI/G
MB	10/01/19	Neptunium-236	-0.000103	0.0161	0.0343	U	PCI/G
MB	10/01/19	Plutonium-236	-0.000103	0.0161	0.0343	U	PCI/G
MB	10/01/19	Plutonium-239/240	0.0136	0.021	0.0343	U	PCI/G
MB	10/01/19	Plutonium-242	-0.00349	0.00869	0.0205	U	PCI/G
MB	10/01/19	Plutonium-244	0.00166	0.0134	0.0273	U	PCI/G
MB	10/01/19	Neptunium-236	-0.000103	0.0161	0.0343	U	PCI/G
MB	10/01/19	Plutonium-236	-0.000103	0.0161	0.0343	U	PCI/G
MB	10/01/19	Plutonium-239/240	0.0136	0.021	0.0343	U	PCI/G
MB	10/01/19	Plutonium-242	-0.00349	0.00869	0.0205	U	PCI/G
MB	10/01/19	Plutonium-244	0.00166	0.0134	0.0273	U	PCI/G
MB	10/02/19	Americium-241	0.00666	0.00922	0.0149	U	PCI/G
MB	10/02/19	Americium-243	-0.00904	0.0101	0.025	U	PCI/G
MB	10/02/19	Curium-243/244	-0.000681	0.00451	0.0105	U	PCI/G
MB	10/02/19	Curium-245/246	0.0028	0.00689	0.011	U	PCI/G
MB	10/02/19	Americium-241	0.00666	0.00922	0.0149	U	PCI/G
MB	10/02/19	Americium-243	-0.00904	0.0101	0.025	U	PCI/G
MB	10/02/19	Curium-243/244	-0.000681	0.00451	0.0105	U	PCI/G
MB	10/02/19	Curium-245/246	0.0028	0.00689	0.011	U	PCI/G
MB	10/03/19	Neptunium-237	-0.00942	0.00983	0.034	U	PCI/G
MB	10/03/19	Neptunium-237	-0.00942	0.00983	0.034	U	PCI/G
MB	10/06/19	Plutonium-241	-1.73	2.96	5.17	U	PCI/G
MB	10/06/19	Plutonium-241	-1.73	2.96	5.17	U	PCI/G
MB	09/14/19	Actinium-225	0.00347	0.00599	0.0102	U	PCI/G
MB	09/14/19	Actinium-227	-0.00426	0.00691	0.0111	U	PCI/G
MB	09/14/19	Actinium-228	0.00172	0.00891	0.0074	U	PCI/G
MB	09/14/19	Antimony-125	-0.00156	0.00212	0.00369	U	PCI/G
MB	09/14/19	Barium-137m	0.000465	0.000829	0.00152	U	PCI/G
MB	09/14/19	Bismuth-212	-0.00187	0.0198	0.0206	U	PCI/G
MB	09/14/19	Bismuth-213	0.000392	0.00241	0.00438	U	PCI/G
MB	09/14/19	Bismuth-214	0.00023	0.00447	0.00318	U	PCI/G
MB	09/14/19	Cesium-134	0.000164	0.000895	0.00161	U	PCI/G
MB	09/14/19	Cesium-137	0.000491	0.000876	0.00161	U	PCI/G
MB	09/14/19	Cobalt-60	-0.0000373	0.000839	0.00157	U	PCI/G
MB	09/14/19	Europium-152	0.0000892	0.00243	0.0044	U	PCI/G
MB	09/14/19	Europium-154	-0.000499	0.00263	0.00449	U	PCI/G
MB	09/14/19	Europium-155	-0.000984	0.00289	0.00485	U	PCI/G
MB	09/14/19	Holmium-166m	-0.000448	0.0014	0.00243	U	PCI/G
MB	09/14/19	Lead-210	0.0327	0.405	0.243	U	PCI/G
MB	09/14/19	Lead-212	-0.000982	0.00237	0.00291	U	PCI/G
MB	09/14/19	Lead-214	0.000969	0.00438	0.00375	U	PCI/G
MB	09/14/19	Neptunium-239	0.00293	0.00759	0.0121	U	PCI/G
MB	09/14/19	Niobium-94	-0.000215	0.000806	0.0014	U	PCI/G
MB	09/14/19	Potassium-40	-0.0163	0.0185	0.0242	U	PCI/G
MB	09/14/19	Promethium-147	-1.86	19.7	33.3	U	PCI/G
MB	09/14/19	Protactinium-231	-0.00488	0.0113	0.0201	U	PCI/G
MB	09/14/19	Radium-226	0.00023	0.00447	0.00318	U	PCI/G
MB	09/14/19	Radium-228	0.00172	0.00891	0.0074	U	PCI/G
MB	09/14/19	Sodium-22	0.000207	0.000906	0.00161	U	PCI/G
MB	09/14/19	Tellurium-125m	-0.0492	0.241	0.376	U	PCI/G
MB	09/14/19	Thallium-208	0.000223	0.00199	0.00142	U	PCI/G
MB	09/14/19	Thorium-231	-0.00181	0.0167	0.0271	U	PCI/G
MB	09/14/19	Thorium-234	0.0221	0.0978	0.0685	U	PCI/G
MB	09/14/19	Thulium-171	-1.03	1.08	1.14	U	PCI/G
MB	09/14/19	Tin-126	-0.000176	0.00207	0.00352	U	PCI/G
MB	09/30/19	Iodine-129	0.288	0.492	0.932	U	PCI/G

Table B-1. Complete Results from the GEL Laboratory

Sample no.	Analysis date	Parameter	Result	Uncertainty	MDC[a]	Qualifier[b]	Units
MB	09/30/19	Iodine-129	0.288	0.492	0.932	U	PCI/G
MB	09/25/19	Technetium-99	0.0693	0.297	0.503	U	PCI/G
MB	09/25/19	Strontium-90	-0.00587	0.00783	0.0147	U	PCI/G
MB	09/25/19	Yttrium-90	-0.00587	0.00783	0.0147	U	PCI/G
MB	09/28/19	Nickel-63	-0.192	0.272	0.472	U	PCI/G
MB	09/27/19	Nickel-63	0.493	0.426	0.711	U	PCI/G
MB	09/26/19	Actinium-225	-0.00142	0.0198	0.0365	U	PCI/G
MB	09/26/19	Actinium-227	0.00437	0.0127	0.0239	U	PCI/G
MB	09/26/19	Actinium-228	0.0153	0.0147	0.0181	U	PCI/G
MB	09/26/19	Antimony-125	-0.0029	0.00458	0.00774	U	PCI/G
MB	09/26/19	Barium-137m	-0.000358	0.00177	0.0029	U	PCI/G
MB	09/26/19	Bismuth-212	0.00447	0.0257	0.0493	U	PCI/G
MB	09/26/19	Bismuth-213	-0.00338	0.00573	0.0097	U	PCI/G
MB	09/26/19	Bismuth-214	0	0.00826	0.00592	UI	PCI/G
MB	09/26/19	Cesium-134	-0.000351	0.00172	0.00322	U	PCI/G
MB	09/26/19	Cesium-137	-0.000378	0.00186	0.00306	U	PCI/G
MB	09/26/19	Cobalt-60	0.00123	0.00189	0.00396	U	PCI/G
MB	09/26/19	Europium-152	-0.000776	0.00469	0.00843	U	PCI/G
MB	09/26/19	Europium-154	0.00407	0.00527	0.0112	U	PCI/G
MB	09/26/19	Europium-155	-0.000575	0.00549	0.00944	U	PCI/G
MB	09/26/19	Holmium-166m	0.00172	0.00296	0.00582	U	PCI/G
MB	09/26/19	Lead-210	0.282	0.495	0.927	U	PCI/G
MB	09/26/19	Lead-212	0.000526	0.00538	0.00714	U	PCI/G
MB	09/26/19	Lead-214	0.00242	0.00618	0.00758	U	PCI/G
MB	09/26/19	Neptunium-239	0.00507	0.0136	0.0241	U	PCI/G
MB	09/26/19	Niobium-94	0.00102	0.00168	0.00336	U	PCI/G
MB	09/26/19	Potassium-40	-0.00554	0.0265	0.0476	U	PCI/G
MB	09/26/19	Promethium-147	21.8	38.7	69.5	U	PCI/G
MB	09/26/19	Protactinium-231	0.00205	0.0245	0.0449	U	PCI/G
MB	09/26/19	Radium-226	0	0.00826	0.00592	UI	PCI/G
MB	09/26/19	Radium-228	0.0153	0.0147	0.0181	U	PCI/G
MB	09/26/19	Sodium-22	0.000944	0.00198	0.00401	U	PCI/G
MB	09/26/19	Tellurium-125m	-0.0422	0.518	0.886	U	PCI/G
MB	09/26/19	Thallium-208	0.00128	0.00415	0.00295	U	PCI/G
MB	09/26/19	Thorium-231	-0.0069	0.0312	0.056	U	PCI/G
MB	09/26/19	Thorium-234	0.0229	0.197	0.15	U	PCI/G
MB	09/26/19	Thulium-171	1.55	3.75	3.39	U	PCI/G
MB	09/26/19	Tin-126	0.00125	0.00437	0.00722	U	PCI/G
MB	09/27/19	Actinium-225	0.00365	0.0165	0.0285	U	PCI/G
MB	09/27/19	Actinium-227	0.0029	0.0113	0.0195	U	PCI/G
MB	09/27/19	Actinium-228	0.0048	0.00841	0.0115	U	PCI/G
MB	09/27/19	Antimony-125	-0.00655	0.00709	0.00634	U	PCI/G
MB	09/27/19	Barium-137m	-0.000402	0.00133	0.00236	U	PCI/G
MB	09/27/19	Bismuth-212	0.00506	0.0221	0.0372	U	PCI/G
MB	09/27/19	Bismuth-213	-0.00156	0.00377	0.00677	U	PCI/G
MB	09/27/19	Bismuth-214	0.00202	0.00733	0.00616	U	PCI/G
MB	09/27/19	Cesium-134	0.000549	0.0015	0.00287	U	PCI/G
MB	09/27/19	Cesium-137	-0.000425	0.0014	0.0025	U	PCI/G
MB	09/27/19	Cobalt-60	-0.0000658	0.00138	0.00269	U	PCI/G
MB	09/27/19	Europium-152	-0.00184	0.00367	0.00659	U	PCI/G
MB	09/27/19	Europium-154	-0.0027	0.00413	0.00626	U	PCI/G
MB	09/27/19	Europium-155	0.000257	0.00434	0.0076	U	PCI/G
MB	09/27/19	Holmium-166m	-0.0012	0.00211	0.00364	U	PCI/G
MB	09/27/19	Lead-210	0.25	0.482	0.404	U	PCI/G
MB	09/27/19	Lead-212	-0.0018	0.00324	0.0046	U	PCI/G
MB	09/27/19	Lead-214	-0.00196	0.00376	0.00527	U	PCI/G
MB	09/27/19	Neptunium-239	0.000122	0.0117	0.0203	U	PCI/G
MB	09/27/19	Niobium-94	2.47E-06	0.00134	0.00244	U	PCI/G
MB	09/27/19	Potassium-40	0.00887	0.0245	0.0221	U	PCI/G
MB	09/27/19	Promethium-147	-0.0724	29.8	51.8	U	PCI/G

Table B-1. Complete Results from the GEL Laboratory

Sample no.	Analysis date	Parameter	Result	Uncertainty	MDC[a]	Qualifier[b]	Units
MB	09/27/19	Protactinium-231	-0.0025	0.0175	0.0324	U	PCI/G
MB	09/27/19	Radium-226	0.00202	0.00733	0.00616	U	PCI/G
MB	09/27/19	Radium-228	0.0048	0.00841	0.0115	U	PCI/G
MB	09/27/19	Sodium-22	-0.00119	0.00148	0.00215	U	PCI/G
MB	09/27/19	Tellurium-125m	-0.0902	0.385	0.66	U	PCI/G
MB	09/27/19	Thallium-208	-0.000631	0.00206	0.00295	U	PCI/G
MB	09/27/19	Thorium-231	-0.0092	0.0229	0.0416	U	PCI/G
MB	09/27/19	Thorium-234	0.0523	0.136	0.156	U	PCI/G
MB	09/27/19	Thulium-171	-0.595	1.29	1.9	U	PCI/G
MB	09/27/19	Tin-126	-0.00108	0.00346	0.00545	U	PCI/G
MB	09/28/19	Iodine-129	0.22	0.486	0.904	U	PCI/G
MB	09/28/19	Iodine-129	0.22	0.486	0.904	U	PCI/G
MB	09/29/19	Iodine-129	0.293	0.313	0.73	U	PCI/G
MB	10/02/19	Polonium-210	-0.00874	0.0413	0.0934	U	PCI/G
MB	09/30/19	Thorium-228	0.0914	0.069	0.102	U	PCI/G
MB	09/30/19	Thorium-229	0.076	0.0543	0.0728		PCI/G
MB	09/30/19	Thorium-230	0.0217	0.0541	0.0959	U	PCI/G
MB	09/30/19	Thorium-232	0.0108	0.0299	0.0517	U	PCI/G
MB	09/28/19	Uranium-232	0.00571	0.0447	0.0813	U	PCI/G
MB	09/28/19	Uranium-233/234	0.00219	0.0216	0.0413	U	PCI/G
MB	09/28/19	Uranium-235/236	0.0288	0.0226	0.0276		PCI/G
MB	09/28/19	Uranium-238	-0.00574	0.0251	0.0508	U	PCI/G
MB	10/01/19	Neptunium-236	-0.00091	0.00723	0.0163	U	PCI/G
MB	10/01/19	Plutonium-236	-0.00091	0.00723	0.0163	U	PCI/G
MB	10/01/19	Plutonium-239/240	0.000822	0.00798	0.0163	U	PCI/G
MB	10/01/19	Plutonium-242	-0.0138	0.00969	0.0271	U	PCI/G
MB	10/01/19	Plutonium-244	0.00432	0.0072	0.0102	U	PCI/G
MB	10/01/19	Neptunium-237	0.00113	0.0118	0.0247	U	PCI/G
MB	10/04/19	Plutonium-241	0.556	1.7	2.91	U	PCI/G
MB	09/28/19	Iron-55	-0.308	1.99	2.88	U	PCI/G
MB	09/26/19	Iron-55	1.04	1.55	2.18	U	PCI/G
MB	09/30/19	Iron-55	-0.918	1.6	2.32	U	PCI/G
MB	09/26/19	Iron-55	0.595	1.49	2.14	U	PCI/G
MB	09/26/19	Nickel-63	-0.000638	0.393	0.675	U	PCI/G
MB	09/28/19	Nickel-63	0.192	0.423	0.719	U	PCI/G
MB	09/26/19	Technetium-99	-0.00322	0.24	0.409	U	PCI/G
MB	09/26/19	Technetium-99	-0.00322	0.24	0.409	U	PCI/G
MB	09/25/19	Technetium-99	0.163	0.333	0.562	U	PCI/G
MB	09/28/19	Tritium	2.52	2.14	3.54	U	PCI/G
MB	09/28/19	Tritium	-0.313	2.03	3.7	U	PCI/G
MB	09/28/19	Tritium	-0.313	2.03	3.7	U	PCI/G
MB	09/27/19	Tritium	-1.01	2.03	3.82	U	PCI/G
MB	09/26/19	Carbon-14	1.02	1.35	2.28	U	PCI/G
MB	09/28/19	Carbon-14	0.579	1.45	2.49	U	PCI/G
MB	09/28/19	Carbon-14	0.579	1.45	2.49	U	PCI/G
MB	09/27/19	Carbon-14	1.25	1.71	2.9	U	PCI/G
MB	09/27/19	Nickel-59	-0.294	0.307	0.457	U	PCI/G
MB	09/26/19	Nickel-59	-0.0604	0.363	0.764	U	PCI/G
MB	09/30/19	Nickel-59	0.141	0.68	1.23	U	PCI/G
MB	09/26/19	Strontium-90	-0.00324	0.00412	0.00742	U	PCI/G
MB	09/26/19	Yttrium-90	-0.00324	0.00412	0.00742	U	PCI/G
MB	10/02/19	Nickel-59	0.723	0.774	0.96	U	PCI/G
MB	10/05/19	Strontium-90	-0.00226	0.00787	0.0148	U	PCI/G
MB	10/05/19	Yttrium-90	-0.00226	0.00787	0.0148	U	PCI/G
MB	10/03/19	Americium-241	0.00863	0.0136	0.0204	U	PCI/G
MB	10/03/19	Americium-243	0.00833	0.0163	0.0281	U	PCI/G
MB	10/03/19	Curium-243/244	-0.00287	0.00741	0.0201	U	PCI/G
MB	10/03/19	Curium-245/246	0.00652	0.0115	0.00977	U	PCI/G
MB	10/07/19	Strontium-90	-0.0174	0.00708	0.0142	U	PCI/G
MB	10/07/19	Yttrium-90	-0.0174	0.00708	0.0142	U	PCI/G
MB	10/07/19	Strontium-90	-0.0174	0.00708	0.0142	U	PCI/G
MB	10/07/19	Yttrium-90	-0.0174	0.00708	0.0142	U	PCI/G

Table B-1. Complete Results from the GEL Laboratory

Sample no.	Analysis date	Parameter	Result	Uncertainty	MDC[a]	Qualifier[b]	Units
MB	10/05/19	Thorium-228	0.0217	0.0874	0.16	U	PCI/G
MB	10/05/19	Thorium-229	-0.0516	0.079	0.17	U	PCI/G
MB	10/05/19	Thorium-230	0.0514	0.0582	0.0821	U	PCI/G
MB	10/05/19	Thorium-232	0.00855	0.0375	0.0654	U	PCI/G
MB	10/06/19	Americium-241	0.00145	0.00637	0.0111	U	PCI/G
MB	10/06/19	Americium-243	-0.00875	0.0157	0.0335	U	PCI/G
MB	10/06/19	Curium-243/244	2.39E-10	0.00561	0.011	U	PCI/G
MB	10/06/19	Curium-245/246	0.00407	0.00976	0.0156	U	PCI/G
MB	10/05/19	Americium-241	0.00208	0.0122	0.023	U	PCI/G
MB	10/05/19	Americium-243	-0.00157	0.0141	0.0278	U	PCI/G
MB	10/05/19	Curium-243/244	0	0.00568	0.00615	U	PCI/G
MB	10/05/19	Curium-245/246	0	0.00506	0.00547	U	PCI/G
MB	10/08/19	Strontium-90	-0.0121	0.00604	0.0113	U	PCI/G
MB	10/08/19	Yttrium-90	-0.0121	0.00604	0.0113	U	PCI/G

MB = Method blank

LCS = Laboratory control sample

[a] Minimum detectable concentration

[b] Qualifier flag:

U = Analyte was analyzed for, but not detected above, the MDL, MDA, MDC, or LOD.

UI = Gamma Spectroscopy – uncertain identification.

X = Consult case narrative (see Table B-2).

Table B-2. Case Narrative Description for GEL Samples with X Qualifier

Sample no.	Analysis_date	Radionuclide	Case Narative
11 C	09/30/19	Plutonium-244	Pu-244 result may be biased high due to tailing from the Pu-242 tracer ROI
16 B	10/06/19	Curium-245/246	Result may be biased high due to the zero Cm-245/246 background of the detector biasing the MDC low
16 C	10/06/19	Curium-245/246	Result may be biased high due to the zero Cm-245/246 background of the detector biasing the MDC low
3 A	09/30/19	Plutonium-244	Pu-244 result may be biased high due to tailing from the Pu-242 tracer ROI
3 C	09/30/19	Plutonium-244	Pu-244 result may be biased high due to tailing from the Pu-242 tracer ROI
4 A	10/01/19	Plutonium-244	Pu-244 result may be biased high due to tailing from the Pu-242 tracer ROI
4 A	10/05/19	Americium-243	Result may be biased high due to the zero Am-243 background of the detector biasing the MDC low
4 B	10/05/19	Curium-245/246	Result may be biased high due to the zero Cm-245/246 background of the detector biasing the MDC low
5 A	10/02/19	Plutonium-244	Pu-244 result may be biased high due to tailing from the Pu-242 tracer ROI
5 C	10/01/19	Plutonium-244	Pu-244 result may be biased high due to tailing from the Pu-242 tracer ROI

Table B-3. Complete Results from Test America Laboratory for Sample 2 Split

Sample no.	Analysis date	Parameter	Result	Uncertainty	MDC	Qualifier	Units
2A-S	9/23/19	Pu-242	0.00501	0.0142	0.0277	U	pCi/g
2A-S	10/1/19	Bismuth-212	1.55	0.237	0.212		pCi/g
2A-S	10/1/19	Bismuth-214	1.38	0.148	0.0312		pCi/g
2A-S	10/1/19	Cesium-134	0.00391	0.00424	0.0371	U	pCi/g
2A-S	10/1/19	Cesium-137	0.0713	0.0197	0.0194		pCi/g
2A-S	10/1/19	Cobalt-60	-0.0169	0.00846	0.0251	U	pCi/g
2A-S	10/1/19	Europium-152	0.00994	0.0178	0.068	U	pCi/g
2A-S	10/1/19	Europium-154	0.0219	0.0301	0.0426		pCi/g
2A-S	10/1/19	Europium-155	0.111	0.0474	0.0589		pCi/g
2A-S	10/1/19	Lead-210	1.29	0.605	0.791		pCi/g
2A-S	10/1/19	Lead-212	1.59	0.171	0.0322		pCi/g
2A-S	10/1/19	Lead-214	1.46	0.154	0.0385		pCi/g
2A-S	10/1/19	Neptunium-237	0	0.328	0.541	U G	pCi/g
2A-S	10/1/19	Niobium-94	0.00197	0.0203	0.0228	U	pCi/g
2A-S	10/1/19	Potassium-40	20.5	2.14	0.183		pCi/g
2A-S	10/1/19	Protactinium-231	-0.258	0.758	1.25	U	pCi/g
2A-S	10/1/19	Radium-224	1.59	0.171	0.0322		pCi/g
2A-S	10/1/19	Radium-226	1.38	0.148	0.0312		pCi/g
2A-S	10/1/19	Radium-228	1.46	0.162	0.066		pCi/g
2A-S	10/1/19	Sodium-22	0.014	0.015	0.0245		pCi/g
2A-S	10/1/19	Thallium-208	0.508	0.0588	0.0214		pCi/g
2A-S	10/1/19	Thorium-231	0.0748	0.0901	0.115		pCi/g
2A-S	10/1/19	Thorium-234	1.09	0.258	0.361		pCi/g
2A-S	9/18/19	H-3	-0.107	0.133	0.243	U	pCi/g
2A-S	9/6/19	Percent Moisture	1.8		0.1		%
2A-S	9/6/19	Percent Solids	98.2		0.1		%
2A-S	9/20/19	Sr-90	0.178	0.162	0.262		pCi/g
2A-S	10/16/19	Fe-55	-0.119	1.37	2.36	U	pCi/g
2A-S	10/16/19	Ni-59	0.273	1.06	1.72	U	pCi/g
2A-S	10/16/19	Ni-63	0.791	1.16	1.91	U	pCi/g
2A-S	10/9/19	Pu-241	1.65	1.39	2.28		pCi/g
2A-S	10/2/19	Tc-99	-0.239	0.181	0.312	U	pCi/g
2B-S	9/23/19	Pu-242	0.00735	0.011	0.0187		pCi/g
2B-S	9/23/19	Np-237	0.00491	0.012	0.0235	U	pCi/g
2B-S	9/23/19	Am-243	0.0136	0.0137	0.0102		pCi/g
2B-S	9/23/19	Cm-245/246	0.00342	0.00685	0.0103	U	pCi/g
2B-S	9/23/19	Cm-247/248	0.0141	0.0173	0.027		pCi/g
2B-S	9/23/19	Th-229	0	0.0282	0.0563	U	pCi/g
2B-S	9/24/19	U-233/U-234	1.01	0.178	0.0569		pCi/g
2B-S	9/24/19	U-235/U-236	0.0222	0.0392	0.0709	U	pCi/g
2B-S	9/24/19	U-238	1.05	0.182	0.0454		pCi/g
2B-S	9/24/19	Am-241	0.0133	0.0134	0.00999		pCi/g
2B-S	9/24/19	Cm-242	0	0.00653	0.00979	U	pCi/g
2B-S	9/24/19	Cm-243/244	-0.00326	0.00654	0.025	U	pCi/g
2B-S	9/24/19	Th-227	0.126	0.059	0.02		pCi/g
2B-S	9/24/19	Th-228	1.3	0.179	0.0532		pCi/g
2B-S	9/24/19	Th-230	0.957	0.152	0.0761		pCi/g
2B-S	9/24/19	Th-232	1.23	0.169	0.0273		pCi/g
2B-S	9/24/19	Pu-236	-0.00962	0.00965	0.0296	U	pCi/g
2B-S	9/24/19	Pu-244	0.00719	0.00832	0.00719		pCi/g
2B-S	9/24/19	Pu-239/240	0.0144	0.0137	0.0184		pCi/g
2B-S	9/24/19	Pu-238	0.0048	0.0118	0.023	U	pCi/g
2B-S	10/3/19	Po-210	0.562	0.0877	0.0229		pCi/g
2B-S	10/10/19	U-232	-0.00917	0.0392	0.0759	U	pCi/g
2B-S	9/18/19	C-14	0.495	0.561	0.918		pCi/g
2B-S	9/27/19	Iodine-129	-0.237	0.82	1.37	U	pCi/g
2B-S	10/1/19	Actinium-227	0.0729	0.0562	0.16	U	pCi/g
2B-S	10/1/19	Actinium-228	1.37	0.149	0.0637		pCi/g
2B-S	10/1/19	Antimony-125	-0.00132	0.0361	0.0441	U	pCi/g
2B-S	10/1/19	Bismuth-212	1.62	0.261	0.184		pCi/g

Table B-3. Complete Results from Test America Laboratory for Sample 2 Split

Sample no.	Analysis date	Parameter	Result	Uncertainty	MDC	Qualifier	Units
2B-S	10/1/19	Bismuth-214	1.28	0.141	0.03		pCi/g
2B-S	10/1/19	Cesium-134	0.000974	0.0015	0.0278	U	pCi/g
2B-S	10/1/19	Cesium-137	0.053	0.0119	0.0149		pCi/g
2B-S	10/1/19	Cobalt-60	-0.00389	0.0297	0.02	U	pCi/g
2B-S	10/1/19	Europium-152	0.0182	0.0363	0.0441	U	pCi/g
2B-S	10/1/19	Europium-154	0.0281	0.0384	0.03		pCi/g
2B-S	10/1/19	Europium-155	0.0883	0.0311	0.0387		pCi/g
2B-S	10/1/19	Lead-210	1.25	0.282	0.301		pCi/g
2B-S	10/1/19	Lead-212	1.48	0.194	0.0274		pCi/g
2B-S	10/1/19	Lead-214	1.38	0.149	0.0347		pCi/g
2B-S	10/1/19	Neptunium-237	0.0327	0.189	0.312	U	pCi/g
2B-S	10/1/19	Niobium-94	0.0149	0.0142	0.0161		pCi/g
2B-S	10/1/19	Potassium-40	19.6	2.07	0.169		pCi/g
2B-S	10/1/19	Protactinium-231	0	0.105	1.15	U	pCi/g
2B-S	10/1/19	Radium-224	1.48	0.194	0.0274		pCi/g
2B-S	10/1/19	Radium-226	1.28	0.141	0.03		pCi/g
2B-S	10/1/19	Radium-228	1.37	0.149	0.0637		pCi/g
2B-S	10/1/19	Sodium-22	0.0164	0.0163	0.0177		pCi/g
2B-S	10/1/19	Thallium-208	0.494	0.0567	0.0175		pCi/g
2B-S	10/1/19	Thorium-231	0.0925	0.0495	0.0743		pCi/g
2B-S	10/1/19	Thorium-234	0.781	0.161	0.209		pCi/g
2B-S	9/18/19	H-3	-0.0679	0.138	0.246	U	pCi/g
2B-S	9/6/19	Percent Moisture	2.5		0.1		%
2B-S	9/6/19	Percent Solids	97.5		0.1		%
2B-S	9/20/19	Sr-90	0.213	0.143	0.224		pCi/g
2B-S	10/16/19	Fe-55	-0.0271	1.5	2.63	U	pCi/g
2B-S	10/16/19	Ni-59	0.561	1.08	1.71	U	pCi/g
2B-S	10/16/19	Ni-63	1	1.15	1.88		pCi/g
2B-S	10/9/19	Pu-241	1.65	0.863	1.35		pCi/g
2B-S	10/2/19	Tc-99	-0.103	0.163	0.278	U	pCi/g
2C-S	9/23/19	Pu-242	0.0116	0.0202	0.0358	U	pCi/g
2C-S	9/23/19	Np-237	0.00873	0.021	0.039	U	pCi/g
2C-S	9/23/19	Am-243	-0.00404	0.00809	0.0309	U	pCi/g
2C-S	9/23/19	Cm-245/246	0	0.00811	0.0122	U	pCi/g
2C-S	9/23/19	Cm-247/248	0.00836	0.0167	0.032	U	pCi/g
2C-S	9/23/19	Th-229	-0.0104	0.0121	0.0385	U	pCi/g
2C-S	9/24/19	U-233/U-234	1.06	0.204	0.0994		pCi/g
2C-S	9/24/19	U-235/U-236	0.0462	0.049	0.0707		pCi/g
2C-S	9/24/19	U-238	0.844	0.186	0.131	G	pCi/g
2C-S	9/24/19	Am-241	0.00303	0.0105	0.0232	U	pCi/g
2C-S	9/24/19	Cm-242	-0.00297	0.00595	0.0227	U	pCi/g
2C-S	9/24/19	Cm-243/244	0	0.00595	0.00892	U	pCi/g
2C-S	9/24/19	Th-227	0.0764	0.0441	0.0418		pCi/g
2C-S	9/24/19	Th-228	1.36	0.173	0.0467		pCi/g
2C-S	9/24/19	Th-230	0.859	0.133	0.064		pCi/g
2C-S	9/24/19	Th-232	1.17	0.154	0.0332		pCi/g
2C-S	9/24/19	Pu-236	0	0.00946	0.0226	U	pCi/g
2C-S	9/24/19	Pu-244	0.00471	0.0116	0.0226	U	pCi/g
2C-S	9/24/19	Pu-239/240	0.00709	0.0125	0.0226	U	pCi/g
2C-S	9/24/19	Pu-238	0.00709	0.0157	0.0291	U	pCi/g
2C-S	10/3/19	Po-210	0.494	0.0839	0.0419		pCi/g
2C-S	10/10/19	U-232	-0.0112	0.0225	0.0497	U	pCi/g
2C-S	9/18/19	C-14	1.05	0.577	0.895		pCi/g
2C-S	9/27/19	Iodine-129	0.256	0.974	1.62	U	pCi/g
2C-S	10/1/19	Actinium-227	0.0579	0.0952	0.251	U	pCi/g
2C-S	10/1/19	Actinium-228	1.56	0.171	0.0614		pCi/g
2C-S	10/1/19	Antimony-125	0.0162	0.069	0.0589	U	pCi/g
2C-S	10/1/19	Bismuth-212	1.65	0.249	0.217		pCi/g
2C-S	10/1/19	Bismuth-214	1.42	0.156	0.0381		pCi/g
2C-S	10/1/19	Cesium-134	0.0948	0.0237	0.0209		pCi/g
2C-S	10/1/19	Cesium-137	0.0731	0.0236	0.023		pCi/g

Table B-3. Complete Results from Test America Laboratory for Sample 2 Split

Sample no.	Analysis date	Parameter	Result	Uncertainty	MDC	Qualifier	Units
2C-S	10/1/19	Cobalt-60	0.0138	0.0202	0.0209		pCi/g
2C-S	10/1/19	Europium-152	0.0368	0.0359	0.0705		pCi/g
2C-S	10/1/19	Europium-154	0.0155	0.0274	0.0442	U	pCi/g
2C-S	10/1/19	Europium-155	0.138	0.0563	0.0664		pCi/g
2C-S	10/1/19	Lead-210	1.35	0.668	0.856		pCi/g
2C-S	10/1/19	Lead-212	1.71	0.183	0.0305		pCi/g
2C-S	10/1/19	Lead-214	1.54	0.162	0.0425		pCi/g
2C-S	10/1/19	Neptunium-237	0	0.352	0.582	U G	pCi/g
2C-S	10/1/19	Niobium-94	-0.00464	0.0205	0.0244	U	pCi/g
2C-S	10/1/19	Potassium-40	21.1	2.21	0.192		pCi/g
2C-S	10/1/19	Protactinium-231	-0.258	0.975	1.61	U	pCi/g
2C-S	10/1/19	Radium-224	1.71	0.183	0.0305		pCi/g
2C-S	10/1/19	Radium-226	1.42	0.156	0.0381		pCi/g
2C-S	10/1/19	Radium-228	1.56	0.171	0.0614		pCi/g
2C-S	10/1/19	Sodium-22	-0.0171	0.0189	0.0309	U	pCi/g
2C-S	10/1/19	Thallium-208	0.539	0.0639	0.0248		pCi/g
2C-S	10/1/19	Thorium-231	0.138	0.0818	0.107		pCi/g
2C-S	10/1/19	Thorium-234	1.02	0.268	0.381		pCi/g
2C-S	9/18/19	H-3	-0.0304	0.141	0.249	U	pCi/g
2C-S	9/6/19	Percent Moisture	3.6		0.1		%
2C-S	9/6/19	Percent Solids	96.4		0.1		%
2C-S	9/20/19	Sr-90	0.041	0.161	0.275	U	pCi/g
2C-S	10/16/19	Ni-59	-0.56	0.991	1.7	U	pCi/g
2C-S	10/16/19	Ni-63	0.375	1.09	1.82	U	pCi/g
2C-S	10/16/19	Fe-55	0.259	1.6	2.78	U	pCi/g
2C-S	10/9/19	Pu-241	0.125	0.694	1.18	U	pCi/g
2C-S	10/2/19	Tc-99	-0.0731	0.143	0.243	U	pCi/g
2A-S	9/23/19	Pu-242	0.01104	0.0175	0.0305	U	pCi/g
2A-S	9/23/19	Np-237	0.01106	0.0175	0.0306	U	pCi/g
2A-S	9/23/19	Am-243	-0.007548	0.0107	0.0362	U	pCi/g
2A-S	9/23/19	Cm-245/246	0	0.0107	0.029	U	pCi/g
2A-S	9/23/19	Cm-247/248	-0.003905	0.00782	0.0299	U	pCi/g
2A-S	9/23/19	Th-229	0.03028	0.0216	0.0114		pCi/g
2A-S	9/24/19	U-233/U-234	0.9038	0.185	0.0728		pCi/g
2A-S	9/24/19	U-235/U-236	0.06615	0.0503	0.0284		pCi/g
2A-S	9/24/19	U-238	1.038	0.199	0.058		pCi/g
2A-S	9/24/19	Am-241	0.01882	0.0227	0.0361		pCi/g
2A-S	9/24/19	Cm-242	-0.003686	0.0165	0.0408	U	pCi/g
2A-S	9/24/19	Cm-243/244	-0.003688	0.00739	0.0282	U	pCi/g
2A-S	9/24/19	Th-227	0.1159	0.0584	0.0493		pCi/g
2A-S	9/24/19	Th-228	1.316	0.178	0.052		pCi/g
2A-S	9/24/19	Th-230	1.02	0.156	0.0703		pCi/g
2A-S	9/24/19	Th-232	1.217	0.166	0.0267		pCi/g
2A-S	9/24/19	Pu-236	0	0.00758	0.0205	U	pCi/g
2A-S	9/24/19	Pu-244	0.01602	0.0152	0.0204		pCi/g
2A-S	9/24/19	Pu-239/240	0.008035	0.0178	0.033	U	pCi/g
2A-S	9/24/19	Pu-238	0.0107	0.0152	0.0256		pCi/g
2A-S	10/3/19	Po-210	0.6302	0.0995	0.0426		pCi/g
2A-S	10/10/19	U-232	0.005667	0.034	0.0629	U	pCi/g
2A-S	9/17/19	C-14	0.364	0.559	0.923	U	pCi/g
2A-S	9/28/19	Iodine-129	0	0.326	1.53	U	pCi/g
2A-S	10/1/19	Actinium-227	-0.0693	0.121	0.2	U	pCi/g
2A-S	10/1/19	Actinium-228	1.553	0.167	0.0556		pCi/g
2A-S	10/1/19	Americium-241	0.01662	0.0396	0.0653	U	pCi/g
2A-S	10/1/19	Antimony-125	0.01292	0.0443	0.0429	U	pCi/g
2A-S	10/1/19	Bismuth-212	1.576	0.215	0.169		pCi/g
2A-S	10/1/19	Bismuth-214	1.338	0.144	0.0315		pCi/g
2A-S	10/1/19	Cesium-134	0.08076	0.0224	0.0185		pCi/g
2A-S	10/1/19	Cesium-137	0.06322	0.0179	0.0166		pCi/g
2A-S	10/1/19	Cobalt-60	-0.0122	0.02	0.0201	U	pCi/g

Table B-3. Complete Results from Test America Laboratory for Sample 2 Split

Sample no.	Analysis date	Parameter	Result	Uncertainty	MDC	Qualifier	Units
2A-S	10/1/19	Europium-152	-0.02099	0.059	0.0975	U	pCi/g
2A-S	10/1/19	Europium-154	0.01065	0.0282	0.0331	U	pCi/g
2A-S	10/1/19	Europium-155	0.09216	0.0323	0.0404		pCi/g
2A-S	10/1/19	Lead-210	1.435	0.339	0.356		pCi/g
2A-S	10/1/19	Lead-212	1.602	0.17	0.0222		pCi/g
2A-S	10/1/19	Lead-214	1.455	0.152	0.0283		pCi/g
2A-S	10/1/19	Neptunium-237	0	0.204	0.336	U	pCi/g
2A-S	10/1/19	Niobium-94	0.01615	0.00818	0.0113		pCi/g
2A-S	10/1/19	Potassium-40	21.19	2.19	0.166		pCi/g
2A-S	10/1/19	Protactinium-231	-0.1784	0.733	1.21	U	pCi/g
2A-S	10/1/19	Radium-224	1.602	0.17	0.0222		pCi/g
2A-S	10/1/19	Radium-226	1.338	0.144	0.0315		pCi/g
2A-S	10/1/19	Radium-228	1.553	0.167	0.0556		pCi/g
2A-S	10/1/19	Sodium-22	0.01214	0.0197	0.0198		pCi/g
2A-S	10/1/19	Thallium-208	0.5015	0.0562	0.018		pCi/g
2A-S	10/1/19	Thorium-231	0.1177	0.0611	0.0862		pCi/g
2A-S	10/1/19	Thorium-234	0.9809	0.184	0.229		pCi/g
2A-S	9/18/19	H-3	0.02131	0.144	0.249	U	pCi/g
2A-S	9/6/19	Percent Moisture	1.8		0.1		%
2A-S	9/6/19	Percent Solids	98.2		0.1		%
2A-S	9/20/19	Sr-90	0.1336	0.149	0.244		pCi/g
2A-S	10/9/19	Pu-241	1.382	0.854	1.36		pCi/g
2A-S	10/2/19	Tc-99	-0.07105	0.156	0.264	U	pCi/g
2B-S	10/16/19	Fe-55	0.9805	1.59	2.72	U	pCi/g
2B-S	10/16/19	Ni-59	0.4817	1.09	1.78	U	pCi/g
2B-S	10/16/19	Ni-63	0.426	1.13	1.89	U	pCi/g
MB	10/1/19	Actinium-227	0.01172	0.0208	0.0435	U	pCi/g
MB	10/1/19	Actinium-228	0.006607	0.0118	0.0138		pCi/g
MB	10/1/19	Americium-241	0.002497	0.00561	0.00793	U	pCi/g
MB	10/1/19	Antimony-125	0.002135	0.00314	0.0138	U	pCi/g
MB	10/1/19	Bismuth-212	0.03024	0.0562	0.0939	U	pCi/g
MB	10/1/19	Bismuth-214	-0.0211	0.0115	0.0289	U	pCi/g
MB	10/1/19	Cesium-134	0.002381	0.00722	0.00826	U	pCi/g
MB	10/1/19	Cesium-137	-0.003303	0.00682	0.00874	U	pCi/g
MB	10/1/19	Cobalt-60	0.0002161	0.00597	0.00686	U	pCi/g
MB	10/1/19	Europium-152	0.0002797	0.000624	0.0237	U	pCi/g
MB	10/1/19	Europium-154	0.005856	0.0123	0.00779		pCi/g
MB	10/1/19	Europium-155	0	0.00361	0.0171	U	pCi/g
MB	10/1/19	Lead-210	-0.03349	0.0777	0.109	U	pCi/g
MB	10/1/19	Lead-212	-0.004769	0.00791	0.0132	U	pCi/g
MB	10/1/19	Lead-214	-0.006914	0.00871	0.0141	U	pCi/g
MB	10/1/19	Neptunium-237	0.007025	0.0236	0.0394	U	pCi/g
MB	10/1/19	Niobium-94	-0.0001432	0.000186	0.00622	U	pCi/g
MB	10/1/19	Potassium-40	-0.007605	0.0655	0.0845	U	pCi/g
MB	10/1/19	Protactinium-231	0.04191	0.146	0.245	U	pCi/g
MB	10/1/19	Radium-224	-0.004769	0.00791	0.0132	U	pCi/g
MB	10/1/19	Radium-226	-0.0211	0.0115	0.0289	U	pCi/g
MB	10/1/19	Radium-228	0.006607	0.0118	0.0138		pCi/g
MB	10/1/19	Sodium-22	-0.001575	0.00389	0.0067	U	pCi/g
MB	10/1/19	Thallium-208	0.006689	0.00422	0.00446		pCi/g
MB	10/1/19	Thorium-231	0.009053	0.019	0.0334	U	pCi/g
MB	10/1/19	Thorium-234	0.009272	0.0329	0.0605	U	pCi/g
MB	9/20/19	Sr-90	0.04688	0.178	0.305	U	pCi/g
MB	9/24/19	Am-241	0.009716	0.0103	0.0149		pCi/g
MB	9/24/19	Cm-242	0	0.00381	0.00571	U	pCi/g
MB	9/24/19	Cm-243/244	0.005713	0.00854	0.0146		pCi/g
MB	9/23/19	Am-243	0.003496	0.00857	0.0167	U	pCi/g
MB	9/23/19	Cm-245/246	0	0.00702	0.0168	U	pCi/g
MB	9/23/19	Cm-247/248	0.009044	0.0096	0.0138		pCi/g
MB	9/24/19	Th-227	0.02717	0.0287	0.0434		pCi/g
MB	9/24/19	Th-228	0.02434	0.0332	0.0433		pCi/g

Table B-3. Complete Results from Test America Laboratory for Sample 2 Split

Sample no.	Analysis date	Parameter	Result	Uncertainty	MDC	Qualifier	Units
MB	9/24/19	Th-230	-0.0196	0.0409	0.0575	U	pCi/g
MB	9/24/19	Th-232	0.0001928	0.0118	0.021	U	pCi/g
MB	9/24/19	U-233/U-234	-0.01257	0.0154	0.0421	U	pCi/g
MB	9/24/19	U-235/U-236	0.00391	0.0135	0.0299	U	pCi/g
MB	9/24/19	U-238	0.003135	0.0109	0.024	U	pCi/g
MB	9/23/19	Th-229	0.01982	0.0193	0.0295		pCi/g
MB	9/17/19	C-14	0.6982	0.566	0.91		pCi/g
MB	9/24/19	Pu-236	-0.01714	0.0219	0.0463	U	pCi/g
MB	9/24/19	Pu-244	0.005695	0.0085	0.0145		pCi/g
MB	9/24/19	Pu-239/240	0.01714	0.0148	0.0211		pCi/g
MB	9/24/19	Pu-238	0.01332	0.0183	0.0308		pCi/g
MB	9/23/19	Pu-242	0.003832	0.00767	0.0147	U	pCi/g
MB	9/23/19	Np-237	0.00384	0.00941	0.0184	U	pCi/g
MB	10/3/19	Po-210	0.03514	0.0208	0.0243		pCi/g
MB	10/9/19	Pu-241	0.2983	0.668	1.12	U	pCi/g
MB	9/17/19	H-3	-0.06563	0.135	0.241	U	pCi/g
MB	9/28/19	Iodine-129	0	0.494	1.88	U	pCi/g
MB	10/2/19	Tc-99	-0.07524	0.187	0.318	U	pCi/g
MB	10/10/19	U-232	-0.002028	0.0157	0.0328	U	pCi/g
MB	10/16/19	Fe-55	1.923	1.5	2.46		pCi/g
MB	10/16/19	Ni-59	-0.08678	0.944	1.59	U	pCi/g
MB	10/16/19	Ni-63	-0.009381	1.05	1.77	U	pCi/g
2A-S	9/23/19	Np-237	0.00502	0.0142	0.0278	U	pCi/g
2A-S	9/23/19	Am-243	0.00335	0.015	0.0321	U	pCi/g
2A-S	9/23/19	Cm-245/246	0.0101	0.0117	0.0101		pCi/g
2A-S	9/23/19	Cm-247/248	0.0104	0.0183	0.0332	U	pCi/g
2A-S	9/23/19	Th-229	0.03	0.0223	0.0255		pCi/g
2A-S	9/24/19	U-233/U-234	0.669	0.147	0.0725		pCi/g
2A-S	9/24/19	U-235/U-236	0.0163	0.0327	0.0624	U	pCi/g
2A-S	9/24/19	U-238	1.02	0.186	0.0501		pCi/g
2A-S	9/24/19	Am-241	0.00344	0.0154	0.0329	U	pCi/g
2A-S	9/24/19	Cm-242	0.00337	0.0117	0.0258	U	pCi/g
2A-S	9/24/19	Cm-243/244	0.00674	0.00955	0.0101	U	pCi/g
2A-S	9/24/19	Th-227	0.0721	0.0439	0.0197		pCi/g
2A-S	9/24/19	Th-228	1.38	0.185	0.0557		pCi/g
2A-S	9/24/19	Th-230	1	0.155	0.071		pCi/g
2A-S	9/24/19	Th-232	1.35	0.179	0.027		pCi/g
2A-S	9/24/19	Pu-236	-0.00426	0.0191	0.0471	U	pCi/g
2A-S	9/24/19	Pu-244	0.0127	0.0225	0.0407	U	pCi/g
2A-S	9/24/19	Pu-239/240	0.00426	0.0225	0.0471	U	pCi/g
2A-S	9/24/19	Pu-238	0	0.0295	0.0613	U	pCi/g
2A-S	10/3/19	Po-210	0.582	0.091	0.0384		pCi/g
2A-S	10/10/19	U-232	-0.0309	0.0285	0.068	U	pCi/g
2A-S	9/17/19	C-14	0.608	0.574	0.934		pCi/g
2A-S	9/27/19	Iodine-129	0	0.319	1.65	U	pCi/g
2A-S	10/1/19	Actinium-227	0.0204	0.0773	0.23	U	pCi/g
2A-S	10/1/19	Actinium-228	1.46	0.162	0.066		pCi/g
2A-S	10/1/19	Antimony-125	0.00544	0.0472	0.0571	U	pCi/g

MB = Method blank

[a] Minimum detectable concentration

[b] Qualifier flag:

U = Analyte was analyzed for, but not detected above, the decision level concentration (*Lc*).

G = The MDC was greater than the requested detection level.

Appendix C. Geographical Information Resources

Geographical information system data were obtained from multiple sources and, in many cases, were developed from geo-referenced satellite and other images.

Geographic Information System (GIS) coverages for the maps presented in this report were obtained from the following sites:

- USGS Terrain Data, Land Use, and Digital Line Maps (transportation, streams, rivers, and water bodies) were obtained from WebGIS (http://www.webgis.com)
- Coverages of the fire perimeter were obtained from the Los Angeles County GIS Data Portal https://egis3.lacounty.gov/dataportal/2018/11/21/woolsey-fire-nov-2018-gis-data-applications/ and from the California ARCGIS Hub (https://hub.arcgis.com/)
- Coverages of roads, streams, and water bodies were from the California Geoportal (https://gis.data.ca.gov).

The maps presented in the report were developed using the Surfer® Version 17 software (www.goldensoftware.com). Some of the GIS shapefiles obtained from the resources above were processed using ArcGIS software (www.esri.com). Coordinates of meteorological stations and air samplers and the data from them were provided by Boeing.

Appendix D. Statistical Analysis

Two-sample *t*-tests were performed between mean radionuclide concentrations for background samples taken in the Chatsworth formation (samples 1, 3, 4, and 5) and those taken in the Modelo formation and within the deposition plume (samples 8, 9, 13, 14, 15, and 18).
The two-sample t-test is given by (Huntsberger and Billingsley [1987]; StatTrek.com [2019]):

$$t_{cal} = \frac{\left(\bar{x}_1 - \bar{x}_2\right) - \xi}{\sqrt{\frac{\sigma_1^2}{n_1} + \frac{\sigma_2^2}{n_2}}} \qquad \text{D-1}$$

where

$\bar{x}_1$ and $\bar{x}_2$ = means of samples 1 and 2

σ_1 and σ_2 = standard deviations of samples 1 and 2

ξ = hypothesized difference between samples.

Tabulated *t* values (t_{tab}) are based on the pooled degrees of freedom given by:

$$df = \frac{\left(\frac{\sigma_1^2}{n_1} + \frac{\sigma_1^2}{n_1}\right)^2}{\left(\frac{\left(\sigma_1^2/n_1\right)^2}{n_1 - 1} + \frac{\left(\sigma_2^2/n_2\right)^2}{n_2 - 1}\right)} \qquad \text{D-2}$$

The soil concentrations by layer for ^{226}Ra, ^{228}Ra, ^{230}Th, ^{232}Th, ^{208}Tl, $^{233/234}$U, and ^{238}U are summarized in Table D-1.

Table D-1. Mean and Standard Deviation of Uranium and Thorium Decay Series Radionuclide Concentrations in Samples in the Modelo and Chatsworth Formations

Radionuclide	Location	0–3 cm (pCi g^{-1})	3–6 cm (pCi g^{-1})	6–12 cm (pCi g^{-1})	12-cm Weighted average (pCi g^{-1})
Modelo formation					
Ra-226	13	2.35E+00	2.26E+00	2.00E+00	2.15E+00
Ra-226	14	1.55E+00	1.47E+00	1.54E+00	1.53E+00
Ra-226	15	1.27E+00	1.23E+00	1.33E+00	1.29E+00
Ra-226	16	1.68E+00	1.53E+00	1.52E+00	1.56E+00
Ra-226	18	1.79E+00	1.76E+00	1.88E+00	1.83E+00
Mean		1.73E+00	1.65E+00	1.65E+00	1.67E+00
σ		3.98E-01	3.90E-01	2.77E-01	3.30E-01
n		5.00E+00	5.00E+00	5.00E+00	5.00E+00
Ra-228	13	1.25E+00	1.18E+00	1.15E+00	1.18E+00

Table D-1. Mean and Standard Deviation of Uranium and Thorium Decay Series Radionuclide Concentrations in Samples in the Modelo and Chatsworth Formations

Radionuclide	Location	0–3 cm (pCi g^{-1})	3–6 cm (pCi g^{-1})	6–12 cm (pCi g^{-1})	12-cm Weighted average (pCi g^{-1})
Ra-228	14	1.05E+00	9.94E-01	1.06E+00	1.04E+00
Ra-228	15	1.02E+00	1.01E+00	1.08E+00	1.05E+00
Ra-228	16	1.03E+00	9.22E-01	9.61E-01	9.69E-01
Ra-228	18	1.22E+00	1.24E+00	1.26E+00	1.25E+00
Mean		1.11E+00	1.07E+00	1.10E+00	1.10E+00
σ		1.11E-01	1.34E-01	1.11E-01	1.13E-01
n		5.00E+00	5.00E+00	5.00E+00	5.00E+00
Th-230	13	2.30E+00	2.37E+00	2.15E+00	2.24E+00
Th-230	14	1.52E+00	1.33E+00	1.23E+00	1.33E+00
Th-230	15	9.11E-01	1.12E+00	1.10E+00	1.06E+00
Th-230	16	1.71E+00	1.63E+00	1.57E+00	1.62E+00
Th-230	18	1.86E+00	1.82E+00	2.12E+00	1.98E+00
Mean		1.66E+00	1.65E+00	1.63E+00	1.65E+00
σ		5.08E-01	4.82E-01	4.89E-01	4.78E-01
n		5.00E+00	5.00E+00	5.00E+00	5.00E+00
Th-232	13	8.83E-01	8.32E-01	8.48E-01	8.53E-01
Th-232	14	8.29E-01	7.30E-01	6.15E-01	6.97E-01
Th-232	15	6.99E-01	7.64E-01	7.26E-01	7.29E-01
Th-232	16	8.61E-01	7.22E-01	7.67E-01	7.79E-01
Th-232	18	9.14E-01	7.72E-01	8.64E-01	8.54E-01
Mean		8.37E-01	7.64E-01	7.64E-01	7.82E-01
σ		8.33E-02	4.36E-02	1.01E-01	7.10E-02
n		5.00E+00	5.00E+00	5.00E+00	5.00E+00
Tl-208	13	4.13E-01	4.11E-01	3.49E-01	3.81E-01
Tl-208	14	3.08E-01	2.65E-01	2.96E-01	2.91E-01
Tl-208	15	3.07E-01	3.10E-01	3.25E-01	3.17E-01
Tl-208	16	3.22E-01	2.81E-01	3.06E-01	3.04E-01
Tl-208	18	3.69E-01	3.70E-01	3.74E-01	3.72E-01
Mean		3.44E-01	3.27E-01	3.30E-01	3.33E-01
σ		4.62E-02	6.15E-02	3.18E-02	4.07E-02
n		5.00E+00	5.00E+00	5.00E+00	5.00E+00
U-233/234	13	9.64E-01	8.24E-01	1.01E+00	9.52E-01
U-233/234	14	7.04E-01	8.31E-01	7.43E-01	7.55E-01
U-233/234	15	6.41E-01	6.60E-01	6.12E-01	6.31E-01
U-233/234	16	1.09E+00	1.05E+00	1.08E+00	1.08E+00
U-233/234	18	9.29E-01	9.24E-01	9.48E-01	9.37E-01

Table D-1. Mean and Standard Deviation of Uranium and Thorium Decay Series Radionuclide Concentrations in Samples in the Modelo and Chatsworth Formations

Radionuclide	Location	0–3 cm (pCi g^{-1})	3–6 cm (pCi g^{-1})	6–12 cm (pCi g^{-1})	12-cm Weighted average (pCi g^{-1})
Mean		8.66E-01	8.58E-01	8.79E-01	8.70E-01
σ		1.87E-01	1.43E-01	1.95E-01	1.76E-01
n		5.00E+00	5.00E+00	5.00E+00	5.00E+00
U-238	13	1.00E+00	7.95E-01	1.09E+00	9.94E-01
U-238	14	7.76E-01	6.91E-01	6.78E-01	7.06E-01
U-238	15	6.21E-01	6.70E-01	6.25E-01	6.35E-01
U-238	16	1.23E+00	1.28E+00	1.29E+00	1.27E+00
U-238	18	8.46E-01	9.01E-01	9.05E-01	8.89E-01
Mean		8.95E-01	8.67E-01	9.18E-01	8.99E-01
σ		2.32E-01	2.48E-01	2.79E-01	2.53E-01
n		5.00E+00	5.00E+00	5.00E+00	5.00E+00
Chatsworth formation					
Ra-226	1	1.15E+00	1.11E+00	1.16E+00	1.14E+00
Ra-226	3	1.45E+00	1.39E+00	1.50E+00	1.46E+00
Ra-226	4	1.03E+00	1.10E+00	1.12E+00	1.09E+00
Ra-226	5	1.31E+00	1.33E+00	1.17E+00	1.25E+00
Mean		1.24E+00	1.23E+00	1.24E+00	1.23E+00
σ		1.84E-01	1.51E-01	1.77E-01	1.63E-01
n		4.00E+00	4.00E+00	4.00E+00	4.00E+00
Ra-228	1	1.60E+00	1.66E+00	1.72E+00	1.67E+00
Ra-228	3	1.71E+00	1.86E+00	1.91E+00	1.85E+00
Ra-228	4	1.42E+00	1.50E+00	1.60E+00	1.53E+00
Ra-228	5	1.73E+00	1.99E+00	1.55E+00	1.71E+00
Mean		1.62E+00	1.75E+00	1.69E+00	1.69E+00
σ		1.42E-01	2.16E-01	1.60E-01	1.30E-01
n		4.00E+00	4.00E+00	4.00E+00	4.00E+00
Th-230	1	1.10E+00	1.31E+00	1.11E+00	1.16E+00
Th-230	3	1.24E+00	1.30E+00	1.44E+00	1.36E+00
Th-230	4	8.49E-01	1.01E+00	1.06E+00	9.95E-01
Th-230	5	1.09E+00	1.08E+00	1.26E+00	1.17E+00
Mean		1.07E+00	1.18E+00	1.22E+00	1.17E+00
σ		1.62E-01	1.54E-01	1.70E-01	1.47E-01
n		4.00E+00	4.00E+00	4.00E+00	4.00E+00
Th-232	1	1.21E+00	1.57E+00	1.14E+00	1.26E+00
Th-232	3	1.32E+00	1.25E+00	1.25E+00	1.27E+00
Th-232	4	1.12E+00	1.25E+00	1.18E+00	1.18E+00

Table D-1. Mean and Standard Deviation of Uranium and Thorium Decay Series Radionuclide Concentrations in Samples in the Modelo and Chatsworth Formations

Radionuclide	Location	0–3 cm (pCi g^{-1})	3–6 cm (pCi g^{-1})	6–12 cm (pCi g^{-1})	12-cm Weighted average (pCi g^{-1})
Th-232	5	1.30E+00	1.33E+00	1.33E+00	1.32E+00
Mean		1.24E+00	1.35E+00	1.23E+00	1.26E+00
σ		9.23E-02	1.51E-01	8.28E-02	5.77E-02
n		4.00E+00	4.00E+00	4.00E+00	4.00E+00
Tl-208	1	4.94E-01	4.74E-01	5.39E-01	5.12E-01
Tl-208	3	5.10E-01	5.36E-01	5.77E-01	5.50E-01
Tl-208	4	4.45E-01	4.65E-01	4.67E-01	4.61E-01
Tl-208	5	5.20E-01	5.71E-01	4.78E-01	5.12E-01
Mean		4.92E-01	5.12E-01	5.15E-01	5.09E-01
σ		3.33E-02	5.07E-02	5.19E-02	3.65E-02
n		4.00E+00	4.00E+00	4.00E+00	4.00E+00
U-233/234	1	9.69E-01	9.64E-01	9.77E-01	9.71E-01
U-233/234	3	1.17E+00	1.39E+00	1.69E+00	1.49E+00
U-233/234	4	1.03E+00	1.09E+00	9.29E-01	9.95E-01
U-233/234	5	1.13E+00	9.17E-01	1.13E+00	1.08E+00
Mean		1.07E+00	1.09E+00	1.18E+00	1.13E+00
σ		9.19E-02	2.13E-01	3.50E-01	2.40E-01
n		4.00E+00	4.00E+00	4.00E+00	4.00E+00
U-238	1	9.26E-01	1.02E+00	1.13E+00	1.05E+00
U-238	3	1.19E+00	1.50E+00	1.63E+00	1.49E+00
U-238	4	9.11E-01	1.09E+00	8.95E-01	9.48E-01
U-238	5	9.61E-01	1.18E+00	1.12E+00	1.10E+00
Mean		9.97E-01	1.20E+00	1.19E+00	1.15E+00
σ		1.30E-01	2.13E-01	3.10E-01	2.36E-01
n		4.00E+00	4.00E+00	4.00E+00	4.00E+00

Two tests were performed. In the first test, the null hypothesis and alternative hypotheses were:

$$H_o: u_M = u_C$$
$$H_a: u_M \neq u_C$$

where u_M and u_C are the mean radionuclide concentrations in the Modelo and Chatsworth formations, respectively. A second t-test was performed where the null and alternative hypotheses were:

$$H_o: u_M - u_C \leq 0$$
$$H_a: u_M - u_C \geq 0$$

Results are presented in Table D-2. At the 95% confidence level (i.e., α=0.05), there was no significant difference between the mean ^{226}Ra concentrations in the 0–3 cm and 3–6 cm layer, but there was a significant difference in the 6–12 cm layer. For ^{230}Th, ^{234}U, and ^{238}U there was no significant difference between concentrations in the Chatsworth and Modelo formations in all layers, and thus no significant difference between sample locations in and outside the plume. For ^{232}Th, ^{228}Th, ^{228}Ra, and ^{208}Tl (thorium decay series), a significant difference was observed between the two formations in all layers. Thorium decay series radionuclide concentrations in the Modelo formation and within the plume were *lower* compared to the background samples taken outside the plume and in the Chatsworth formation.

Table D-2. *t*-test Results for Uranium and Thorium Decay Series Radionuclides in Samples Taken in the Modelo and Chatsworth Formations

					Accepted hypothesis[a,b]			
Ra-226	0–3 cm	3–6 cm	6–12 cm	12-cm weighted average	0–3 cm	3–6 cm	6–12 cm	12-cm weighted average
df	5	5	6	6				
t_{cal}	2.46E+00	2.21E+00	2.74E+00	2.59E+00				
t_{tab} (2-tail)	2.57E+00	2.57E+00	2.45E+00	2.45E+00	H_o	H_o	H_a	H_a
u_M	1.73E+00	1.65E+00	1.65E+00	1.67E+00				
u_C	1.24E+00	1.23E+00	1.24E+00	1.23E+00				
t_{tab} (1-tail)	2.57E+00	2.57E+00	2.45E+00	2.45E+00	H_o	H_o	H_a	H_a
Ra-228								
df	5	4	5	6				
t_{cal}	5.77E+00	5.52E+00	6.28E+00	7.17E+00				
t_{tab} (2-tail)	2.57E+00	2.78E+00	2.57E+00	2.45E+00	H_a	H_a	H_a	H_a
u_M	1.11E+00	1.07E+00	1.10E+00	1.10E+00				
u_C	1.62E+00	1.75E+00	1.69E+00	1.69E+00				
t_{tab} (1-tail)	2.57E+00	2.78E+00	2.57E+00	2.45E+00	H_a	H_a	H_a	H_a
Th-230								
df	4	4	5	4				
t_{cal}	2.45E+00	2.09E+00	1.77E+00	2.10E+00				
t_{tab} (2-tail)	2.78E+00	2.78E+00	2.57E+00	2.78E+00	H_o	H_o	H_o	H_o
u_M	1.66E+00	1.65E+00	1.63E+00	1.65E+00				
u_C	1.07E+00	1.18E+00	1.22E+00	1.17E+00				
t_{tab} (1-tail)	2.78E+00	2.78E+00	2.57E+00	2.78E+00	H_o	H_o	H_o	H_o
Th-232								
df	6	3	6	6				
t_{cal}	6.73E+00	7.49E+00	7.54E+00	1.11E+01				
t_{tab} (2-tail)	2.45E+00	3.18E+00	2.45E+00	2.45E+00	H_a	H_a	H_a	H_a
u_M	8.37E-01	7.64E-01	7.64E-01	7.82E-01				

Table D-2. *t*-test Results for Uranium and Thorium Decay Series Radionuclides in Samples Taken in the Modelo and Chatsworth Formations

					Accepted hypothesis[a,b]			
Ra-226	0–3 cm	3–6 cm	6–12 cm	12-cm weighted average	0–3 cm	3–6 cm	6–12 cm	12-cm weighted average
u_C	1.24E+00	1.35E+00	1.23E+00	1.26E+00				
t_{tab} (1-tail)	2.45E+00	3.18E+00	2.45E+00	2.45E+00	H_a	H_a	H_a	H_a
Tl-208								
df	6	6	4	6				
t_{cal}	5.60E+00	4.92E+00	6.26E+00	6.82E+00				
t_{tab} (2-tail)	2.45E+00	2.45E+00	2.78E+00	2.45E+00	H_a	H_a	H_a	H_a
u_M	3.44E-01	3.27E-01	3.30E-01	3.33E-01				
u_C	4.92E-01	5.12E-01	5.15E-01	5.09E-01				
t_{tab} (1-tail)	2.45E+00	2.45E+00	2.78E+00	2.45E+00	H_a	H_a	H_a	H_a
U-234								
df	6	5	4	5				
t_{cal}	2.19E+00	1.87E+00	1.55E+00	1.83E+00				
t_{tab} (2-tail)	2.45E+00	2.57E+00	2.78E+00	2.57E+00	H_o	H_o	H_o	H_o
u_M	8.66E-01	8.58E-01	8.79E-01	8.70E-01				
u_C	1.07E+00	1.09E+00	1.18E+00	1.13E+00				
t_{tab} (1-tail)	2.45E+00	2.57E+00	2.78E+00	2.57E+00	H_o	H_o	H_o	H_o
U-238								
df	6	6	6	6				
t_{cal}	8.36E-01	2.14E+00	1.39E+00	1.51E+00				
t_{tab} (2-tail)	2.45E+00	2.45E+00	2.45E+00	2.45E+00	H_o	H_o	H_o	H_o
u_M	8.95E-01	8.67E-01	9.18E-01	8.99E-01				
u_C	9.97E-01	1.20E+00	1.19E+00	1.15E+00				
t_{tab} (1-tail)	2.45E+00	2.45E+00	2.45E+00	2.45E+00	H_o	H_o	H_o	H_o

a. Null and alternate hypothesis for 1-tailed t-test: H_o: $u_M = u_C$, H_a: $u_M \neq u_C$. t_{val} based on α=0.05.

b. Null and alternate hypothesis for 2-tailed t-test: H_o: $u_M - u_C \leq 0$, H_a: $u_M - u_C \geq 0$. t_{val} based on α=0.05.

References

Huntsberger, D.V. and P.P Billingsley. 1987. *Elements of Statistical Inference: Sixth Edition*. Boston, MA: Allyn and Bacon Inc.

StatTrek 2019. Available at www.stattrek.com. Accessed November 12, 2019.

Appendix E. Potential Dose that Soil Sampling Can Detect

This Appendix evaluates the potential dose that sampling in surface soils would be able to distinguish above background. The comparison of predicted and observed $PM_{2.5}$ concentrations presented in Section 3.4 demonstrates that the source release and atmospheric transport model produced credible results. These results can be used to estimate the amount of deposition that may be observed in soil that would result in radiological dose to a person at the location. This calculation requires several parameters that are calculated from the concentration and deposition values. These parameters are the concentration (X/Q) and deposition (ψ/Q) factors and are given by:

$$X/Q = \frac{X_{air}}{Q}$$
$$\psi/Q = \frac{\psi_{grd}}{Q} \qquad \text{(E-1)}$$

where

X_{air}	=	average $PM_{2.5}$ concentration during the simulated time period (g m^{-3})
ψ_{grd}	=	average deposition rate of $PM_{2.5}$ on the ground surface during the assessment period (g m^{-2} s^{-1})
Q	=	release rate of $PM_{2.5}$ during the simulated time period (g s^{-1})
X/Q	=	concentration factor (s m^{-3})
ψ/Q	=	deposition factor (m^{-2}).

For these calculations, we simulated a 10-hour period starting from the ignition of the fire at 14:24 PST 8 November 2018. During this period, the fire burned across portions of Area IV where known contamination exists and includes regions 1 through 5 identified in Figure 2-2. Concentrations and deposition rates were extracted from grid files generated from CALPOST and viewed using the Surfer® software (Golden Software 2019). Concentration and deposition values at a location on the northeast corner of the Oak Park community where concentration and deposition were the highest were extracted. Using the data in Table 2-2, the total $PM_{2.5}$ emissions for November 8 (regions 1 through 5) was calculated to be 2.99×10^{8} g and the average release rate over 10 hours was 8,304 g s^{-1}. The calculated X/Q and ψ/Q and supporting data are presented in Table E-1.

Table E-1. Parameters Values for Calculation of *X*/*Q* and *ψ*/*Q* at the Oak Park Community[a]

Quantity	Value
10-hr average $PM_{2.5}$ concentration (g m^{-3})	2.93E-04
10-hr average $PM_{2.5}$ deposition (g m^{-2})	8.90E-06
$PM_{2.5}$ release rate for regions 1–5 (g s^{-1})	8.30E+03
X/*Q* (s m^{-3})	3.53E-08
ψ/*Q* (m^{-2})	1.07E-09

[a.] Located at UTM 338750E 3783550N and node row 140 and node column 177 in the file conc-pm25-Nov8.grd for concentration and in the file totalPM2.5dflx-Nov8-10hr-ASCII.grd for deposition.

The effective dose for a given release rate can be calculated using the *X*/*Q* and *ψ*/*Q* values, an exposure scenario, and dose coefficients. These calculations focus on three anthropogenic radionuclides that have been detected on the SSFL: ^{137}Cs, ^{90}Sr, and ^{239}Pu, and the naturally occurring radionuclide ^{226}Ra. The effective dose for a person exposed to radionuclides in the plume and deposited on the ground is calculated by:

$$D = Q\left[\begin{array}{l}\left(X/Q \times BR \times ET_{inh} \times DC_{inh}\right) + \left(X/Q \times ET_{sub} \times \dfrac{3600\text{ s}}{\text{hour}} \times DC_{sub}\right) \\ + \left(\psi/Q \times RT \times ET_{ext} \times \dfrac{3600\text{ s}}{\text{hour}} \times DC_{ext}\right)\end{array}\right] \quad \text{(E-2)}$$

where

Q	=	release rate (pCi s^{-1})
BR	=	breathing rate (m^3 hr^{-1})
ET_{inh}	=	exposure time for inhalation (hours)
DC_{inh}	=	dose coefficient for inhalation (mrem pCi^{-1})
ET_{sub}	=	exposure time for submersion (hours)
DC_{sub}	=	submersion dose coefficient (mrem m^3 s^{-1} pCi^{-1})
RT	=	release time (36,000 s)
ET_{grd}	=	exposure time for exposure from radionuclides deposited on the ground (hours)
DC_{grd}	=	ground plane dose coefficient (mrem m^2 s^{-1} pCi^{-1}).

Equation (E-2) is solved for *Q* for an effective dose that is protective of human health (i.e., the limiting dose). The exposure scenario assumes the person inhales SSFL-derived radionuclides entrained in the smoke plume and resides at their residence for a year[1] following the fire where they receive external radiation from radionuclides that have deposited on the ground. The *Q* value is then used in the following equation to calculate the surface soil concentration:

$$C_{soil} = \frac{Q \times \psi/Q \times RT}{\rho_b \times T} \quad \text{(E-3)}$$

[1] Radiation standards are stated on an annual basis.

where

ρ_b = bulk density (g m^{-3})
T = thickness of soil layer (m).

The exposure scenario assumes that during the fire, the person is engaged in light activity 50% of the time and moderate activity for the remainder. Mean breathing rates for light and moderate activity for a person 31 to 41 years old from EPA (2011) are 0.012 m^3 min^{-1} (0.72 m^3 hr^{-1}) and 0.027 m^3 min^{-1} (1.62 m^3 hr^{-1}), respectively, for a weighted mean of 1.17 m^3 hr^{-1}.

During the following year, default occupancy factors from RESRAD v7.2 (Kamboj et al. 2018) were adapted. These factors include 50% of the time spent indoors, 25% of the time spent outdoors, 25% of the time spent away from the home, and an indoor gamma shielding factor of 0.7. The occupancy factor multiplied by the number of hours in a year (8,760) gives the exposure time to radionuclides deposited on the ground. The occupancy factor (*OF*) and exposure time for ground exposure (EF_{grd}) is calculated as:

$$OF = 0.5 \times 0.7 + 0.25 \times 1.0 + 0.25 \times 0.0 = 0.6$$
$$ET_{grd} = 0.6 \times 8760 \text{ hours} = 5256 \text{ hours}$$

Parameters for the dose calculation are summarized in Table E-2. Dose coefficients, shown in Table E-3 are from DOE (2011a) for inhalation and from EPA (2019) for external exposure (submersion and ground plane).

Table E-2. Parameters Used in the Dose Calculation

Parameter	Value	Units	Reference or comments
Breathing rate, *BR*	1.17	m^3 hr^{-1}	Calculated from data in EPA (2011)
Occupancy factor, *OF*	0.6	---	Calculated based on Kamboj et al. (2018)
Inhalation exposure time, ET_{inh}	10	hours	Based on plume passage time
Submersion exposure time, ET_{sub}	10	hours	Based on plume passage time
Ground exposure time, ET_{grd}	5256	hours	Calculated based on Kamboj et al. (2018)
Bulk density, ρ_b	1.0E6	g m^{-3}	Assumed surface soil value
Soil layer thickness, *T*	0.03	m	Sampling depth for surface soil

Table E-3. Dose Coefficients used in Dose Calculations

Radio-nuclide	Progeny[a]	Inhalation solubility Type[b]	Inhalation DC (mrem pCi^{-1})	Ground plane DC (mrem-m^2 pCi^{-1} s^{-1})	Submersion in air DC (mrem-m^3 pCi^{-1} s^{-1})
^{137}Cs[c]		F	1.70E-05	2.90E-14	1.44E-12
	^{137m}Ba	F	[e]	1.44E-12	9.84E-11
^{239}Pu		M	6.22E-02	1.55E-16	1.22E-14
^{90}Sr[d]		M	1.45E-04	2.41E-14	1.49E-12
	^{90}Y	M	[e]	5.44E-13	1.18E-11

Radio-nuclide	Progeny[a]	Inhalation solubility Type[b]	Inhalation DC (mrem pCi^{-1})	Ground plane DC (mrem-m^2 pCi^{-1} s^{-1})	Submersion in air DC (mrem-m^3 pCi^{-1} s^{-1})
^{226}Ra		M	1.41E-02	1.51E-14	1.11E-12
	^{214}Bi	M	[e]	3.70E-12	2.67E-10
	^{214}Pb	M	[e]	6.07E-13	4.11E-11

a. Radioactive progeny that are in secular equilibrium in the environment.
b. Default solubility class from ICRP (1996).
c. External doses for ^{137}Cs includes the dose from ^{137}Cs plus the dose from ^{137m}Ba × a branching fraction of 0.944.
d. External doses for ^{90}Sr includes the dose from ^{90}Sr plus the dose from ^{90}Y × a branching fraction of 1.0.
e. Inhalation dose coefficient includes these progeny.

The calculated *Q* values for limiting doses of 0.01 mrem, 0.1 mrem, and 1.0 mrem are presented in Table E-4 along with unit doses (*UD*) for the inhalation, submersion, and external exposure pathways. Release inventories are calculated with Equation E-2 solved for *Q*. Unit dose factors are the quantities in Equation E-2 for the inhalation, submersion, and external exposure pathways for a 1 pCi Q value. Thus, the *UD* values and *Q* values are calculated by:

$$\begin{aligned} UD_{inh} &= 1\text{ pCi} \times \left(X/Q \times BR \times ET_{inh} \times DC_{inh} \right) \\ UD_{sub} &= 1\text{ pCi} \times \left(X/Q \times ET_{sub} \times \frac{3600\text{ s}}{\text{hour}} \times DC_{sub} \right) \\ UD_{ext} &= 1\text{ pCi} \times \left(\psi/Q \times RT \times ET_{ext} \times \frac{3600\text{ s}}{\text{hour}} \times DC_{ext} \right) \end{aligned} \tag{E-4}$$

and

$$Q = \frac{D_L}{UD_{inh} + UD_{sub} + UD_{ext}} \tag{E-5}$$

where D_L is the limiting dose (0.01 mrem, 0.1 mrem, and 1.0 mrem).

Table E-4. Radionuclide Release Inventories (*Q*) that Result in an Annual Effective Dose of 0.01 mrem, 0.1 mrem, and 1.0 mrem at Oak Park and Unit Dose Factors

Radio-nuclide	*Q* for 0.01 mrem (pCi)	*Q* for 0.1 mrem (pCi)	*Q* for 1.0 mrem (pCi)	Inhalation unit dose (mrem pCi^{-1})	Submersion unit dose (mrem pCi^{-1})	External unit dose (mrem pCi^{-1})
^{137}Cs	3.52E+11	3.52E+12	3.52E+13	1.58E-16	3.33E-18	2.82E-14
^{239}Pu	1.74E+10	1.74E+11	1.74E+12	5.76E-13	4.31E-22	3.14E-18
^{90}Sr	7.77E+11	7.77E+12	7.77E+13	1.34E-15	4.68E-19	1.15E-14
^{226}Ra	1.56E+9	1.56E+10	1.56E+11	1.31E-13	1.52E-19	6.26E-12

The surface soil concentration that corresponds to the limiting dose can be compared to analytical detection limits (Section 5.3) and background concentrations (Section 4.2.2) to determine if the activity deposited on soil surface could be detected by sampling. The soil concentrations from deposition were calculated for three limiting effective doses: 1.0 mrem, 0.1 mrem, and 0.01 mrem (Table E-5). These effective doses are a factor of 100, 1,000, and 10,000 times lower than the annual effective dose limit above background from human sources recommended by the International Commission on Radiological Protection (ICRP), National Council on Radiation Protection and Measurements (NCRP), and implemented in DOE-Order 458.1 (DOE 2011b) of 100 mrem. Moreover, these effective doses are well below the average effective dose from natural background a typical person normally receives in a year of about 310 mrem (NCRP 2009). As shown in Table E-5, if a 0.1 mrem annual effective dose was received by an individual residing near Oak Park, then the soil sampling would be able to detect the presence of anthropogenic radionuclides deposited on soil from the Woolsey fire above that which is currently present in soil. For a dose of 0.01 mrem, estimated soil concentrations would be difficult to distinguish from background. Radium-226 is naturally occurring, has a high background concentration value relative to the other three radionuclides, and is released to the air from any natural wildfire. A ^{226}Ra release from either a natural or anthropogenic source resulting in an effective dose of 10 mrem could theoretically be detected in soil.

Table E-5. Results of Soil Concentration Calculation for Limiting Effective Dose

	Soil concentration from deposition for limiting effective dose (pCi g^{-1})				
Radionuclide	1.0 mrem	0.1 mrem	0.01 mrem	MDC (pCi/g)[a]	Background (pCi/g)[b]
^{137}Cs	1.26	0.126	0.0126	0.007	0.229
^{239}Pu	0.062	0.0062	6.20×10^{-4}	0.005	0.0134
^{90}Sr	2.78	0.278	0.0278	0.015	0.0735
^{226}Ra	5.59×10^{-3}	5.59×10^{-4}	5.59×10^{-5}	0.02	1.88

a. Minimum detectable concentration, see Table 5-2.
b. Background threshold value, see Table 4-2.

Thus, the sampling sensitivity should detect SSFL radionuclides deposited on the soil surface from the fire that would result in an effective dose of 0.1 mrem to an individual. Sensitivity of detecting natural occurring radionuclides that were also used in SSFL operations is complicated because naturally occurring radionuclides are present in all soils and vegetation and are released to the air during a fire. For example, radionuclides of the uranium and thorium decay series have anthropogenic sources on the SSFL but also are found naturally in soils in varying abundances.

Cesium-137 is an important radionuclide because it has a low MDC (i.e., readily detected in soil), has the highest measured concentration of the long-lived fission products detected on the SSFL (1,600 pCi g^{-1} in 1989; 819 pCi g^{-1} decay corrected to 2018), and as it is relatively immobile in soils, it would not leach away like ^{90}Sr. Plutonium isotopes were also measured on the SSFL but concentrations were substantially lower than those of ^{137}Cs or ^{90}Sr. Thus, ^{137}Cs is a good indicator of radionuclide releases from the Woolsey fire burning across SSFL.

References

DOE (U.S. Department of Energy). 2011a. *Derived Concentration Technical Standard*. DOE-Std-1196-2011. U.S. Department of Energy, Washington, D.C.

DOE. 2011b. *Radiation Protection of the Public and Environment*. DOE Order 458.1. U.S. Department of Energy, Washington, D.C. February.

EPA (U.S. Environmental Protection Agency). 2011. *Exposure Factors Handbook*. EPA/600/R-090/052F. U.S. EPA, Office of Research and Development, Washington, D.C.

EPA. 2019. *External Exposure to Radionuclides in Air, Water and Soil*. EPA-402/R19/002. U.S. EPA, Office of Radiation and Indoor Air, Washington, D.C.

Golden Software. 2019. Surfer Version 17.1.288. Golden Software LLC, Golden, CO. (www.goldensoftware.com).

ICRP (International Commission on Radiological Protection). 1996. Age-dependent Doses to Members of the Public from Intake of Radionuclides: Part 5 Compilation of Ingestion and Inhalation Dose Coefficients. Publication 72. International Commission on Radiological Protection, Oxford, UK.

Kamboj, S., E. Gnanapragasam, and C. Yu. 2018. *User's Guide for the RESRAD Onsite Code Version 7.2*. ANL/EVS/TM-18/1. Argonne National Laboratory, Argonne, IL.

NCRP (National Council on Radiation Protection and Measurements). 2009. *Ionizing Radiation Exposure of Population of the United States*. NCRP Report No. 160. National Council on Radiation Protection and Measurements, Bethesda, MD.

T 803.536.4883 F 803.534.1995 417 Till Road Neeses, South Carolina 29107 www.racteam.com